Tissue-specific Butyrophilin-like Molecules are Master Regulators of Intraepithelial γδ T cell Composition

Rafael Provenzano Di Marco Barros

University College London

and

The Francis Crick Institute

PhD Supervisor: Professor Adrian Clive Hayday

A thesis submitted for the degree of

Doctor of Philosophy

University College London

09 2016

Declaration

I Rafael Di Marco Barros confirm that the work presented in this thesis is my own. Where information has been derived from other sources, I confirm that this has been indicated in the thesis.

Abstract

Many epithelial barriers are constitutively populated by large numbers of organ-specific γδ T cells that collectively make up a substantial proportion of the body's T cells. In mice, these intraepithelial lymphocytes (IEL) display striking site-specific T cell receptor (TCR) Variable (V)γ chain usage, such that Vγ5$^+$, Vγ6$^+$ and Vγ7$^+$ T cells form lifelong associations with the murine epidermis, uterine and the small intestinal epithelium, respectively. The maintenance of IEL composition is critically important to host physiology and its disruption in murine epidermis is associated with dysregulated cutaneous inflammation and heightened susceptibility to carcinogenesis. Furthermore, tumour-associated γδ T cell gene-expression signatures were recently found to be the greatest correlate with overall survival in a genome-wide expression analysis of ~18,000 human tumours. Thus, there is considerable interest in identifying molecules that regulate infiltration, composition and activation of tissue-resident γδ T cells.

Skint1 is a *Butyrophilin-like (Btnl)* gene expressed by thymic medullary epithelium and suprabasal keratinocytes, which shapes DETC composition. However, as neither *Skint1* nor DETC are conserved, a general mechanism by which epithelia shape IEL composition remains unelucidated. Here we show that enterocyte *Btnl1* expression shapes small intestinal IEL composition by driving extrathymic maturation and expansion of Vγ7$^+$ IEL *in trans* upon their arrival in the gut. Uninfluenced by microbial or solid food antigens, this mechanism evokes the Major Histocompatibility Complex-driven selection of αβ T cell repertoires. Consistent with this, we show that *Btnl1* together with *Btnl6* elicits specific TCR-dependent responses of intestinal Vγ7$^+$ cells *in vitro*. From these data, a generalizable mechanism emerges whereby organ-specific expression of Btnl molecules enables epithelial cells to actively shape the lifelong composition of their signature IEL compartments. Moreover, by identifying selection elements that regulate signature γδ IEL, our models also provide novel avenues to study the unique contributions of discreet IEL compartments to host immunity.

Acknowledgements

Firstly, I would like to express my gratitude to Professor Adrian Hayday, whose supervision, mentorship, encouragement and limitless excitement about this project has been key to my development as a scientist. These have been the most formative years of my life and I am very appreciative of the opportunity I was given to undertake such an exciting project in such a great laboratory. I would also like to acknowledge my thesis committee, Professor Hans Stauss and Professor Caetano Reis e Sousa for their support, mentorship and advice throughout my studies; Professor Ulrich Steinhoff and his wife Karen, who introduced me to Marburg, welcomed me into their home, and helped me perform some critical experiments presented in this thesis; The UCL MBPhD programme; and my funders, Cancer Research UK and the Medical Research Council.

Several members of the Hayday lab (past and present) were instrumental in my scientific training and in the execution of this project. In fact, I feel truly privileged to have been trained by and to have worked alongside such a brilliant group of people. Special thanks are due to Melanie Wencker who trained and mentored me during my first 18 months in the lab; to Anett Jandke, Natalie Roberts and Pierre Vantourout who made crucial contributions to the Btnl1 project and who trained and supported me throughout my time here (especially while I was writing this thesis - you were all fantastic! - Thank you so much!); to Livija Deban, who introduced me to mucosal immunology, supported, mentored and trained me; to Robin Dart, for his enthusiasm in expanding the Butyrophilin project into the human; to Rosie Hart, for bringing our favourite cells to life in her beautiful images; to the 3i team, for introducing me to radar plots and for contributing to the paper and this thesis!; and to Yin Wu, for luring me into the immunosurveillance lab all those years ago! This list could very easily continue, as I have been incredibly fortunate to work and collaborate with virtually every member of the Hayday lab - thank you all!

Outside of the laboratory, my friends and family have always been supportive of me and for that I am very thankful. In particular, special thanks are due to my mum who holds much of the responsibility for my long-standing interest in immunology. Furthermore, although they live a bit further away, my sister and my dad have

always been incredibly supportive and always available for a short notice phone call whenever I have needed a boost in morale. Finally, I want to thank Danielle, my girlfriend of 8 years, whose love and support has driven me every step of the way. Thank you for everything! This work is dedicated to her.

Table of Contents

Table of figures

List of tables

Abbreviations

-/-	Knock-out
AF	Alexa-fluor
aly/aly	Alymphoplasia
AOM	Azoxymethane
APC	Antigen-presenting cell
BiTg	Bitransgenic
BTN	Butyrophilin
BTNL	Butyrophilin-like
CMV	Cytomegalovirus
D	Day
DAMP	Danger-associated molecular pattern
DC	Dendritic cell
DETC	Dendritic epidermal T cell
DIG	Digoxigenin
DMBA	Dimethylbenz[*a*]anthracene
DMEM	Dulbecco's Modified Eagle's Medium
DN	Double negative
DNA	Deoxyribonucleic acid
Dox	Doxycycline
DP	Double positive
DTT	Dithiothreitol
E	Embryonic day of gestation
EdU	5-ethynyl-2 deoxyuridine
ERMAP	Erythroblast membrane associated protein
EV	Empty vector
FACS	Fluorescence activated cell sorting
FAF	Food-antigen-free
FCS	Foetal calf serum
GF	Germ-free
GFP	Green fluorescent protein
Gzm	Granzyme

HBSS	Hank’s balanced salt solution
HMBPP	(E)-4-hydroxy-3-methyl-but-2-enyl pyrophosphate
Hr	Hour
ICER	Inducible cAMP early repressor of transcription
IEL	Intraepithelial lymphocyte
IFN	Interferon
Ig	Immunoglobulin
IL	Interleukin
IMPC	International Mouse Phenotyping Consortium
iNKT	Invariant natural killer T
IPP	Isopentenyl pyrophosphate
IRES	Internal ribosome entry site
ITIM	Immunoreceptor tyrosine-based inhibitory motif
IV	Intravenous
JAML	Junctional adhesion molecule-like protein
L1	Btnl1
L3	BTNL3
L4	Btnl4
L6	Btnl6
L8	BTNL8
LSS	Lymphoid stress surveillance
LSSR	Lymphoid stress surveillance response
LT	Lymphotoxin
M	Million
MAIT	Mucosa-associated invariant T
MCS	Multiple cloning site
MFG	Milk fat globule
MHC	Major histocompatibility complex
MLN	Mesenteric lymph node
MOG	Myelin oligodendrocyte protein
NKR	Natural killer receptor
pAg	Phospho-antigen
pAgPC	Phospho-antigen-presenting cell
PALP	Phosphotyrosine-rich aggregates located on projections

PAMP	Pathogen-associated molecular pattern
PBS	Phosphate-buffered saline
PCR	Polymerase chain reaction
PP	Peyer's patch
PRR	Pattern recognition receptor
PVR	Poliovirus receptor
qRT-PCR	Quantitative reverse transcription polymerase chain reaction
RAG	Recombination-activating gene
RBC	Red blood cell
RNA	Ribonucleic acid
SI	Small intestine
SiTg	Single transgenic
SP	Single positive
T_c	Cytotoxic T cell
T_h	Helper T cell
TCR	T cell receptor
TCS	Tissue culture supernatant
TdT	Terminal deoxynucleotidyl transferase
Tg	Transgenic
TLA	Thymus leukaemia antigen
TLR	Toll-like receptor
TNF	Tumour necrosis factor
TNFR	Tumour necrosis factor receptor
TP	Triple positive
TPA	12-O-tetradecanoylephorbol
TRE	Tetracycline response element
T_{RM}	Tissue-resident memory
UV	Ultra-violet
W	Week
WT	Wild type
γδ17	IL-17-producing γδ T cell
γδIFNγ	IFNγ-producing γδ T cell

Chapter 1. Introduction

The study of immunology stems from the earliest observations of immune memory and the potent prophylactic properties of vaccination against infectious disease. In seeking to better understand the biology underlying these observations, seminal work from several groups has outlined a sequence of cellular and molecular interactions that describe the host response to microbial challenge. Such pathways are now described in some detail in all immunology textbooks and their study has uncovered numerous molecular targets for pharmacological immunomodulation in the clinic. While the immune system has evolved under considerable selection pressure to respond to microbial challenge, it is increasingly acknowledged that non-microbial challenges such as mechanical tissue perturbation, genotoxic stress and cellular transformation can also activate immune cells. Such responses to dysregulated or stressed 'self' may contribute to the exacerbation or initiation of autoinflammatory pathology and are directly implicated in tumour immunosurveillance. In order to better understand the contribution of these emerging immunological pathways to host defence and host pathology, research has focussed on identifying key cellular effectors and characterising their development; their functional potential(s); and the molecular interactions that govern their effector function(s).

1.1 The immune responses to environmental challenge

1.1.1 Microbial Challenge

The immune response to microbial challenge is the best-studied system in mammalian immunology and is subdivided into innate and adaptive phases. During the innate phase, myeloid-derived antigen-presenting cells (APC) such as dendritic cells (DCs) employ germline-encoded pattern recognition receptors (PRRs) to mount rapid responses to pathogen-associated molecular patterns (PAMPs) and danger-associated molecular patterns (DAMPs) (Janeway, 1989; Janeway and Medzhitov, 2002; Matzinger, 2002; Zelenay and Sousa, 2013) (**Figure 1.1**). Upon activation, DCs deploy local effector responses, recruit additional leukocytes and migrate to local lymphoid tissues to prime the adaptive phase of the immune response. Adaptive immunity is antigen-specific and driven by T and B cells that

utilise recombination-activating-gene (RAG)-mediated somatic gene rearrangement to generate a vast repertoire of antigen-specific immune receptors (Davis and Bjorkman, 1988; Hozumi and Tonegawa, 1976). At the lymphoid tissue, DCs present processed microbial antigens via major histocompatibility complex (MHC) to naïve antigen-specific $\alpha\beta$ T cells (**Figure 1.1**).

The engagement of cognate antigen *via* the T cell receptor (TCR) drives clonal expansion and functional differentiation of naïve T cells into mature effector T cells. Effector T cells home to affected tissues and drive the adaptive immune response (Banchereau and Steinman, 1998). Upon resolution of infection, some antigen-specific lymphocytes persist as long-lived memory cells that can be rapidly mobilized to provide symptomatic immunity to re-infection by the same pathogen (Sallusto et al., 1999; Zinkernagel et al., 1996). Thus, while innate immunity comprises rapid responsiveness to conserved molecular patterns associated with microbial invasion, adaptive immunity is delayed, antigen-specific and can generate long lasting immunological memory.

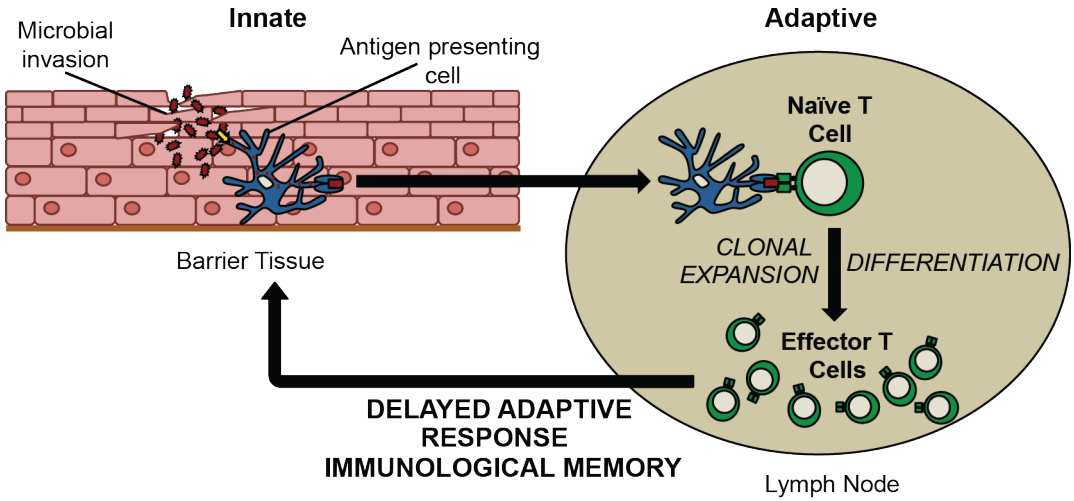

Figure 1.1 The immune response to microbial challenge

Innate - Locally resident myeloid-derived APCs rapidly detect microbial invasion by engaging PAMPs and DAMPs *via* germline-encoded PRRs (Janeway and Medzhitov, 2002; Matzinger, 2002; Zelenay and Sousa, 2013). Microbial components are internalised, processed into smaller peptides and presented on cell surface MHC molecules. Activated APCs migrate to local draining lymph nodes to prime the adaptive response. Antigens derived from cytosolic (intracellular) pathogens are presented *via* MHC class I to naïve $CD8^+$ $\alpha\beta$ T cells. Antigens derived from extracellular pathogens are presented *via* MHC class II to naïve $CD4^+$ $\alpha\beta$ T cells.

Adaptive - TCR engagement of cognate antigen presented on cell surface MHC drives a process of clonal expansion and differentiation, whereby a naïve T cell acquires its mature effector function (e.g. IFNγ *versus* IL-17 production). $CD4^+$ helper T (T_h) cells promote the activation of $CD8^+$ cytotoxic T cells (T_c), which comprise antigen-specific effectors of cell-mediated adaptive immunity. T_h cells also promote activation of naïve B cells, which differentiate into antibody-secreting plasma cells. While T cells home to affected tissues to clear the infection, plasma cells secrete antigen-specific antibodies into the circulation, where they opsonise target pathogens. As clonal expansion, functional maturation and tissue homing takes time, *adaptive* immune responses are often delayed by several days. However, following resolution of infection, some antigen specific T cells and B cells persist as memory cells, providing symptomatic immunity to re-infection by the same pathogen.

1.1.2 Tissue-resident T cells with innate-like *response* modes

Whilst the textbook model for immune activation (**Figure 1.1**) provides an extremely useful frame of reference, it sequesters the contribution of myeloid-derived and lymphoid-derived cells to the afferent arm of the innate response and the efferent arm of the adaptive response, respectively. As such, the model fails to ascribe specific roles to the myriad populations of lymphocytes that are constitutively enriched for in non-lymphoid barrier tissues such as the skin and the gut, where they are optimally positioned to contribute to the earliest phases of the *innate* immune response. Prominent among these are large populations of T cells that exist in a functionally pre-activated state, enabling them to deploy effector functions in response to *innate* stimuli (e.g. inflammatory cytokines), in the absence of concomitant TCR engagement, functional differentiation and clonal expansion (Brennan et al., 2013; Fan and Rudensky, 2016; Lanier, 2013; Shires et al., 2001; Strid et al., 2008). The description of these cells as *innate-like* T cells reflects their expression of an Rag-rearranged TCR and their capacity for unconventional *innate* activation, *via* signals delivered through non-clonally distributed germ-line encoded receptors (Wencker et al., 2013). In other words, while these cells are designated as T cells, they may participate in both *innate* and *adaptive* immunity.

Tissue-resident T cells with *innate* response capabilities include 'conventional' MHC-restricted $\alpha\beta$ tissue-resident memory (T_{RM}) cells (Fan and Rudensky, 2016; Guo et al., 2012) but also include several subsets of 'unconventional' $\alpha\beta$ and $\gamma\delta$ T cells (Godfrey et al., 2015). 'Unconventional' T cells are named as such because they are not restricted to classical MHC, display restricted TCR repertoires and home directly to non-lymphoid tissue following their development in the thymus. They include intraepithelial T lymphocytes (IEL) that occupy various human and murine epithelia, *invariant* natural killer T (iNKT) cells and mucosa-associated invariant T (MAIT) cells, both of which are enriched for in the liver and the intestinal mucosa (Chandra and Kronenberg, 2015; Cheroutre et al., 2011; Godfrey et al., 2015; Shires et al., 2001).

T_{RM} cells and unconventional T cell subsets differentiate *via* discreet developmental pathways, but their acquisition of mature effector function, *innate* responsiveness and tissue-residency shares a requirement for strong or agonist-mediated TCR

stimulation. Hence, T_{RM} cells are the differentiated products of a naïve T cells that have engaged a TCR agonist antigen in a peripheral lymphoid organ (Guo et al., 2012; Schenkel et al., 2016; Schenkel and Masopust, 2014; Sheridan and Lefrançois, 2011); and 'Unconventional' T cells are the differentiated products of cells that acquire their mature effector potential, *innate* responsiveness and tissue homing phenotype following strong TCR-mediated signalling in the thymus (so called 'agonist-selection' **Figure 1.2**) (Baldwin et al., 2004; McDonald et al., 2014; Moran et al., 2011; Stritesky et al., 2012; Wencker et al., 2013). Although for MAIT cells this may occur shortly after thymic egress in a non-lymphoid tissue (Leeansyah et al., 2014).

In summary, non-lymphoid barrier tissues are constitutively populated by multiple subsets of 'conventional' and 'unconventional' T cells that share a legacy of TCR-driven maturation and a capacity to rapidly respond to *innate* stimuli. While some of these subsets achieve functional maturation in the thymus and home directly to their tissue of residence, other subsets are the products of antigen-specific clonal expansion and functional differentiation of naïve T cells into T_{RM} cells. Collectively, these T cells are hypothesized to be key drivers of immunological stress response pathways and their enrichment in non-lymphoid tissue optimally positions them to serve as sentinels of tissue stress (**Figure 1.3**).

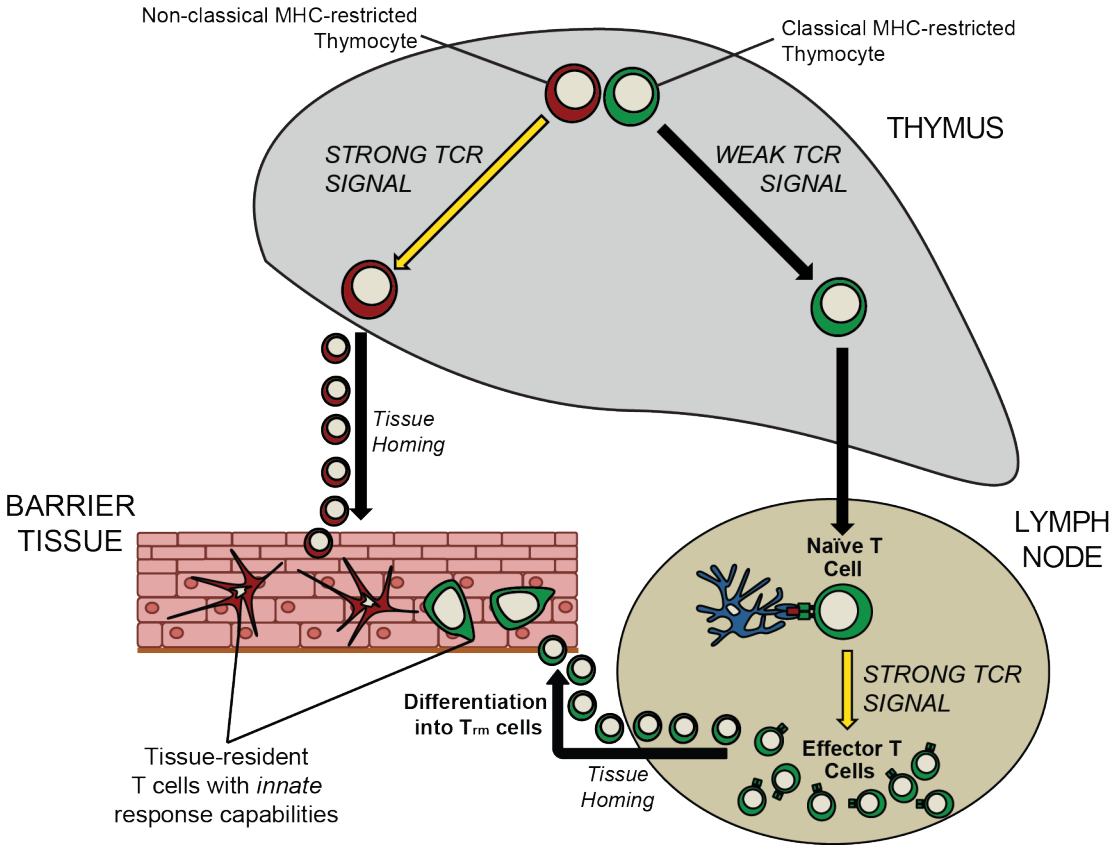

Figure 1.2 Developmental pathways of tissue-resident T cells with *innate* response capabilities

Classical MHC-restricted - Thymocytes are positively selected by weak TCR signalling in the thymus, as strong TCR signalling is associated with their negative selection and clonal deletion. Positively selected cells differentiate into naïve $CD4^+$ or $CD8^+$ T cells and home to peripheral lymphoid organs. Here they await a rare encounter with cognate antigen during microbial infection. Strong cognate antigen-driven TCR signalling is associated with acquisition of mature effector function and tissue-homing capabilities, enabling these cells to migrate to affected tissues and deploy adaptive immunity. Following resolution of infection, the adaptive immune response contracts but some antigen-specific T cells persist, do not recirculate and are peripherally maintained as T_{RM} cells.

Non-classical MHC-restricted - Thymocytes experience strong TCR signalling during agonist selection in the thymus. Thymic differentiation of these cells is associated with acquisition of mature effector function, tissue-homing and *innate* response capabilities. Many such cells are peripherally maintained (see later).

1.1.3 The lymphoid stress surveillance response

The immune response that ensues downstream of stress-induced *innate* activation of tissue-resident T cells is described as the Lymphoid Stress Surveillance Response (LSSR) (Hayday, 2009). Much like PAMP/DAMP-driven activation of myeloid-derived APCs, the LSSR drives rapid deployment of pro-inflammatory and cytotoxic effector functions, recruitment of additional leukocytes and modulation of *adaptive* immune responses (Hayday, 2009; Nitahara et al., 2006; Strid et al., 2011). By positioning T cell activation in the afferent arm of *innate* immunity, the LSSR challenges the textbook model of immune responsiveness and broadens the contribution of T cells to host immunity (**Figure 1.3**) (Hayday, 2009).

Tissue dysregulation can be directly communicated to tissue-resident *innate-like* T cells via germ-line encoded receptors such as toll-like receptors (TLRs), which engage PAMPs during microbial invasion (Martin et al., 2009); receptors for inflammatory cytokines (Gray et al., 2011; Sutton et al., 2009; Wencker et al., 2013); and natural killer receptors (NKR) such as NKG2D (Shafi et al., 2011; Strid et al., 2008). Ligands for NKG2D are MHC Class-I-related molecules of the MICA/MICB and ULBP families in humans and Rae1, H60 and Mult1 in mice. These ligands are up-regulated during cellular stress and are expressed on primary tumours (Girardi et al., 2001; Vantourout et al., 2014); on mechanically perturbed epithelia (Strid et al., 2011); and in sites of on-going inflammation (Groh et al., 1996).

The NKG2D axis is a model for the LSSR and is likely to represent one of many stimulatory trans-cellular interactions that occur between tissue-resident T cells and their epithelial or stromal neighbours (Chodaczek et al., 2012; Strid et al., 2008; Swamy et al., 2010; Witherden et al., 2010; 2012). NKG2D is constitutively expressed by $CD8^+$ T_{RM} cell compartments (Hüe et al., 2004; Xing et al., 2014) and by a large proportion of 'unconventional' T cells, of which intraepithelial $\gamma\delta$ T cells are the prototype (Hayday, 2009; Strid et al., 2011; 2008).

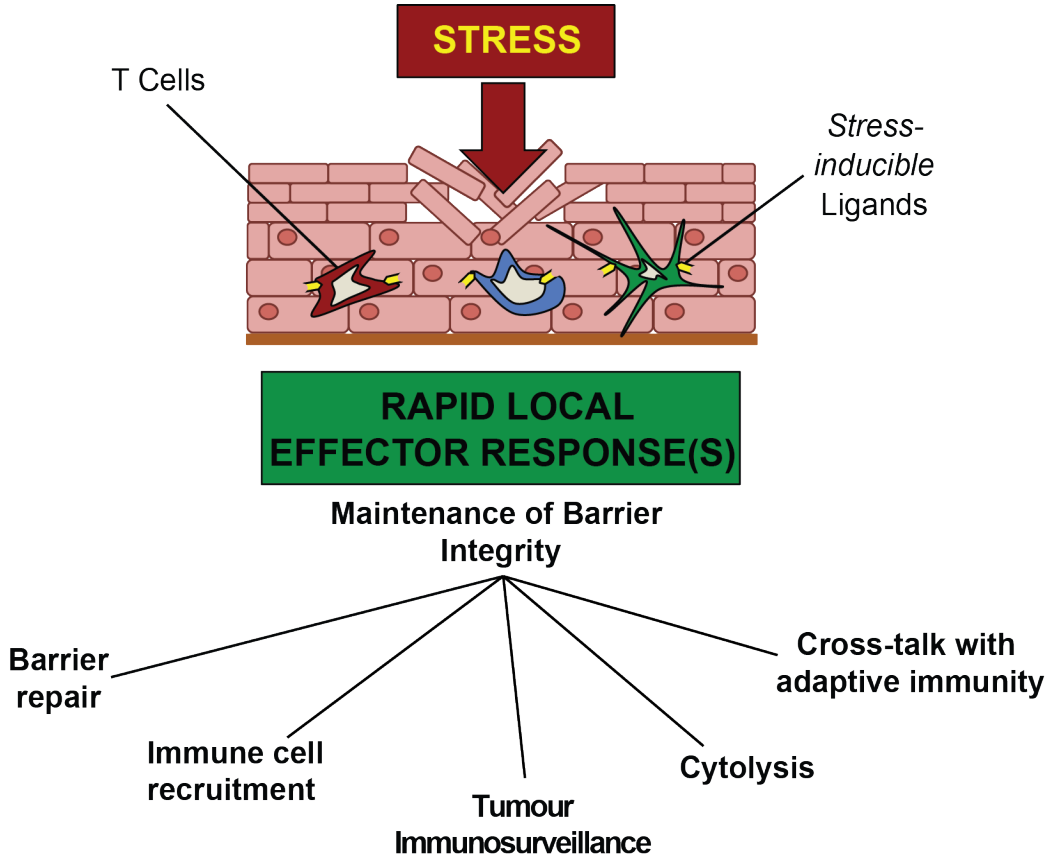

Figure 1.3 The lymphoid stress surveillance response

The lymphoid stress surveillance response (LSSR) describes the rapid activation of tissue-resident T cells in response to various forms of barrier perturbation that occur during microbial or non-microbial challenge. Their activation can take place independently of TCR engagement, *via* receptors for stress-inducible ligands (e.g. NKG2D), cytokine receptors or PRRs. The LSSR has been directly implicated in the maintenance of barrier integrity; in leukocyte recruitment; in tumour immunosurveillance; and in modulating down-stream adaptive immune responses.

1.2 γδ T cells: Prototypic mediators of lymphoid stress surveillance

1.2.1 Evolutionary conservation

γδ T cells, αβ T cells and B cells comprise a tripartite of antigen-specific lymphocytes that utilize somatic gene rearrangement to generate their defining antigen receptors (Hayday, 2000). Discovery of the TCRγ gene locus was unanticipated (Hayday et al., 1985; Saito et al., 1984) and was made prior to the identification of tissue-resident lymphocytes that express them (Borst et al., 1987; Brenner et al., 1986; Jitsukawa et al., 1987; Stingl et al., 1987). Whilst a consensus has yet to be reached regarding the precise role of γδ T cells in human immunology, their conservation across ~450 million years of vertebrate evolution would attest to a significant contribution (Chen et al., 2009; Rast et al., 1997). Furthermore, recent studies of adaptive immunity in the Lamprey, a primitive extant jawless vertebrate, have identified 3 families of lymphocyte-like cells expressing somatically rearranged 'variable lymphocyte receptors' (VLR-A, -B, or -C) (Kasamatsu et al., 2010). While VLR-B is secreted much like B cells secrete immunoglobulin, VLR-A and VLR-C are expressed at the cell surface, evoking thought-provoking parallels with αβ and γδ T cells. Indeed, the enrichment of VLR-C^+ cells in barrier tissues (e.g. the epidermis) and of VLR-A^+ cells in the circulation mirrors the anatomical distribution of most γδ and αβ T cells, respectively (Hirano et al., 2013). Taken together, these studies provide compelling arguments that the three families of antigen-specific lymphocytes carry out critical, non-overlapping functions that merit their conservation across the evolution of vertebrates.

1.2.2 Highly ordered development and site-specific TCR usage

In all vertebrates that have been analysed, γδ T cells are among the first T cells to emerge from the embryonic thymus, with rearrangement of TCRγδ genes detectable by embryonic day (E)13 in the mouse, E10 in the chicken and by gestational week 8 in the human (Hayday, 2000). Emergence of these T cells during embryogenesis is highly ordered and characterized by the sequential appearance of thymocytes bearing specific TCRs. In humans, the foetal circulating

γδ T cell compartment is initially dominated by $V\gamma9^+V\delta2^+$ cells, which progressively decrease in representation as $V\delta1^+$ and $V\delta3^+$ T cells emerge (Dimova et al., 2015). Subsequently, $V\gamma9^+V\delta2^+$ T cells persist in the adult circulation, whereas $V\delta1^+$ and $V\delta3^+$ T cells home to tissues such as the intestinal mucosa and skin (Holtmeier et al., 2001; Pang et al., 2012).

Highly ordered development is also observed in mice, where distinct waves of γδ T cells characterised by TCRVγ chain usage sequentially emerge from the embryonic thymus. First to appear at embryonic day (E)13 are progenitors for $V\gamma5^+V\delta1^+$ dendritic epidermal T cells (DETC), which exclusively populate the murine epidermis (Asarnow et al., 1988; Havran and Allison, 1988; Kuziel et al., 1987; Stingl et al., 1987). These are shortly followed by $V\gamma6^+V\delta1^+$ thymocytes, which predominantly home to epithelia in the reproductive tract and tongue (Itohara et al., 1990); and $V\gamma7^+$ thymocytes, that are mostly found as IEL in the small intestinal epithelium (Asarnow et al., 1988; Kyes et al., 1989). Henceforth, $V\gamma5^+$ DETC, $V\gamma6^+$ uterine IEL and $V\gamma7^+$ small intestinal IEL are considered to be the signature γδ IEL compartments of the mouse (**Figure 1.4**).

$V\gamma5^+$ DETC and $V\gamma6^+$ IEL are exclusively generated from foetal thymic progenitors and so must be peripherally maintained in their respective tissues (Ramond et al. 2013; Haas et al. 2012; Muñoz-Ruiz et al. 2016). As their development precedes detectable expression of terminal deoxynucleotidyl transferase (TdT), they express canonical TCRs lacking junctional diversity that is normally generated *via* random nucleotide addition during Rag-mediated gene rearrangement (Haas et al., 2012; Muñoz-Ruiz et al., 2016; Ramond et al., 2013; Y. Zhang et al., 1995). By contrast, small intestinal $V\gamma7^+$ IEL arise from bone marrow progenitors and accordingly, can be reconstituted in adult bone marrow chimeras (Schluns et al., 2004). While they do display somewhat greater TCR diversity, their repertoire does not overlap with and is significantly less diverse than systemic γδ T cell subsets (Hayday, 2000; Kyes et al., 1989).

Signature DETC compartments with restricted or monoclonal TCR repertoires also exist in rats, cows, and cynomolgus macaques (Hayday, 2000; Hein and Dudler, 1997; Mohamed et al., 2015; Van Rhijn et al., 2007). Likewise, intra-epidermal VLR-C^+ lymphocyte-like cells of the lamprey are reported to display a restricted

antigen receptor repertoire that does not overlap with that of circulating cells (Hirano et al., 2013). Humans also have γδ IEL, which are thought to comprise ~40% of the intestinal IEL compartment and mostly express a $V\gamma4^+$ TCR, evoking a similarity with site-specific TCRVγ chain usage observed in mice (**Figure 1.4**) (Di Marco Barros et al., 2016; Landau et al., 1995). In summary, γδ T cells deploying site-specific TCRs, including signature IEL compartments, are both abundant and conserved across jawed vertebrates. The presence of similarly oligoclonal IEL-like cells in jawless vertebrates attests to the significance of site-specific antigen-receptor specificity within these enigmatic immune compartments.

The generation of an invariant or oligoclonal T cell compartment *via* RAG-mediated somatic gene rearrangement was unprecedented prior to the characterization of murine dendritic epidermal $V\gamma5^+V\delta1^+$ T cells (DETC) (Asarnow et al., 1988). Such IEL are poorly suited to the antigen-sampling requirements of conventional adaptive immunity but are optimally positioned to serve as sentinels for barrier stress. Indeed, the signature associations of specific γδTCRs with particular epithelia has led to suggestions that these cells recognise antigens from a commonly encountered site-specific pathogen, or self-encoded molecules that are indicative of barrier dysregulation (Janeway et al., 1988; Vantourout and Hayday, 2013). This hypothesized feature, along with the capacity of these cells to be activated independently of TCR engagement via *bona fide innate* receptors represents a significant crossover of *innate* and *adaptive* immunity. Thus, the biology of γδ IEL strongly supports their designation as prototypic *innate-like* tissue-resident effectors of LSS (Hayday, 2009).

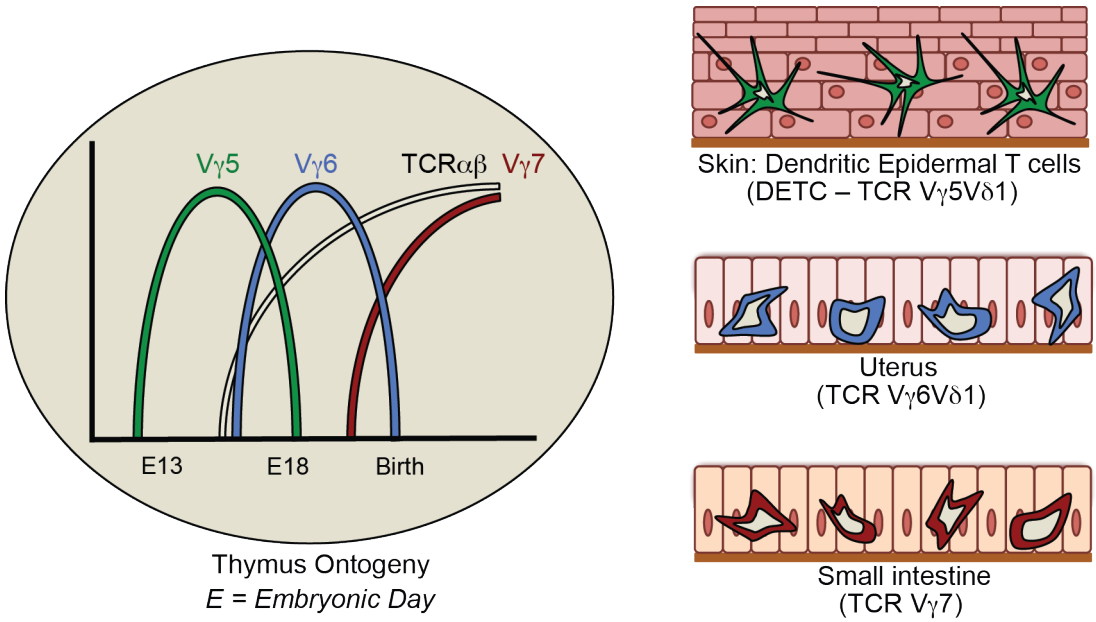

Figure 1.4 γδ IEL development and composition is tightly regulated

γδ IEL progenitors emerge from the embryonic thymus in iconic waves characterized by TCRVγ chain usage. $V\gamma5^+$ and $V\gamma6^+$ thymocytes home directly to the epidermis and uterine epithelium, respectively. $V\gamma7^+$ thymocytes emerge in late embryonic/early post-natal stages. Notably $V\gamma7^+$ IEL can also develop in athymic NU/NU mice, so is not clear whether $V\gamma7^+$ thymocytes and/or an extrathymic pool of progenitors give rise to $V\gamma7^+$ IEL *in vivo* (this will be discussed in subsequent sections). Schematic adapted from: (Carding and Egan, 2002)

1.2.3 γδ IEL composition is critical for lymphoid stress surveillance

The striking evolutionary conservation of site-specific IEL compartments indicates that their composition is tightly regulated and may be important to host physiology. Whilst there are no mouse models exclusively deficient in IEL, perturbation of γδ IEL composition has been experimentally achieved in TCRδ$^{-/-}$ mice, which carry a genetic disruption in the TCR Cδ gene segment (Itohara et al., 1993); and in Vγ5$^{-/-}$ Vδ1$^{-/-}$ mice, which carry targeted disruptions in TCRVγ5 and TCRVδ1 gene loci (Hara et al., 2000; Mallick-Wood et al., 1998). TCRδ$^{-/-}$ mice globally lack γδ T cells and their epithelia are populated by polyclonal αβ T cells. Vγ5$^{-/-}$Vδ1$^{-/-}$ mice lack canonical DETC, but carry polyclonal γδ T cells in their place. Studies using these mutant mice have implicated signature γδ IEL as a critical component of the LSSR (**Figure 1.3**).

1.2.3.1 Tumour immunosurveillance

TCRδ$^{-/-}$ and Vγ5$^{-/-}$Vδ1$^{-/-}$ mice are both reported to display increased susceptibility to chemically-induced cutaneous carcinogenesis, by cutaneous application of dimethylbenz[*a*]anthracene (DMBA) and 12-O-tetradecanoylephorbol (TPA) (Dalessandri et al., 2016; Girardi et al., 2001; Strid et al., 2008). TCRδ$^{-/-}$ mice have also been shown to display increased susceptibility to colorectal carcinoma, following intraperitoneal injection of azoxymethane (AOM) (Matsuda et al., 2001). Given that the IEL compartments of TCRδ$^{-/-}$ and epidermis T cells of Vγ5$^{-/-}$Vδ1$^{-/-}$ mice are populated by polyclonal αβ and γδ T cells, respectively, these studies suggest that signature or canonical γδ IEL subsets perform critical and non-redundant roles in tumour immunosurveillance.

1.2.3.2 Cross-talk with adaptive immunity

The LSSR has been implicated in modulating adaptive immune responses, *via* cellular and molecular pathways that are contingent on intact γδ IEL compartments. In support of this, a common phenotype reported during epithelial challenge of TCRδ$^{-/-}$ mice manifests as αβ T cell-mediated immunopathology at mucosal sites (Hayday et al., 2000). In the gut, it has been shown that TCRδ$^{-/-}$ but not TCRβ$^{-/-}$ or

TCR$\delta^{-/-}\beta^{-/-}$ mice display enhanced intestinal bleeding during infection with the natural coccidian parasite, *Eimeria Vermiformis* (Roberts et al., 1996). In the skin, TCR$\delta^{-/-}$ but not TCR$\delta^{-/-}\beta^{-/-}$ display spontaneous and augmented hypersensitivity responses upon cutaneous application of TPA (Girardi et al., 2002). These adverse phenotypes could be rescued in the skin by adoptively reconstituting signature V$\gamma5^{+}$ DETC (Girardi et al., 2002), and could be rescued in the gut by adoptive transfer of intestinal IEL (Roberts et al., 1996). Additional studies have also implicated intestinal $\gamma\delta$ IEL in the regulation of intestinal immunopathology during 2,4,6-trinitrobenzene sulfonic acid (TNBS)-induced colitis (Inagaki-Ohara et al., 2004), and during infection with *Nippostronglyus brasiliensis,* a gastrointestinal nematode parasite (Inagaki-Ohara et al., 2011). Thus, the signature $\gamma\delta$ IEL compartments of the skin and the gut are thought to be critical for effective regulation of barrier immune responses.

More recently, the LSSR in the skin was shown to be involved in the induction of antigen-specific atopy (Strid et al., 2011). DETC can be activated by acute up-regulation of NKG2D ligands (e.g. *Rae-1*) in neighbouring keratinocytes, which commonly occurs in response to mild cutaneous abrasion (Strid et al., 2011; 2008). When such mechanical perturbation was accompanied by exposure to ovalbumin, wild-type (WT) but not V$\gamma5^{-/-}$V$\delta1^{-/-}$ or NKG2D-deficient mice generated ova-specific immune responses, characterised by significant increases in serum ova-specific IgE (Strid et al., 2011). Altogether, these studies demonstrate that activation of LSSR can elicit highly pleiotropic downstream effects on adaptive immunity and that each of these are contingent on the presence of a signature $\gamma\delta$ IEL compartment.

1.2.3.3 Maintenance of barrier integrity

Signature $\gamma\delta$ IEL are increasingly becoming recognised for their role in the maintenance of effective barrier function. V$\gamma5^{+}$ DETC have been shown to display constitutive and stress-inducible up-regulation of IL-13 expression, which is thought to promote the transition of keratinocytes through the epidermis (Dalessandri et al., 2016). In their absence, the epidermis of TCR$\delta^{-/-}$ mice display a greater degree of trans-epidermal water loss and enhanced expression of *Rae-1*, indicative of steady-state barrier dysregulation (Dalessandri et al., 2016). Given that IL-13-

deficient mice also display increased sensitivity to chemically-induced cutaneous carcinogenesis, it is possible that its selective production by canonical DETC is required for their role in tumour immunosurveillance (Dalessandri et al., 2016; Girardi et al., 2001; Strid et al., 2008).

Following a full thickness punch biopsy of mouse skin, DETC are also thought to promote timely wound healing, possibly through their stress-inducible production of keratinocyte growth factor-1 and insulin-like growth factor 1 (Boismenu and Havran, 1994; Sharp et al., 2004). However, although TCR$\delta^{-/-}$ mice do display marked delay in re-epithelialization, these studies have not specifically identified canonical DETC-deficiency to be the cause (Havran and J. M. Jameson, 2010).

In the gut, it is possible that γδ IEL fulfil a similar role to DETC in the promotion of epithelial integrity. Indeed, TCR$\delta^{-/-}$ mice have been shown to display increased systemic translocation of *Salmonella typhimurium* ≤4 hours after oral inoculation (Edelblum et al., 2015; Hirano et al., 2013; Ismail et al., 2011). Further studies have also shown rescue of this phenotype by adoptively transferring V$\gamma7^{+}$ IEL into TCR$\delta^{-/-}$ mice, whereas non-signature V$\gamma7^{-}$ IEL were insufficient (Dalton et al., 2006; Walker et al., 2013). However, as intestinal γδ IEL do not constitutively express IL-13, their promotion of barrier integrity appears to be driven *via* alternative undefined mechanisms (Fahrer et al., 2001; Shires et al., 2001).

The various studies of mice with perturbed γδ IEL compartments have identified a multitude of potential contributions that these cells could make to host physiology. Furthermore, they have often been able to show, particularly in the skin, that such contributions are highly dependent on a single signature γδ T cell subset (e.g. V$\gamma5^{+}$V$\delta1^{+}$ DETC). How such monoclonal or oligoclonal T cell compartments are able to regulate such pleiotropic functions is not fully understood, nor is it well understood how signature γδ T cell compartments are selected for maintenance at a particular anatomical site.

1.3 The development and maintenance of IEL composition

1.3.1 Intestinal IEL composition

Intestinal IEL are found at a density of approximately 1 lymphocyte per 5-10 epithelial cells (Cheroutre et al., 2011). Given the extensive surface area of the small intestine, this may be one of the largest T cell compartments in the body. Unlike the epidermis where >90% of T cells express the canonical $V\gamma5^+V\delta1^+$ TCR, the small intestinal epithelium is jointly occupied by $\gamma\delta$ and $\alpha\beta$ IEL, in roughly equal proportion. Most $\gamma\delta$ IEL express CD8$\alpha\alpha$ homodimers and can be subdivided according to TCRVγ chain usage. The majority (~60%) of $\gamma\delta$ IEL express TCRVγ7, whereas the remainder express TCRVγ1 (~30%) or TCRVγ4 (~10%) (Cheroutre et al., 2011; Kawaguchi et al., 1993). By contrast, $V\gamma1^+$ and $V\gamma4^+$ T cells comprise ~70% of the systemic $\gamma\delta$ T cell compartment (Haas et al., 2012).

$\alpha\beta$ IEL include non-MHC restricted *innate-like* T cells that express the CD8$\alpha\alpha$ homodimer and MHC-restricted T cells that express CD8$\alpha\beta$ or CD4, although $CD4^+$ cells are usually a minor subset (Hayday et al., 2001). Collectively, $CD4^+$ and $CD8\alpha\beta^+$ IEL constitute an intestinal T_{RM} compartment that accumulates throughout life, following repeated exposure to foreign antigens (**Figure 1.2**) (Bandeira et al., 1990; Sheridan and Lefrançois, 2011; Sheridan et al., 2014). A small proportion of T_{RM} cells may also acquire co-expression of CD8$\alpha\alpha$ homodimers, which is thought to arise during strong TCR signalling in the presence of cytokines such as TGFβ and retinoic acid, both of which are present in the gut microenvironment (Y. Huang et al., 2011; Mucida et al., 2013; Reis et al., 2013). In summary, the small intestinal epithelium is predominantly occupied by $V\gamma7^+$, $TCR\beta^+CD8\alpha\alpha^+$ or $TCR\beta^+CD8\alpha\beta^+$ IEL, alongside smaller subsets of $\gamma\delta$ and $\alpha\beta$ T cells.

Intestinal IEL are not uniformly distributed as IEL density is greatest in the proximal small intestine and progressively decreases towards the caecum (H. Suzuki et al., 2000). Furthermore, while $\gamma\delta$ and $TCR\beta^+CD8\alpha\alpha^+$ IEL display their greatest abundance in the proximal small intestine, $TCR\beta^+CD4^+$ and $TCR\beta^+CD4^+CD8\alpha\alpha^+$ IEL are more abundant in the distal small intestine, which could suggest these cells perform site-specific functions (H. Suzuki et al., 2000). Unlike the small intestine,

colonic IEL are predominantly (>80%) αβ T cells (Kuo et al., 2001). In considering how signature γδ IEL subsets may develop and persist in a given anatomical site, it is necessary to briefly review γδ and αβ T cell and IEL development.

1.3.2 Thymic development of αβ and γδ T cells

T cell development conventionally occurs in the thymus where bone marrow-derived haematopoietic lymphoid progenitors differentiate into naïve or *innate-like* αβ or γδ T cells. It is generally accepted that a common thymic progenitor has the capacity to generate both αβ and γδ T cells, however this does not rule out the possibility that some subsets of T cells derive from distinct progenitor pools (Haks et al., 2005; Hayes et al., 2005; Kreslavsky et al., 2008; Ramond et al., 2013; Zarin et al., 2014). T cell progenitors infiltrate the thymus at the cortico-medullary junction as TCR^-, $CD4^-CD8^-$ double negative cells and their differentiation can be divided into 4 stages (DN1→DN4) according to their cell surface expression of CD25 and CD44 (**DN1**-$CD44^+CD25^-$ → **DN2**-$CD25^+CD44^+$ → **DN3**-$CD25^+CD44^{low}$ → **DN4**-$CD25^{lo}CD44^{lo}$) (Rothenberg et al., 2008). RAG-mediated rearrangement of the TCRβ, γ and δ gene loci begins at DN2 and is largely completed by DN3 (Ciofani and Zúñiga-Pflücker, 2010). Cells that productively rearrange a γδ TCR adopt a DN γδ T cell fate, whereas cells that fail to do so can assemble a pre-TCR, composed of TCRβ and pre-TCRα. The pre-TCR delivers weak ligand-independent signals and drives DN thymcoytes to adopt a $CD4^+CD8^+$ double positive (DP) αβ T cell fate (Dudley et al., 1995; Prinz et al., 2006).

1.3.2.1 Conventional αβ T cell selection

Several experimental systems have demonstrated that TCR signalling is a key regulator of T cell lineage commitment. While strong signals delivered through a γδ TCR drive thymocytes to a DN γδ T cell fate, weak ligand-independent signals delivered through a pre-TCR drive thymocytes to a DP αβ T cell fate (Haks et al., 2005; Hayes et al., 2005; Kreslavsky et al., 2008; Zarin et al., 2014). DP thymocytes rearrange the TCRα gene locus in order to assemble mature TCRαβ heterodimers that serve as substrates for MHC-mediated positive and negative selection (**Figure 1.5**) (Germain, 2002). During selection, highly self-reactive cells

experience strong TCR signalling and die by apoptosis, whereas non self-reactive cells die by neglect. Positively selected cells are weakly self-reactive, experience intermediate levels of TCR signalling and adopt a $CD4^+$ or $CD8^+$ single positive (SP) αβ T cell fate in accordance with their restriction to MHC class II or class I, respectively.

1.3.2.2 Developmental pre-programming of γδ T cells

The role of negative selection during γδ T cell development is poorly defined (Hayday, 2009; Vantourout and Hayday, 2013). However, several subsets of *innate*-like γδ T cell progenitors are understood to require agonist selection downstream of strong TCR signals, driven by their engagement of largely undefined TCR ligands (Jensen et al., 2008; Muñoz-Ruiz et al., 2016; Turchinovich and Hayday, 2011; Wencker et al., 2013). Agonist selection describes the selection of γδ and αβ thymocytes that developmentally engage agonist TCR ligands, experience a strong TCR signal but are not negatively selected (**Figure 1.5**) (Baldwin et al., 2004; Hogquist and S. C. Jameson, 2014). Many agonist-selected γδ T cells (e.g. DETC and $Vγ6^+$ IEL) are thought to derive exclusively from foetal thymic progenitors and are developmentally pre-programmed with pre-defined effector functions (e.g. IFNγ *versus* IL-17 production) and tissue-homing capabilities (**Figure 1.5**) (Ribot et al., 2009; Turchinovich and Hayday, 2011).

Developmental pre-programming is mediated *via* TCR signalling, in conjunction with co-stimulation *via* a range of germ-line encoded receptors (Ribeiro et al., 2015). This pathway is best described for IFNγ-producing γδ T cells, which critically depend on TCR stimulation; *trans*-conditioning from DP thymocytes; and co-stimulation through CD27 and lymphotoxin (LT) receptor, both of which are members of the tumour necrosis factor (TNF) receptor superfamily (**Figure 1.5**) (Muñoz-Ruiz et al., 2016; Pennington et al., 2003; Ribot et al., 2009; Silva-Santos et al., 2005; Turchinovich and Hayday, 2011).

Because of developmental pre-programming, IFNγ-producing γδ T cells and thymocytes can be distinguished from IL-17-producing γδ T cells and thymocytes by their constitutive cell surface expression of CD27 and by their distinct gene expression signature. This gene expression signature includes regulators of G

protein signalling, *Rgs1* and *2*; *Tbx21*; the inducible cAMP early repressor of transcription (ICER); and various transcription factors from the nerve growth factor-induced B family (e.g. *Nr4a1*) (Malhotra et al., 2013; Narayan et al., 2012; Pennington et al., 2003; Ribot et al., 2009; Silva-Santos et al., 2005). This gene expression signature is also shared with intestinal TCR$\alpha\beta$CD8$\alpha\alpha^+$ and $\gamma\delta$ IEL, which also express CD27 and produce IFNγ upon stimulation (Malinarich et al., 2010; Montufar-Solis et al., 2007; Pennington et al., 2003). By contrast, these genes are not highly expressed by intestinal TCRβCD8$\alpha\beta^+$ T_{RM} IEL, which do produce IFNγ but develop *via* conventional MHC-mediated selection and antigen-dependent peripheral activation (**Figure 1.2**) (Masopust et al., 2006; Pennington et al., 2003; Schenkel and Masopust, 2014; Yamagata et al., 2004). Given their similar gene expression signatures, it is possible that signature intestinal $\gamma\delta$ IEL, TCRβ^+CD8$\alpha\alpha^+$ IEL and *innate*-like CD27$^+$ $\gamma\delta$ T cells receive similar signals (e.g. agonist selection) during their development.

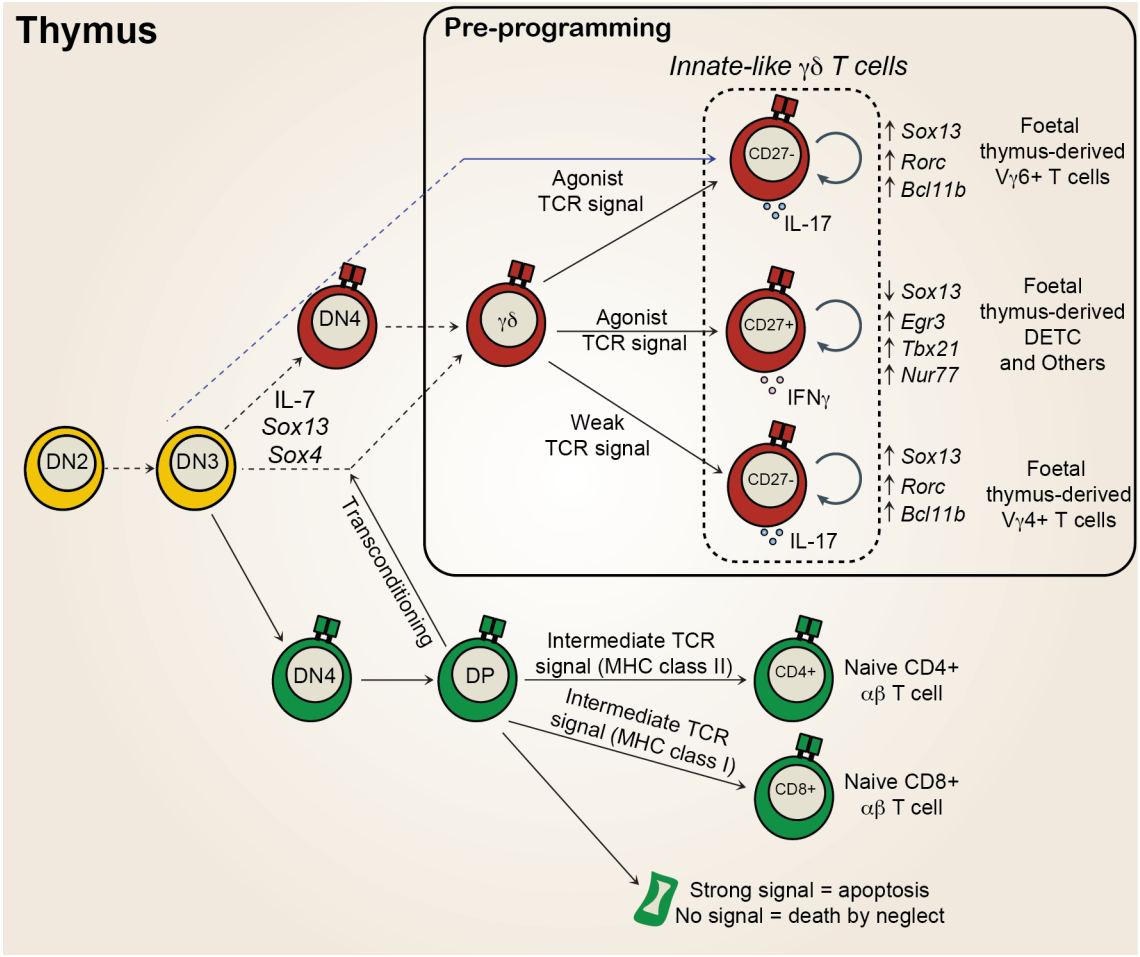

Figure 1.5 Model for thymic development of γδ/αβ T cells

αβ T cell selection - Cells that fail to productively rearrange TCRγ/δ gene loci can assemble the αβ TCR and undergo MHC-mediated positive and negative selection. Due to selection, it is estimated that <5% of the αβTCRs generated through Rag-mediated rearrangement in the thymus are represented in the periphery (Goldrath and Bevan, 1999).

γδ T cell differentiation - Some γδ T cells, including IL-17 producing subsets (γδ17) and DETC, exclusively derive from foetal thymic progenitors (Haas et al., 2012; Ramond et al., 2013). However, other subsets, such as *innate*-like CD27$^+$ IFNγ-producing cells may also derive from adult bone marrow (Muñoz-Ruiz et al., 2016). Rearrangement of TCRγ/δ gene loci depends on IL-7 cytokine, which regulates chromatin accessibility at this site (Schlissel et al., 2000; Ye et al., 2001). The transcription factors Sox4 and Sox13 are known to promote γδ T cell differentiation (Melichar et al., 2007).

γδ T cell pre-programming - Signalling through the TCR, CD27 and the LT receptor (LTRβ) are each required for the developmental pre-programming of most IFNγ-producing γδ T cells (γδIFNγ). Their thymocyte precursors interact with thymic medullary epithelial cells, which express CD70 (the TNF ligand for CD27) (Tesselaar et al., 2003); and DP thymocytes, which produce LT and mediate additional *trans*-conditioning (Silva-Santos et al., 2005). While CD27$^+$ γδIFNγ cells down-regulate *Sox13* and *Sox4* and up-regulate genes such as *Tbx21* and *Egr3*,

CD27$^-$ γδ17 cells maintain *Sox13 and Sox4* expression and up-regulate *Rorc*. The curved arrows highlight the fact that many such γδ T cell subsets exclusively derive from the foetal thymus and are peripherally maintained.

γδ T cell agonist selection - It was originally postulated that TCR agonist ligand engagement drives γδ thymocytes towards an CD27$^+$ γδIFNγ cell fate, whereas weaker ligand-independent signalling drives cells towards a 'default' CD27$^-$ γδ17 cell fate (Jensen et al., 2008). While the requirement for strong TCR signalling in γδIFNγ cells has been substantiated in various studies (Muñoz-Ruiz et al., 2016; Turchinovich and Pennington, 2011; Wencker et al., 2013), recent reports have identified additional complexity in the developmental requirements for γδ17 cells (Muñoz-Ruiz et al., 2016; Wencker et al., 2013). In particular, these studies demonstrated that: a) all γδ17 cells depend on developmental TCR-associated signalling; and b) Vγ6$^+$ (but not Vγ4$^+$) CD27$^-$ γδ17 cells require high levels of cell surface γδ TCR expression to develop, suggesting they may require strong agonist-mediated selection. Given these developments, further studies are now required to identify the contribution of TCR ligands (*versus* ligand-independent signalling) to the development of these discreet populations of γδ17 cells (Turchinovich and Pennington, 2011).

An alternative pathway for γδ17 cells - It was recently shown that γδ17 cells can be derived from DN2 but not DN3 or DN4 foetal thymocytes *in vitro* (Shibata et al., 2014). These data suggest that foetal-derived γδ17 cells could bi-pass the DN3 and DN4 stages of thymocyte development *in vivo*. In order to account for this possibility, a blue dashed arrow is included in the above model. Figure adapted from: (Vantourout and Hayday, 2013).

1.3.3 Thymic agonist selection of intestinal *innate*-like αβ IEL

T cells expressing the CD8αα homodimer are rare in the circulation but are abundant in the small intestinal epithelium. Their TCR repertoire is both oligoclonal and site-specific as it does not overlap with that of lymph node αβ T cells or with TCRβ$^+$CD8αβ$^+$ cells in the small intestinal epithelium or lamina propria (Arstila et al., 2000; Cheroutre et al., 2011; Mayans et al., 2014; McDonald et al., 2014; Regnault et al., 2016; Rocha et al., 1991). While TCRβ$^+$CD8αα$^+$ IEL are not restricted to classical MHC class I/II or CD1, they do depend on developmental interactions with non-classical MHC class Ib molecules. As such, β2m$^{-/-}$ but not CD1- or classical MHC class I/II-deficient mice are depleted for most TCRβ$^+$CD8αα$^+$ IEL (Capone et al., 2003; G. Das et al., 2000; Fujiura et al., 1996; Park et al., 1999).

Because TCRβ$^+$CD8αα$^+$ IEL display such a restricted, site-specific TCR repertoire, they are thought to comprise self-reactive αβ T cells. Consistent with this, they develop independently of the microbiome and of diet-derived protein antigens, and in DBA/2 (M1s^a IE$^+$) mice, express TCRVβ (Vβ6, Vβ8.1 and Vβ11$^+$) chains that are normally negatively selected by thymic super-antigens (Bandeira et al., 1990; Hayday et al., 2001; Rocha et al., 1991). Furthermore, mice transgenic for TCRs that display high but not low affinity for thymic ligands preferentially generate TCRβ$^+$CD8αα$^+$ cells *in vivo* (Leishman et al., 2002; Yamagata et al., 2004). Thus, it is generally considered that TCRβ$^+$CD8αα$^+$ IEL are generated from self-reactive thymocytes that are positively selected by strong, agonist-mediated TCR signalling (Baldwin et al., 2004).

Consistent with this notion, co-stimulation-deficient CD28$^{-/-}$ or B7$^{-/-}$ mice display marked defects in the negative selection of super-antigen-reactive thymocytes, which instead develop into TCRβ$^+$CD8αα$^+$ IEL (Pobezinsky et al., 2012). Using this system, it was shown that the development of these thymocytes was characterized by their up-regulation of CD122, CD5, CD69 and PD-1, all of which are markers associated with agonist selection (Azzam et al., 2001; Hanke et al., 1994; Ishida et al., 1992; McDonald et al., 2014). Furthermore, their development was also characterized by their transition from the DP compartment, back into the DN

compartment, revealing a major divergence in the developmental pathways of conventional MHC-restricted αβ T cells *versus* agonist-selected TCRβ$^+$CD8αα$^+$ IEL (**Figure 1.6**).

Because agonist ligands for TCRβ$^+$CD8αα$^+$ IEL are mostly unidentified, studies have sought to characterise the importance of αβ TCR specificity in their agonist selection and lineage commitment. By analysing the development of thymocytes bearing transgenic TCRs cloned from TCRβ$^+$CD8αα$^+$ (*unconventional*) and TCRβ$^+$CD8αβ$^+$ (*conventional*) IEL, it was shown that *unconventional* TCRs exclusively drove the development of *innate-like* CD8αα$^+$TCRαβ$^+$ or CD4$^-$CD8$^-$ TCRαβ$^+$ IEL. By contrast, thymocytes expressing *conventional* TCRs gave rise to intestinal TCRαβ$^+$CD8αβ T_{RM} cells (Mayans et al., 2014; McDonald et al., 2014). Taken together, these data strongly attest to the importance of TCR specificity in determining the lineage determination of αβ thymocytes. The implication is that only thymocytes bearing agonist ligand-reactive TCRs develop into TCRβ$^+$CD8αα$^+$ IEL.

The mechanism by which strong TCR signalling drives agonist selection of some αβ T cells and clonal deletion of others is poorly understood. Some studies have suggested that agonist-selection may take place within a tight perinatal window, prior to the establishment of efficient clonal deletion (Hayday et al., 2001; Lin et al., 1999). However, this model would not accommodate the fact that TCRβ$^+$CD8αα$^+$ IEL can be reconstituted from adult bone marrow chimeras (Schluns et al., 2004). Other studies have proposed that TCRβ$^+$CD8αα$^+$ cells develop extrathymically, or avoid negative selection by exiting the thymus at the DN stage (Guy-Grand et al., 1991; Lambolez et al., 2005; 2002; Naito et al., 2008). However, lineage tracing studies have shown that these cells uniformly transition through a DP status at some point of their development (G. Eberl and Littman, 2004). An alternative possibility is that TCRβ$^+$CD8αα$^+$ IEL derive from distinct haematopoietic progenitors that are intrinsically pre-programmed to survive agonist selection. Some evidence for this was provided by a study that showed TCRβ$^+$CD8αα$^+$ IEL to derive from a rare population of CD8αα-expressing DP thymocytes (so called triple positive; TP cells) (Gangadharan et al., 2006). As the CD8αα homodimer is thought to repress TCR signalling and promote T cell survival (Cheroutre and

Lambolez, 2008; Y. Huang et al., 2011; Leishman et al., 2001; Madakamutil et al., 2004; Olivares-Villagómez et al., 2008), it was suggested that up-regulation of CD8αα in a subset of (possibly pre-committed) DP thymocytes serves to rescue them from clonal deletion during strong TCR signalling (Gangadharan et al., 2006). Although precise details regarding the development of TCRβ$^+$CD8αα$^+$ IEL remain under investigation, these various studies have outlined a prototypic pathway for the agonist selection of self-reactive IEL. This pathway differs from conventional MHC-mediated selection because it may require up-regulation of CD8αα at the DP stage (i.e. a TP stage) (Gangadharan et al., 2006); because it involves strong TCR signalling (Mayans et al., 2014; McDonald et al., 2014; Rocha et al., 1991; Yamagata et al., 2004); and because it may involve down-regulation of CD4 and CD8 prior to thymic export (Lambolez et al., 2005; McDonald et al., 2014) (**Figure 1.6**).

1.3.4 The extrathymic development of intestinal γδ IEL

Athymic NU/NU mice harbour no uterine or epidermal IEL and likewise have very few αβ T cells but their intestinal epithelium contains substantial numbers of γδ IEL (20-30% of that in euthymic mice) (Guy-Grand et al., 1991; Nonaka et al., 2005). The intestinal mucosa is thought to support extrathymic γδ T cell development in specialised lymphoid organs called cryptopatches that are found in the crypt lamina propria (Kanamori et al., 1996; Naito et al., 2008; Saito et al., 1998). These small lymphoid compartments are enriched in immature haematopoietic lin$^-$ cells expressing receptors for stem cell factor and IL-7 (c-kit$^+$IL7R$^+$), which reconstitute mature γδ IEL when adoptively transferred to thymectomized immunodeficient recipients (Lambolez et al., 2002; Saito et al., 1998). γδ IEL can also be reconstituted by transplantation of donor bone marrow into thymectomized lympho-depleted recipients, and is associated with the sequential appearance of cryptopatch structures, CD3$^-$ and then CD3$^+$ IEL (K. Suzuki et al., 2000). Consistent with the capacity of the intestinal mucosa to support γδ T cell development, enterocyte-specific expression of an IL-7 transgene alone can rescue γδ IEL development in IL-7$^{-/-}$ mice (Laky et al., 2000). Thus, there is a significant body evidence to suggest the small intestinal mucosa can support the extrathymic lymphopoiesis of γδ IEL (**Figure 1.6**). An extrathymic pathway of development

would represent a significant difference between γδ IEL and thymic agonist-selected TCRβ$^+$CD8αα$^+$ IEL.

Although extrathymic γδ T cell development clearly takes place in NU/NU mice, a number of studies have questioned this pathway and the extent to which it contributes to γδ IEL development in euthymic mice (**Figure 1.6**). For example, neonatal thymectomy is associated with a substantial depletion of both intestinal γδ and αβ IEL, suggesting that thymic transit may be a key component intestinal IEL development (Lefrançois and Olson, 1994). In support of this, sub-cutaneous re-engraftment of thymic lobes into thyemectomized adults can rescue the intestinal IEL compartment (Lefrançois and Olson, 1994). Furthermore, as γδ IEL still develop in Rorγt-deficient mice that are significantly depleted of cryptopatches, the relevance of these lymphoid aggregates to IEL development has been questioned (G. Eberl, 2005; G. Eberl and Littman, 2004; Naito et al., 2008). Other studies have used transgenic mice expressing green fluorescent protein (GFP) downstream of the *Rag2* promoter, to test whether TCR rearrangement is detectable amongst cryptopatch cells or IEL. Whilst GFP^{HI} cells, indicative of recent or active *Rag* expression, were abundant in Peyer's patches and mesenteric lymph nodes (MLN) of athymic mice, they were undetectable amongst IEL or cryptopatch cells of euthymic or athymic animals, which directly challenges the proposed pathway for extrathymic T cell development (Guy-Grand et al., 2003), although this too has been contested (Ishikawa et al., 2007).

Most recently, it has been proposed that low frequencies of Vγ7$^+$ intestinal IEL progenitors continuously emerge from the thymus and require prior activation in Peyer's patches before infiltrating the gut epithelium (Guy-Grand et al., 2013). However, this model is difficult to reconcile with the virtually unimpaired development of Vγ7$^+$ IEL in NU/NU alymphoplasia (aly/aly) mice that are athymic and lack all lymph nodes, Peyer's patches and isolated lymphoid follicles (Nonaka et al., 2005). Hence, the developmental pathway and selection of signature γδ IEL remains largely unresolved (Hayday and Gibbons, 2008).

The potential of the intestinal mucosa to support γδ T cell development has not been the focus of most recent studies, despite its potential relevance to the lifelong maintenance of γδ IEL. Indeed, extrathymic development may represent a critical

pathway by which signature tissue-resident immune compartments are replenished beyond thymic evolution. Hence these pathways could have profound implications for immunological senescence in the LSSR and merit further study.

1.3.4.1 Agonist selection of intestinal γδ IEL

Although the developmental pathway of signature γδ IEL remains unresolved, it is generally thought that these cells are also developmentally agonist-selected. In order to study the importance of γδ TCR specificity and test the contribution of agonist ligand engagement to the development of intestinal γδ IEL, various groups have analysed γδ TCR-transgenic (Tg) mouse models. The G8 γδ TCR is known to engage the non-polymorphic MHC class Ib molecule TL^b (T22), which is normally expressed on thymic medullary and small intestinal epithelial cells of C57Bl/6 mice (Adams et al., 2005; 2008; Crowley et al., 2000; Shin et al., 2005). By comparing γδ IEL development in $T22^{+ve}$ *versus* $T22^{-ve}$ G8-TCR-Tg mice, it was shown that although intestinal γδ IEL can develop independently of T22, they require its expression to adopt the signature $Thy1^-CD8\alpha\alpha^+$ cell surface phenotype of most γδ IEL (Hayday et al., 2001; Lin et al., 1999). Furthermore, while G8-TCR-Tg thymocytes were abundant in the thymus of $T22^{+ve}$ neonates, they were largely undetectable in that of adults, suggesting that they had been negatively selected. Hence, G8-TCR-Tg IEL in $T22^{+ve}$ mice developed exclusively from neonatal progenitors and required TCR agonist ligand engagement in the thymus and/or gut in order to attain phenotypic maturity (Lin et al., 1999).

Further substantiating these observations, the intestinal γδ IEL of mice rendered transgenic for the expression of non-gut IEL associated γδTCRs (e.g. the DETC $V\gamma5^+V\delta1^+$ TCR) are also reported to display an unconventional $Thy1^+CD8\alpha\alpha^-$ cell surface phenotype (Bonneville et al., 1990). Thus, studies of γδ IEL development in γδ TCR-Tg mice support the notion that signature intestinal γδ IEL require agonist selection to attain phenotypic maturity.

To further test this model outside of a TCR-Tg system, Jensen et al., (2009) analysed the cell surface phenotype of T10/T22-reactive intestinal γδ IEL in C57Bl/6 ($T10/T22^+$) *versus* $\beta2m^{-/-}$ (T10/T22-deficient) mice. ~1% of all mouse γδ T cells have been shown to engage T10/T22 *via* their TCRδ chain. These T cells are

readily identified using fluorescently-conjugated T22 tetramers and have been shown to emerge from the thymus irrespective of whether or not their TCR ligands (T10/T22) are expressed (Jensen et al., 2008). Staining of intestinal γδ IEL with T22 tetramers showed that T22-reactive cells displayed a $CD122^{HI}$ phenotype in C57Bl/6 mice and a $CD122^{LO}$ phenotype in $\beta2m^{-/-}$ mice (Jensen et al., 2009). As up-regulation of CD122 is a hallmark of agonist selection (Jensen et al., 2008; Lewis et al., 2006; Turchinovich and Hayday, 2011), this study attested to the importance of developmental agonist ligand-engagement in the phenotypic maturation of small intestinal γδ IEL. However, as these conclusions are based on data acquired in a very small subset (~1%) of γδ IEL, the extent to which it applies to the full γδ IEL compartment is unclear.

1.3.5 Intestinal factors regulating γδ IEL composition

Following their putative agonist selection and migration to the gut epithelium, there are several factors that peripherally determine the mature composition of γδ IEL. These factors include self-expressed cytokines but also include exogenous diet-derived components. Interestingly, each of these factors are equally critical for the peripheral maintenance of signature DETC (De Creus et al., 2002; Kadow et al., 2011; Kawai et al., 1998).

1.3.5.1 IL-15 signalling

Several cytokines, including IL-2, IL-4, IL-7, IL-9, IL-15 and IL-21 engage distinct multimeric cytokine receptor complexes that each make use of the common γ chain receptor subunit (CD132). CD132 is constitutively expressed on most lymphocytes and has been implicated in several immune processes, including T cell development, maintenance, activation and memory generation (Schluns and Lefrançois, 2003; Waickman et al., 2015). Its critical role in immune function is illustrated by the syndrome of severe combined immunodeficiency (SCID) seen in individuals that carry a loss of function mutation in the γ_C gene (Noguchi et al., 1993).

IL-15 primarily exists in complex with IL15Rα and is *trans*-presented from intestinal enterocytes to IEL expressing CD132 and IL-2Rβ (CD122) (Stonier and Schluns,

2010). This *trans*-cellular interaction is critical for the peripheral expansion and maintenance of signature $V\gamma7^+$ IEL and $TCR\beta^+CD8\alpha\alpha^+$ IEL (Lai et al., 2008). Consistent with this, IL-$15R\alpha^{-/-}$ and IL-$15^{-/-}$ mice are markedly depleted in $TCR\beta^+CD8\alpha\alpha^+$ IEL and $\gamma\delta$ IEL, the development of which can be rescued in IL-$15R\alpha^{-/-}$ mice by enterocyte-specific expression of an IL15Rα transgene (Ma et al., 2009; H. Suzuki et al., 1997). It has also been shown that haematopoietic expression of CD122 and stromal expression of IL-15 and IL-15Rα are critical for the reconstitution of $V\gamma7^+$ and $TCR\beta^+CD8\alpha\alpha^+$ IEL from adult donor bone marrow (Schluns et al., 2004). Given that thymic lobes from IL-$15R\alpha^{-/-}$ mice can still give rise to $\gamma\delta$ and $TCR\beta^+CD8\alpha\alpha^+$ IEL when engrafted into WT hosts (Lai et al., 2008), it is the intestinal IL-15 that is critical for the establishment and long-term maintenance of signature IEL subsets. The impact of IL-15 signalling on intestinal IEL may be mediated by driving their proliferation (Lodolce et al., 1998) and/or by promoting their long-term survival *via* up-regulation of anti-apoptotic molecules such as Bcl-2 (Ma et al., 2009).

As the up-regulation of CD122 is one hallmark of agonist selection, one could expect agonist-selected $TCR\beta^+CD8\alpha\alpha^+$ or $\gamma\delta$ IEL to have a selective survival advantage in the small intestinal epithelium (Hanke et al., 1994; Jensen et al., 2008; Turchinovich and Hayday, 2011). In this regard, it is conspicuous that $V\gamma1^+$ IEL are not dependent on IL-15 signalling for their reconstitution in adult bone marrow chimeras (Schluns et al., 2004). Perhaps this suggests that $V\gamma7^+$ but not $V\gamma1^+$ cells are agonist-selected to up-regulate CD122 and henceforth preferentially survive in their shared small intestinal niche. Such a model could explain why $V\gamma7^+$ cells are the predominating $\gamma\delta$ IEL subset in this location (Kawaguchi et al., 1993).

1.3.5.2 Aryl hydrocarbon receptor

The aryl hydrocarbon receptor (AhR) is a ligand-activated transcription factor that is probably best known for its role in mediating the toxic effects of dioxins, which include hazardous bi-products of industrial processes (Connor and Aylward, 2007). This receptor is expressed by various subsets of immune cells, including $\gamma\delta$ IEL, but is also expressed by several non-lymphoid tissues (e.g. epithelia). AhR-deficiency is associated with several phenotypes, including a reduction in splenic and lymph

node lymphocytes, chronic liver fibrosis and a marked depletion in small intestinal γδ and TCRβ^{+}CD8αα^{+} IEL (Fernandez-Salguero et al., 1995; Y. Li et al., 2011). The impact of AhR on intestinal IEL is independent of the epithelium as its expression was shown to be specifically required in RAG-dependent lymphoid cells for IEL development (Y. Li et al., 2011).

Intestinal ligands for the AhR are thought to include tryptophan derivatives that are specific to plants (e.g. indole-3-carbinol). Such ligands are particularly enriched for in cruciferous vegetables such as cabbage and are found in the normal mouse diet. Synthetic diets deficient in such ligands were found to deplete intestinal γδ IEL, whereas diets containing these ligands were found to maintain them (Y. Li et al., 2011). Thus, whilst the development of signature γδ IEL occurs independently of the microbiome (Bandeira et al., 1990; Kawaguchi et al., 1993), their maintenance in the small intestinal epithelium is contingent on their continued exposure to exogenous ligands for the AhR (**Figure 1.6**).

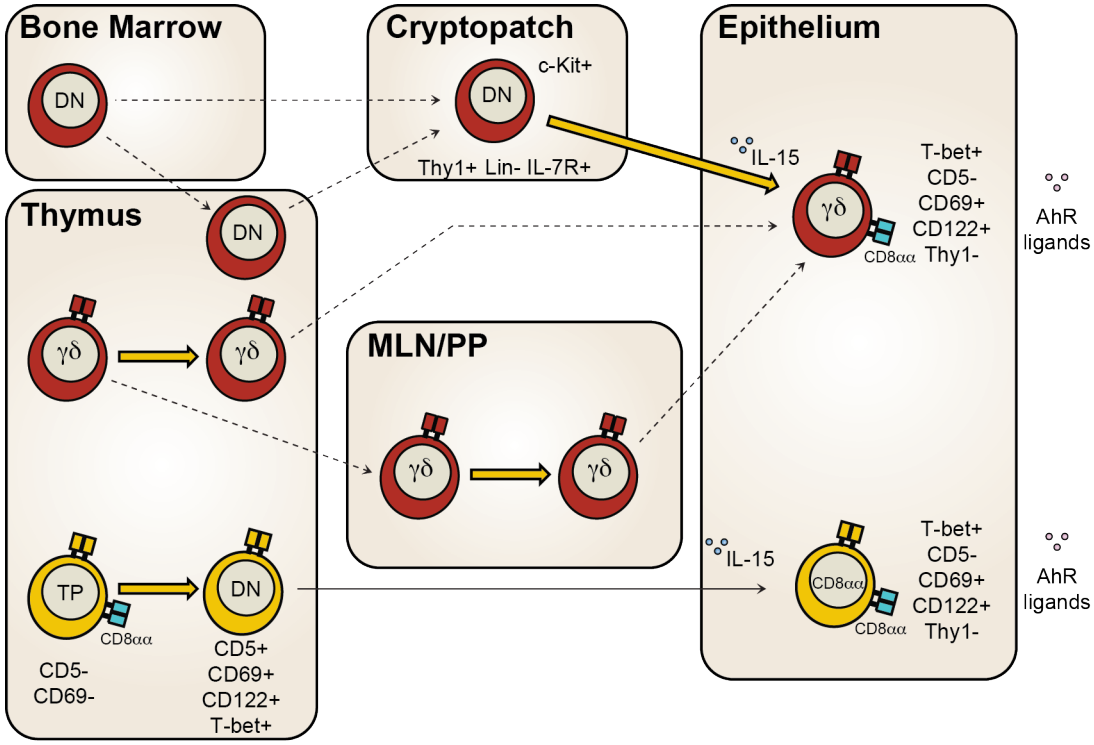

Figure 1.6 Model for the development of γδ and TCRβ$^+$CD8αα$^+$ IEL

γδ IEL development - Strong TCR signals downstream of agonist selection (yellow arrow) are thought to drive acquisition of a mature cell surface phenotype in γδ IEL precursors. Agonist selection may take place in the neonatal thymus (Lin et al., 1999); mesenteric lymph node (MLN) or Peyer's patch (PP) (Guy-Grand et al., 2013); or during infiltration into the small intestinal epithelium (Lambolez et al., 2002). γδ IEL may develop *via* a thymic (G. Eberl and Littman, 2004) or extrathymic (Guy-Grand et al., 1991; Lambolez et al., 2002; Naito et al., 2008) pathway.
TCRβ$^+$CD8αα IEL development - A small subset of DP thymocytes express the CD8αα homodimer, which is thought to promote their survival during agonist ligand engagement (Gangadharan et al., 2006). Agonist selection is associated with acquisition of a CD122$^+$CD5$^+$CD69$^+$ DN cell surface phenotype. These cells migrate to the small intestinal epithelium and adopt a CD8αα$^+$CD5$^-$CD69$^+$ cell surface phenotype (Mayans et al., 2014; McDonald et al., 2014).
IEL maintenance - Signalling through the IL-15 receptor expressed by agonist-selected IEL and aryl hydrocarbon receptor (AhR) is critical for the peripheral maintenance of γδ and TCRβ$^+$CD8αα$^+$ IEL (Y. Li et al., 2011; Ma et al., 2009; Schluns et al., 2004).

1.3.6 *Skint1:* a tissue-restricted selecting element

Studies of small intestinal IEL development have outlined a prototypic pathway through which signature intestinal γδ and αβ IEL compartments develop (**Figure 1.6**). This pathway involves agonist selection, which drives up-regulation of CD122, and peripheral maintenance, which is at least partly mediated by signals received through CD122 and the AhR. Within this model, agonist-selection may serve to endow signature IEL subsets with the responsiveness to IL-15 (*via* up-regulation of CD122) that is required for their selective maintenance in a given epithelia. This could explain why $V\gamma7^+$ IEL predominate over $V\gamma1^+$ and $V\gamma4^+$ IEL in the small intestinal epithelium and could also explain why $V\gamma5^+$ IEL comprise >90% of epidermal T cells. However, it fails to explain how discreet compartments of γδ IEL establish and maintain their signature associations with specific epithelial tissues (i.e. $V\gamma7^+$ and $TCR\beta^+CD8\alpha\alpha^+$ with gut; $V\gamma5^+$ with skin). While research has been successful in identifying a multitude of functional and phenotypic hallmarks of tissue-resident T cells, very little is actually known about the factors that constitutively regulate tissue-resident T cell composition (Fan and Rudensky, 2016). In this regard, a singular insight has been provided by the discovery of *Skint1*.

Skint1 is the founding member of a novel immunoglobulin superfamily of trans-membrane proteins related to B7 and is exclusively expressed in thymic medullary epithelial cells and suprabasal keratinocytes (Boyden et al., 2008). Mice that carry a loss-of-function mutation in *Skint1* lack canonical DETC and consequently display spontaneous and augmented cutaneous hypersensitivity responses (Lewis et al., 2006). The ablation of canonical DETC in *Skint1* mutant mice is primarily a developmental defect as DETC progenitors fail to acquire functional and phenotypic maturity in the thymus and fail to home to the skin (Barbee et al., 2011; Lewis et al., 2006; Turchinovich and Hayday, 2011). Consequently, DETC progenitors in *Skint1* mutant mice carry a pre-agonist-selected $CD27^{LO}CD122^{LO}TCR^{LO}$ cell surface phenotype and produce IL-17 rather than IFNγ upon stimulation *ex vivo* (**Figure 1.5**) (Barbee et al., 2011; Lewis et al., 2006; Turchinovich and Hayday, 2011). Developmental interactions with *Skint1*-

expressing thymic medullary epithelial cells are therefore critical for normal DETC development.

While the receptor for *Skint1* on DETC has not been identified, there is evidence to suggest that its impact is mediated *via* a TCR-associated pathway. Consistent with this, the phenotypic maturation of DETC in *Skint1* mutant thymic lobes can be rescued in foetal thymic organ culture (FTOC) by providing soluble TCRVγ5-specific agonist antibody. Furthermore, cell surface expression of *Skint1* is necessary for this pathway as it can be inhibited in WT FTOC by providing Skint1-IgV-specific blocking antibodies (Lewis et al., 2006; Salim et al., 2016). Thus, the data are consistent with *Skint1* engaging a receptor on DETC progenitors, to drive a molecular pathway that can be phenocopied using TCR agonist antibodies.

Further substantiating the notion of TCR involvement in DETC development, a gene expression analysis of Vγ5$^+$ thymocytes in WT *versus Skint1* mutant mice identified a *Skint1*-dependent gene expression signature that was indicative of strong TCR signalling. This gene expression signature could be also elicited in adult $\gamma\delta$ thymocytes by TCR agonist antibody stimulation (Turchinovich and Hayday, 2011). While these data would be consistent with *Skint1* engaging the canonical DETC TCR, direct evidence for this has not been shown and it does not preclude it acting as a co-stimulator. In either case, the impact of *Skint1* provides a clear example of how a thymus- and skin-restricted epithelial element can selectively elicit TCR-associated pathways to drive the development of a signature IEL compartment.

1.3.7 Canonical DETC have a selective survival advantage in the skin

Although *Skint1* is also expressed by epidermal keratinocytes, it remains to be established whether peripheral *Skint1* expression is necessary to retain canonical DETC *in situ*. That notwithstanding, there is some evidence to suggest that DETC expressing canonical TCRs experience a selective survival advantage *in situ*. This was elegantly demonstrated in a study where TdT expression was forcibly induced in neonatal DETC progenitors by replacing its promoter with that for Lck (Aono et al., 2000). The approach was successful as both the foetal thymus and newborn skin of these mutant mice was enriched for DETC expressing non-canonical TCRs with non-germline encoded junctional sequences. However, such cells failed to

persist and were largely replaced by canonical DETC by 10 weeks of age. Thus, DETC expressing canonical TCRs display a selective survival and/or proliferation advantage *in situ* in neonatal skin.

In support of this, the epidermis of mice that carry a genetic disruption in the TCRVδ1 gene segment (Vδ1$^{-/-}$ mice) remains enriched for Vγ5^{+} T cells that selectively increase in density from post-natal week 1 to week 16. By contrast, no such enrichment in Vγ5^{+} cells is seen in *Skint1* mutant mice (Lewis et al., 2006). Moreover, Vγ5$^{-/-}$ mice, which also lack canonical DETC, are enriched for cells expressing TCRs that are reactive to the 17D1 antibody (Mallick-Wood et al., 1998). 17D1 binds a conformational epitope present on canonical Vγ5^{+}Vδ1^{+} TCRs and accordingly, does not bind to any T cells in the replacement polyclonal γδ epidermal T cell compartment of *Skint1* mutant mice. Thus, in the presence of functional *Skint1*, Vγ5$^{-/-}$ and Vδ1$^{-/-}$ mice are each able to generate replacement DETC expressing γδ TCRs with features conserved from that of the canonical DETC TCR. If *Skint1* really is driving the selective peripheral expansion of DETCs bearing specific TCRs, one would expect the enrichment in Vγ5^{+} and 17D1-reactive epidermal T cells (in Vδ1$^{-/-}$ and Vγ5$^{-/-}$ mice) to be ablated when these strains are crossed with *Skint1*-mutant mice.

1.3.8 DETC constitutively engage keratinocytes

To test whether any TCR signalling occurs at the steady state and during challenge in canonical DETC, a recent study has employed *intravital* imaging and confocal microscopy to visualise DETC activation *in situ* (Chodaczek et al., 2012). During the steady state, DETC extend several apically orientated dendrites that are anchored to suprabasal keratinocyte tight junctions, forming contacts enriched for TCR and phosphorylated intracellular signalling components (e.g. phospho-CD3ζ). Consistent with TCR specificity being important in the formation of these contacts, such phosphotyrosine-rich aggregates located on projections (PALPs) are not observed in rare populations of Vγ5^{-} DETC, or in replacement DETC in TCRδ$^{-/-}$ mice (Chodaczek et al., 2012). These data would be consistent with DETC TCR constitutively signalling at the steady state in cells specifically expressing the canonical DETC TCR. Such signals could promote the selective expansion and/or

maintenance of canonical DETC *in situ*. Furthermore, they may also drive the constitutive transcription of IL-13 that has been reported in these cells (Dalessandri et al., 2016). In support of this model, conditional deletion of the linker for activated T cells (LAT) in TCRδ^+ cells specifically reduces the proliferative capacity of DETC in neonatal skin and in adult skin following full thickness punch biopsies (B. Zhang et al., 2015).

In addition to promoting their maintenance, constitutive TCR signalling may serve to keep DETC in a functionally pre-primed state that enables them to rapidly respond to the stress-inducible engagement of NKG2D (Strid et al., 2011; 2008), junctional adhesion molecule-like protein (JAML) (Witherden et al., 2010) or CD100 at their cell surface (Witherden et al., 2012). In the context of constitutive TCR signalling, the overt and possibly deleterious activation of DETC in the absence of stress may be prevented by their developmental attenuation of TCR responsiveness, which has been shown to occur during *Skint1*-mediated selection in the thymus (Wencker et al., 2013). Indeed, altered responsiveness to TCR stimulation has also been reported for $\gamma\delta$17 cells, in addition to putative 'agonist-selected' intestinal $\gamma\delta$ and TCRβ^+CD8$\alpha\alpha^+$ IEL, suggesting it may be an important feature in the biology of several *innate-like* T cell subsets (Malinarich et al., 2010; Wencker et al., 2013).

In summary, *Skint1* is an organ-specific determinant of canonical DETC composition. Its expression in thymic medullary epithelial cells is critical for the selective agonist selection of DETC progenitors and its expression in keratinocytes may be required for PALP formation, or for selectively promoting DETC survival *in situ*. The discovery of *Skint1* has fuelled the hypothesis that various epithelia express tissue-restricted selecting elements that shape the lifelong composition of their signature $\gamma\delta$ IEL compartments. In support of this, several species that express a functional *Skint1* orthologue, including rats, cows and cynomolgus macaques, possess epidermal or skin-resident $\gamma\delta$ T cell compartments with highly restricted $\gamma\delta$TCR repertoires (Hayday, 2000; Hein and Dudler, 1997; Mohamed et al., 2015; Van Rhijn et al., 2007). That notwithstanding, the prospect that *Skint* genes might offer a generalizable mechanism by which tissue-resident $\gamma\delta$ T cells may be selected and maintained has been widely questioned. This is because

neither DETC nor *Skint1* is conserved in humans, and because the expression of *Skint* gene family members is predominately restricted to the skin and thymus (Boyden et al., 2008; Mohamed et al., 2015).

1.4 The Butyrophilins: emerging regulators of γδ T cells

S*kint* genes constitute a subfamily of butyrophilin-like (*BTNL*/*Btnl*) genes that are closely related to the B7 family of co-stimulators/repressors that are themselves thought to have close evolutionary relationships to MHC (Abeler-Dörner et al., 2012; Afrache et al., 2012; Henry et al., 1999). The butyrophilins (*BTN/Btn*) derive their name (*'butter-loving'*) from the prototypic founder *BTN1A1/Btn1a1*, which is highly expressed in epithelial cells of lactating mammary glands; encodes a major protein constituent of milk fat globules (MFG); and is critically required for MFG secretion (Franke et al., 1981; Jack and Mather, 1990; Ogg et al., 2004). Following the discovery of murine *Skint1*, human BTN3 genes were found to be key regulators of the TCR-dependent activation of human circulating $V\gamma9^{+}V\delta2^{+}$ T cells (Harly et al., 2012).

1.4.1 The Butyrophilin gene family

The extended *BTN*/*Btn* gene family contains up to 14 gene groups that are believed to have been present in a common Eutherian ancestor (Afrache et al., 2012). While some groups have been stably conserved across species (e.g. *BTN1*), some groups have been lost (e.g. *BTN3* in rodents) and others have undergone tandem duplication within specific lineages (e.g. *Skint* in rodents), consistent with rapid evolution and selection (Afrache et al., 2012). Human *BTN* genes can be sub-divided into three phylogenetically associated subfamilies, ***BTN1*** (*BTN1A1*), ***BTN2*** (*BTN2A1, BTN2A2, BTN2A3*) and ***BTN3*** (*BTN3A1, BTN3A2, BTN3A3*). Two of these genes are conserved in the mouse including ***Btn1*** (*Btn1A1*) and ***Btn2*** (*Btn2a2*). However, the mouse has many more butyrophilin-like (*Btnl*) genes, including ***Btnl****1, 2, 4, 5, 6, 7*, *9* and *10*, the closely related ***Skint****1 - 11,* erythroblast membrane associated protein (***Ermap***) and myelin oligodendrocyte glycoprotein (***Mog***). Of these, only *Btnl2, Btnl9, Mog and Ermap* have clear orthologues in humans (*BTNL2, BTNL9, MOG* and *ERMAP*), whereas *SKNTL* and *BTNL10* are predicted to encode pseudogenes. The human genome additionally contains *BTNL3* and *BTNL8*, which are not conserved in the mouse (Abeler-Dörner et al., 2012; Afrache et al., 2012; Rhodes et al., 2016) (**Figure 1.7**).

Most *BTN/Btn* and *BTNL/Btnl* genes encode integral membrane proteins with two extracellular immunoglobulin (Ig) domains (IgC and IgV) and an intracellular B30.2 domain (also termed PRY/SPRY) (Rhodes et al., 2016; 2005). The exceptions to this are *BTN2A3* (likely a pseudogene and/or non-functional) and *BTN3A2* which lack a B30.2 domain; *BTNL2/Btnl2* which encodes four extracellular domains (2xIgV and 2xIgC) and lacks the B30.2; and *MOG/Mog* and *ERMAP/Ermap*, which both contain a single extracellular IgV (although *MOG* lacks a B30.2) (Rhodes et al., 2016) (**Figure 1.7**). B30.2 (PRY/SPRY) domains are found on ~150 human and ~700 eukaryotic proteins but their function in immunity is best characterized in TRIM proteins, where they appear to have evolved to bind specific endogenous or exogenous ligands (Woo et al., 2006). For example, rhesus TRIM5α encodes a viral restriction factor that binds human immunodeficiency virus (HIV) capsid via its B30.2 domain and targets it for proteasome degradation (Pertel et al., 2011). By contrast, the B30.2 domain of TRIM21 serves as a high affinity intracellular Fc receptor that binds IgG-opsonised viral particles as they enter the cell cytoplasm. This interaction subsequently drives antibody-dependent intracellular neutralisation pathways (Rhodes and Trowsdale, 2007). Both of these highly specific protein interactions are thought to be enhanced by multimerization of TRIM proteins, which enables these molecules to serve as high avidity intracellular *innate* PRRs (Mische et al., 2005).

As TRIM genes are often located in close proximity to BTN/BTNL gene clusters, it is possible that these families share an evolutionary link and that the biological activity of BTNs/BTNLs may be similarly regulated by multimerization and/or by their engagement of intracellular ligands via B30.2 domains. Indeed, this appears to be the case for the prototypic member Btn1a1, where both multimerization (Robenek et al., 2006) and intracellular binding of xanthene oxidoreductase (XOR) by the B30.2 domain (Jeong et al., 2009) has been proposed to regulate MFG secretion from the apical membrane of lactating mammary gland epithelium (Franke et al., 1981; Ogg et al., 2004).

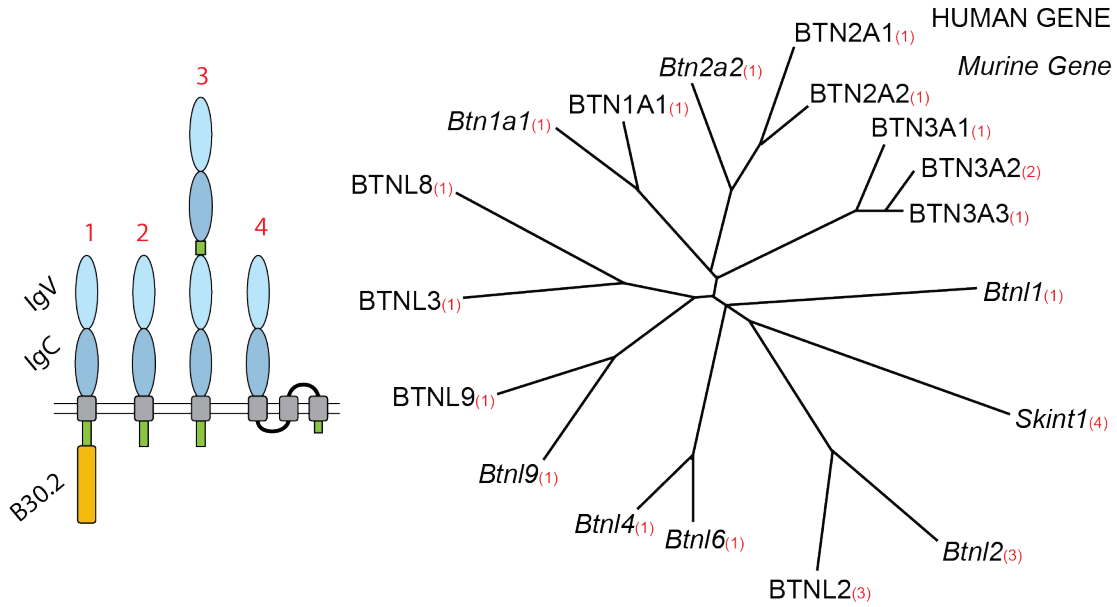

Figure 1.7 Predicted structure and phylogenetic tree of Butyrophilin gene family
Adapted from: (Abeler-Dörner et al., 2012; Rhodes et al., 2016)

1.4.2 BTN3 is a key regulator of human Vγ9$^+$Vδ2$^+$ T cell activation

Vγ9$^+$Vδ2$^+$ T cells are the most abundant γδ T cell subset in the human circulation and display rapid TCR-dependent responsiveness during accumulation of low-molecular-mass phospho-antigens (pAg) that are intermediary products of isoprenoid synthesis (Hayday, 2009; Karunakaran and Herrmann, 2014; Pang et al., 2012). Isopentenyl pyrophosphate (IPP) is a key building block for isoprenoids that are generated in most eukaryotes *via* the mevalonate pathway and in various plants and microorganisms *via* the non-mevalonate pathway (Karunakaran and Herrmann, 2014). IPP itself is a weak pAg and vastly less potent than its precursor in the non-mevalonate pathway, (E)-4-hydroxy-3-methyl-but-2-enyl pyrophosphate (HMBPP). The potency of HMBPP is such that infection by HMBPP-producing microorganisms (e.g. *mycobacterium tuberculosis*) can drive extensive clonal expansion of Vγ9$^+$Vδ2$^+$ cells, increasing their representation among circulating T cells from ~1-5%, to as much as 50% (M. Eberl et al., 2003; Shen et al., 2002).

IPP accumulates during dysregulation of mevalonate metabolism, which can occur during cellular transformation or viral infection and can also occur when IPP-metabolizing enzymes are pharmacologically inhibited by aminobisphosphonates (Gober et al., 2003; J. M. Jameson et al., 2010; Thurnher and Gruenbacher, 2015; van Beek et al., 1999). Indeed, aminobisphosphonate-pulsed cells are potent activators of Vγ9$^+$Vδ2$^+$ T cells and are often used for functional assays *in vitro* (H. Das et al., 2001). As pAgs are too small to directly crosslink the Vγ9$^+$Vδ2$^+$ TCR, activation of these T cells is contingent on cell:cell contact with a human or primate 'pAg-presenting cell' (pAgPC) expressing the three isoforms of *BTN3* (*BTN3A1, BTN3A2, BTN3A3*). *BTN3* is ubiquitously expressed in human cells and is critical for pAg-mediated activation of Vγ9$^+$Vδ2$^+$ T cells (Harly et al., 2012). Hence, short hairpin RNA-mediated knock-down of any single *BTN3* isomer in a pAgPC substantively diminishes its capacity to activate Vγ9$^+$Vδ2$^+$ T cells *in vitro* (Rhodes et al., 2015).

BTN3A1 is believed to be particularly important for pAg-presentation as its over-expression (alone) in *BTN3A1/3A2/3A3* 'triple knock-down' cells (but not that of BTN3A2/3A3) is sufficient to fully rescue pAg-presenting capabilities (Harly et al.,

2012). The $V\gamma9^{+}V\delta2^{+}$ TCR is directly implicated in this pathway as its expression in TCR-deficient jurkat T cell lines is sufficient to confer pAg-reactivity (H. Das et al., 2001). While these data are strongly indicative of BTN3A1 mediating its impact *via* the $V\gamma9^{+}V\delta2^{+}$ TCR, direct binding of BTN3A1 to the TCR has not been reproducibly demonstrated and its mechanism of action remains unclear (Rhodes et al., 2015; Sandstrom et al., 2014; Vavassori et al., 2013). Recent data suggest that pAgs bind to the B30.2 domain of BTN3A1 (Sandstrom et al., 2014), eliciting conformational changes to the protein (Sebestyen et al., 2016) that enable its direct engagement of the TCR or a co-receptor, or its recruitment of additional factors that engage the TCR (Karunakaran and Herrmann, 2014; Riaño et al., 2014).

Studies of murine *Skint1* and human *BTN3* have identified two non-orthologous members of the same extended gene family that regulate TCR-dependent processes in discreet subsets of γδ T cells. While *Btn* genes are conserved amongst placental mammals, closely related gene families have also been identified in zebrafish, xenopus and chickens (Afrache et al., 2012; Salomonsen et al., 2014). Moreover in chickens, which are particularly abundant in γδ T cells, several of these *Btn*-related *BG* genes have been shown to display tissue-restricted expression (Berndt et al., 2006; Salomonsen et al., 2014). Collectively, these studies suggest that butyrophilin and butyrophilin-related gene families are strong candidates for evolutionarily conserved regulators of γδ T cell biology and tissue-specific composition.

1.5 Summary and thesis aims

The mammalian immune system has evolved to mediate rapid responsiveness to both microbial and non-microbial environmental challenge. In order to cope with the latter, organisms deploy organ-specific *innate*-like T cells that constitutively monitor tissue stress. Such cells can rapidly deploy site-specific effector responses and can modulate downstream adaptive immunity, which helps to ensure that the overall immune response is appropriate to the context and nature of an environmental challenge. Prominent among these cells are the γδ IEL, which in several species have been shown to display striking site-specific TCRVγ chain usage. Their appropriate anatomical compartmentalization within an organism is critical for stress surveillance as its perturbation has profound implications for barrier integrity, tumour immunosurveillance and tissue immunopathology. While much is known regarding the phenotypic and functional hallmarks of these cells, very little is known about how their critical compartmentalisation is established and regulated.

In an attempt to determine how such compartmentalisation is established, research has focussed on characterising the developmental pathways of αβ and γδ IEL. Collectively, these studies have provided a prototypic outline for IEL development, which involves their developmental agonist selection, followed by their peripheral maintenance in discreet epithelia. While providing important information, these studies have failed to establish how discreet populations of γδ T cells, defined by their TCR Vγ chain usage, establish and maintain their life-long associations with specific epithelial tissues.

In this regard the discovery of *Skint1* as an organ-specific regulator of DETC composition has provided an important clue. The expression of *Skint1* in thymic medullary epithelium, where it is necessary for DETC selection, and in suprabasal keratinocytes, where it may be necessary for DETC maintenance, suggests that discreet epithelia could deploy tissue-specific elements to shape their local γδ IEL compartments (**Figure 1.8**). However, the prospect that *Skint* genes offer a generalizable mechanism by which γδ IEL are selected has been questioned because neither DETC nor *Skint1* is conserved in humans, and because the *Skint* genes are mostly expressed in the skin and thymus.

That notwithstanding, *Skint* genes are closely related to *BTN/Btn/BTNL/Btnl* genes that are conserved in humans and are emerging as key regulators of γδ TCR-dependent processes. Specifically, the three isomers of BTN3 are now known to be critical for the TCR-dependent activation of human $V\gamma9^{+}V\delta2^{+}$ T cells. As *Skint1* and *BTN3* represent non-orthologous members of the same extended gene family, their shared regulation of γδ T cell biology challenges the commonly held notion that these immune cells are highly species-specific with few or no conserved features (Kazen and Adams, 2011). Furthermore, as *BTN/BTNL* genes and *BTN*-related genes appear to be conserved across evolution, these studies fuel the hypothesis that this extended gene family may contain several subset-specific regulators of γδ T cell selection, maintenance and/or activation. To begin testing this hypothesis, this thesis will seek to establish whether murine *Btnl* genes regulate small intestinal γδ IEL composition.

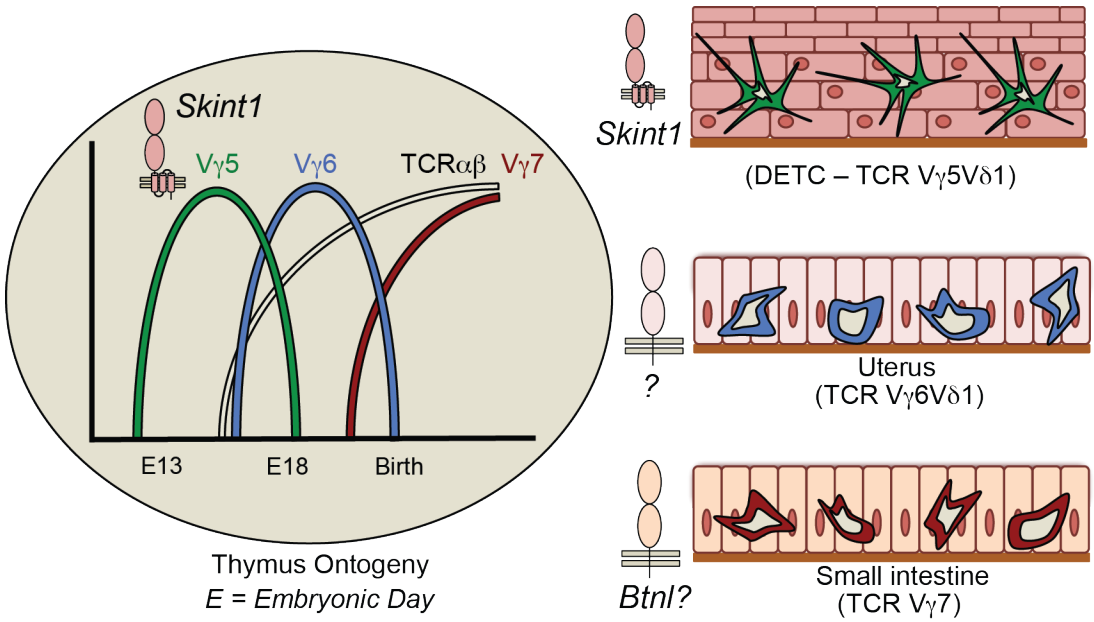

Figure 1.8 Regulation of γδ IEL composition

This schematic depicts the hypothesis that will be tested by this thesis: Do intestinal *Btnl* genes regulate the composition of signature small intestinal γδ IEL? Adapted from: (Carding and Egan, 2002).

1.5.1 Are Btnl1, 4 and 6 determinants of signature intestinal γδ IEL?

Within the murine *Btn* family, the genes most homologous to *Skint1* are *Btnl1, Btnl4* and *Btnl6* (Abeler-Dörner et al., 2012; Bas et al., 2011). All three of these genes are conspicuously expressed in small intestinal enterocytes and are encoded within the MHC II locus of chromosome 17. Interestingly, this is a region that has previously been associated with regulating intestinal γδIEL composition (Lefrançois et al., 1990; Pereira et al., 1997). *In vivo*, Btnl1 protein is detected on essentially all villus enterocytes, where it displays apical perinuclear enrichment and instances of juxtaposition with IEL (Bas et al. 2011). Taken together, each of these features makes Btnl1, Btnl4 and Btnl6 strong candidates for site-specific regulators of signature intestinal γδ IEL composition.

1.5.2 Specific aims

The aim of this thesis is to test the hypothesis that organ-specific products of *Btnl* genes serve to establish and maintain the lifelong composition of signature small intestinal γδ IEL (**Figure 1.8**).

To test this hypothesis, my primary objectives are as follows:

- To characterise the phenotypic maturation of signatory intestinal Vγ7$^+$ IEL in WT mice.
- To identify the developmental time point and anatomical location where Vγ7$^+$ IEL acquire their mature cell surface phenotype.
- To determine the impact of *Btnl1* and *Btnl4* in this process through a comprehensive analysis of *Btnl1*$^{-/-}$ and *Btnl4*$^{-/-}$ mice.
- To investigate the mechanisms by which *Btnl* genes mediate their impact on γδ T cells.

Chapter 2. Materials & Methods

For full details regarding buffer recipes, cytokines, antibodies, chemicals, materials, kits and DNA based reagents, please refer to the appendix.

2.1 Mice

All Animal experiments were undertaken in full compliance with UK Home Office regulations and under a project license to Prof. Adrian Hayday (80/2480). Experiments included 2-36 week-old (as indicated) male and female mice. Wild-type (WT) C57Bl/6 mice were obtained from Charles River and Harlan. 3 independently derived embryonic stem (ES) cells for *Btnl1*$^{-/-}$ (Btnl1$^{tm1(KOMP)Mbp}$) and ES cells for *Btnl4*$^{-/-}$ (Btnl4$^{tm1(KOMP)Mbp}$) mice were obtained from the international mouse phenotyping consortium (IMPC) (project IDs: CSD67994 and CSD81524). WT and *Btnl*-knockout lines were generated and maintained at The Francis Crick Institute's Biological resource facilities. B6.Cg-Foxn1<Nu>/J (NU/NU) mice were obtained from the Jackson Laboratory. Nur77.gfp mice were kindly provided by K. Hogquist (Moran et al., 2011). Alymphoplasia (aly/aly) mice were previously described (Shinkura et al., 1999). For timed pregnancies, mice were mated overnight and E0 was considered as the day a vaginal plug was observed.

2.1.1 Germ-free mice and food antigen-free nutrition

C57Bl/6 mice maintained on germ-free or on solid-food antigen-free diets were bred at the Institute for Medical Microbiology and Hospital Epidemiology, University of Marburg, Germany where all experiments were conducted according to the German animal protection law.

Germ-free (GF) mice were kept in plastic isolators (Metall and Plastik, Germany) with autoclaved food, bedding and water. Sterility of animals was checked bi-weekly by culturing faeces in thioglycollate medium under aerobic and anaerobic conditions for at least ten days. All handling procedures for GF mice were conducted in a laminar flow hood under sterile conditions. All experiments were conducted according to the German animal protection law.

Food antigen-free (FAF) mice were raised on an amino acid-containing diet for up to five generations. Pellets of FAF diet (ssniff, S7242-E014/-E714) contained all essential vitamins, minerals, trace elements, fat, dextrin, sucrose and free amino acids equimolar to the protein content of normal rodent chow (LASQCdietRod16, LASvendi).

2.1.2 Generation of doxycyclin inducible Btnl-1 transgenic (Tg) mice

Doxycycline (Dox)-inducible *Btnl1*-Tg mice were generated by injection of *Btnl1*$^{-/-}$ blastocysts with a linearised cassette containing a CMV-promoter regulated by a tetracycline response element (TRE) upstream of the Btnl1-ORF. The TRE/CMV cassette has been previously described (Oppenheim et al., 2005). R26-rtTA-M2 (Hochedlinger et al., 2005) or Villin-rtTA-M2 (Roth et al., 2009) mice were bred to homozygosity for *Btnl1*-deficiency and backcrossed onto *Btnl*-Tg mice for 3 generations to facilitate global (R26) or local (Villin) induction of *Btnl1* transgene expression. Doxycycline was administered to the drinking water (1mg/ml Dox, 2% sucrose). Ctrl water contained 2% sucrose. Water was changed 3 times a week.

2.2 Immune cell isolation protocols

2.2.1 Intestinal intraepithelial lymphocytes

Intraepithelial lymphocytes (IEL) were isolated from the entire length of the small intestine as previously described (Wencker et al., 2013). In brief, small intestinal tissue was opened longitudinally and thoroughly washed in ice-cold PBS prior to processing. Intestinal tissue was cut into 0.5-1cm long pieces and incubated for 20min at room temperature on a turning wheel, in 50ml falcon tubes containing 10ml RPMI:Dithiothreitol (DTT) solution. Tissue suspensions were centrifuged and the RPMI:DTT solution was decanted. Tissues were re-suspended in 10ml ‘IEL recovery medium’ and vortexed for 4 minutes at maximum speed. Supernatants containing cell suspension were harvested through 70μm nylon cell strainers. Tissues were then re-suspended in 10ml of fresh IEL recovery medium to repeat vortexing and filtration steps. The cell strainers were each washed with 30ml PBS.

To recover IEL, cells were pelleted and re-suspended in 40% percoll. Samples were centrifuged on a 20/40/80% percoll density gradient at 700g for 30min. IEL were harvested from the 40% to 80% Percoll interface.

2.2.2 Isolation of murine thymocytes

Thymus lobes were dissected and transferred to ice cold PBS. Blood vessels were removed under a dissection microscope. Lobes were mechanically disaggregated and passed through a 70 μm cell strainer. Cell suspensions were collected for staining.

2.2.3 Isolation of bone marrow cells

4-6 week old donor mice were sacrificed to harvest femurs and tibias. Bone scissors were used to cut the proximal and distal ends of the femur/tibia. Bones were flushed with ice cold sterile Hank's Balanced Salt Solution (HBSS) through a 27G needle/syringe. Clumps were disaggregated using a 19G needle/syringe, passed through a 40μM cell strainer and collected in a 50ml falcon tube. Cells were pelleted and re-suspended in 1ml of red blood cell lysis buffer (shaken at room temperature for 2 minutes). Cells were washed with HBSS and re-suspended at an appropriate concentration.

2.3 Flow Cytometry

2.3.1 Antibodies

Flow cytometry was performed using the following antibodies, coupled to the indicated fluorochromes (see Appendix for Cat. Numbers). **Fluorophore-conjugated antibodies for mouse**: CD3 APC Cy7 (17A2); CD3 PerCPCy5.5 (145-2C11); TCRβ Brilliant Violet 421 (H57-597); TCRβ APC (H57-597); CD122 PE (TMβ1); CD122 Brilliant Violet 421 (TMβ1); CD122 APC (TMβ1); TIGIT PE (GIGD7); CD45RB APC Cy7 (C363-16A); Thy1.2 Brilliant Violet 510 (53-2.1); Lag3 PerCP-efluor 710 (C9B7W); CD5 PE (53-7.3); CD24 FITC (M1/69); CD24 PECy7 (M1/69); CD8α PECy7 (53-6.7); CD8α PECy7 (53-6.7); TCR Vδ4 FITC (GL-2); TCR Vδ4 PE (GL-2); CD8β PerCpCy5.5 (YTS156.7.7); CD25 PerCpCy5.5 (PC61); CD69 PECy7 (H1.2F3); CCR9 PECy7 (CW-1.2); CD44 PECy7 (IM7); TCRVγ7

(F2.67) was provided by Pablo Pereira (Institut Pasteur, Paris, France); TCRVγ1 APC (2.11); TCRVγ4 APC (UC3-10A6); TCRδ BV421 (GL3); Ki67 FITC (B56/MOPC-21); CD45 Qdot 605 (30-F11); CD5 Brilliant Violet 510 (53-7.3); TCRδ PeCy7 (GL3); CD161/NK1.1 Brilliant Violet 650 (PK136); CD4 Brilliant Violet 786 (GK1.5); CD8α AlexaFluor 700 (53-6.7); CD25 APC (PC61); GITR PE (DTA-1); CD44 FITC (IM7); CD62L PerCP-Cy5.5 (MEL-14); KLRG1 BV421 (2F1); CD11c BV786 (HL3); CD11b BV510 (M1/70); F4/80 PerCPCy5.5 (BM8); Ly6G APC (1A8); Ly6C AlexaFluor 700 (AL-21); CD103 PE (M290); CD317 Brilliant Violet 650 (927); MHCII/IA/IE FITC (2G9); CD86 Pe-Cy7 (GL1); CD3 Brilliant Violet 421 (145-2C11); CD19 Brilliant Violet 421 (1D3); CD161/NK1.1 (lin) Brilliant Violet 421 (PK136); IgG1 PE (A85-1); B220 (CD45R) AlexaFluor 700 (RA3-6B2); IgM Brilliant Violet 786 (R6-60.2); IgD PerCPCy5.5 (11-26c.2a); GL-7 AlexaFluor 647 (GL7); CD95 PECy7 (Jo2); CD138 Brilliant Violet 650 (281-2); CD21/35 FITC (7G6); CD23 Brilliant Violet 421 (B-ly6). **Other antibodies**: DYKDDDDK-PE (Flag); DYKDDDDK-APC (Flag); HA-DyLight 650; 6x-Histidine-PE; LEAF-Purified Hamster IgG Isotype Control (HTK888); LEAF-Purified anti-mouse CD3 (2C11)

Commercial antibodies were purchased from Biolegend, eBioscience, BD-Bioscience, Thermo Fisher Scientific or Miltenyi (see appendix). Viability dyes (near IR or Blue) were from Invitrogen. All cell surface and intracellular stains were performed in 96-well V-bottom plates.

2.3.2 Production of anti-TCRVγ7 antibody

F2.67 Hybridoma was cultured in DMEM supplemented with glutamine, penicillin/streptomycin, sodium pyruvate, non-essential amino acids, β-mercapto ethanol and 5% foetal calf serum (FCS). Anti-TCRVγ7 (F2.67, provided by Pablo Pereira [Insitut Pasteur, Paris, France]) was purified from hybridoma supernatant using the mouse tissue culture supernatant (TCS) purification system (abcam). Purified anti-TCRVγ7 was conjugated to biotin (EZ-Link Sulfo-NHS-LC Biotinylation Kit, Thermo Fisher Scientific) or to Alexa-Fluor(AF)647 (labelling kit, Thermo Fisher Scientific).

2.3.3 Viability dye

Viability dyes were used at a dilution factor of 1:1000 in phosphate buffered saline solution (PBS). Cells were stained for 15-20 minutes at 4^{o}C and then washed with FACS buffer prior to cell surface staining. Live/Dead Fixable Blue Dead Cell Stain Kit (Thermo Fisher) was used for all staining panels apart from spleen and mesenteric lymph node immunophenotyping. Zombie NIR^{TM} Fixable Viability Kit (Biolegend) was used for spleen and mesenteric lymph node immunophenotyping experiments.

2.3.4 Cell surface stain

Cells were incubated in 20μl F_C block for 15 minutes at 4^{o}C. Antibodies were diluted in FACS buffer to produce a 2X concentrated stock solution. 20μl of 2X antibody mix was added to each well containing cells suspended in F_C block. Cell surface stains were performed for 25-30 minutes at 4^{o}C. Samples were either analysed on the same day as staining, or fixed for 4mins at room temperature (shielded from light) in 4% paraformaldehyde, stored overnight at 4^{o}C and analysed the following morning.

2.3.5 Ki67 intracellular stain

Ki-67 staining was performed after cell surface stains on cells fixed and permeabilzed using the Foxp3 staining buffer kit in accordance with the manufacturer's instructions (eBioscience). In brief, cells were re-suspended in Fixation/Permebilization solution and left for 30 minutes at room temperature shielded from light. Cells were then washed twice in permeabilization buffer and re-suspended in 30μl Ki67 antibody mix (1:30 in permeabilization buffer). Cells were incubated for 30 minutes at room temperature, washed in permeabilization buffer and then washed and re-suspended in FACS buffer for analysis.

2.3.6 EdU Click-iT assay

EdU incorporation was assessed by flow cytometry 3 hours post-intraperitoneal injection (50mg/kg) (Click-iT EdU AF647 Assay Kit, Invitrogen). EdU Click-iT

reaction was performed according to manufacturer's instructions in 96-well V-bottom plates in 70μl reaction mix.

All flow cytometry data analysis performed on FlowJo (Version 9.9).

2.3.7 Spleen and mesenteric lymph node immunophenotyping

Comprehensive immunophenotyping of mesenteric lymph node (MLN) and splenic immune cells in *Btnl1*$^{-/-}$, *Btnl1*$^{+/-}$ and C57Bl/6 mice, was performed using a platform developed by the Wellcome trust Infection and Immunity Immunophenotyping (3i) consortium (www.immunophenotyping.org). Briefly, spleen and MLN were digested in collagenase (1mg/ml)/DNAse (0.1mg/ml) in 2% foetal calf serum (FCS) phosphate buffered saline (PBS +Ca/Mg) for 20 minutes at 37^{o}C. Samples were filtered through 30μm cell strainers, and shaken for 2 minutes at room temperature in red blood cell (RBC) lysis buffer (SIGMA). Samples were washed in PBS, centrifuged and plated on 96-well V-Bottom plates for staining. All stains were performed at 4^{o}C for 20 minutes. Full details regarding the phenotyping panels and gating strategy are included (see Appendix). Samples were acquired on a BD LSR Fortessa X-20 equipped with 405nm (40mW), 488nm (50mW), 561nm (50mW) and 640nm (100mW) lasers.

2.4 Quantitative-RT-PCR, transfection and lentiviral transduction.

2.4.1 MODE-K transfectants/transductants

MODE-K cell transductants were generated and kindly provided by Dr Vantourout for this study. Briefly, the self-inactivating lentiviral vector pCSIGPW (SFFV promoter – Multiple Cloning Site [MCS] – IRES-GFP – CMV promoter – Puromycin^{R}) was constructed by replacing the Puromycin^{R}/mIR cassette from the pAPM vector (Pertel et al., 2011) by a custom EcoRI-XhoI-PmeI-NotI-BamHI-XbaI-MluI MCS. The IRES-GFP cassette was cloned by PCR from the pIRES2-eGFP vector (Clonetech) using the BamHI/XbaI sites. The CMV promoter was cloned by PCR from the pCDNA3.1+ vector (Thermo Fischer Scientific) using the MluI/ClaI sites. The Puromycin resistance gene was cloned by PCR from the pGIPZ vector (Dharmacon) using the ClaI/AgeI sites. The pCSIGHW variant was generated by

exchanging the puromycin resistance gene with a hygromycin B resistance gene, which was cloned by PCR from the pLHCX vector (Clontech).

cDNAs were (sub-)cloned into pCSIGPW or variant vectors. *Btnl1*, *Btnl4* and *Btnl6* were previously described (Bas et al., 2011).

Transfections were carried out in HEK293T cells using PEI (3:1 PEI:DNA ratio, Polysciences). Btnl/BTNL expression was checked 48h post-transfection. Lentiviral particles were produced in HEK293T cells by co-transfection of pCSIGPW or pCSIGHW either empty (empty vector; EV) or containing *Btnl* cDNA, pCMVΔR8.91 (HIV-1 *tat*/*rev*/*gag*/*pol*) (Zufferey et al., 1997), and pHIT/G (MLV *env*) (Fouchier et al., 1997). Transduced cells were treated with puromycin and hygromycin 48h post-transduction for 7 days, sorted on the basis of GFP expression and used for functional assays.

2.4.2 Quantitative RT–PCR.

For whole tissue analysis, the small intestine was divided into 3 segments (proximal 1/3, medial 1/3 and distal 1/3) and a 0.5cm piece of whole small intestine was taken from the middle of each. Tissue was either frozen in RNAlater or directly lysed in RLT lysis buffer (supplemented with β mercaptoethanol [1:100]), in 2ml eppendorf tubes in a tissue lyser (Qiagen; with metal beads). RNA was purified using the Qiagen RNeasy kit, according to manufacturer's instructions. Cellular samples were flow stored into 400μl of IEL recovery medium in 1.5ml eppendorf tubes (4^{o}C). Sorted cells were pelleted, and lysed in RLT lysis buffer (supplemented with β mercaptoethanol [1:100]) prior to RNA purification (Qiagen RNeasy kit).

cDNA was synthesized using Superscript-II (Invitrogen) and analysed using Power-Sybr-green assay (Invitrogen) using a ViiA7 Real-time PCR machine (Applied Biosystems).

2.4.3 qRT-PCR primers

Btnl1 For: 5'-TGACCAGGAGAAATCGAAGG-3'
Btnl1 Rev: 5'-CACCGAGCAGGACCAATAGT-3'

Btnl4 For: 5'- CATTCTCCTCAGAGACCCACACTA-3'
Btnl4 Rev: 5'- GAGAGGCCTGAGGGAAGAA-3'
Bntl6 For: 5'-GCACCTCTCTGGTGAAGGAG-3'
Btnl6 Rev: 5'-ACCGTCTTCTGGACCTTTGA-3'
β-Actin For: 5'-CAGCTTCTTTGCAGCTCCTT-3'
β-Actin Rev: 5'-CACGATGGAGGGGAATACAG-3'
Sox13 For: 5'-CTCCAGGCCTTCCCAGAC-3'
Sox13 Rev: 5'-CATGGACTTCCAGCGAGAAC-3'
Rorγc For: 5'-GGTGACCAGCTACCAGAGGA-3'
Rorγc Rev: 5'-CCACATACTGAATGGCCTCA-3'
Tbp For: 5'-GGGGAGCTGTGATGTGAAGT-3'
Tbp Rev: 5'-CCAGGAAATAATTCTGGCTCA-3'
CycloFor: 5'- CAAATGCTGGACCAAACACAA-3'
Cyclo Rev: 5'- CCATCCAGCCATTCAGTCTTG-3'

2.5 Southern Blotting

2.5.1 Genomic DNA extraction

Genomic DNA was extracted from tail tissue. Tissue was incubated overnight (shaking at 56°C) in 360μl tail buffer + 15μl Proteinase K (10mg/ml stock). 125μl 5M NaCl was added to precipitate debris, which was pelleted before harvesting the supernatant. Supernatant was transferred to a tube containing 250μl isopropanol. Samples were centrifuged, isopropanol decanted and pellets were re-suspended in 500μl 70% ethanol. Samples were centrifuged, ethanol decanted and pellets were air dried for ~1hr at room temperature. DNA was eluted in milliQ H_2O.

2.5.2 DNA digestion, electrophoresis and Southern blotting

10-20μg genomic DNA was digested with the indicated restriction enzymes (AseI, EcoRI or KpnI) under conditions recommended by manufacturer's instructions (New England Biolabs). Digested DNA was ethanol precipitated, mixed with bromophenol blue loading buffer and ran on 0.8% agarose gel (constant voltage: 40V overnight). Agarose gel was incubated at room temperature with depurination buffer for (10mins with gentle agitation); then with denaturation buffer (30mins with

gentle agitation); then with neutralisation buffer (30mins with gentle agitation); then rinsed with milli-Q water.

DNA was blotted overnight by capillary action onto a nitrocellulose membrane in 20X SSC buffer. Nitrocellulose blotted DNA was cross-linked by ultra-violet (UV) radiation, then dried for 1 hour at room temperature.

2.5.3 Probe generation

Digoxigenin (DIG)-labelled DNA probes were generated by PCR of genomic DNA using the following primers:

Btnl1 For: 5'-ACTGGCTTCCTCAGAGTCAT-3'
Btnl1 Rev: 5'-CAGTAGTGAATGGCCCCTGA-3'
Btnl4 For: 5'-GACCAACGCTTCCCTACCTC-3'
Btnl4 Rev: 5'-GCCTTGGGTCCAACAAGACA-3'
Btnl1-Ex3-F2: 5'- GGTTTTCTGTGAAGGGACCA -3'
Btnl1-Ex4-R2: 5'- GGTCTGCAACTCAGAGGAGG -3'

PCR amplification was performed using REDTaq polymerase (Sigma) and DIG-labeled deoxynucleotide solution mix (Roche)

2.5.4 Probe hybridization/detection

All steps were performed according to manufacturer's instructions (Roche). Blots were hybridized in DIG-Easy-hyb buffer overnight at 65^{o}C; washed for 2x 5 minutes at room temperature in 2xSSC/0.1%SDS; washed for 2x 15 minutes in 0.1xSSC/0.1%SDS; and then rinsed in PCR grade water. Blocking was performed using DIG-blocking reagent for 30mins at room temperature. Detection antibody was diluted 1:10,000 in DIG-blocking reagent and incubated with the blot for 30mins at room temperature. Blots were then washed for 2x 15 minutes in wash buffer, equilibrated for 5 minutes in detection buffer and developed using the DIG-Luminescence Detection Kit.

2.6 MODE-K co-culture and IEL stimulation assays

2.6.1 IEL Stimulation

96-well U-bottom plates were coated overnight at 4°C with 50μl PBS containing 10μg/ml LEAF-purified anti-mouse CD3ε or Hamster IgG Isotype Control (Biolgend). Wells were washed once with PBS 1X and IEL were seeded at a density of 10^5/well in complete RPMI (see Appendix). IEL were stimulated overnight (16-18hrs) at 37°C and 10% CO_2.

2.6.2 IEL:MODE-K co-cultures

MODE-K transductants were maintained in 'MODE-K culture medium' at 37°C/5% CO_2. Co-cultures were performed at 37°C/10% CO_2 in 'complete RPMI' (see Appendix).

10^5 MODE-K cells were seeded onto each well of a 48-well plate 24hrs prior to co-culture experiments (Day -1). At Day 0, 'MODE-K culture medium' was replaced with 'complete RPMI' and 10^5 unsorted or (where indicated) positively FACS-sorted (CD45+Vγ7+) IEL were seeded onto MODE-K monolayers. Cells were co-cultured for 4 hours, 6 hours or 16-18 (overnight) hours (as indicated) prior to harvesting for analysis.

For transwell assays, $2x10^5$ MODE-K cells were seeded onto 24-well transwell plates (3μm pore size - Corning) 24h prior to the addition of $3x10^5$ IEL, either in direct contact (below), sequestered from (above), or split 50:50 with MODE-K cells (above and below the transwell). Cells were harvested after 16-18 hours of co-culture.

2.7 Bone Marrow Chimeras and Adoptive IEL Transfers

2.7.1 Bone marrow chimeras

10-12 week-old recipient mice were irradiated with 2 doses of 480 Rad, 3-4 hours apart, 24 hours prior to tail vein intravenous (IV) injection with $5\text{-}10x10^6$ donor bone marrow cells. Analysis was performed 4-12 weeks later (as indicated).

2.7.2 Adoptive IEL transfer

IEL harvested from 4 week-old WT mice were column-purified using CD45 microbeads (MACS Miltenyi biotec) and IV-injected into 6 week-old TCR$\delta^{-/-}$ and TCR$\delta^{-/-}$.*Btnl1*$^{-/-}$ recipients. Analysis was performed 2-3 weeks later.

2.8 Microscopy

2.8.1 Gut whole mount staining

Thesis presents 4 maximum intensity projection images kindly provided by Dr Hart.

2.8.1.1 Day 1 – Fixation and primary stain

Proximal 1/3 of small intestine was harvested and flushed with ice cold PBS. Fat was removed and tissue was cut longitudinally. Using a scalpel, 2x 2-3mm wide sections of gut wall were harvested and incubated in Zamboni's fixative for 2hrs at room temperature (gentle agitation). Samples were washed 5 times for 5 minutes with washing buffer (gentle agitation) and then blocked for 1 hour (with gentle agitation) at room temperature with normal goat serum (Block A). Primary stain: αCD3 (17A2-*unconjugated*) in Block A overnight at 4^{o}C with gentle agitation. See appendix for buffer/fixative details.

2.8.1.2 Day 2 – Secondary stain

Samples were washed 4 times for 5 minutes with washing buffer (gentle agitation), before incubating with 'Block B' for 3hrs at room temperature (gentle agitation). After blocking, samples were incubated with conjugated antibodies (TCRβ-BV421, Vγ7-AF647, Vδ4-FITC, Goat anti-Rat IgG Alexa Fluor 555) diluted in 'Block B' overnight at 4^{o}C (gentle agitation). See appendix for buffer details.

2.8.1.3 Day 3 – Mounting and image acquisition

Samples were washed 4 times for 5 minutes in washing buffer (gentle agitation) at room temperature. Then they were mounted as whole tissues in vectashield for confocal analysis. Z-Sections were acquired on a confocal-LSM-710 microscope

(Zeiss) and processed and analysed using Imaris Software (Bitplane Scientific Solutions). See appendix for buffer details.

2.8.1.4 Imaris Image analysis

3D image analysis on z-stacks was carried out using Imaris (Bitplane). The surfaces tool was used to identify $CD3^+$ cells. Voxels outside of these structures were set to zero in each of the channels to create masks.

2.8.2 Histology

Thesis presents histology data acquired in collaboration with the Francis Crick Institute Experimental Histopathology Core Facility.

2.8.2.1 BrdU incorporation in intestinal epithelium

Mice were injected intraperitoneally with BrdU (50mg/kg; Sigma) 3 hours prior to sacrifice. Intestinal tissue was harvested, flushed with ice cold PBS, cut longitudinally and fixed as a gut roll. BrdU incorporation was assessed by immunohistochemistry in paraffin-embedded histological sections of the gut roll.

2.8.2.2 RNAscope

RNAscope analysis was performed on paraffin-embedded sections using probes and kits obtained from Advanced Cell Diagnostics Inc. using the RNAscope 2.0 HD Reagent Kit-BROWN. Reference sequences are as follows: *Btnl1*.NM_001111094.1 (576-1723); *Btnl4* NM030746.1 (560-968); *Btnl6*.NM_030747.1 (245-1552).

2.9 RNA sequencing

RNA sequencing was performed in collaboration with the Francis Crick Institute Advanced Sequencing Core Facility. $V\gamma7^+CD122^{hi}$ and $V\gamma7^+CD122^{lo}$ IEL were flow sorted from pooled D14-17 pups directly into RLT plus micro buffer (supplemented with 1:100 β mercaptoethanol). RNA was prepared using the RNA-Micro-plus kit (Qiagen). cDNA libraries were generated using the KAPA Stranded RNA-seq Kit with RiboErase (HMR) (KAPA BIOSYSTEMS). Paired-end sequencing was

performed on a HiSeq 2500 (illumina) using rapid run chemistry (read length: 100bp).

2.9.1 Bioinformatics analysis of RNA sequencing

101 base-pair paired-end reads were aligned and quantified using RSEM (v1.2.11) (B. Li and Dewey, 2011) with Bowtie2. Reads were aligned to a transcriptome constructed from the mm10 mouse genome and a UCSC knownGene gtf file. A mean alignment rate of 57.4 million fragments per sample was observed. Using the gene level quantification, only detected genes (mean TPM value across all samples > 1; 13,313 genes) were selected. Differential expression between the $CD122^{hi}$ and $CD122^{lo}$ $V\gamma7^{+}$ IEL groups using DESeq2 (M. I. Love et al., 2014) was identified by taking into account the paired structure within the replicate groups. Using an FDR of 0.01 2664 phenotype dependent gene expression effects were identified.

2.10 Quantification and Statistical Analysis

2.10.1 Cell enumeration

Total thymocyte and IEL yields were analysed on an electronic cell counter (CASY counter; INNOVATIS), which determined live lymphocyte events by cell diameter and electrical conductivity. Subset counts in thesis (e.g. total enumeration of $V\gamma7^{+}$ IEL) were calculated as: Total lymphocyte yield x ($V\gamma7^{+}$ [%live events] / 100).

2.10.2 Statistics

Unless stated otherwise, bar/spider charts display mean ±SD and p values were derived from unpaired two tailed t-tests, assuming equivalent SD (*ns* $p>0.05$).

Chapter 3. Signature Small Intestinal Intraepithelial γδ T cells

3.1 Introduction

Signature Vγ5$^+$ DETC carry a mature cell surface phenotype characterised by high levels of cell surface TCR, CD45RB and CD122 and low levels of CD24 and CD62L (Lewis et al., 2006; Sumaria et al., 2011). Their thymic progenitors acquire this signature phenotype during their developmental interactions with *Skint1*-expressing thymic medullary epithelial cells (Lewis et al., 2006). Hence, mice that carry a loss-of-function mutation in *Skint1* lack canonical DETC because their progenitors experience developmental defects in the thymus, fail to attain phenotypic and functional maturity and fail to home to the skin (Barbee et al., 2011; Boyden et al., 2008; Lewis et al., 2006).

The developmental up-regulation of CD122 that occurs during *Skint1*-mediated DETC selection is also associated with agonist selection of developing thymocytes (Baldwin et al., 2004; Hanke et al., 1994). Agonist selection describes positive selection of thymocytes that engage their TCR ligand in the thymus, experience strong TCR signalling but do not undergo clonal deletion. Examples of such 'agonist-selected' cells include iNKT cells and TCRβ$^+$CD8αα$^+$ intestinal IEL (Hogquist and S. C. Jameson, 2014). Although there is no direct evidence of Skint1 engaging the DETC TCR, phenotypic maturation of DETC progenitors in the thymus of *Skint1*-mutant mice can be rescued *in vitro* by supplementing FTOC with agonist antibodies specific for the Vγ5$^+$ TCR (Lewis et al., 2006). Moreover, *Skint1*-mediated selection has been shown to induce a gene expression signature in DETC progenitors associated with strong TCR signalling (Turchinovich and Hayday, 2011). This expression signature includes up-regulation of *Tbx21*, *Egr3*, *Tnfrsf9* and down-regulation of *Rorc, and Sox13* and can be phenocopied in adult γδ thymocytes by direct TCR stimulation *in vitro* (Turchinovich and Hayday, 2011). Therefore, it is considered that *Skint1* regulates the developmental agonist selection of DETC progenitors.

TCRβ$^+$CD8αα$^+$ IEL comprise a subset of self-reactive 'agonist-selected' intestinal αβ IEL that are not restricted by classical MHC (Cheroutre et al., 2011; Oh-hora et al., 2013; Rocha et al., 1991). Thymic agonist selection of TCRβ$^+$CD8αα$^+$ IEL progenitors is also associated with up-regulation of CD122 and T-bet, which in the small intestine phenotypically differentiates TCRβ$^+$CD8αα$^+$ IEL from MHC-restricted TCRβ$^+$CD8αβ$^+$ or CD4$^+$ IEL subsets (Klose et al., 2014; McDonald et al., 2014; Pennington et al., 2003). While TCRβ$^+$CD8αα$^+$ IEL appear to be phenotypically and functionally distinct from TCRβ$^+$CD8αβ$^+$ and CD4$^+$ IEL, they share many features with bulk γδ IEL. For example, most γδ and TCRβ$^+$CD8αα$^+$ IEL share a similar cell surface phenotype, including their expression of CD122 and the CD8αα homodimer, a negative regulator of TCR signalling (Cheroutre and Lambolez, 2008). Both populations also express Lag3, while lacking CD5 and Thy1, and contain sub-populations of cells that express various members of the Ly49 family of inhibitory NK receptors (Denning et al., 2007; Klose et al., 2014). Moreover, γδ IEL and TCRβ$^+$CD8αα$^+$ IEL share expression of several genes, including inducible cAMP early repressor of transcription (*ICER*), regulator of G protein signalling 2 (*Rgs2*) and *FcεRIγ*, many of which are shared by DETC but not by TCRβ$^+$CD8αβ$^+$ IEL (Denning et al., 2007; Pennington et al., 2003). Thus, by various phenotypic metrics DETC, intestinal γδ IEL and intestinal TCRβ$^+$CD8αα$^+$ IEL share more in common with each other than with populations of intestinal MHC-restricted αβ IEL.

Given that DETC and TCRβ$^+$CD8αα$^+$ IEL acquire various features of their mature phenotype during an agonist selection process in the thymus. We hypothesized that γδ IEL development may be similarly defined by an agonist-selection-type process regulated by a *Skint1*-like gene. To study this, we first sought to characterise the phenotypic profile of signature small intestinal γδ IEL, identify the developmental time point at which it is acquired and where possible, identify parallels with *Skint1*-selected DETC selection or agonist-selected TCRβ$^+$CD8αα$^+$ IEL.

3.2 Phenotypic profile of signature γδ IEL

3.2.1 Vγ7$^+$ IEL are signature intestinal γδ IEL

Previous studies have shown that most small intestinal γδ T cells colonise the gut shortly after birth (Lefrançois and Olson, 1994; Torow et al., 2015) and that Vγ7$^+$ T cells predominate among small intestinal γδ IEL (Kawaguchi et al., 1993). To verify this, we determined γδ IEL composition in adult mice by flow cytometry of freshly recovered cells. Consistent with with previous reports (Chennupati et al., 2010; Kawaguchi et al., 1993; Pereira et al., 1997), Vγ7$^+$ cells were the predominant intestinal γδ IEL subset comprising ~60% of the compartment. Vγ1$^+$ cells comprised ~25% and the remaining ~15% mostly expressed Vγ4 (**Figure 3.1A**; *data not shown*).

Most αβ IEL were positive for CD8α, which was expressed as a CD8αα homodimer by ~50% and as a CD8αβ heterodimer by ~40%. The remaining 10% of αβ IEL either expressed CD8αα alongside CD8αβ (~5%), or were CD8α$^-$ and mostly CD4$^+$ (~5%) (**Figure 3.1A;** *data not shown*). Furthermore, a small but variable proportion of cells co-expressed CD4 with CD8αα, as has been also been reported in the literature (*data not shown*) (Y. Huang et al., 2011; Mucida et al., 2013; Reis et al., 2013; 2014).

DETC are among the first T cells to emerge from the embryonic thymus and populate the neonatal epidermis (Aono et al., 2000; Ramond et al., 2013). To assess when Vγ7$^+$ IEL first populated the small intestinal epithelium, we recovered IEL from 2 to 3-week old suckling mouse pups and analysed γδ IEL composition by flow cytometry. Between 2 to 3 weeks of age, the representation of Vγ7$^+$ T cells increased from ~40% to >60% of γδ IEL (**Figure 3.1B**). By week 3, these cells had become the predominant γδ IEL subset and were maintained as such for at least 9 months thereafter. Hence, it was concluded that Vγ7$^+$ IEL were the signature small intestinal γδ IEL and that these cells became the predominant intestinal γδ IEL subset by 3 weeks of age.

3.2.2 Vγ7$^+$ IEL carry an agonist-selected cell surface phenotype

As discussed, *Skint1*-mediated selection of DETC progenitors is associated with the acquisition of a mature CD122^{HI}CD45RB^{HI}TCR^{HI} cell surface phenotype and down-regulation of *Sox13* and *Rorc*. To establish whether signature small intestinal Vγ7$^+$ IEL carried a similar 'agonist-selected' phenotype, freshly recovered IEL from 3-5 week old weanling mice were analysed. From day 21 to 40 (D21-40), Vγ7$^+$ cells expressed uniformly high levels of CD122, the IL-2R/IL-15Rβ sub-unit; and of TIGIT, an inhibitory co-receptor. By contrast, Vγ7$^-$ (CD3$^+$TCRβ$^-$) IEL were largely negative for cell surface expression of both markers (**Figure 3.2A**). Vγ7$^+$ IEL also expressed the highest levels of cell surface TCR (by anti-CD3 antibody) relative to αβ and to Vγ7$^-$ γδ IEL and expressed ~4-fold lower levels of *Sox13* and *Rorc* relative to Vγ7$^-$ cells (**Figure 3.2B**). Thus, amongst small intestinal γδ IEL, Vγ7$^+$ cells from 21 to 40 day-old mice selectively adopted a mature agonist selected phenotype reminiscent of *Skint1*-selected DETC.

By contrast to the differences in cell surface expression of TCR, CD122 and TIGIT, Vγ7$^+$ IEL were almost indistinguishable from Vγ7$^-$ cells with regards to their expression of CD44, CD45RB, and CCR9 (**Figure 3.2C**). To identify additional features that may differentiate putative 'selected' Vγ7$^+$ IEL from Vγ7$^-$ IEL, we sought to assess the extent to which these distinct T cell populations phenocopied the reported 'agonist-selected' phenotype of TCRβ$^+$CD8αα$^+$ IEL. As mentioned previously TCRβ$^+$CD8αα$^+$ IEL cells are defined by their expression of the CD8αα homodimer, CD69 and Lag3, and are largely negative for CD5 and Thy1 (Denning et al., 2007; Gangadharan et al., 2006; Ma et al., 2009; McDonald et al., 2014). Whereas almost 100% of Vγ7$^+$ IEL expressed the CD8αα homodimer, only ~70% of Vγ7$^-$ IEL were CD8αα$^+$ (**Figure 3.2D**). Furthermore, while Vγ7$^+$ IEL uniformly expressed high levels of CD69 and Lag3, and were mostly (~90%) negative for CD5 and Thy1; a significantly greater proportion of Vγ7$^-$ IEL were negative for Lag3 (~50%), expressed lower levels of CD69 and were positive for CD5 and Thy1 (30-40%) (**Figure 3.2D**). These results indicate that Vγ7$^+$ IEL more closely phenocopy 'agonist-selected' TCRβ$^+$CD8αα$^+$ IEL than Vγ7$^-$ IEL.

Taken together, these data demonstrate that intestinal Vγ7^{+} IEL selectively phenocopy Vγ5^{+} DETC and TCRβ^{+}CD8$\alpha\alpha^{+}$ IEL in that they carry a cell surface phenotype (CD122^{HI}, TCR^{HI}, TIGIT^{HI}, CD8$\alpha\alpha^{+}$, CD69^{HI}, Lag3^{HI}, CD5^{LO}, Thy1^{LO}), consistent with a prior agonist selection.

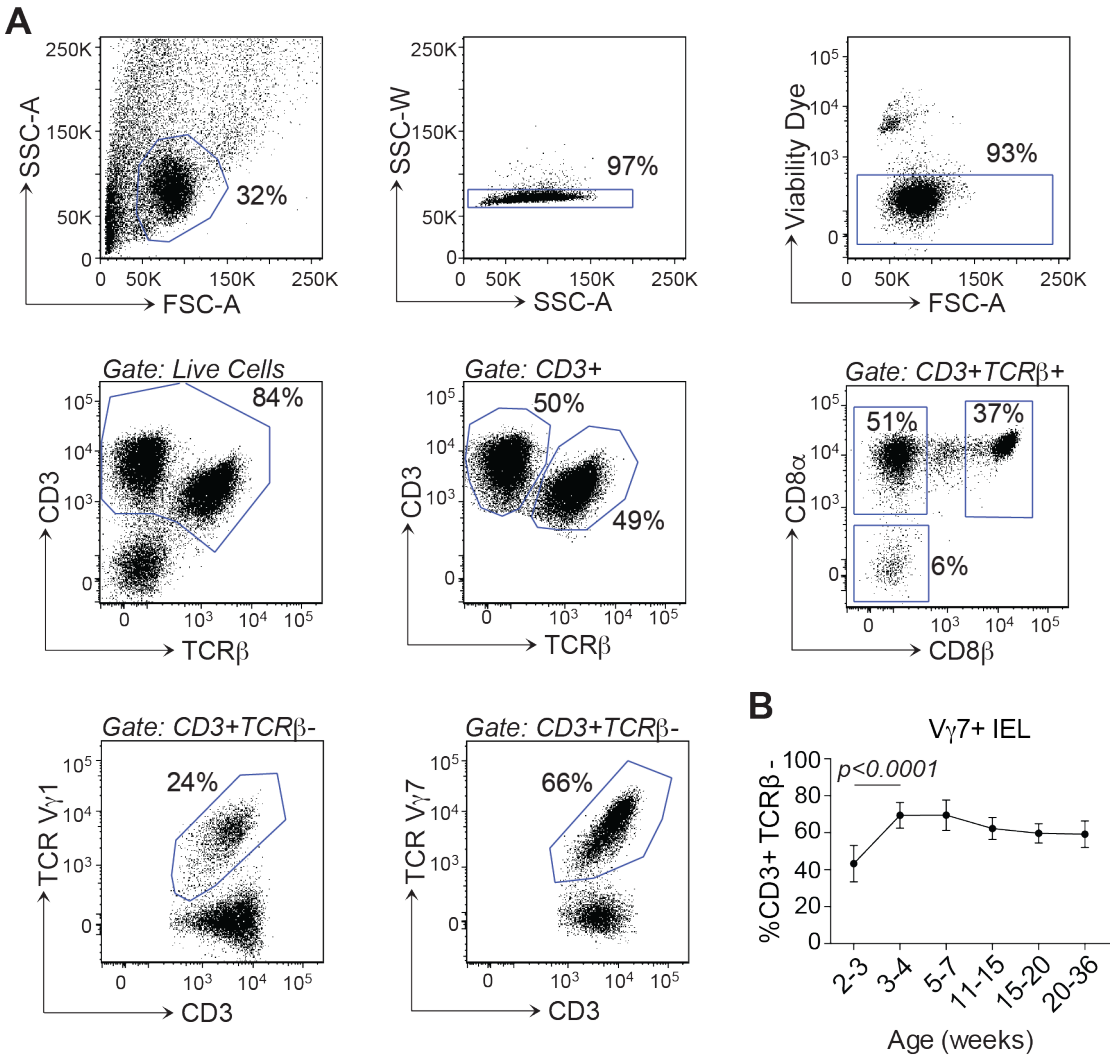

Figure 3.1 Composition of small intestinal IEL

A) Gating strategy for small intestinal Vγ7$^+$ IEL in 12 week(W)-old C57Bl/6 mice (*n≥12*). **B)** Representation of Vγ7$^+$ IEL over time (W20-36 ➔ *n=5*; other time points ➔ *n≥12*). Panel (**A**) includes data representative of ≥3 experiments. Panel (**B**) includes data pooled from >20 independent experiments.

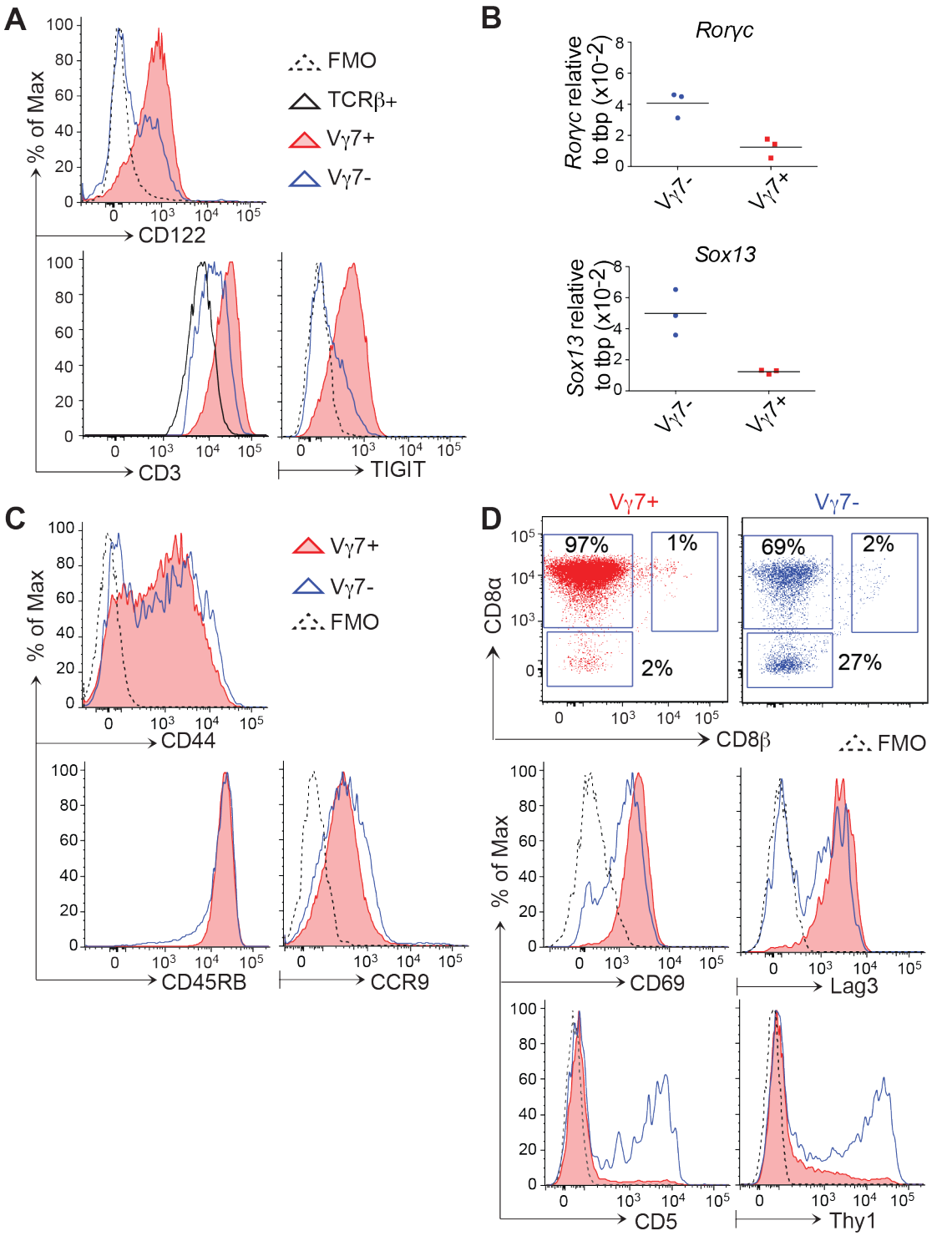

Figure 3.2 Phenotype of small intestinal γδ IEL in 21-40 day-old mice

A) Cell surface phenotypes of Vγ7$^+$, Vγ7$^-$ (CD3$^+$TCRβ$^-$Vγ7$^-$) and αβ IEL from 21-40 day-old mice (*n*≥*8*). **B)** Gene expression by qRT-PCR in Vγ7$^+$ *vs.* Vγ7$^-$ γδ IEL (*n*=*3*). **C-D)** Cell surface phenotypes of Vγ7$^+$ and Vγ7$^-$ (CD3$^+$TCRβ$^-$Vγ7$^-$) IEL from 21-40 day-old mice (*n*≥*8*). Data are representative of 1 (**B**), or ≥3 independent experiments (**A,C,D**). Data in panel (**B**) provided by Dr Jandke.

3.3 Intestinal selection of Vγ7$^+$ IEL

3.3.1 Neonatal small intestine harbours putative Vγ7$^+$ IEL precursors

Having defined the phenotype of signature Vγ7$^+$ IEL in mice at D21-40 (CD122^{HI}TCR^{HI}Lag3^{HI}CD5$^-$Thy1$^-$CD8αα$^+$) (**Figure 3.2**), these cell surface markers were used to identify the time point and anatomical location in which Vγ7$^+$ IEL attain phenotypic maturity. Interestingly, a number of studies have suggested that intestinal γδ IEL develop or mature extra-thymically (Lambolez et al., 2002; Lefrançois and Olson, 1994; Naito et al., 2008; Saito et al., 1998; K. Suzuki et al., 2000). In support of this hypothesis, significant numbers of intestinal γδ IEL, but not DETC or αβ IEL, develop in athymic NU/NU mice (Almeida et al., 2015; Guy-Grand et al., 1991; Nonaka et al., 2005). Furthermore, it has been shown that enterocyte-specific transgenic expression of IL-7 in IL-7$^{-/-}$ mice is sufficient to restore intestinal γδ IEL development in the absence of thymic output (Laky et al., 2000). Hence, small intestinal microenvironments appear to have a unique capacity to support extrathymic development and/or differentiation of Vγ7$^+$ IEL.

To test whether extrathymic maturation takes place in euthymic C57Bl/6 mice, the cell surface phenotype of Vγ7$^+$ IEL from 14 to 17 day-old mice was analysed by flow cytometry. We chose these specific time points because earlier time points were associated with T cell yields that were too small to analyse. Furthermore, previous data (**Figure 3.1B**) suggested that Vγ7$^+$ IEL are a minority of γδ IEL at this stage and thus may contain a greater representation of recently infiltrated Vγ7$^+$ T cells. In support of an extrathymic intestinal pathway of differentiation, the analysis identified an enrichment of Vγ7$^+$ IEL carrying an 'immature' CD122^{LO} cell surface phenotype between post-natal days (D)14 to 17, relative to weanling mice (D21-40) (**Figure 3.3A**).

These putative precursor cells could also be distinguished from Vγ7$^+$ IEL at D21-40 by low levels of cell surface TCR (by anti-CD3), CD122 and TIGIT, lack of expression of Lag3 and CD8α, and increased expression of Thy1 and CD5 (**Figure 3.3A**). Furthermore, a small proportion of Vγ7$^+$ IEL at D14-17 expressed CD24 (heat stable antigen), whereas CD24 expression was not seen after D21 (**Figure**

3.3A). Thus, the data suggest that 'immature' Vγ7$^+$ IEL could constitute a precursor to signature CD122^{HI}TCR^{HI} Vγ7$^+$ IEL that predominate amongst intestinal $\gamma\delta$ IEL from D21 (**Figure 3.1B, 3.2**).

To define the composite cell surface phenotype of a putative Vγ7$^+$ IEL precursor cell in D14-17 mice, we found that 'immature' cells could be segregated from 'mature' counterparts according to CD122$^{LO(MFI<200)}$Thy1$^+$, and CD122$^{HI(MFI>500)}$Thy1$^-$ status, respectively (**Figure 3.3B**). Applying this gating strategy to a comparative analysis of D14 *versus* D28 Vγ7$^+$ IEL, ~40% of Vγ7$^+$ IEL were classed as 'immature' at D14, compared to ~10% of Vγ7$^+$ IEL at D28. Combining this gating strategy with stringent phenotypic analysis of CD5, CD24, CD8α and Lag3 expression (**Figure 3.3A**), the phenotype of 'mature' Vγ7$^+$ IEL (CD122^{HI}Thy1$^-$CD8α^+Lag3$^+$CD24$^-$CD5$^-$) showed no overlap with putative 'immature' precursors (CD122^{LO}Thy1$^+$CD8α^-Lag3$^-$ CD24$^+$CD5$^+$) (*n*≥7; p<0.0001 *for statistical analysis of each marker individually*) (**Figure 3.3B**). Likewise, high expression of cell surface TCR and TIGIT also segregated with 'mature' CD122^{HI} Vγ7$^+$ IEL and not with 'immature' CD122^{LO} counterparts (**Figure 3.3C**). Thus, Vγ7$^+$ IEL at D14-17 were enriched for putative 'immature' precursor cells that carried a cell surface phenotype similar to Vγ7$^-$ $\gamma\delta$ IEL in weanling (W3-6) mice (**Figure 3.2A, D**) and to non-selected DETC progenitors in *Skint1*-mutant mice (CD122^{LO}, TCR^{LO}, CD24$^+$) (Lewis et al., 2006).

3.3.2 No evidence for intrathymic maturation of Vγ7$^+$ thymocytes

Having characterised a putative Vγ7$^+$ precursor population in neonatal small intestinal epithelium, we next sought to determine whether any component of the Vγ7$^+$ IEL phenotype is acquired by Vγ7$^+$ thymocytes. To test this, we used flow cytometric analysis to study Vγ7$^+$ thymocytes across 4 developmental time points (D1-D7; D14-D18; W3-W5; W5-W8) to compare their cell surface phenotype to that of signature Vγ7$^+$ IEL (**Figure 3.2**). Importantly, these time points span the first 8 weeks of life, encompassing peak thymus activity in C57Bl/6 mice (Hsu et al., 2003). Across all 4 time-points Vγ7$^+$ thymocytes were a rare population, totalling ~10,000 cells at D1-7, ~30,000 cells at D14-D18, ~40,000 cells at W3-W5, and ~20,000 cells at W5-W8 (**Figure 3.4A**). During W3-W5, Vγ7$^+$ thymocytes carried an 'immature' cell surface phenotype characterised by low CD45RB expression, high

CD5 expression and greater Thy1 expression relative to $V\gamma7^+$ IEL harvested from the same mouse (**Figure 3.4B**). The 'immature' cell surface phenotype of $V\gamma7^+$ thymocytes was replicated across the 4 time points analysed (**Figure 3.4C**). $V\gamma7^+$ thymocytes were also $CD8\alpha^-$ and expressed significantly lower CD122 levels and TCR (by anti-CD3), relative to $V\gamma7^+$ IEL from the same mouse (**Figure 3.4D**). Hence, there was no evidence for intra-thymic maturation of $V\gamma7^+$ thymocytes, which instead appeared to more closely phenocopy putative intestinal precursors of $V\gamma7^+$ IEL as they carried an 'immature' TCR^{LO}, $CD122^{LO}$, $Thy1^+$, $CD5^+$, $CD8\alpha^-$ cell surface phenotype.

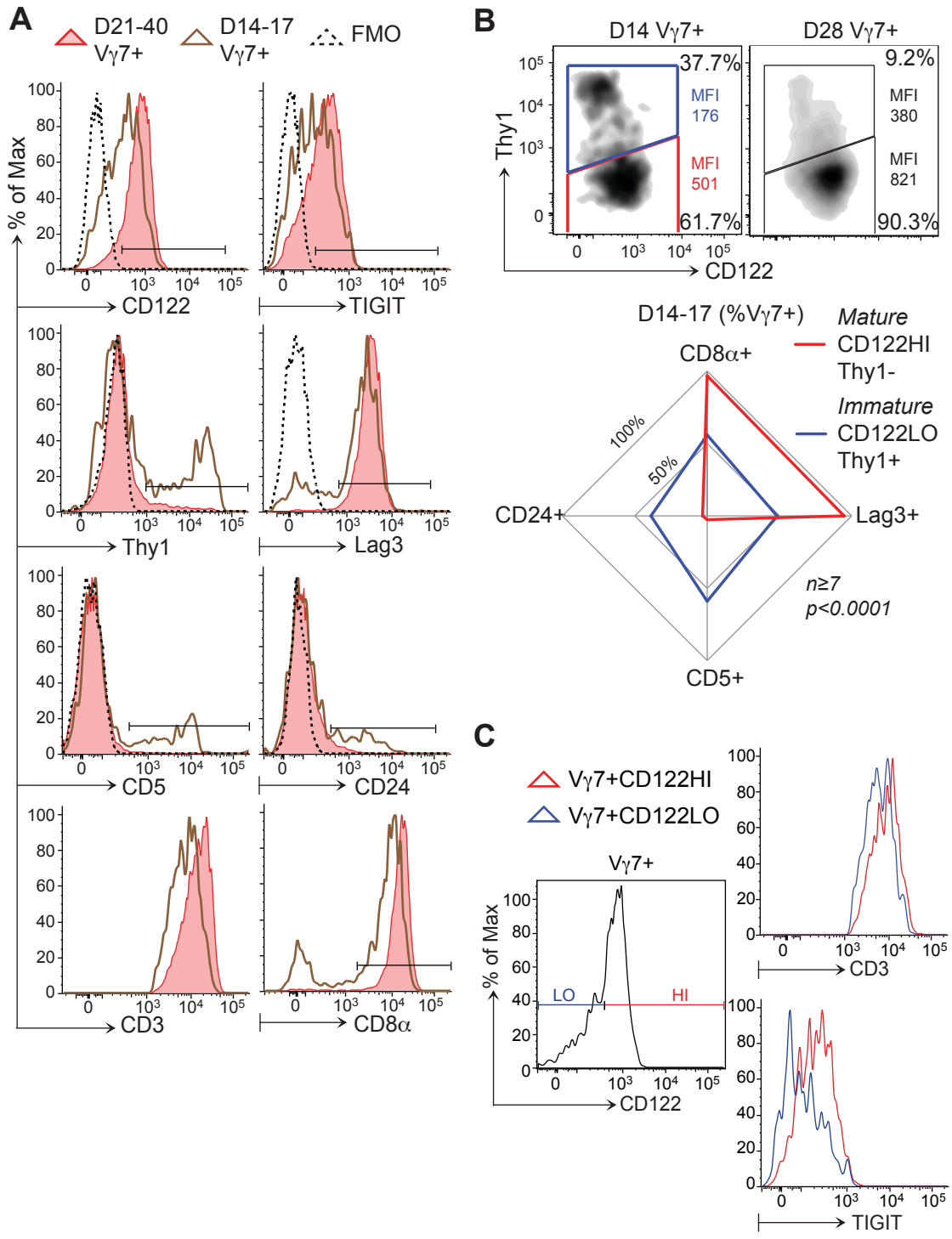

Figure 3.3 Phenotype of small intestinal Vγ7+ IEL in neonatal mice

A) Cell surface phenotypes of $V\gamma7^+$ IEL at postnatal day (D)14-17 *vs.* D21-40 (*n*≥7). **B)** *Upper:* Cell surface phenotype of $V\gamma7^+$ IEL at D14 *vs.* D28 (Median fluorescence intensity [MFI] corresponds to CD122). *Lower:* Cell surface phenotypes of $CD122^{HI}Thy1^{-}V\gamma7^+$ vs. $CD122^{LO}Thy1^+V\gamma7^+$ IEL at D14-17 (*n*≥7). **C)** Cell surface TIGIT expression at D14-17 in $V\gamma7^+CD122^{HI}$ *vs.* $V\gamma7^+CD122^{LO}$ IEL (*n*≥7). Data are representative of ≥3 (**A**,**B**-*upper*,**C**) experiments. Panel (**B**-*lower*) includes data pooled from ≥4 independent experiments.

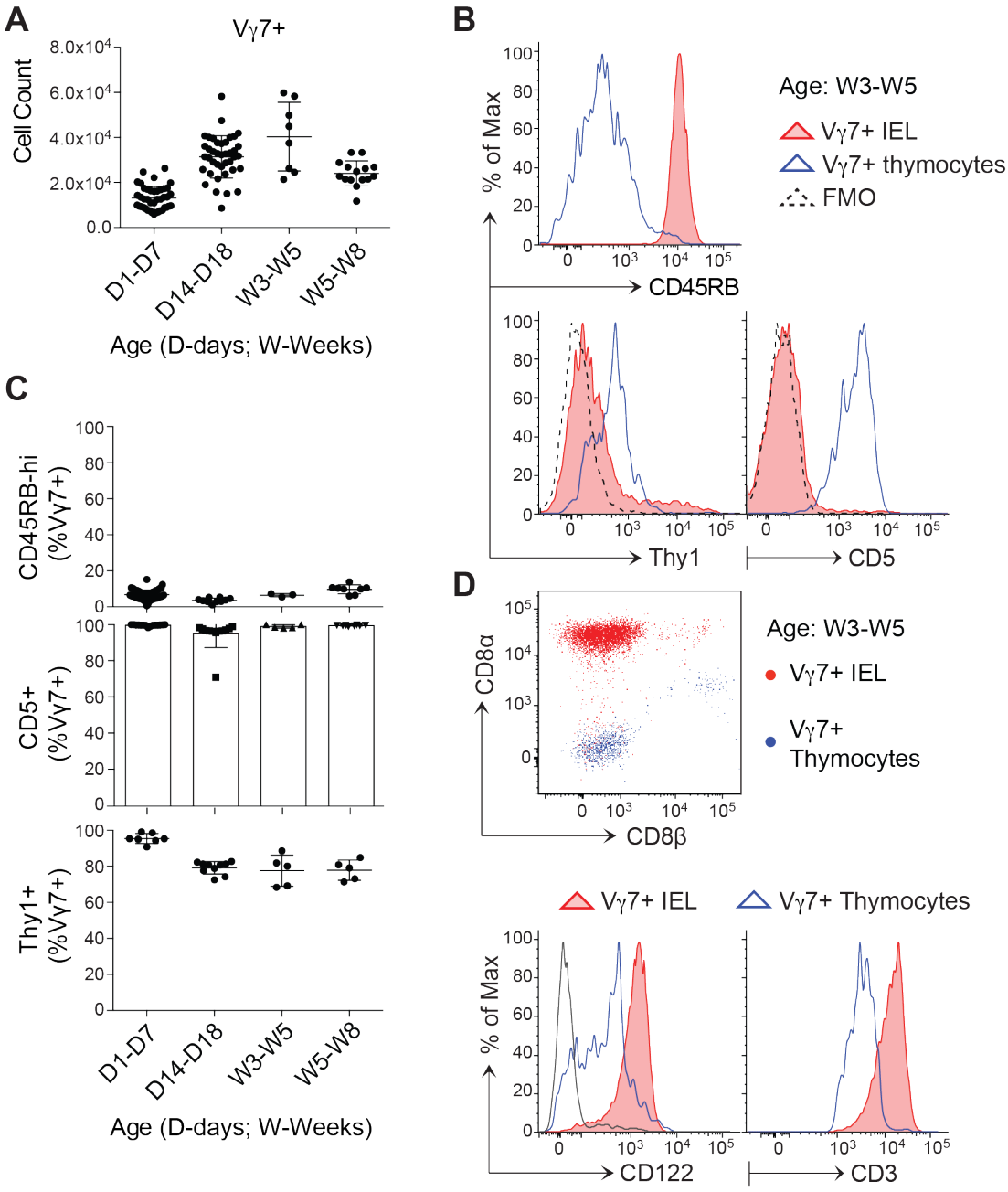

Figure 3.4 Phenotype of Vγ7$^+$ thymocytes

A) Quantification of Vγ7$^+$ thymocytes assayed by flow cytometry. **B)** Cell surface phenotypes of Vγ7$^+$ IEL and thymocytes (*n=5*). **C)** Cell surface phenotypes of Vγ7$^+$ thymocytes at indicated time points. **D)** Cell surface phenotypes of Vγ7$^+$ IEL and thymocytes (*n=5*). Data are representative of ≥2 (**B,D**) independent experiments. Panels include data pooled from >3 (**C**) or >6 (**A**) independent experiments.

3.3.3 Vγ7$^+$ IEL develop independently of the thymus or most peripheral lymphoid organs

Given that there was no evidence for intrathymic maturation of Vγ7$^+$ thymocytes, we sought to assess whether Vγ7$^+$ IEL could attain phenotypic maturity *via* extrathymic pathways in athymic NU/NU mice. To do this, we analysed γδ IEL composition and CD122 expression by flow cytometry of freshly recovered Vγ7$^+$ IEL. While adult (W8-13) NU/NU mice were depleted in αβ IEL (<10% of CD3$^+$ IEL), they retained a substantive compartment of γδ IEL that comprised >90% of all CD3$^+$ cells (**Figure 3.5A**). Absolute numbers of Vγ7$^+$ IEL in adult NU/NU mice were roughly ~3 fold lower than age-matched euthymic controls (~1.5M *versus* ~0.5M cells; *data not shown*). However, the representation of Vγ7$^+$ IEL amongst γδ IEL in NU/NU mice (~80%) was comparable, if not slightly enriched relative to euthymic controls (~70%). To better assess γδ IEL composition in NU/NU mice, GL2 analysis was included. GL2 antibody specifically engages the TCRVδ4$^+$ chain and ~20% of γδ IEL in euthymic and NU/NU mice were Vγ7$^+$GL2$^+$ (**Figure 3.5A**). Furthermore, Vγ7$^+$ IEL in NU/NU mice were uniformly CD122^{HI}, indicative of phenotypic maturity. Thus, we concluded that despite a reduction in absolute cell count, the development and maturation of Vγ7$^+$ and Vγ7$^+$GL2$^+$ IEL was unaffected by thymus-deficiency.

A recent study suggested that Vγ7$^+$ IEL require priming in PP or MLN before homing to the epithelium (Guy-Grand et al., 2013). To test this we analysed γδ IEL composition and CD122 expression in alymphoplasia (aly/aly) mice. aly/aly mice carry a partially penetrant loss-of-function point mutation in NF-κb-inducing kinase (Nik). As Nik is upstream of NF-κb activation in TNFSFR signal transduction, its loss of function impairs LTβR signalling during lymphoid tissue organogenesis and thus gives rise to mice that lack all lymph nodes, Peyer's patches and isolated lymphoid follicles (Fütterer et al., 1998; Shinkura et al., 1999). By contrast to athymic mice, aly/aly mice that had been surgically confirmed to lack peripheral and mesenteric lymph nodes, displayed comparable absolute numbers of Vγ7$^+$ (~2M) and Vγ7$^+$GL2$^+$ (~200,000) cells relative to age-matched controls (**Figure 3.5B**). Their γδ IEL compartments were enriched for Vγ7$^+$ IEL (~80%) and they

displayed a similar proportion of $V\gamma7^+GL2^+$ cells (~10%). Furthermore, $V\gamma7^+$ IEL were uniformly $CD122^{HI}$ suggesting they did not depend on priming in peripheral lymphoid organs for development (**Figure 3.5B**). Indeed, these findings further substantiate a report that found normal γδ IEL composition in aly/aly mice that were simultaneously athymic (Nonaka et al., 2005).

3.3.4 $V\gamma7^+$ IEL can develop independently of the microbiome and of dietary protein antigen

Given that $V\gamma7^+$ IEL could mature normally in NU/NU and aly/aly mice, we considered intestinal factors that may drive their local maturation. Strong candidates included antigens derived from the microbiome and/or diet. To test the effects of such factors, we analysed IEL composition and cell surface phenotype by flow cytometry of cells recovered from adult (W9-13) C57Bl/6 mice raised in total germ-free (GF) conditions, on a protein-antigen free diet (FAF) or on a protein-antigen free diet in germ-free conditions (GF/FAF). These 'antigen-free' mice were compared to C57Bl/6 controls raised in conventional specific pathogen-free conditions (SPF). Whereas γδ IEL made up ~50% of $CD3^+$ cells in SPF mice, their representation increased to ~60% in GF mice and ~75% in FAF and GF/FAF mice (**Figure 3.6**). Hence, αβ T cell but not γδ T cell recruitment to the small intestinal epithelium appeared to be partially dependent on the microbiome and greatly dependent on food-derived antigens, consistent with previous reports (Bandeira et al., 1990).

The decrease in αβ IEL representation in GF/FAF mice was predominantly attributed to loss of $TCR\beta^+CD8\alpha\beta^+$ cells which decreased from ~350,000 cells in SPF mice to ~150,000 in GF and ~100,000 in FAF and GF/FAF (**Figure 3.6**). $TCR\beta^+CD8\alpha^-$ IEL were also reduced in number, but these were a minor proportion to begin with (*data not shown*). By contrast, the representation of $V\gamma7^+$ IEL remained unchanged in GF, FAF and GF/FAF relative to SPF mice, making up ~60% of all γδ IEL irrespective of the antigen-exposure status of the mouse. Consequently, their mean absolute cell number increased slightly from ~400,000 cells in SPF mice, to ~500,000 cells in GF and FAF/GF mice and ~650,000 cells in FAF mice, possibly compensating for αβ IEL depletion that occurred under these

conditions (**Figure 3.6**). On analysis of CD122 expression, we found that $V\gamma7^+$ IEL from GF, FAF and GF/FAF mice were uniformly $CD122^{HI}$, indicating that they had attained phenotypic maturity in the absence of these exogenous local antigens. Hence, $V\gamma7^+$ IEL development and maturation was not dependent on a thymus, priming in peripheral lymphoid organs, or antigens derived from dietary proteins and the microbiome.

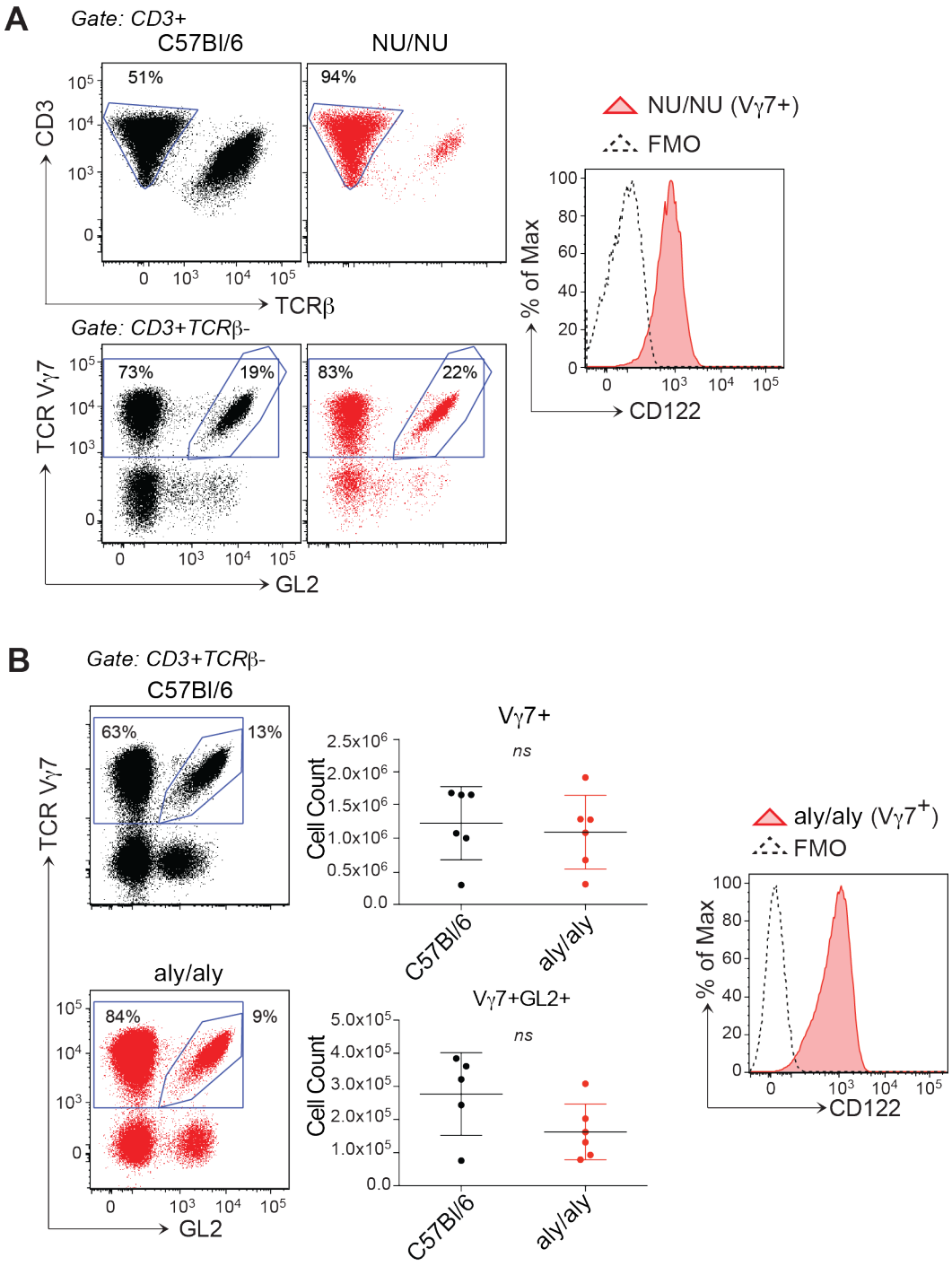

Figure 3.5 Analysis of Vγ7$^+$ IEL in NU/NU and aly/aly mice

A) *Left:* IEL composition in W8-14 wild type (WT) *vs.* NU/NU mice. The GL2 antibody detects the *TRDV2-2-encoded* Vδ4 chain. *Right:* Cell surface CD122 expression on NU/NU Vγ7$^+$ IEL (n≥12). **B)** γδ IEL composition (*left)*, cell count (*middle)* and cell surface CD122 expression (*right*) in W8-12 WT *vs.* alymphoid (aly/aly) mice. Panel (**A**) presents data representative of ≥3 independent experiments. Panel (**B**) presents data pooled from 2 independent experiments.

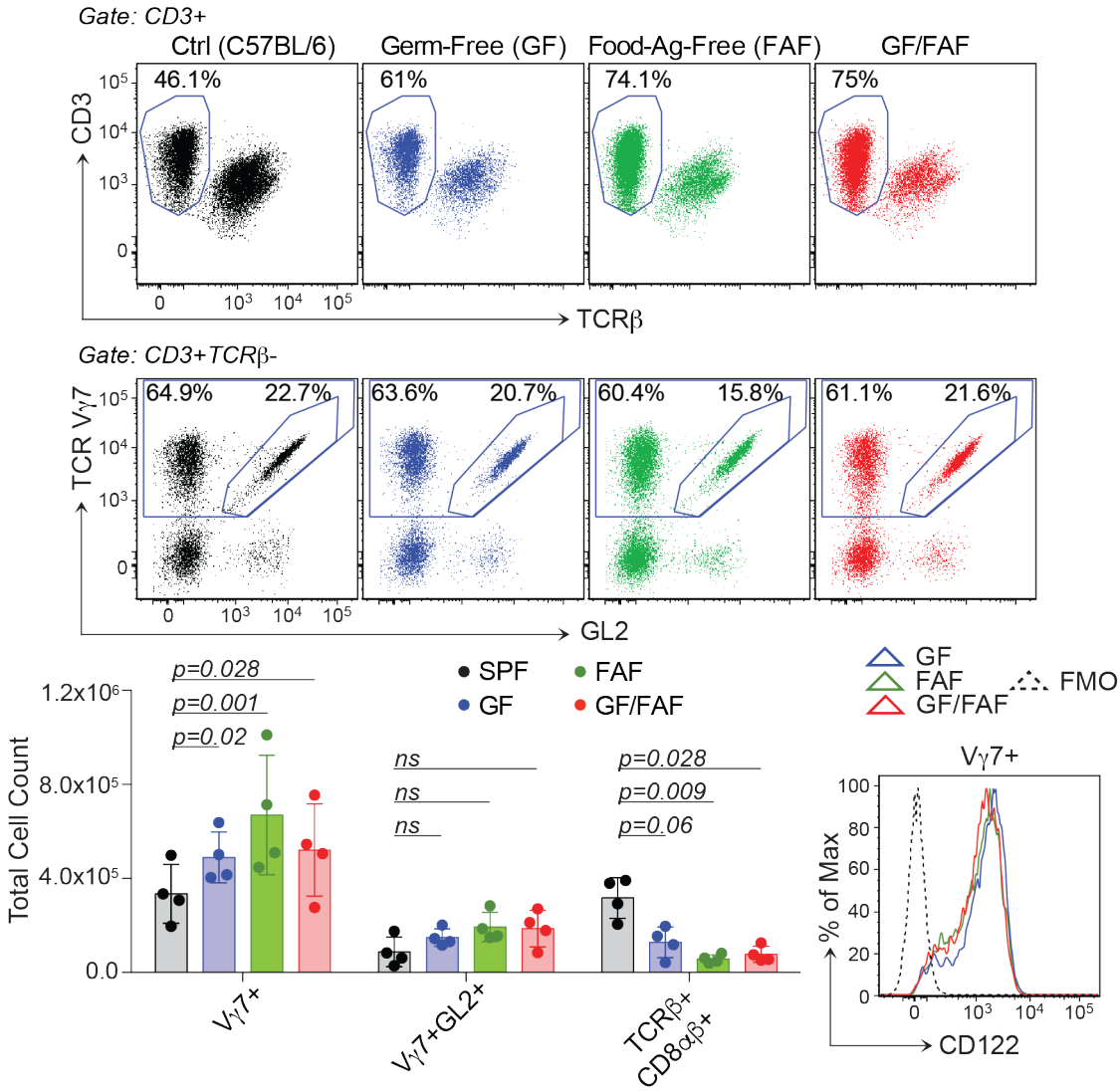

Figure 3.6 IEL development in germ-free and food antigen-free mice

IEL composition (*upper*), cell count (*lower left*), and CD122 expression (*lower right*) in SPF, germ-free (GF), food antigen-free (FAF), or GF-FAF C57Bl/6 mice at W9-13 (*n*≥*4*). Data are representative of 1 (GF-FAF) or 2 (SPF, GF, FAF) independent experiment(s).

3.3.5 Putative maturation checkpoint of Vγ7$^+$ IEL associated with significant changes in gene expression profile

Having established that Vγ7$^+$ IEL can develop independently of the thymus, peripheral lymphoid organs, the microbiome and diet-derived protein antigens, we considered that these cells' development and maturation may be driven by a germline-encoded factor similar to *Skint1*. *Skint1*-mediated selection of DETC progenitors is associated with their acquisition of a gene expression signature, which was characterised by a genome-wide expression analysis of Vγ5$^+$ foetal thymocytes in WT *versus* *Skint1*-mutant mice (Turchinovich and Hayday, 2011). Similar analyses have since been performed to compare the gene expression profile of 'immature' CD24^{HI} to 'mature' CD24^{LO} Vγ1$^+$, Vγ4$^+$ and Vγ1$^+$Vδ6$^+$ thymocytes (Narayan et al., 2012). However, the paucity of 'mature' Vγ7$^+$ thymocytes at any point during the first 8 weeks of life (**Figure 3.4A-D**) has hitherto prohibited any comparable analysis of their intrathymic development (Narayan et al., 2012). As our analysis of small intestinal Vγ7$^+$ IEL at D14-17 had identified both immature and mature Vγ7$^+$ IEL (**Figure 3.3B**), we proceeded to compare their gene expression profiles. To do this, RNA was purified from flow-sorted CD122^{HI}Vγ7$^+$ IEL and CD122^{LO}Vγ7$^+$ IEL that had been isolated from pooled D14-D17 mice on four separate occasions and subject to RNA sequencing (**Figure 3.7A**) (GEO accession number: GSE85422).

Altogether, 2664 genes showed statistically significant up- or down-regulation between CD122^{HI} and CD122^{LO} Vγ7$^+$ IEL. Consistent with their distinct cell surface phenotypes, many of these differentially regulated genes were identified as encoding cell surface proteins (**Figure 3.7A**-*GO Term: Cell Surface*). Furthermore, there was full concordance between gene expression profile and the cell surface phenotypes that we had defined in 'mature' and 'immature Vγ7$^+$ IEL (**Figure 3.3B**). Thus, we concluded that our purification strategy had been successful and that the data were representative of the two populations of interest.

To define the extent to which peripheral Vγ7$^+$ IEL maturation phenocopied *Skint1*-mediated DETC selection, we compared our gene list to genes that had previously been shown to be up- or down-regulated across the *Skint1*-mediated selection

checkpoint (Turchinovich and Hayday, 2011) (**Figure 3.7B**). Many genes that were up- (e.g. *Tnfrsf9* [4-1BB/CD137], *Xcl1* [lymphotactin]) or down-regulated (e.g. *Sox13, Sox4*, *Bcl11b*) in CD122^{HI} *versus* CD122^{LO} Vγ7^{+} cells, were similarly up- or down-regulated across the *Skint1*-selection checkpoint of DETC progenitors (**Figure 3.7B**). Of note, *Rorc* and *Tbx21* did not meet the stringent statistical cut off applied during our re-analysis of the *Skint1*-selection microarray dataset (hence, neither are included in **Figure 3.7B**). However, it was shown by qRT-PCR that *Tbx21* is up-regulated and *Rorc* is down-regulated during *Skint1*-mediated selection (Turchinovich and Hayday, 2011) and likewise, both genes were similarly up- and down-regulated in CD122^{HI} *versus* CD122^{LO} Vγ7^{+} IEL. Hence, both the *Skint1*-selection checkpoint of DETC progenitors and the putative peripheral maturation checkpoint of Vγ7^{+} IEL in D14-17 mice were associated with up-regulation of *Tbx21, Tnfrsf9*, *Xcl1* and *Tbx21* and down-regulation of *Sox13, Sox4, Rorc and Bcl11b*.

Deep gene ontology analysis revealed a striking enrichment of cell cycle genes in CD122^{HI} relative to CD122^{LO} Vγ7^{+} cells, which suggested these cells might be selectively expanding *in situ* (**Figure 3.7A**). Indeed, selective expansion at this early time point (D14-17) could explain the increase in abundance of Vγ7^{+} IEL from postnatal W2 to W3 (**Figure 3.1B**). To verify that this increase in abundance was not an artefact of variation in IEL recovery between suckling pups and weaned mice, we employed confocal microscopy to assess $\gamma\delta$ IEL composition in proximal small intestinal whole mounts at D17 relative to D21. Confocal analysis revealed an ~4-fold enrichment of Vγ7^{+} IEL at D21 relative to D17 in the proximal gut ($p=0.002$) (**Figure 3.8A**). Thus, we concluded that the peripheral maturation of Vγ7^{+} IEL might be accompanied by their selective expansion, enabling them to achieve representational predominance amongst small intestinal $\gamma\delta$ IEL by postnatal D21.

3.3.6 Vγ7^{+} IEL selectively expand *in situ*

To test our hypothesis that Vγ7^{+} IEL selectively cycled *in situ* in the neonatal gut, IEL were isolated at various time points and analysed for Ki67 expression by flow cytometry. Ki67 expression identifies all non-quiescent cells outside of G_0 in the cell cycle. Consistent with Vγ7^{+} IEL undergoing selective cycling *in situ*, as many as 2-

fold more Vγ7$^+$ cells stained positive for Ki67 relative to Vγ7$^-$ IEL at every time point between D14 and W5-7 (**Figure 3.8B**). From D14-16 to D21-24, the proportion of Vγ7$^+$ IEL expressing Ki67 increased from ~50% to almost 100%, which correlated with the increase in representation of 'mature' CD122^{HI}Thy1$^-$ cells at each of these time points (~60% and ~90%, respectively) (**Figure 3.8B; 3.3B**). By contrast ~25% of Vγ7$^-$ γδ IEL were Ki67$^+$ between D14-16, ~60% were Ki67$^+$ at D19, and <50% of Vγ7$^-$ cells were Ki67$^+$ from D21-24 to W5-7. By W5-7 Ki67 expression in the Vγ7$^+$ compartment had significantly declined and approached the levels of expression seen in Vγ7$^-$ IEL. In mice over 11 weeks old, IEL were mostly quiescent and Ki67 expression was virtually indistinguishable between the 2 compartments (**Figure 3.8B**). These data suggest that Vγ7$^+$ IEL selectively cycle in neonatal mice, from at least D14 to W5-7, after which the intestinal γδ IEL compartment as a whole is largely quiescent.

Because Ki67 is a broad marker of non-quiescence and may not necessarily correlate with cell division, we also compared DNA synthesis in Vγ7$^+$ IEL to Vγ7$^-$ IEL by incorporation of the thymidine analogue 5-ethynyl-2 deoxyuridine (EdU), during a 3hr pulse *in vivo* at D28. Whereas ~10% of Vγ7$^+$ IEL incorporated EdU, only ~4% of Vγ7$^-$ IEL were EdU$^+$ ($p<0.0001$) (**Figure 3.8C**). Furthermore, the rate of EdU incorporation in Vγ7$^+$ IEL was comparable to rapidly cycling CD8αβ$^+$ thymocytes, ~10% of which also incorporated EdU over a 3hr pulse (**Figure 3.8C**). Taken together, these data provide compelling evidence that the small intestinal epithelium accommodates the selective expansion of signature Vγ7$^+$ IEL between D14 and W5-7.

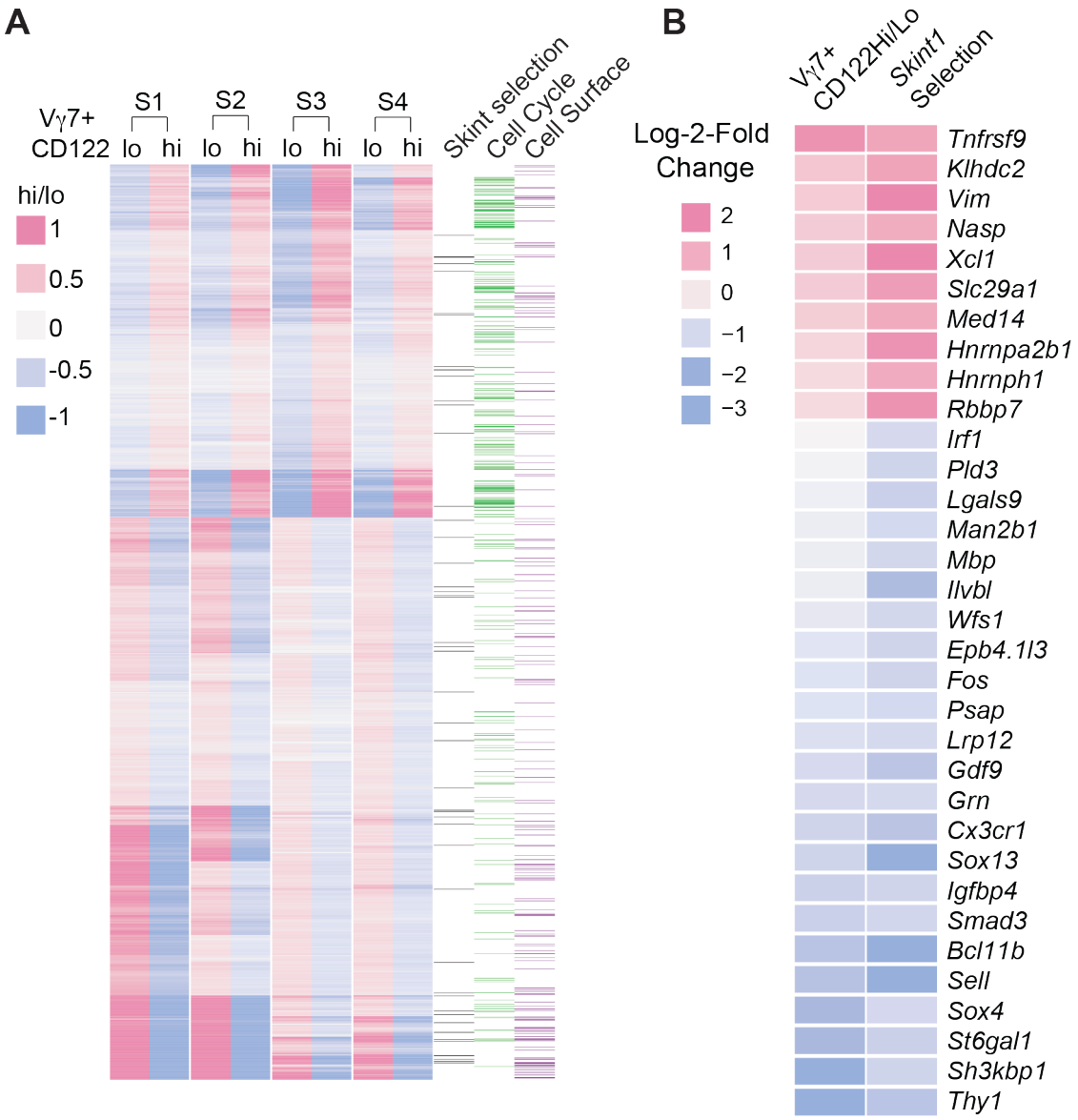

Figure 3.7 Gene expression analysis of neonatal small intestinal Vγ7^{+} IEL

A) Heat map of genes differentially regulated (log-2-FoldChange) between Vγ7^{+}CD122^{hi} and Vγ7^{+}CD122^{lo} IEL sorted from post-natal day (D)14-17 mouse pups. Data generated by total RNA sequencing ('cell cycle' & 'cell surface' GO terms annotated). Fold changes are scaled to median expression values across the samples. **B)** Heat map of genes differentially regulated between Vγ7^{+}CD122^{HI} and Vγ7^{+}CD122^{LO} IEL from D14-D17 mice and between *Skint1*-selected and non-selected Vγ5^{+} DETC progenitors (*n=4*). Data are representative of 1 experiment.

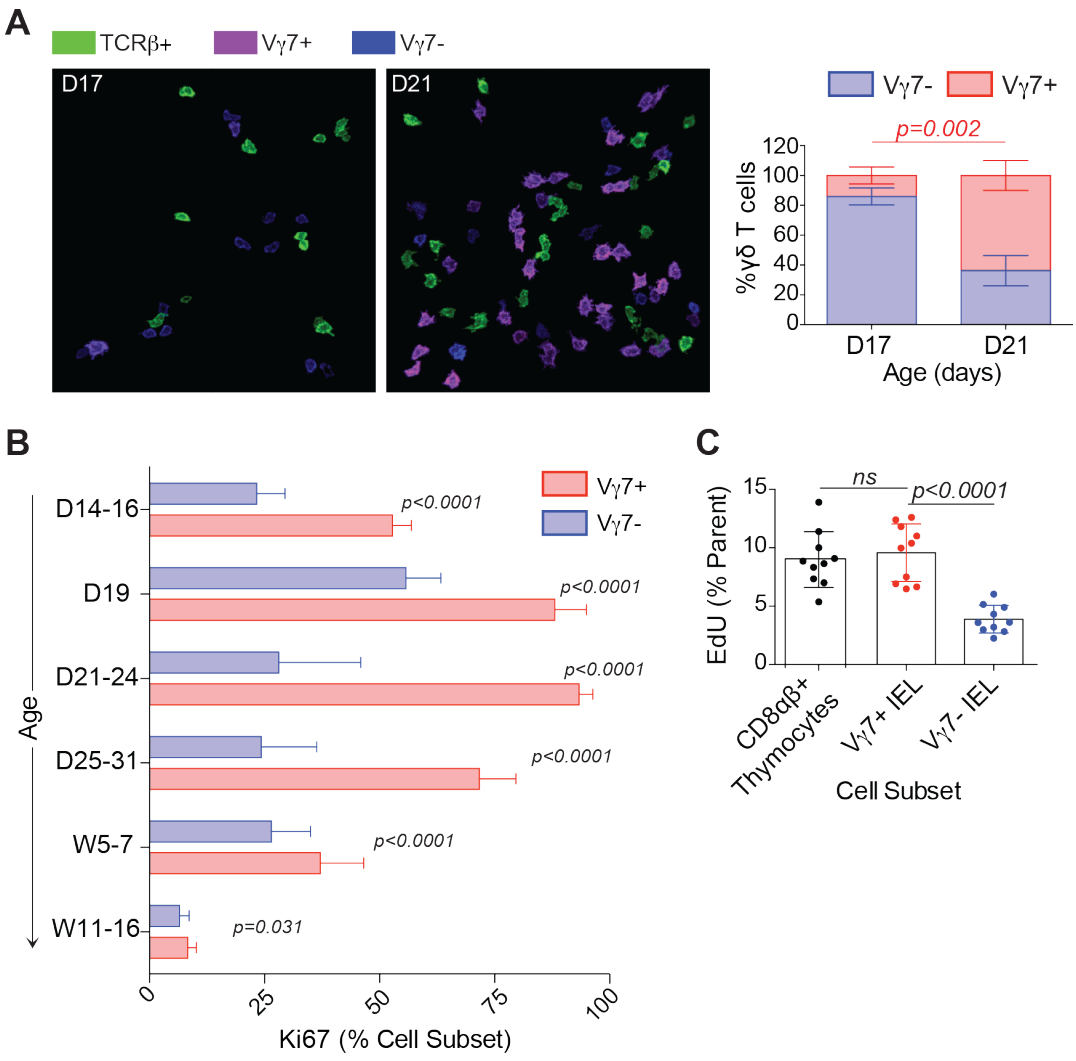

Figure 3.8 Cell cycle analysis of small intestinal γδ IEL

A) IEL composition assessed by confocal microscopy of proximal small intestinal whole mounts from post-natal day (D)17 (*left*) and D21 (*middle*) mice (*n=3*). *Right:* Quantification corresponding to confocal images. **B)** Ki67 expression in $V\gamma7^+$ *vs.* $V\gamma7^-$ IEL directly *ex vivo* (D19➔*n=4; all others*➔*n=8-27*). **C)** EdU incorporation during 3hr pulse *in vivo* in $V\gamma7^+$ and $V\gamma7^-$ ($CD3^+TCR\beta^-V\gamma7^-$) IEL and $CD8\alpha\beta^+$ thymocytes from 4 week-old mice assessed by flow cytometry. Panel (**A**) is representative of 1 experiment. Some panels include data pooled from 3 (**C**) or >20 (**B**) independent experiments. Data in panel (**A**) provided by Dr Hart.

3.4 Conclusions

Our studies have demonstrated that the small intestinal epithelium harbours signature V$\gamma7^+$ IEL that selectively expand *in situ* as the neonatal mouse develops into an adult. Having characterised the mature composition and cell surface phenotype of signature V$\gamma7^+$ IEL, we were able to show that this immune compartment develops in the absence of a thymus and peripheral lymph nodes, isolated lymphoid follicles and Peyer's patches. Their development was also not dependent on exogenous antigens derived from the microbiome or dietary protein.

Consistent with previous reports (Narayan et al., 2012), our studies have found no evidence for intra-thymic maturation of V$\gamma7^+$ thymocytes. However, they do provide some evidence to support an extra-thymic intestinal pathway of development for these cells. Phenotypically 'immature' V$\gamma7^+$ IEL were enriched for in the small intestinal epithelium of 14 to 17 day old animals. These putative precursors were characterized by their CD122^{LO}TCR^{LO}Thy1$^+$ status, which was reminiscent of pre-selection DETC in *Skint1*-mutant mice. Furthermore, several genes that were found to be up- or down-regulated in 'mature' CD122^{HI} *versus* 'immature' CD122^{LO} V$\gamma7^+$ IEL, were similarly up- or down-regulated by *Skint1*-mediated selection in DETC progenitors. While these data are consistent with CD122^{LO} V$\gamma7^+$ IEL being 'pre-selection precursors' of their CD122^{HI} counterparts, our study did not include a lineage-tracing analysis to conclusively demonstrate a true precursor-product relationship. Hence, we conclude that CD122^{LO} V$\gamma7^+$ IEL potentially represents an extra-thymic pre-selected precursor of CD122^{HI} V$\gamma7^+$ IEL.

Having defined the phenotypic hallmarks of V$\gamma7^+$ IEL and time frame over which it was universally acquired in the small intestinal epithelium, we proceeded to study the endogenous *Skint1*-like factors that may regulate these cells' development or maturation.

Chapter 4. *Btnl* genes in Vγ7$^+$ IEL development

4.1 Introduction

In seeking endogenous *Skint1*-like molecules that may regulate the development and composition of signature small intestinal γδ IEL, we turned our attention to the extended BTN/Btn gene family, to which *Skint* genes are closely related (Abeler-Dörner et al., 2012; Afrache et al., 2012). Outside of the *Skint* family, *Btnl1, Btnl4* and *Btnl6* display the greatest homology to *Skint1* (Bas et al., 2011). As with most butyrophilin(-like) genes, *Btnl1*, *Btnl4* and *Btnl6* encode type I membrane proteins with 2 extracellular Ig domains, a single transmembrane region and an intracellular B30.2 (PRY/SPRY) domain (see Chapter 1) (Rhodes et al., 2016). As *Skint1* has three transmembrane regions and lacks a B30.2 domain, its homology to *Btnl1*, *Btnl4*, and *Btnl6* is concentrated in its extracellular Ig domains (IgC and IgV), which features a strikingly similar amino acid sequence (**Figure 1.7**) (Bas et al., 2011).

Btnl1, Btnl4 and *Btnl6* are exclusively highly expressed in small intestinal enterocytes and are each encoded within the MHC class II locus, in a region of the genome that has previously been associated with regulating the variation in γδ IEL composition across genetically distinct inbred mouse strains (Lefrançois et al., 1990; Pereira et al., 1997). *In vivo,* Btnl1 protein forms heteromeric complexes with Btnl6 and reportedly displays a perinuclear staining pattern, which occasionally co-colocalizes with CD3$^+$ IEL (Bas et al., 2011; Lebrero-Fernández et al., 2016). *In vitro*, over-expressed *Btnl1* has been shown to regulate the effector response of intestinal epithelial cell lines during their incubation with IFNγ-rich supernatants of activated intestinal IEL (Bas et al., 2011). Given their selective expression in small intestinal enterocytes and striking similarity to *Skint1*, *Btnl1*, *Btnl4* and *Btnl6* are strong candidates for organ-specific regulators of signature small intestinal γδ IEL development. In support of this, it was recently shown that murine intestinal epithelial cell lines co-expressing *Btnl1* and *Btnl6* could selectively stimulate Vγ7$^+$ T cells *in vitro* (Lebrero-Fernández et al., 2016).

Having characterized a putative extrathymic pathway for the maturation and expansion of Vγ7$^+$ IEL (see Chapter 3), we hypothesized that it could be regulated by *Btnl1, Btnl4* and/or *Btnl6*. However, as there is very little known regarding the

function of *Btnl1*, *Btnl4* and *Btnl6* in the biological context of small intestinal physiology, we started by analysing the ontogeny of *Btnl* expression in small intestinal enterocytes.

To investigate the role of *Btnl1* and *Btnl4* in detail and to test our hypothesis that intestinal *Btnl* genes may regulate the peripheral maturation of signature intestinal Vγ7$^+$ IEL we obtained *Btnl1* and *Btnl4* knockout mice and tested the impact of *Btnl1*- and *Btnl4*-deficiency *in vivo* on the composition of $\gamma\delta$ IEL and systemic immune cell populations.

4.2 Ontogeny of intestinal *Btnl* gene expression

4.2.1 Intestinal *Btnl1*, *Btnl4* and *Btnl6* expression is detectable from post-natal day 7

To analyse the onset of *Btnl1, Btnl4* and *Btnl6* expression in the murine gut, qRT-PCR was performed on RNA purified from small intestinal tissue harvested at 12 time points between E15 and post-natal D37 (E15, D6, 7, 13, 14, 16, 17, 18, 21, 25, 28, 37). Proximal small intestinal tissue was selectively harvested for this assay because this is the region of the small intestine that has the greatest density of $\gamma\delta$ IEL (H. Suzuki et al., 2002; Tamura et al., 2003). *Btnl1, Btnl4* and *Btnl6* were all detectable before, during and after post-natal W2-3 (**Figure 4.1A**). *Btnl4* was first detected at E15, *Btnl1* and *Btnl6* became detectable by post-natal D6. *Btnl1* expression additionally increased by ~2-fold at D13 and expression of the three *Btnl* genes continued into adulthood (**Figure 4.1A**) (Bas et al., 2011; Lebrero-Fernández et al., 2016). Thus, the expression of the three *Btnl* genes was detectable within and beyond the developmental window of postnatal D14 to D21, which would be in agreement with their hypothezised role in regulating Vγ7$^+$ IEL maturation and expansion (**Figure 3.1B; 3.3 3.7; 3.8)**.

4.2.2 *Btnl1* expression is concentrated in post-mitotic villus enterocytes in the proximal 2/3 of the small intestine

To assess where in villus microanatomy *Btnl1 message* is expressed, analysis by RNAscope was performed on paraffin-embedded histological sections of small intestinal tissue. Proximal gut tissue was harvested from adult (W8-W10) mice that

had received a 3 hour pulse with bromodeoxyuridine (BrdU) (see Materials and methods), a thymidine analogue that incorporates into cells in S phase. *Btnl1* expression was detected in small intestinal epithelium, where it was concentrated in post-mitotic differentiated villus enterocytes and poorly detectable in rapidly dividing $BrdU^+$ crypt cells and the lamina propria (**Figure 4.1B**). The enrichment of *Btnl1* in post-mitotic villus enterocytes was detectable from post-natal D7 and showed no significant difference in its distribution when compared to small intestinal sections from D25 or adult (W8-10) mice (**Figure 4.1B,C**). Thus, the expression and anatomical distribution of *Btnl1* was established early in post-natal small intestine and was maintained as such into adulthood.

Previous studies have shown that γδ IEL density is greatest in the proximal small intestine and greatly decreases towards the ileum and colon (H. Suzuki et al., 2002; 2000; Tamura et al., 2003). To test whether the macroanatomical distribution of *Btnl1* expression along the length of the gut correlated with γδ IEL density, RNAscope analysis was performed on paraffin embedded gut sections taken from the proximal, medial and distal 1/3 of the small intestine and from the colon (**Figure 4.1C**). Histological analysis showed that *Btnl1* was poorly expressed in colon enterocytes relative to small intestinal enterocytes (**Figure 4.1D**). This was further substantiated by qRT-PCR, which identified a ≤2-fold and ≤10-fold enrichment of *Btnl1* in the proximal 2/3 of the small intestine relative to the distal 1/3 and colon, respectively (**Figure 4.1E**). In summary, *Btnl1* expression correlated with the reported gradient of γδ IEL as it was highly expressed in the proximal 2/3 of the small intestine and poorly expressed in the distal portion. Both the anatomical distribution of *Btnl1* expression and the temporal onset of *Btnl1*, *Btnl4* and *Btnl6* expression would accommodate their potential role in regulating $V\gamma7^+$ IEL development.

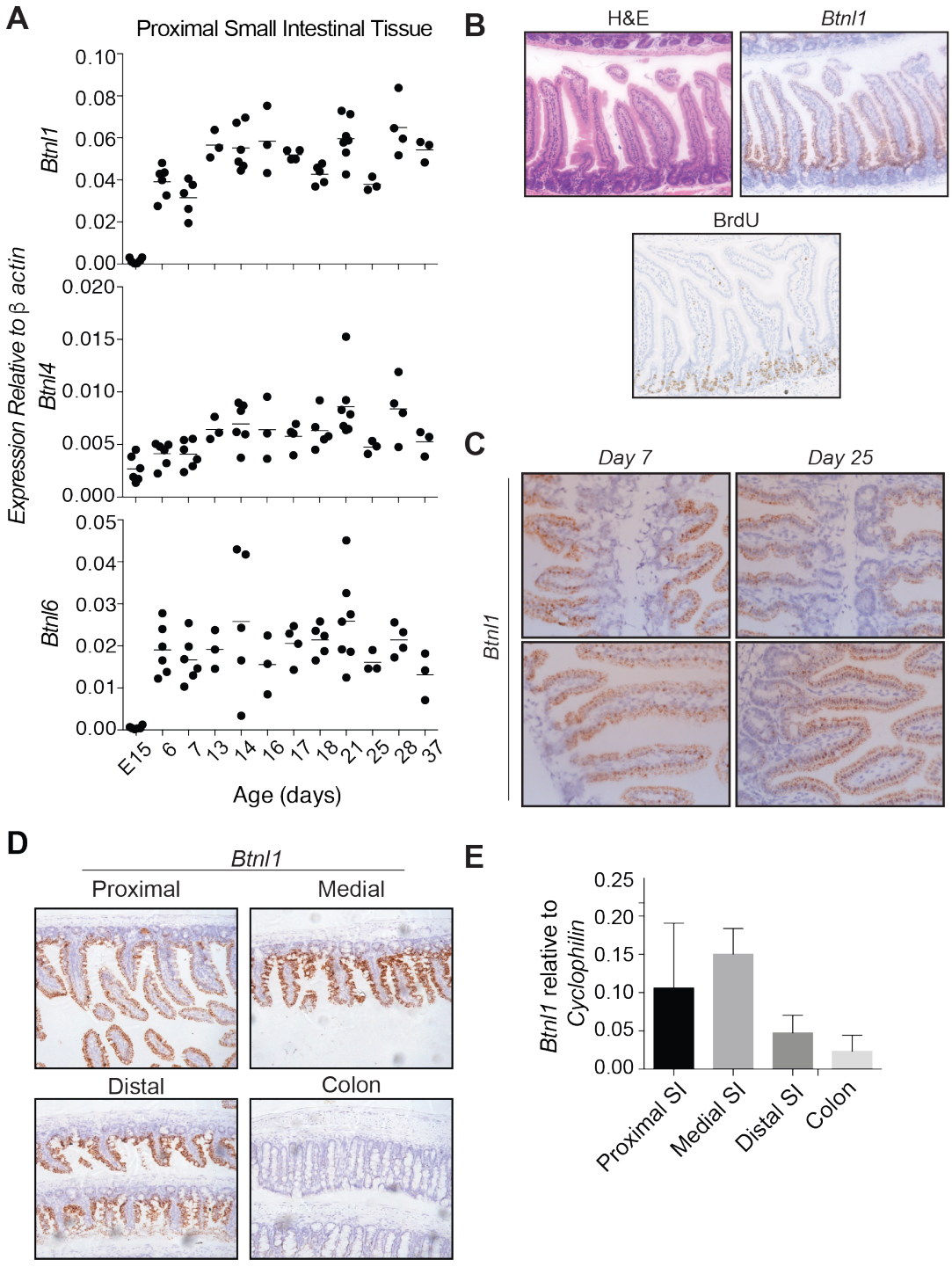

Figure 4.1 Intestinal expression of *Btnl* genes

A) Analysis of *Btnl1, Btnl4 and Btnl6* expression in proximal small intestine by qRT-PCR. **B)** *Top:* Histological analysis (H&E, *left), Btnl1* expression (RNAScope, *right*) and BrdU incorporation *vivo* (*bottom*) 3hrs after intraperitoneal injection, in paraffin-embedded sections of proximal small intestine (*n*≥*3*). **C-D)** RNAscope analysis of *Btnl1* expression (*n*≥*3*). **E)** Analysis of *Btnl1* expression by qRT-PCR (*n*=*3*). Data are representative of 1 (**B**) or ≥2 (**C,D,E**) independent experiments. Panel (**A**) includes data pooled from 2 independent experiments. qRT-PCR data provided by Dr Jandke (**A**) and Dr Cipolat (**E**).

4.3 Validation of *Btnl1*$^{-/-}$ and *Btnl4*$^{-/-}$ mice

To test the impact of *Btnl1* and *Btnl4* on the development of intestinal IEL, we obtained three independently generated strains of *Btnl1*$^{-/-}$ mice (CSD67994) and one of *Btnl4*$^{-/-}$ (CSD81524), that were each generated by targeted mutagenesis of embryonic stem (ES) cells by the International Knockout Mouse Consortium (IKMC) (**Figure 4.2A**). *Btnl1*$^{-/-}$ mice lack exons 3 and 4 of the *Btnl1* gene, which encode the extracellular IgV and IgC domains, respectively. *Btnl4*$^{-/-}$ mice lack exons 2-9, which encode most of the extracellular, transmembrane and intracellular domains of the peptide. Exons from both genes were targeted by homologous recombination and replaced by a cassette encoding a LacZ reporter construct and a neomycin resistance gene, which was used to select for targeted ES cells (**Figure 4.2A**).

4.3.1 *Btnl1* and *Btnl4* alleles were successfully targeted in *Btnl1*$^{-/-}$ and *Btnl4*$^{-/-}$ mice

Gene knockouts were confirmed by Southern blotting of genomic DNA purified from *Btnl1*$^{+/-}$ ES cells and tail tissue of C57Bl/6 (WT), *Btnl1*$^{-/-}$, *Btnl4*$^{-/-}$, and *Btnl4*$^{+/-}$ mice. DNA was digested with AseI for Btnl1 analysis or KpnI for Btnl4 analysis. Digoxigenin (DIG)-labelled DNA probes were generated to target an intronic region 5' to the *Btnl1* gene and 3' to the Btnl4 gene (**Figure 4.2A)**. As predicted from sequence information, WT *Btnl1* migrated at 7.095Kb, whereas targeted *Btnl1* migrated at 17.9Kb. WT *Btnl4* migrated at 7.8Kb, whereas targeted *Btnl4* migrated at 3.7Kb (**Figure 4.2B**). Successful targetting of *Btnl1* was further validated by additional Southern blots, probing for the intronic sequence 3' to the *Btnl1* gene and for insertion of the LacZ cassette (*data not shown*).

To verify that *Btnl1* and *Btnl4* expression was ablated in *Btnl1*$^{-/-}$ and *Btnl4*$^{-/-}$ mice, RNAscope analysis was performed on paraffin-embedded small intestinal tissue sections taken from WT, *Btnl1*$^{-/-}$ and *Btnl4*$^{-/-}$ mice. *Btnl1*, *Btnl4* and *Btnl6* all displayed similar enrichment in post-mitotic villus enterocytes in WT tissue (**Figure 4.3A**). No *Btnl1* and *Btnl4* expression was detected in *Btnl1*$^{-/-}$ and *Btnl4*$^{-/-}$ tissue respectively. By contrast non-targetted genes (e.g. *Btnl6*) were consistently detected in *Btnl1*$^{-/-}$ and *Btnl4*$^{-/-}$ mice. These data demonstrate that RNAscope

probes are both sensitive and specific to their respective targets. Further analysis of gene expression in *Btnl1*$^{-/-}$ mice found no detectable thymic expression (by qRT-PCR) of *Btnl1* and additionally demonstrated that thymic *Btnl1* expression in WT mice was >10^7-fold lower than that detected in small intestinal tissue (**Figure 4.3B**). Taken together, these data confirm that *Btnl1*$^{-/-}$ and *Btnl4*$^{-/-}$ mice do indeed lack expression of *Btnl1* and *Btnl4*, respectively.

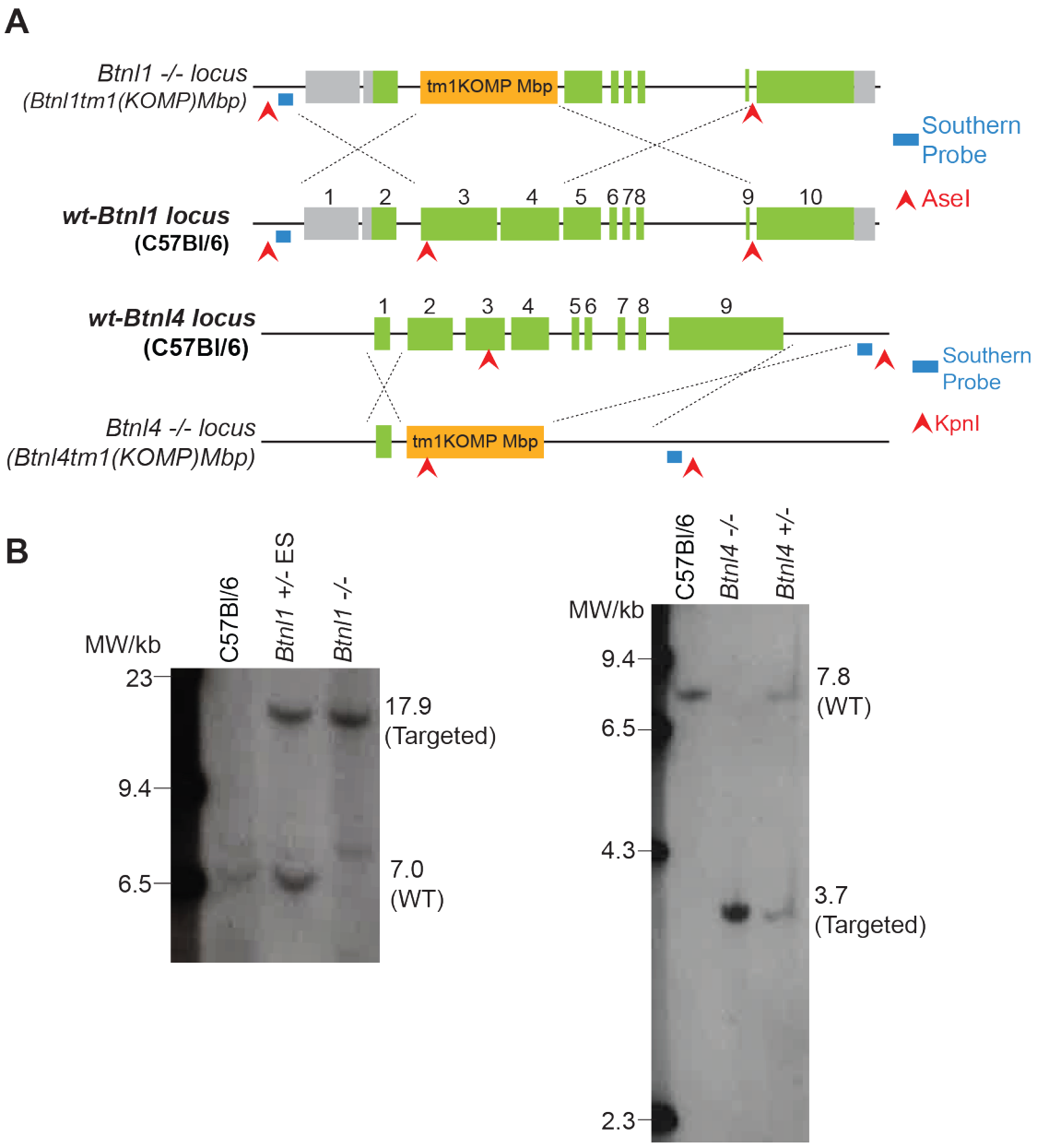

Figure 4.2 Btnl1$^{-/-}$ and Btnl4$^{-/-}$ mice

A) Organisation of WT and targeted loci for *Btnl1* and *Btnl4*. Grey: untranslated region; green: translated region; orange: targeting cassette. Knockout ES cell clones were obtained from the Knockout Mouse Project Repository (KOMP) IKMC-ID 67994 (Btnl1) and 81524 (Btnl4). **B)** DNA analysis by southern blot for targeting of alleles in *Btnl1*$^{-/-}$ (*left*) and *Btnl4*$^{-/-}$ (*right*) mice. Genomic DNA was digested using the indicated restriction enzymes (red arrowheads). Probes were generated to bind sequences upstream of *Btnl1* and downstream of *Btnl4* (blue bars: See materials and methods). Panel (**B**) is representative of 1 (*right*) or 2 (*left*) independent experiments. Data in panel (**B**-*right*) provided by Dr Jandke.

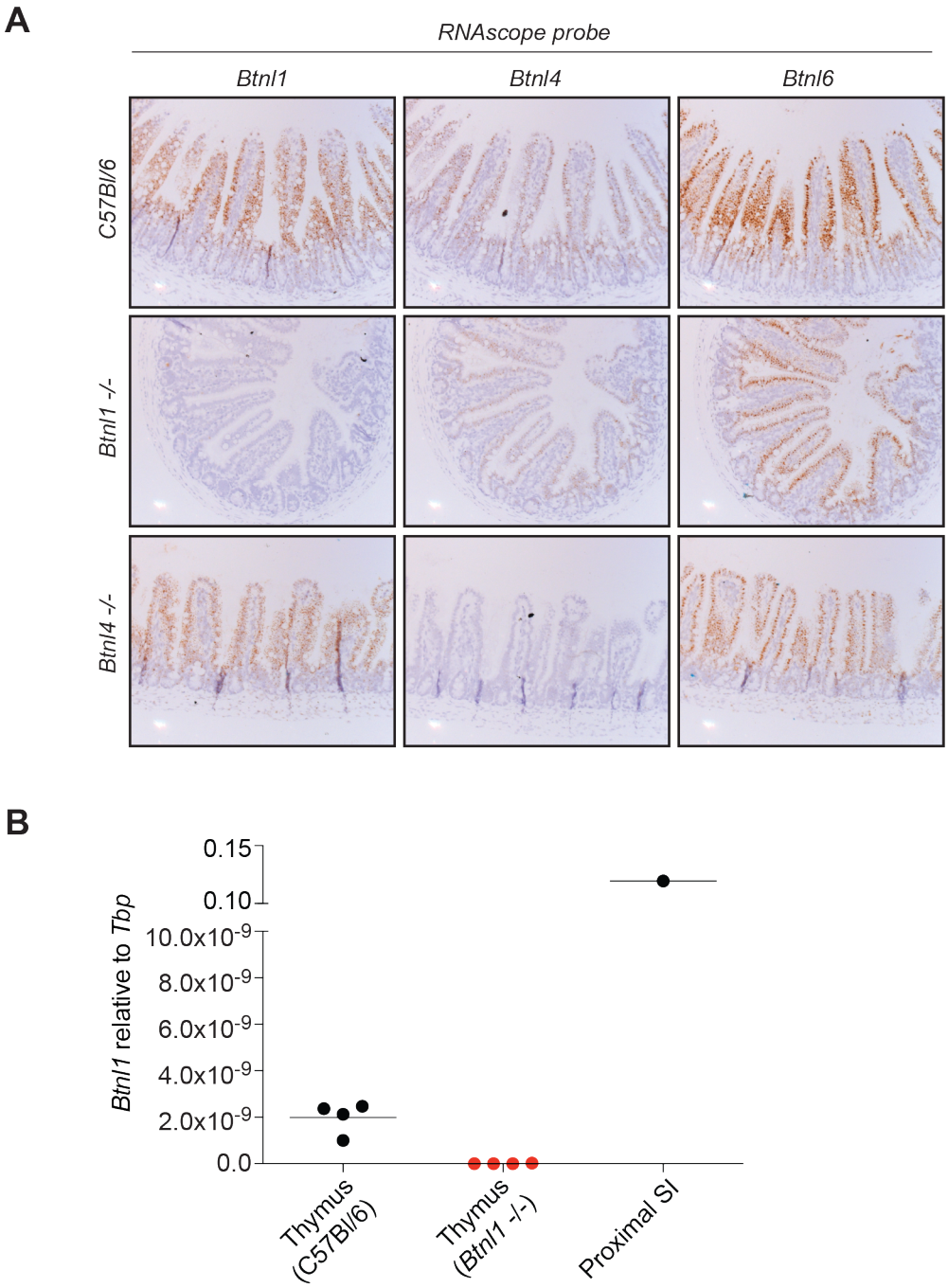

Figure 4.3 Btnl expression in *Btnl1*$^{-/-}$ and *Btnl4*$^{-/-}$ mice

A) Histological analysis of *Btnl1, Btnl4 and Btnl6* expression by RNAscope (*n*≥*3*). **B)** Analysis of *Btnl1* expression by qRT-PCR. Panel (**A**) is representative of 1 experiment. Data in panel (**B**) provided by Dr Roberts.

4.4 Impact of *Btnl* genes on IEL development *in vivo*

4.4.1 *Btnl1* but not *Btnl4* is critical for the development of signature intestinal Vγ7$^+$ IEL

To determine the impact of *Btnl1* on intestinal Vγ7$^+$ IEL development, IEL composition was assayed by flow cytometry of cells freshly recovered from the small intestine of adult (W6-15) WT *versus* *Btnl1*$^{-/-}$ mice. In three independently generated *Btnl1*$^{-/-}$ mouse strains, there was a ~3-fold reduction in the representation of Vγ7$^+$ IEL and an ≤8-fold reduction in that of Vγ7$^+$GL2$^+$ IEL amongst γδ IEL relative to WT and *Btnl1*$^{+/-}$ mice (**Figure 4.4**). This decrease in the representation of Vγ7$^+$ IEL translated into a ~90% reduction in absolute numbers of Vγ7$^+$ and Vγ7$^+$GL2$^+$ IEL in *Btnl1*$^{-/-}$ relative to WT mice (*p<0.0001)* (**Figure 4.4**). Loss of Vγ7$^+$ IEL was mostly compensated for by an expansion of *innate-like* TCRβ$^+$CD8αα$^+$ IEL (~1Million [M] cells in WT *versus* ~2M cells in *Btnl1*$^{-/-}$, *p<0.0001*) and a smaller increase in Vγ7$^-$ γδ IEL (0.9M in WT *versus* 1.6M in *Btnl1*$^{-/-}$, *p=0.0012*), which included both Vγ1$^+$ and Vγ4$^+$ IEL (**Figure 4.5A**). By contrast, there was no significant change in the absolute numbers of MHC-restricted TCRβ$^+$CD8αβ$^+$ and TCRβ$^+$CD8α$^-$ (mostly CD4$^+$) IEL (**Figure 4.4**). To exclude the formal possibility that *Btnl1* deficiency selectively impacted upon the recovery of Vγ7$^+$ IEL from the small intestinal epithelium, analysis of IEL composition by confocal microscopy was performed on whole mounts of proximal small intestinal tissue. Corroborating the data acquired by flow cytometry, *Btnl1*$^{-/-}$ mice displayed almost total depletion of Vγ7$^+$ IEL, which was associated with an expanded TCRβ$^+$ IEL compartment (**Figure 4.5B**). Thus, *Btnl1* expression was critical for the normal development of signature Vγ7$^+$ IEL.

By contrast to the profound and selective impact of *Btnl1* on Vγ7$^+$ IEL development, flow cytometry of small intestinal IEL recovered from adult (W12) *Btnl4*$^{-/-}$ mice revealed no significant differences in the representation of Vγ7$^+$ or Vγ7$^+$GL2$^+$ IEL relative to age-matched WT controls (**Figure 4.6A**). Furthermore, there was no significant difference in the absolute cell numbers of Vγ7$^+$, Vγ7$^+$GL2$^+$, Vγ7$^-$, TCRβ$^+$CD8αα$^+$ and TCRβ$^+$CD8αβ$^+$ recovered from the small intestine of *Btnl4*$^{-/-}$

relative to WT mice. Hence, *Btnl1* but not *Btnl4* was required for the development of signature intestinal Vγ7$^+$ IEL.

4.4.2 *Btnl1* is critical for the athymic development of signature intestinal Vγ7$^+$ IEL

As *Btnl1* is strongly expressed specifically in small intestinal villus epithelium, we considered that the impact of *Btnl1* is mediated extra-thymically and within the small intestine (**Figure 4.3A,B**). To test the contribution of *Btnl1* to *bona fide* extrathymic Vγ7$^+$ IEL development, *Btnl1*$^{-/-}$ mice were crossed with athymic NU/NU mice and the IEL composition was analysed by flow cytometry of cells freshly recovered from the small intestine. NU/NU.*Btnl1*$^{-/-}$ mice displayed a ~3-fold and ≤10-fold reduction in the representation of Vγ7$^+$ and Vγ7$^+$GL2$^+$ IEL amongst $\gamma\delta$ IEL, respectively, relative to age matched NU/NU controls (**Figure 4.6B**). As was shown for euthymic *Btnl1*$^{-/-}$ mice (**Figure 4.4**), this depletion in Vγ7$^+$ IEL equated to a >90% reduction in the overall number of Vγ7$^+$ and Vγ7$^+$GL2$^+$ cells recovered from the small intestine of NU/NU.*Btnl1*$^{-/-}$ relative to NU/NU mice (**Figure 4.6B**). Given these data, we concluded that although NU/NU mice harbour 3-4-fold fewer intestinal $\gamma\delta$ IEL relative to euthymic mice (Guy-Grand et al., 1991), the Vγ7$^+$ IEL that do develop are similarly dependent on *Btnl1*. Moreover, as NU/NU mice lack most $\alpha\beta$ IEL, these data refute the possibility that *Btnl1* deficiency drives expansion of TCRβ^+CD8$\alpha\alpha^+$ IEL, rather than depletion of Vγ7$^+$ IEL. In summary, *Btnl1* was critical for the development of Vγ7$^+$ IEL in euthymic and athymic mice.

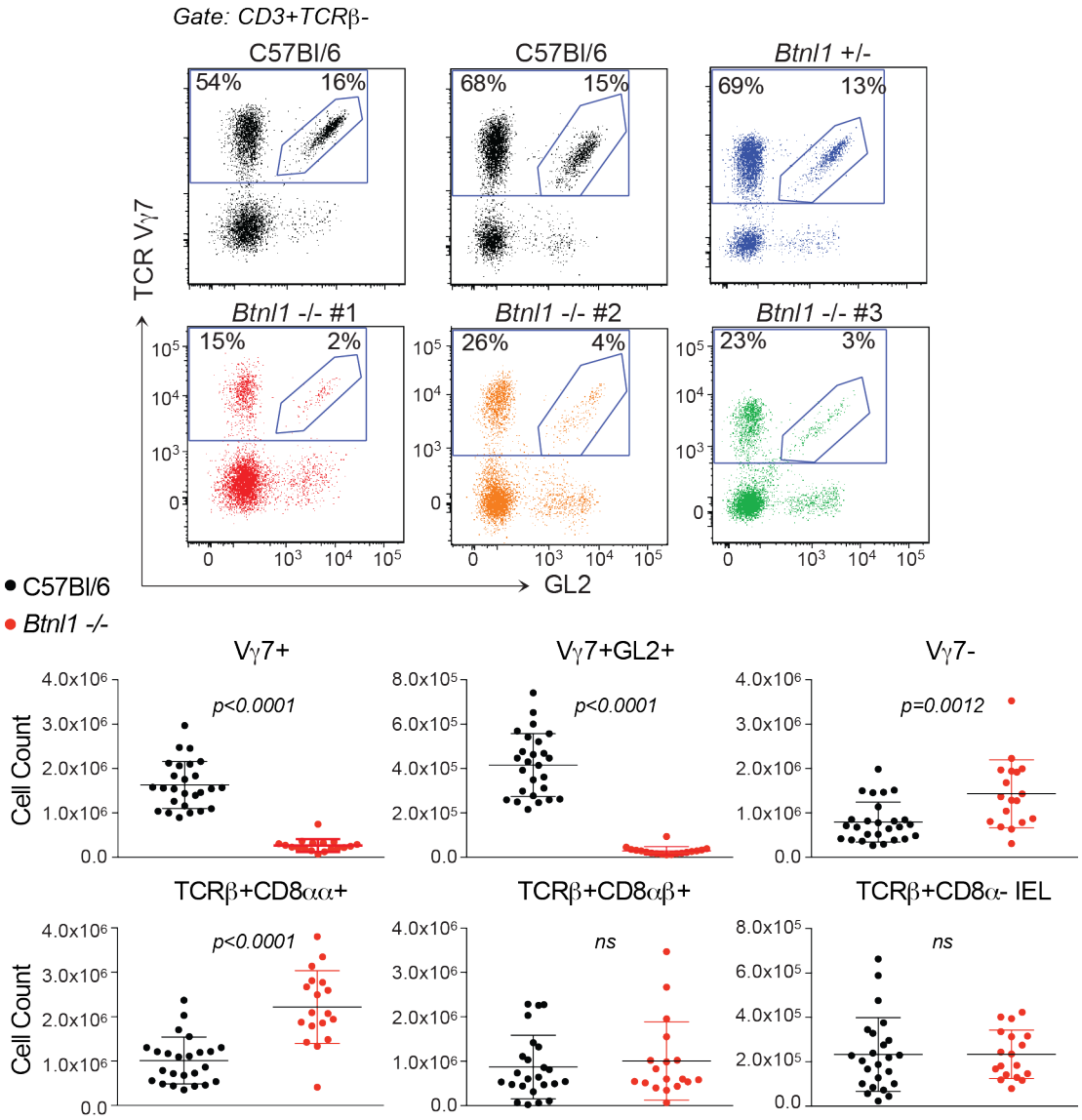

Figure 4.4 IEL composition in *Btnl1*$^{-/-}$ mice

Upper: Representative dot plots from 3 independently derived *Btnl1*$^{-/-}$ lines and associated controls (n≥6). *Lower:* Enumeration of IEL subsets in W6-15 WT *vs.* *Btnl1*$^{-/-}$ mice by flow cytometry. Lower panel includes data pooled from 6 independent experiments.

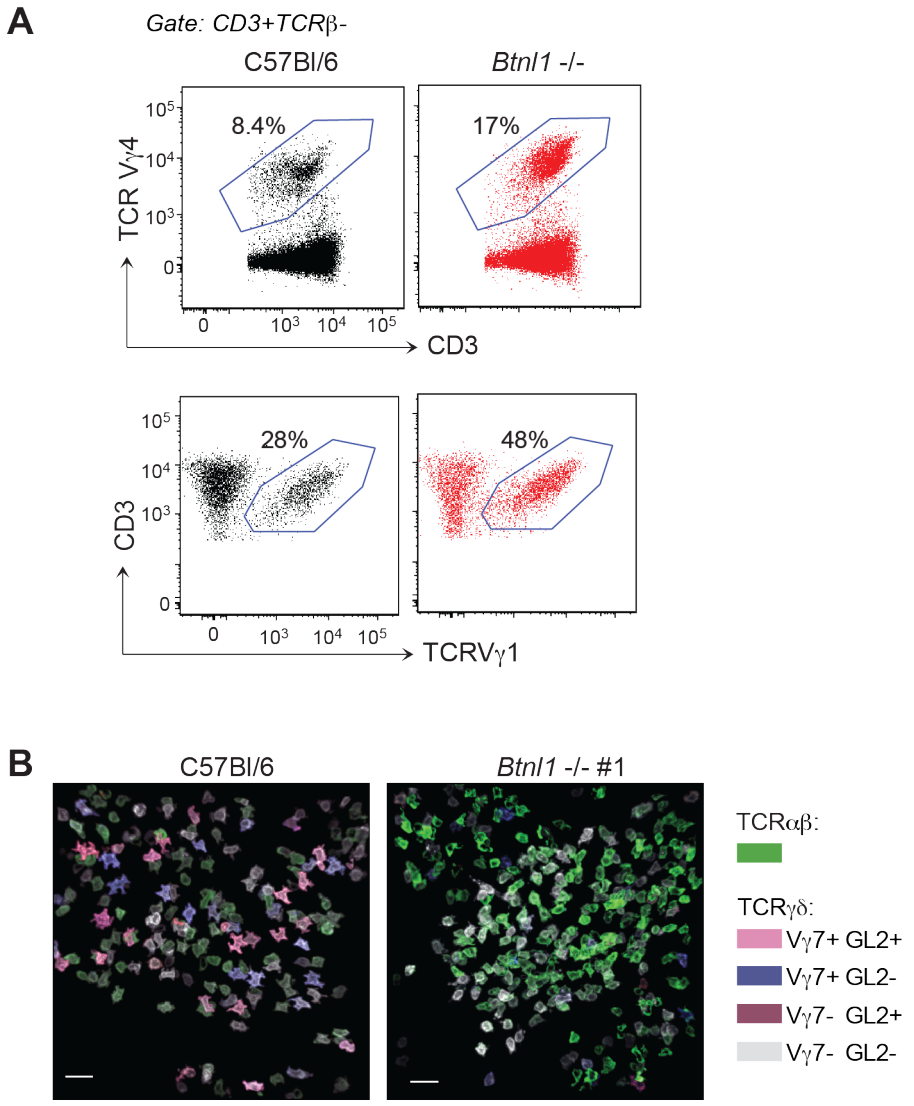

Figure 4.5 IEL composition in *Btnl1*$^{-/-}$ mice

A) TCRVγ1 and TCRVγ4 chain usage amongst small intestinal γδ IEL in WT *vs.* *Btnl1*$^{-/-}$ mice (n=8-16) **B)** Representative maximum intensity projections from confocal analysis of IEL composition in proximal small intestinal whole-mounts from adult WT *vs.* *Btnl1*$^{-/-}$ mice. (*n=3*). Data are representative of 1 (**B**), or >4 (**A**) independent experiments. Data in panel (**B**) provided by Dr Hart.

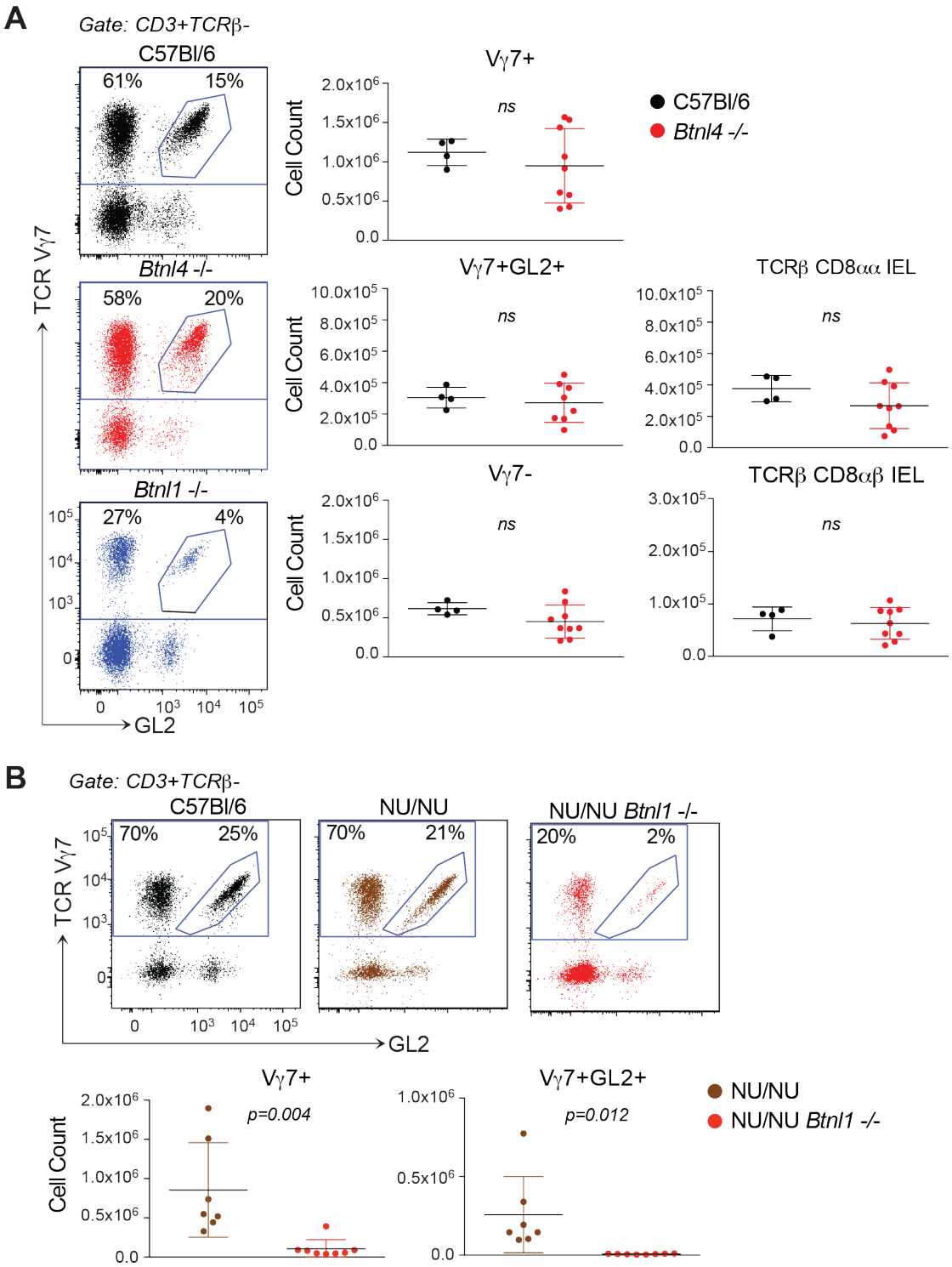

Figure 4.6 IEL composition in *Btnl1*$^{-/-}$ and *Btnl4*$^{-/-}$, NU/NU and NU/NU.*Btnl1*$^{-/-}$ mice

A) γδ IEL composition (*left*) and absolute numbers (*right*) of γδ and αβ IEL subsets in W12 WT *vs. Btnl4*$^{-/-}$ mice. **B)** γδ IEL composition (*upper*) and absolute numbers (*lower*) of Vγ7^{+} and Vγ7^{+}GL2^{+} IEL in W10-12 NU/NU *vs.* NU/NU.*Btnl1*$^{-/-}$ mice. Panels (**A**) and (**B**) each include data pooled from 2 independent experiments. Data in panel (**A**) provided by Dr Jandke.

4.5 The specificity of *Btnl1* for Vγ7$^+$ IEL

4.5.1 *Btnl1* has no impact on systemic immune cell composition

The impact of the *Skint1* mutation is highly specific to signature Vγ5$^+$ DETC and has no reported consequences for systemic immune composition (Barbee et al., 2011; Boyden et al., 2008; Lewis et al., 2006; Turchinovich and Hayday, 2011). To test the specificity of *Btnl1* for Vγ7$^+$ IEL, a comprehensive multi-parametric flow cytometry analysis of immune cell composition was performed in cells freshly isolated from the mesenteric lymph nodes and spleen of *Btnl1*$^{-/-}$, *Btnl1*$^{+/-}$ and WT adult (W10-W11) mice. The analysis was designed and performed by the Infection and Immunity Immunophenotyping (3i) consortium and included a complete analysis of mesenteric lymph node (MLN) T cell composition and splenic T cell, B cell and myeloid cell composition (see materials and methods). There was no significant difference in splenic T cell, B cell and myeloid cell or MLN T cell composition between WT, *Btnl1*$^{+/-}$ and *Btnl1*$^{-/-}$ mice (**Figure 4.7; 4.8**). Furthermore, flow cytometric analysis of TCRVγ chain usage within splenic and MLN γδ T cell compartments revealed no significant difference in the representation of Vγ1$^+$ (~50%), Vγ4$^+$ (~25%), Vγ7$^+$ (<10%) and Vγ1/4/6$^-$ triple negative (~10%) γδ T cells between adult (W10-11) WT, *Btnl1*$^{+/-}$ and *Btnl1*$^{-/-}$ mice (**Figure 4.9**). Therefore we concluded that *Btnl1* had no detectable impact on the composition of these systemic immune compartments.

4.5.2 *Btnl1* has no impact on the development of Vγ7$^+$ thymocytes

To check whether *Btnl1* has an impact on Vγ7$^+$ thymocyte development, flow cytometric analysis was employed to quantify and phenotype Vγ7$^+$ thymocytes from WT, *Btnl1*$^{+/-}$ and *Btnl1*$^{-/-}$ mice at postnatal D4-5, D14-15 and W5-W8. There was no significant difference in the absolute numbers of Vγ7$^+$ or Vγ7$^+$GL2$^+$ thymocytes in *Btnl1*$^{-/-}$ mice relative to WT mice at D14-15 and W5-8, or relative to *Btnl*$^{+/-}$ mice at D4-5 (**Figure 4.10A**). Furthermore, there was no detectable difference in cell surface phenotype in Vγ7$^+$ thymocytes from *Btnl1*$^{-/-}$ mice relative to WT mice at D14-15 and W5-8, or relative to *Btnl*$^{+/-}$ mice at D4-5 (**Figure 4.10B**). Indeed, as previously shown (**Figure 3.4A-D**), Vγ7$^+$ and Vγ7$^+$GL2$^+$ thymocytes were mostly

CD122^{-} or CD122^{LO}, CD45RB^{LO}, CD5^{+}, CD24^{+}, CD69^{-} and Thy1^{+} (**Figure 4.10B**). Hence, Vγ7^{+} thymocytes retained an 'immature' cell surface phenotype irrespective of *Btnl1* expression over the first 8 weeks of life, during which thymus activity is at its peak in C57Bl/6 mice (Hsu et al., 2003). There was therefore no evidence that *Btnl1* had any impact outside of the small intestinal signature Vγ7^{+} IEL compartment.

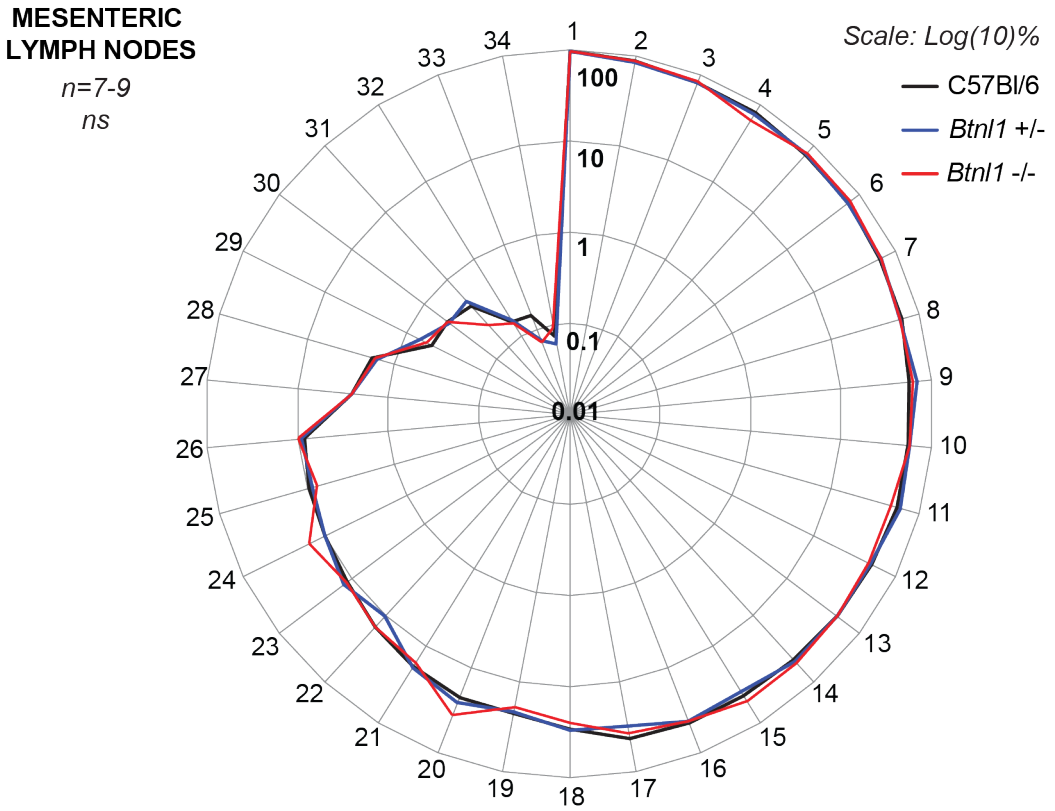

MESENTERIC LYMPH NODES

1	Total αβ T cells - % of total T cells	18	Effector CD4- NKT cells - % of CD4- NKT cells
2	CD4+ T helper cells - % of CD4+	19	Effector γδ T cells - % of γδ T cells
3	Resting CD4+ T helper cells - % of CD4+	20	Resting CD4+ NKT cells - % of CD4+ NKT cells
4	Effector CD4+ NKT cells - % of CD4+ NKT cells	21	Effector CD4+ T helper cells - % of CD4+ T helper cells
5	Resting γδ T cells - % of γδ T cells	22	KLRG1+ NK cells - % of NK cells
6	Resting CD4- NKT cells - % of CD4- NKT cells	23	Total Treg cells - % of CD4+
7	Naive CD8+ T cells - % of CD8+	24	KLRG1+ CD4+ NKT cells - % of CD4+ NKT cells
8	Total T cells - % of CD45+	25	Effector CD8+ T cells - % of CD8+
9	Total CD4+ NKT cells - % of NKT cells	26	Resting CD8+ T cells - % CD8+
10	Total CD4+ T cells - % of αβ T cells	27	Total γδ T cells - % of total T cells
11	Effector NK cells - % of NK cells	28	KLRG1 Treg cells - % of Treg
12	Effector Treg cells - % of Treg	29	Total NKT cells - % of CD45+
13	CD5+ γδ T cells - % of γδ T cells	30	Total NK cells - % of CD45+
14	Resting Treg cells - % of Treg	31	KLRG1+ CD4- NKT cells - % of CD4- NKT cells
15	Resting NK cells - % of NK cells	32	KLRG1+ CD4+ T helper cells - % of CD4+ T helper cells
16	Total CD8+ T cells - % of αβ T cells	33	KLRG1+ γδ T cells - % of γδ T cells
17	Total CD4- NKT cells - % of NKT cells	34	KLRG1+ CD8+ T cells - % of CD8+

Figure 4.7 Mesenteric lymph node immune composition in WT, *Btnl1*$^{+/-}$ and *Btnl1*$^{-/-}$ mice

Mesenteric lymph node T cell composition assayed by multi-parametric flow cytometry in W10-11 adult mice. Data are presented as Log_{10}(% indicated subset). Radar plot presents mean values (*n=8*). Data are representative of 1 experiment performed in collaboration with Dr Laing and 3i team.

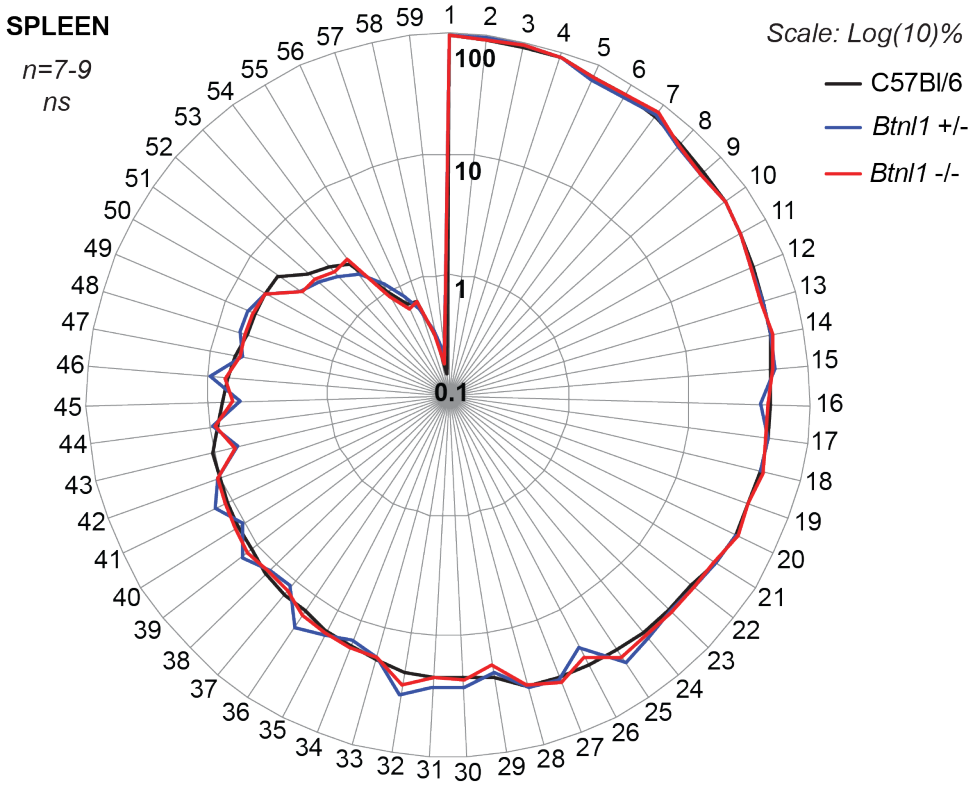

SPLEEN

1 Total B2 cells - % of B cells
2 Total αβ T cells - % of total T cells
3 Effector CD4+ NKT cells - % of CD4+ NKT cells
4 CD4+ T helper cells - % of CD4+
5 Resting NK cells - % of NK cells
6 Resting CD4+ T helper cells - % of CD4+ T helper cells
7 Conventional DC (cDC) - % of DC
8 Naive CD8+ T cells - % of CD8+
9 Resting Treg cells - % of Treg
10 Total CD4+ NKT cells - % of NKT cells
11 Total CD4+ T cells - % of αβ T cells
12 Resting γδ T cells - % of γδ T cells
13 Resting CD4- NKT cells - % of CD4- NKT cells
14 Conventional CD11b type DC - % of cDC
15 B2 t3 + f1 + f2 + gc cells - % of B2 cells
16 KLRG1+ NK cells - % of NK cells
17 Conventional CD8α type DC - % of cDC
18 Effector CD4- NKT cells - % of CD4- NKT cells
19 Total B cells - % of CD45+
20 Effector γδ T cells - % of γδ T cells
21 Total CD8+ T cells - % of αβ T cells
22 Follicular 2 B cells - % of B2 cells
23 Total CD4- NKT cells - % of NKT cells
24 Effector Treg cells - % of Treg
25 Granulocytes + monocytes - % of myeloid cells
26 Total DC - % of myeloid cells
27 CD5+ γδ T cells - % of γδ T cells
28 Total T cells - % of CD45+
29 Plasmacytoid DC - % of DC
30 Effector CD4+ T helper cells - % of CD4+ T helper cells
31 Effector NK cells - % of NK cells
32 Granulocytes - % of myeloid cells
33 B2 t1 + t2 cells - % of B2 cells
34 B2 marginal zone + precursor cells - % of B2 cells
35 Resting CD8+ T cells - % of CD8+ T cells
36 CD103+ CD8α+ DC - % of CD8+ cDC
37 Transitional 1 B cells - % of B2 cells
38 Monocytes - % of myeloid cells
39 Eosinophils - % of myeloid cells
40 Marginal zone B cells - % of B2 cells
41 Transitional 3 + follicular 1 B cells - % of B2 cells
42 Total Treg cells - % of CD4+
43 Resting CD4+ NKT cells - % of CD4+ NKT cells
44 Effector CD8+ T cells - % of CD8+
45 Macrophages - % of myeloid cells
46 Total myeloid cells - % of CD45+
47 Total γδ T cells - % of total T cells
48 KLRG1+ Treg cells - % of Treg
49 Transitional 2 B cells - % of B2 cells
50 Marginal zone precursor B cells - % of B2 cells
51 KLRG1+ CD4+ NKT cells - % of CD4+ NKT cells
52 B1a cells - % of B cells
53 Total NK cells - % of CD45+
54 KLRG1+ CD4- NKT cells - % of CD4- NKT cells
55 Total NKT cells - % of CD45+
56 KLRG1+ CD4+ T helper cells - % of CD4+ T helper cells
57 KLRG1+ CD8+ T cells - % of CD8+
58 KLRG1+ γδ T cells - % of γδ T cells
59 Germinal centre B cells - % of B2 cells

Figure 4.8 Splenic immune compartments in WT, *Btnl1*$^{+/-}$ and *Btnl1*$^{-/-}$ mice

Splenic T cell, B cell and myeloid cell composition assayed by multi-parametric flow cytometry in W10-11 adult mice. Data are presented as Log_{10}(% indicated subset). Radar plot presents mean values (*n=8*). Data are representative of 1 experiment performed in collaboration with Dr Laing and 3i team.

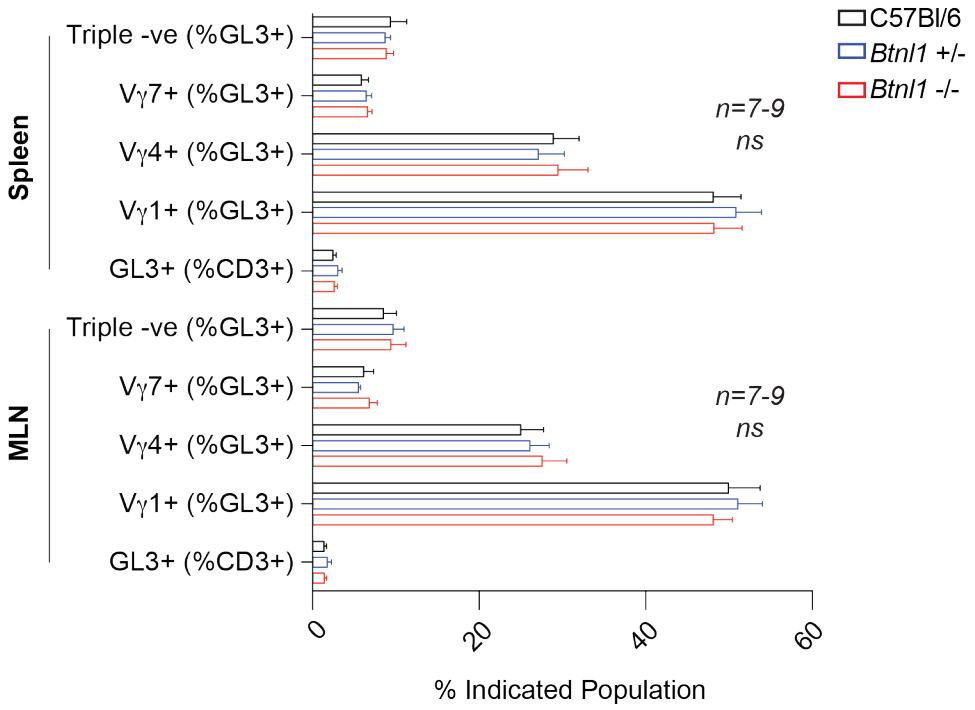

Figure 4.9 Splenic/Mesenteric lymph node γδ T cell composition in WT, *Btnl1*$^{+/-}$ and *Btnl1*$^{-/-}$ mice

Splenic and mesenteric lymph node γδ T cell composition assayed by multi-parametric flow cytometry in W10-11 adult mice (*n=8*). Data are representative of 1 experiment.

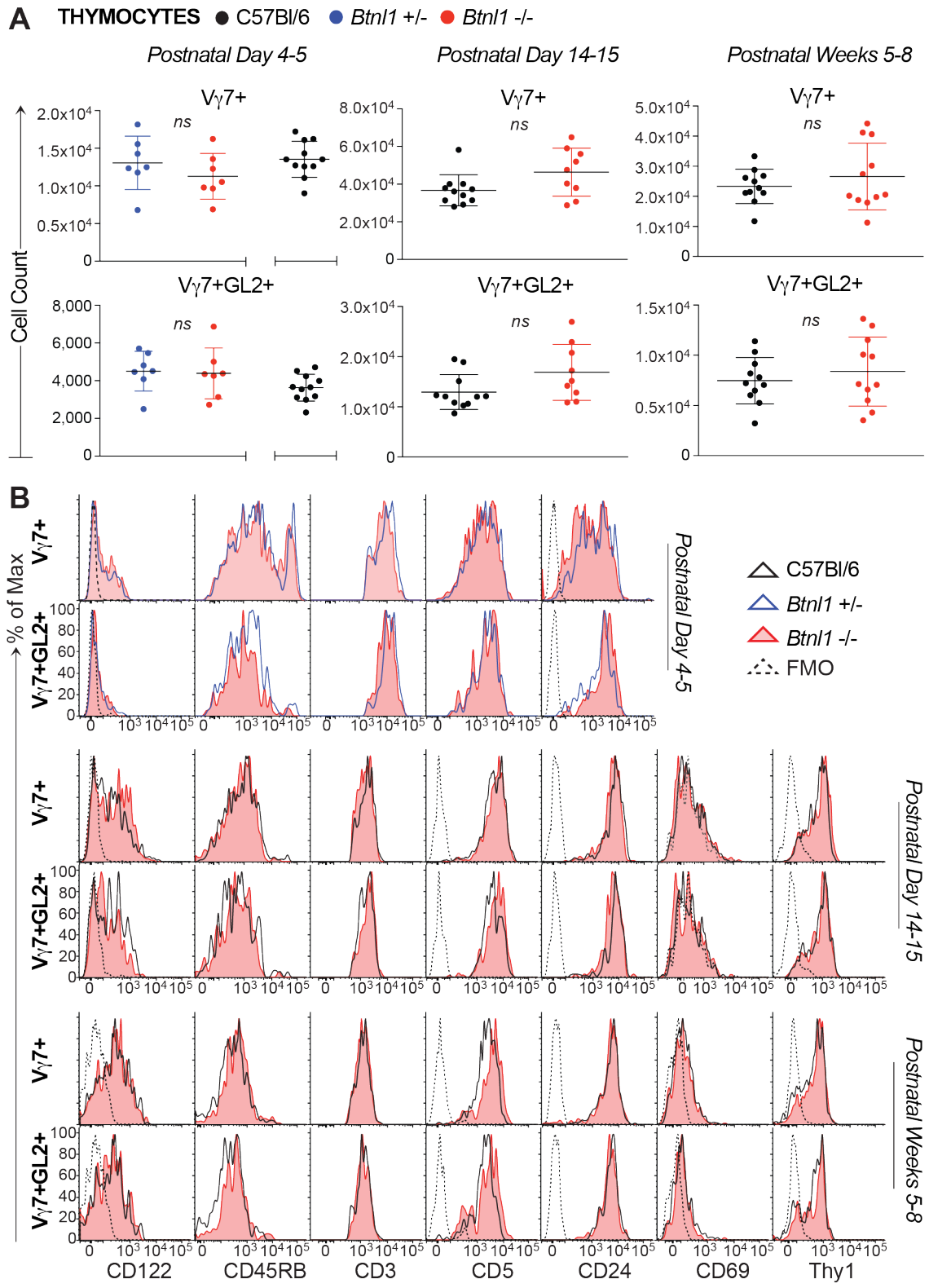

Figure 4.10 Vγ7^{+} thymocytes in *Btnl1*$^{-/-}$ mice

A) Enumeration of Vγ7^{+} and Vγ7^{+}GL2^{+} thymocytes from WT, *Btnl1*$^{+/-}$ and *Btnl1*$^{-/-}$ mice at indicated time points. **B)** Cell surface phenotypes of Vγ7^{+} and Vγ7^{+}GL2^{+} thymocytes from WT, *Btnl1*$^{+/-}$ and *Btnl1*$^{-/-}$ mice at indicated time points ($n \geq 6$). Panels (**A**) and (**B**) include data pooled from ≥3 independent experiments.

4.6 Conclusion

In agreement with previous reports, we have shown that *Btnl1, Btnl4* and *Btnl6* are strongly expressed in the small intestinal epithelium (Bas et al., 2011), and that their expression is more specifically within post-mitotic, differentiated villus enterocytes. Given that *Btnl1*- but not *Btnl4*-deficiency was associated with a striking depletion in signature small intestinal V$\gamma7^+$ IEL, we conclude that *Btnl1* but not *Btnl4* is critically required for the development of V$\gamma7^+$ IEL.

Btnl1$^{-/-}$ mice displayed no overt difference in the composition of their systemic T cell, B cell and myeloid cell compartments relative to WT controls. Furthermore, thymic *Btnl1* expression is almost negligible and accordingly, its deficiency had no effect on the development of V$\gamma7^+$ thymocytes. Hence, the impacts of *Btnl1* appear to be mediated extrathymically and are specific to signature intestinal V$\gamma7^+$ IEL. Consistent with this, *bona fide* extrathymic development of V$\gamma7^+$ IEL was impaired in NU/NU.*Btnl1*$^{-/-}$ relative to NU/NU mice. In summary, we conclude that *Btnl1* is critical for an extrathymic component of signature intestinal V$\gamma7^+$ IEL development. We next proceeded to investigate the impact of intestinal *Btnl1* on the extrathymic development of signature V$\gamma7^+$ IEL, which we further sought to characterise.

Chapter 5. Impact of *Btnl1* on extrathymic Vγ7$^+$ IEL maturation

5.1 Introduction

We previously demonstrated that at postnatal D14-D17, Vγ7$^+$ IEL in WT mice were enriched for cells that carried an 'immature' TCR^{LO}CD122^{LO}CD24$^+$ cell surface phenotype, reminiscent of pre-selection DETC progenitors in *Skint1*-mutant mice (**Figure 3.3A-C**). Furthermore, relative to 'mature' CD122^{HI} Vγ7$^+$ IEL, putative CD122^{LO}Vγ7$^+$ 'immature' precursors expressed greater levels of *Bcl11b*, *Sox13* and *Sox4* and lower levels of *Tnfrsf9, Xcl1* and *Tbx21* (**Figure 3.7**), suggesting Vγ7$^+$ IEL may *peripherally* transition through a similar developmental checkpoint to DETC progenitors in the thymus.

Having shown that *Btnl1* was a critical determinant for the development of signature small intestinal Vγ7$^+$ IEL (**Figure 4.4; 4.5A-B**), we next sought to determine how its impact was mediated. Given that *Btnl1* is exclusively highly expressed in small intestinal epithelium (**Figure 4.1A-E**) (Bas et al., 2011), and that its deficiency was not associated with a thymic, splenic or MLN immune phenotype (**Figure 4.7; 4.8; 4.9; 4.10A-B**), we hypothesized that *Btnl1* regulated the peripheral selection of Vγ7$^+$ IEL in *trans* from small intestinal villus enterocytes. Within this model, we also considered that selective interactions with *Btnl1*-expressing enterocytes could be driving the selective expansion of signature Vγ7$^+$ IEL *in situ*, in the small intestine of neonatal and weanling mice (**Figure 3.8A-C**).

To test this, we phenotypically characterized the 'residual' Vγ7$^+$ IEL found in *Btnl1*$^{-/-}$ mice; we assessed whether haematopoietic expression of *Btnl1* was necessary for Vγ7$^+$ IEL development; and we established an inducible *Btnl1* transgenic mouse model to assess the impact or re-introducing *Btnl1* into *Btnl1*$^{-/-}$ mice.

5.2 Phenotypic status of 'residual' Vγ7$^+$ IEL in *Btnl1*$^{-/-}$ mice

5.2.1 *Btnl1*$^{-/-}$ mice are enriched for putative CD122^{LO} Vγ7$^+$ IEL precursors that fail to selectively expand *in situ*

To test whether residual Vγ7$^+$ IEL in *Btnl1*$^{-/-}$ mice carried a pre-selection CD122^{LO}TCR^{LO}TIGIT^{LO} phenotype (**Figure 3.3A**) (Lewis et al., 2006), flow cytometric analysis was performed on IEL freshly isolated from postnatal D21 to D35 *Btnl1*$^{-/-}$ mice. By contrast to age-matched WT controls, a greater proportion of Vγ7$^+$ and Vγ7$^+$GL2$^+$ IEL in *Btnl1*$^{-/-}$ mice carried a CD122^{LO}TIGIT^{LO} phenotype, although TCR (by anti-CD3) expression was comparable (**Figure 5.1A**). Furthermore, 'residual' Vγ7$^+$ IEL from D35 *Btnl1*$^{-/-}$ mice phenocopied their WT counterparts in D14 mice (**Figure 3.3B**), as ~50% of the population carried the 'immature' CD122^{LO}Thy1$^+$ phenotype (**Figure 5.1B**). Indeed, 'Immature' cells were also enriched for putative CD8α$^-$Lag3$^-$CD5$^+$CD24$^+$ precursors, which was virtually undetectable in the CD122^{HI}Thy1$^-$ Vγ7$^+$ compartment (**Figure 5.1B**). While Vγ7$^+$ IEL in *Btnl1*$^{-/-}$ mice showed no overall difference in cell surface TCR expression to age-matched WT counterparts (n≥4; *p<0.003 for statistical analysis of each marker individually*) (**Figure 5.1A**), high *versus* low TCR expression did segregate with CD122^{HI}TIGIT^{HI} and CD122^{LO}TIGIT^{LO} Vγ7$^+$ cells, respectively (**Figure 5.1C**). Thus, it was concluded that 21-35 day-old *Btnl1*$^{-/-}$ mice were enriched for the putative CD122^{LO}Thy1$^+$CD8α$^-$Lag3$^-$CD5$^+$CD24$^+$ Vγ7$^+$ IEL precursors that had previously been identified in 14-17 day old WT mice (**Figure 3.3A-C**).

To investigate whether Vγ7$^+$ IEL failed to undergo selective expansion in the absence of *Btnl1*, EdU incorporation in 28 day-old mice was assayed by flow cytometry of IEL recovered after a 3hr EdU pulse *in vivo*. While ~10% of Vγ7$^+$ and Vγ7$^+$GL2$^+$ IEL in WT mice incorporated EdU over this time frame, ~6% of Vγ7$^+$ and ~5% of Vγ7$^+$GL2$^+$ IEL in *Btnl1*$^{-/-}$ mice were found to do so (*p<0.0001*) (**Figure 5.2A**). Furthermore, EdU incorporation in *Btnl1*$^{-/-}$ 'residual' Vγ7$^+$ IEL failed to phenocopy rapidly dividing CD8αβ$^+$ thymocytes, ~10% of which were EdU$^+$, and instead more closely resembled Vγ7$^-$ IEL, ~4% of which were EdU$^+$ (**Figure 5.2A**). Hence, the depletion of Vγ7$^+$ IEL in *Btnl1*$^{-/-}$ mice may be at least partly due to a failure in selectively expanding this compartment *in situ*. Consistent with this, a significantly

smaller proportion of Vγ7$^+$ IEL expressed Ki67 at post-natal D14-16 (*p<001*), D21-24 (*p<0.0001*), D25-31 (*p<0.0001*) and W5-7 (*p=0.0001*) (**Figure 5.2B**). From W11-16, most >90% of Vγ7$^+$ IEL were quiescent in both WT and *Btnl1*$^{-/-}$ mice and there was no significant difference in Ki67 expression. Taken together, these data suggest that selective interactions with *Btnl1*-expressing small intestinal enterocytes may drive phenotypic maturation and expansion of Vγ7$^+$ IEL, such that by D21 they form the predominant and signature intestinal γδ IEL compartment.

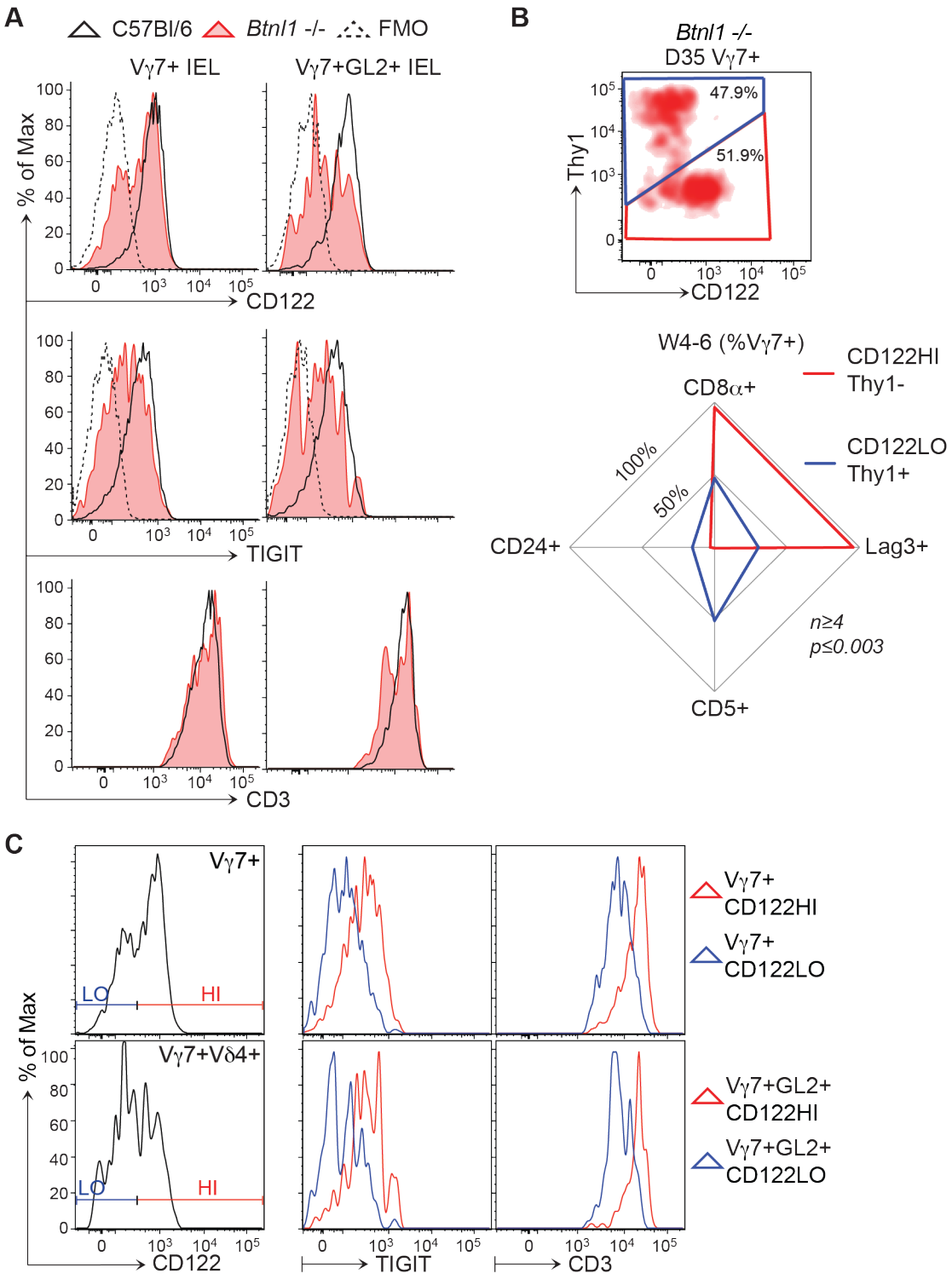

Figure 5.1 'Residual' Vγ7^{+} IEL in *Btnl1*$^{-/-}$ mice

A) Surface phenotypes of Vγ7^{+} and Vγ7^{+}GL2^{+} IEL from W3-5 *Btnl1*$^{-/-}$ mice (*n*≥8) **B)** *Upper:* Thy1 and CD122 expression by Vγ7^{+} IEL from D35 *Btnl1*$^{-/-}$ mice (*n=8*); *Lower:* Surface phenotypes of CD122^{HI}Thy1^{-} *vs.* CD122^{LO}Thy1^{+} Vγ7^{+} IEL from W4-6 *Btnl1*$^{-/-}$ mice (*n≥4*). **C)** CD3 and TIGIT expression in CD122^{HI} *vs.* CD122^{LO} Vγ7^{+} IEL (shown in figure 4.10A) from *Btnl1*$^{-/-}$ mice (*n*≥8). Data are representative of ≥3 experiments. Panel (**B**) includes data pooled from ≥3 experiments.

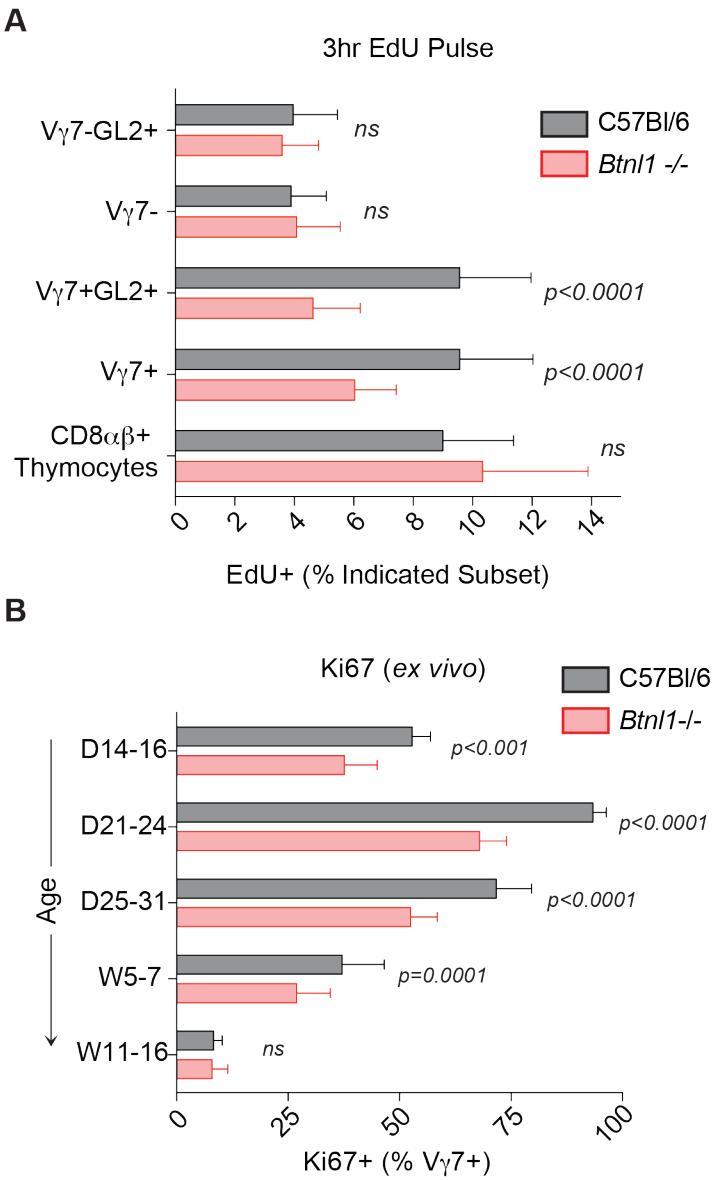

Figure 5.2 Post-natal expansion of Vγ7^{+} IEL in *Btnl1*$^{-/-}$ mice

A) EdU incorporation during 3hr pulse *in vivo* in γδ IEL and CD8αβ thymocytes from W4 WT *vs. Btnl1*$^{-/-}$ mice (Vγ7^{-} gated from CD3^{+}TCRβ^{-} cells) (n≥9). **B)** Ki67^{+} expression in Vγ7^{+} IEL freshly isolated from WT *vs. Btnl1*$^{-/-}$ mice (D14➔*n≥4;* All other time points➔*n=8-27*). Panels include data pooled from 3 (**A**) or >8 (**B**) independent experiments.

5.2.2 *Btnl1* acts in *trans* from small intestinal enterocytes

To test our hypothesis that enterocyte *Btnl1* expression confers a selective advantage to $V\gamma7^+$ IEL *in trans*, we established conditions (see materials and methods) by which adult (W5-W6) bone marrow could reconstitute signature $V\gamma7^+$ and $V\gamma7^+GL2^+$ IEL compartments in irradiated adult (W8-W10) $TCR\delta^{-/-}$ recipients. Analysis of IEL composition was performed by flow cytometry of freshly recovered cells. Following bone marrow transfer, it took 5-6 weeks for $V\gamma7^+$ IEL to reliably reconstitute to a level at which they were the predominating (60-70%) $\gamma\delta$ IEL subset. However, it took ≥10 weeks for the reconstituted $\gamma\delta$ IEL compartment to attain a 40% representation amongst total $CD3^+$ IEL (**Figure 5.3A**). Using these conditions, it was shown that WT and *Btnl1*$^{-/-}$ bone marrow were equally capable at reconstituting signature $CD122^{HI}$ $V\gamma7^+$ IEL **Figure 5.3B**). Hence, haematopoietic expression of *Btnl1* was dispensable for the reconstitution and phenotypic maturation of donor bone marrow-derived $V\gamma7^+$ IEL.

To determine whether host *Btnl1* expression was required for $V\gamma7^+$ IEL reconstitution, *Btnl1*-sufficient $CD45.1^+$ bone marrow was transferred into irradiated $CD45.2^+$ congenic WT or *Btnl1*$^{-/-}$ hosts. Analysis of IEL composition was performed 4-5 weeks post bone marrow transfer. Although overall reconstitution of intestinal IEL in 'T cell sufficient' WT and *Btnl1*$^{-/-}$ hosts was less effective that that observed in $TCR\delta^{-/-}$ mice (**Figure 5.3A,B**), ~40% of the reconstituted $CD45.1^+CD3^+TCR\beta^-$ IEL were $V\gamma7^+$ in WT hosts, whereas only ~17% were $V\gamma7^+$ in *Btnl1*$^{-/-}$ hosts (**Figure 5.4A**). Moreover, the reconstituted $V\gamma7^+$ and $V\gamma7^+GL2^+$ IEL compartment was mostly $CD122^{HI}$ in WT hosts and $CD122^{LO}$ in *Btnl1*$^{-/-}$ hosts (**Figure 5.4A**). Hence, both the efficiency of $V\gamma7^+$ IEL reconstitution and the capacity to support $V\gamma7^+$ IEL maturation was highly dependent on host *Btnl1* expression. Complementing these findings, $CD45^+$ IEL purified from 21 to 35 day-old mice could reconstitute the intestinal $V\gamma7^+$ IEL compartment of recipient $TCR\delta^{-/-}$ mice, albeit very inefficiently. However, this too was greatly impaired in $TCR\delta^{-/-}$.*Btnl1*$^{-/-}$ recipients (**Figure 5.4B**). Taken together, these data support the notion that enterocyte-expressed *Btnl1* acts *in trans* to promote the selective phenotypic maturation and expansion of signature $V\gamma7^+$ IEL precursors as they arrive in the gut epithelium.

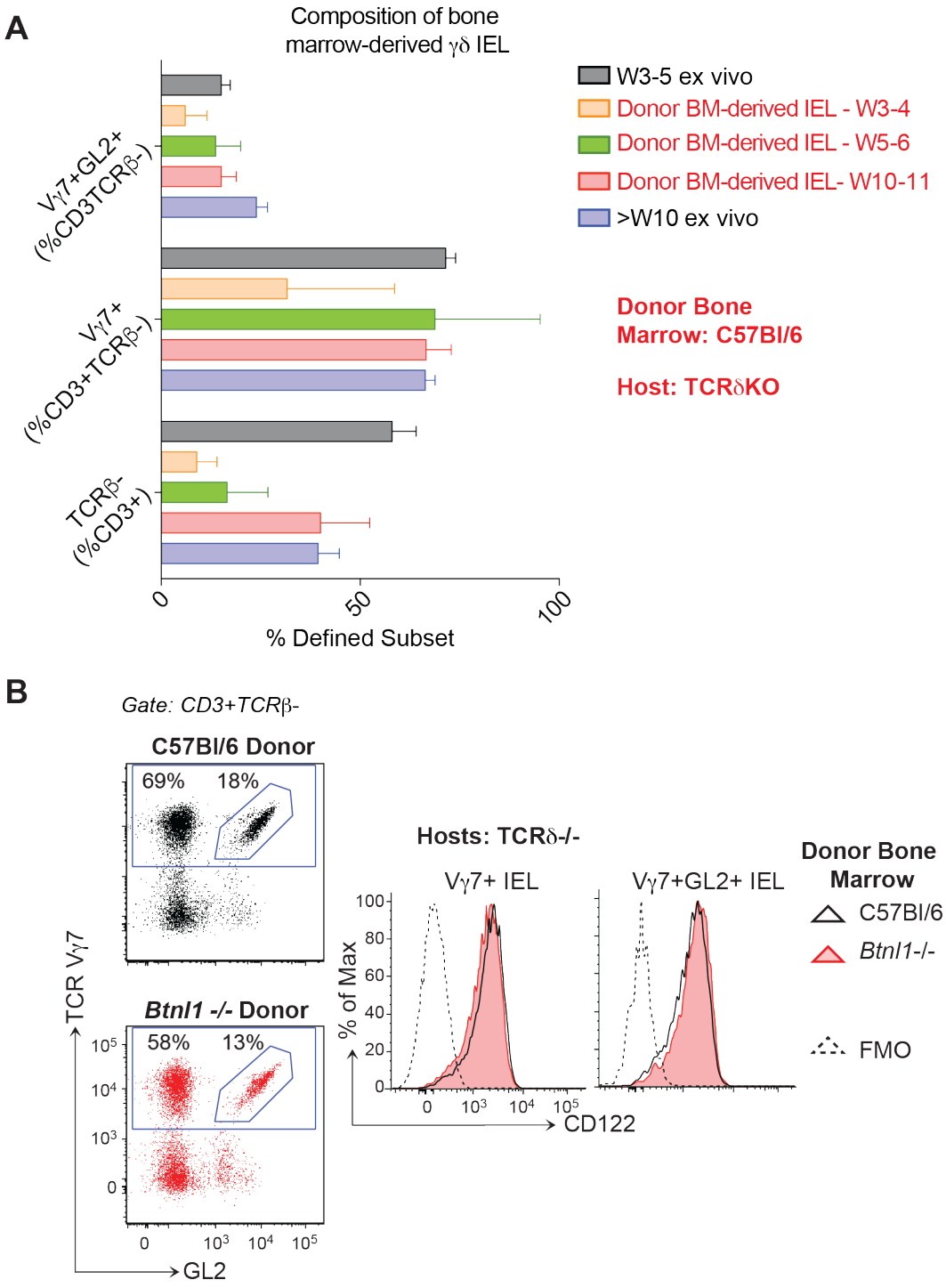

Figure 5.3 Reconstitution of signature Vγ7^{+} IEL from adult donor bone marrow

A) Intestinal IEL composition assayed by flow cytometry in irradiated TCRδ$^{-/-}$ hosts at indicated time-points after reconstitution with adult (W5-6) WT bone marrow (*n*≥*3*). **B)** γδ IEL composition and cell surface phenotype in irradiated TCRδ$^{-/-}$ hosts 8-10 weeks after reconstitution with WT *vs. Btnl1*$^{-/-}$ bone marrow (*n*≥*7*). Data are representative of 1 (**A**) or 3 (**B**) independent experiments.

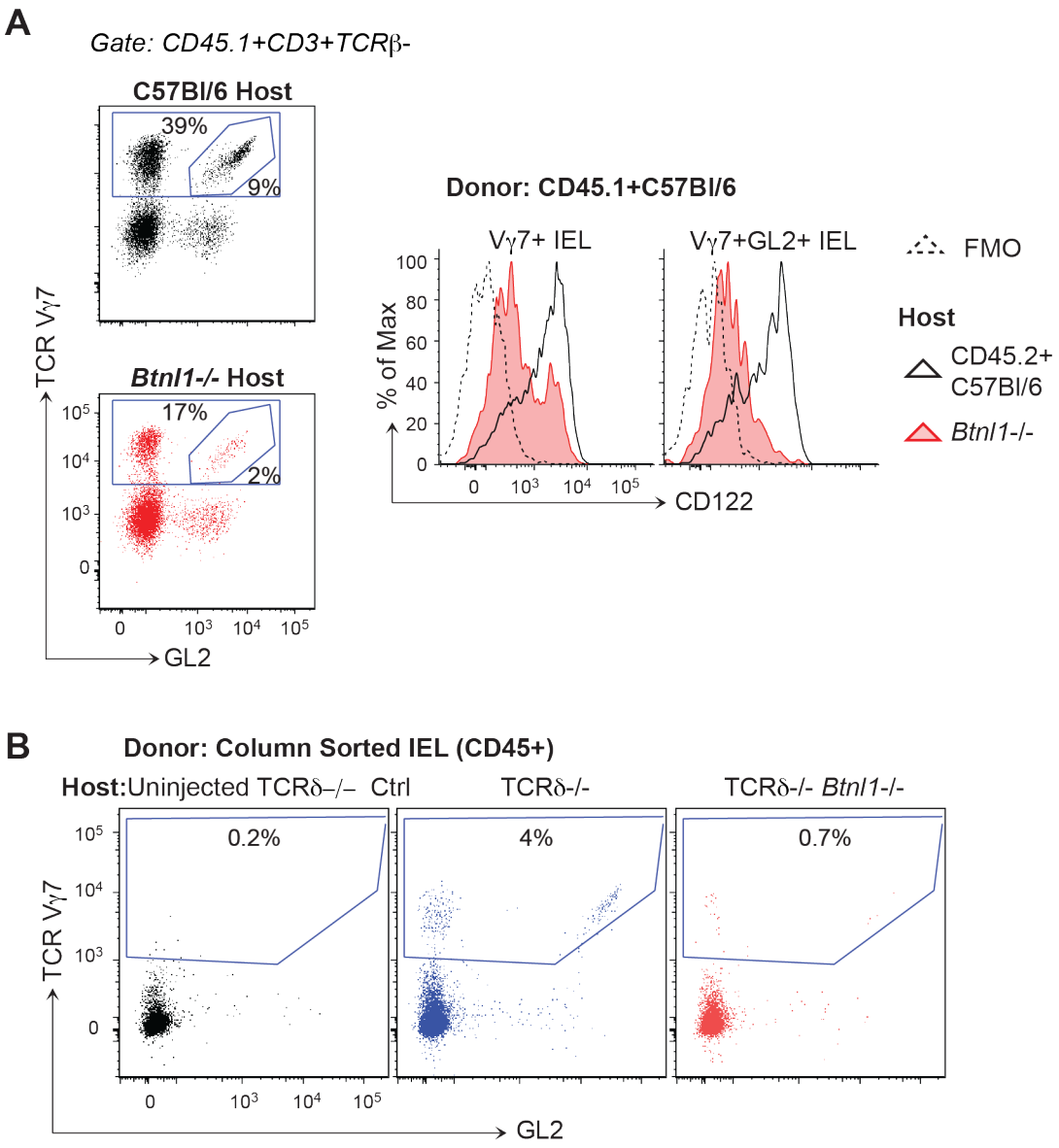

Figure 5.4 Reconstitution of Vγ7^{+} IEL in *Btnl1*$^{-/-}$ mice

A) CD45.1^{+} γδ IEL composition and cell surface phenotype in irradiated CD45.2^{+} WT *vs. Btnl1*$^{-/-}$ hosts 4-5 weeks after reconstitution with adult (W5-6) CD45.1^{+} bone marrow (*n*=7). **B)** γδ IEL composition 2-3 weeks after adoptive transfer of (CD45^{+}) IEL column-purified from weanling (W4-5) mice into W6 WT.TCRδ$^{-/-}$ *vs. Btnl1*$^{-/-}$.TCRδ$^{-/-}$ hosts. (*n*=6). Panels (**A**) and (**B**) are each representative of 2 independent experiments.

5.3 Transgenic rescue of Vγ7$^+$ IEL deficiency in *Btnl1*$^{-/-}$ mice

5.3.1 Generation of an inducible *Btnl1* transgenic mouse

Having established that *Btnl1* acts in *trans* to regulate the intestinal maturation and expansion of Vγ7$^+$ IEL, we considered whether re-introduction of *Btnl1* expression would be sufficient to rescue maturation and/or expansion of 'residual' Vγ7$^+$ IEL in *Btnl1*$^{-/-}$ mice. We thus generated *Btnl1*$^{-/-}$ mice transgenic (Tg) for *Btnl1* under the control of a doxycycline (Dox)-inducible promoter, an approach previously used to generate Dox-inducible Rae-1-Tg mice (Oppenheim et al., 2005; Strid et al., 2008). Briefly, *Btnl1*$^{-/-}$ blastocysts were injected with a linearized cassette containing the Btnl1-open reading frame (ORF) downstream of a tetracycline-responsive element (TRE) controlling a minimal cytomegalovirus (CMV) promoter (**Figure 5.5A**). Successful insertion of the *Btnl1*-transgene in *Btnl1*$^{-/-}$ pups was confirmed by Southern blotting of genomic DNA purified from tail tissue and digested with EcoRI. As predicted by the genomic and transgene sequences, WT *Btnl1* migrated at 7.3kB and the *Btnl1* transgene migrated at 2.3kB (**Figure 5.5A,B**).

To induce *Btnl1* expression, *Btnl1*-Tg$^+$ mice were crossed with *Btnl1*$^{-/-}$ mice expressing the reverse tetracycline trans-activator (rtTA-M2) regulated by the ubiquitous *Rosa26* promoter (R26.rtTA) (Hochedlinger et al., 2005); or by the enterocyte-specific Villin promoter (Villin.rtTA) (Roth et al., 2009). Bi-transgenic (BiTg) *Btnl1*$^{-/-}$ offspring generated from these crosses inherited both the *Btnl1*-Tg and the reverse tetracycline transactivator (rt-TA) and could inducibly express *Btnl1* globally (R26.rtTA) or locally (Villin.rtTA) in response Dox treatment (**Figure 5.6**). As previously reported, supplementation of drinking water with low-dose (1mg/ml) Dox had minimal impact on gut health (Roth et al., 2009). Dox water is bitter in taste, so to incentivise its consumption we supplemented it with 2% sucrose and accordingly, treated BiTg negative controls with 2% sucrose alone (ctrl water). To control for any non-specific effects of Dox, single transgenic (SiTg) mice that had only inherited the *Btnl1*-Tg (SiTg) were also Dox-treated.

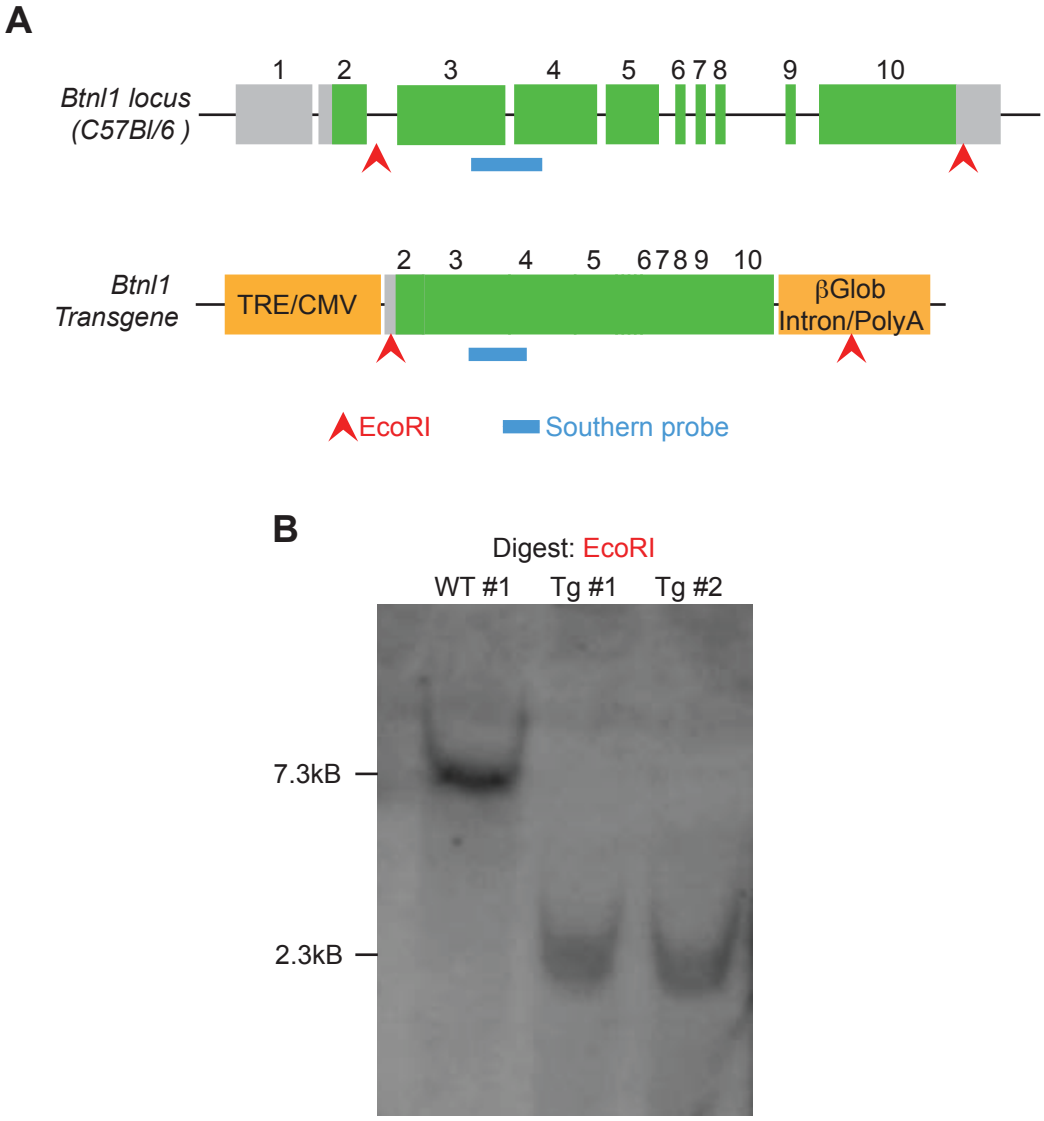

Figure 5.5 Generation of a Dox-inducible *Btnl1* transgenic mouse

A) *Upper:* Schematic representation of the WT *Btnl1* locus. *Lower:* TRE-*Btnl1* transgene construct. The linearized TRE/CMV cassette has been previously described (Oppenheim et al., 2005). Grey: unstranslated region; green: translated region; orange: upstream-tetracycline response element/CMV promoter and downstream-β-globulin/polyA tail. **B)** DNA analysis by Southern blot to detect transgene insertion. Genomic DNA was digested with EcoR1 as indicated (arrowheads) and a probe (blue bar) targeting the indicated region (Exon3/4 boundary in ORF) was generated to detect the WT and targeted allele. Panel (**B**) is representative of ≥2 independent experiments. Data provided by Efstathios Theodoridis.

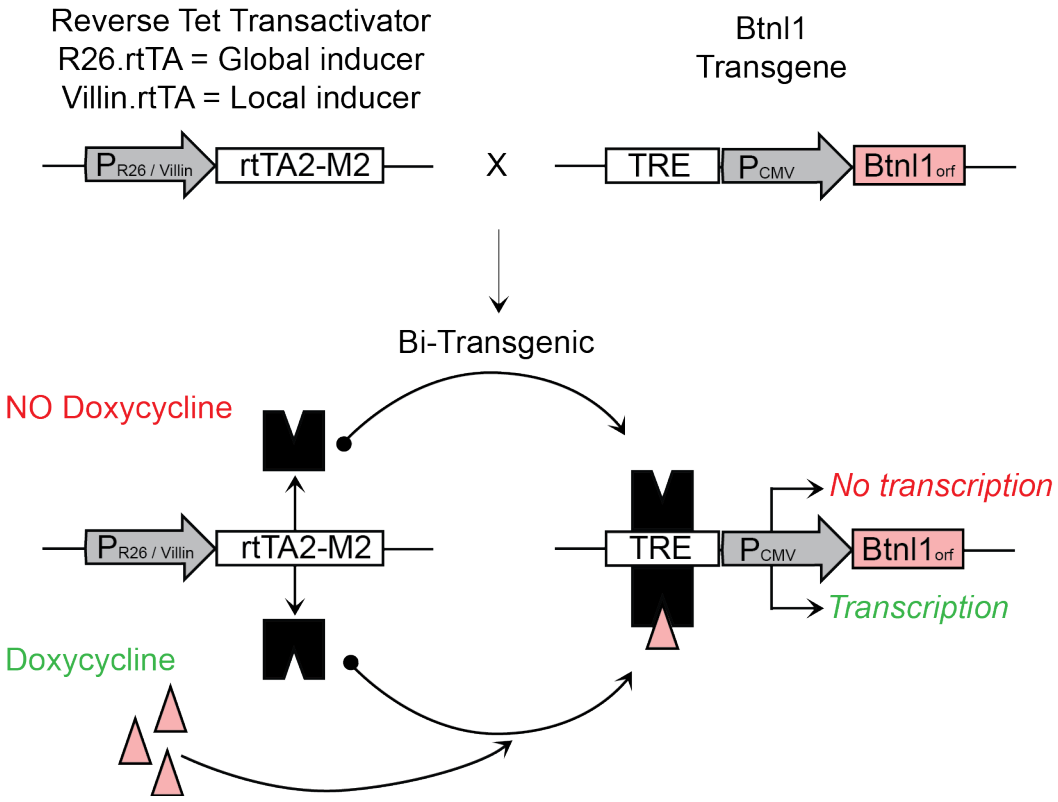

Figure 5.6 Schematic of *Btnl1* induction in Bi-transgenic mice

Doxycycline treatment specifically induces *Btnl1* transcription in mice that are Bi-transgenic for the *Reverse Tetracycline (Tet) Transactivator* (rtTA2-M2) and *Btnl1*. **R26.rtTA^{+} BiTg** mice inducibly express *Btnl1* **globally**. **Villin.rtTA^{+} BiTg** mice inducibly express *Btnl1* **locally** in enterocytes. Schematic adapted from: (Strid et al., 2008).

5.3.2 Global *Btnl1* induction elicits selective stimulation and phenotypic rescue of Vγ7$^+$ IEL

To verify the Dox-dependency of *Btnl1* induction in BiTg mice, *Btnl1* expression was assayed by qRT-PCR in adult (W7-13) BiTg, SiTg and *Btnl1*$^{-/-}$ mice after two weeks of Dox treatment. Dox-treated mice were compared to untreated WT and ctrl-water-treated BiTg mice. Consistent with the mouse genotypes, Dox-dependent *Btnl1* expression was detected in BiTg but not in SiTg or *Btnl1*$^{-/-}$ mice (**Figure 5.7A**). Although the magnitude of *Btnl1* expression in BiTg mice was ~5-fold lower than in WT mice, its induction was highly dependent on Dox-treatment, with little to no leaky expression in littermate controls (**Figure 5.7A**). Thus, BiTg mice provided a well-controlled system to study the impact of *de novo Btnl1* expression in *Btnl1*$^{-/-}$ mice.

To examine the impact of such global *Btnl1* induction, adult (W7-13) BiTg and littermate controls were treated with Dox or Ctrl water for 1-2 weeks before IEL composition and phenotype analysis. Dox-treated BiTg mice displayed no significant differences in the frequency and absolute cell numbers of signature Vγ7$^+$ and Vγ7GL2$^+$ cells relative to littermate controls (**Figure 5.7B**). Hence, *Btnl1* expression over this time frame did not rescue the signature Vγ7$^+$ IEL compartment. However, the proportion of CD122^{HI} cells within the Vγ7$^+$ IEL compartment increased from <50% in ctrl-treated BiTg and Dox-treated SiTg to >70% in Dox-treated BiTg mice (**Figure 5.8A**). Furthermore, most CD122^{HI} cells were additionally Ki67$^+$, indicating that they had been selectively stimulated out of quiescence. The proportion of CD122$^+$Ki67$^+$ cells amongst Vγ7$^+$ IEL was up to 4-fold higher in Dox-treated BiTg mice (>40%) than in ctrl-treated BiTg (<10%) and Dox-treated SiTg (<10%) mice (**Figure 5.8A**). Such stimulation was specific to the Vγ7$^+$ IEL compartment, as ~50% of Vγ7$^+$ IEL in BiTg mice were Ki67$^+$ following Dox-treatment, relative to <20% of TCRβ$^+$ and Vγ7$^-$ γδ IEL. Indeed, TCRβ$^+$ and Vγ7$^-$ γδ IEL displayed no Dox-dependent changes in Ki67 expression (**Figure 5.8B**). In summary, global *Btnl1* induction in adult BiTg mice partially phenocopied Vγ7$^+$ IEL maturation in neonatal mice, as it selectively elicited up-regulation of CD122 and Ki67 expression but failed to achieve numerical expansion of this signature IEL compartment.

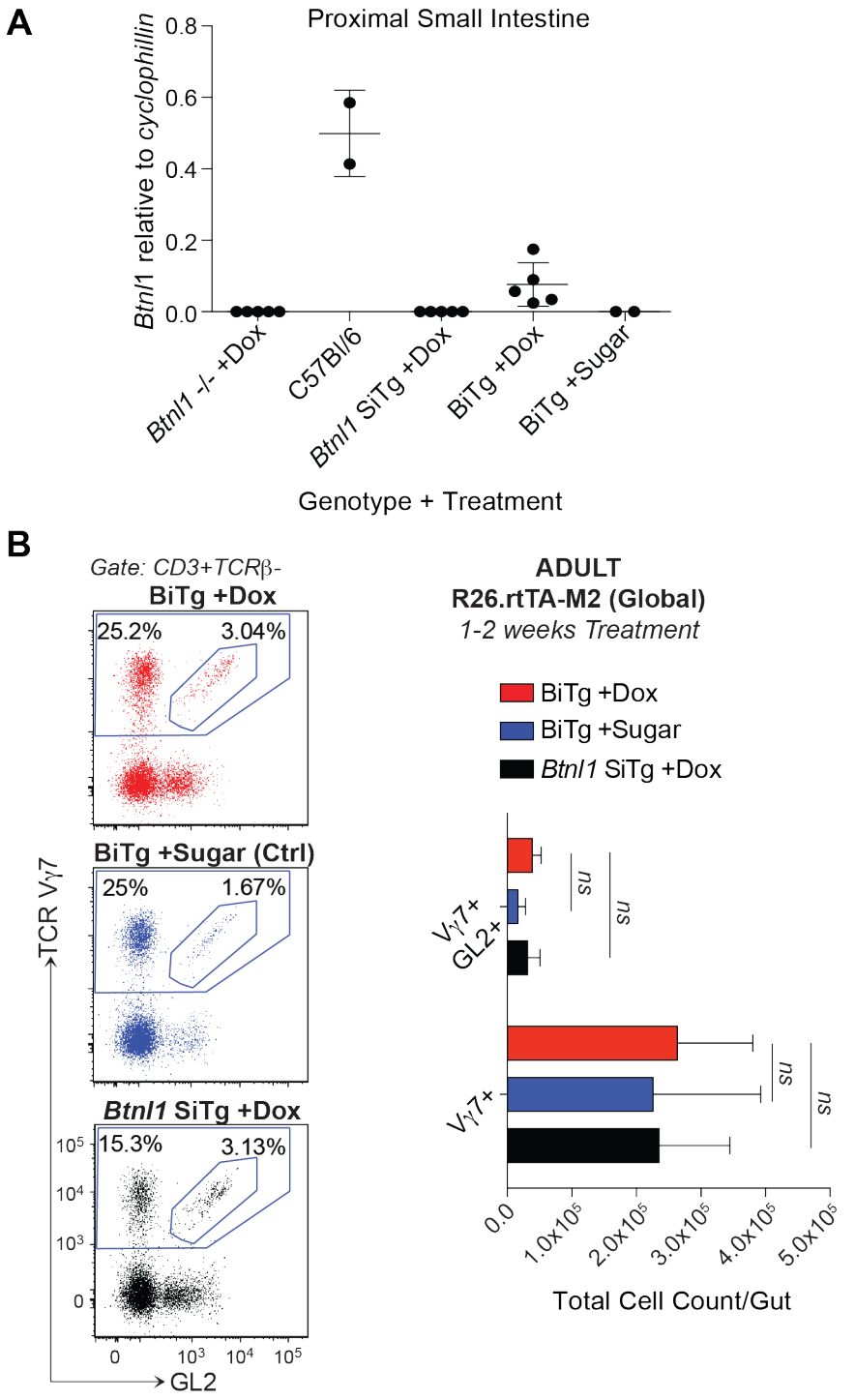

Figure 5.7 IEL composition in Doxycycline-treated adult Bi-transgenic mice

A-B) 7-13 week old *Btnl1*$^{-/-}$ SiTg and BiTg mice were treated with Dox-water (1mg/ml Dox; 2% sucrose) or Ctrl-water (2% sucrose) for 1-2 weeks. **A)** *Btnl1* expression by qRT-PCR *vs.* untreated WT mouse. **B)** γδ IEL composition (*Left*) and absolute cell numbers (*Right*) assessed by flow cytometry (sugar➔*n=3-5;* rest➔n=*4-14*). Panels include data representative of 2 (**A**) or ≥3 (**B**-*left*) independent experiments. Panel (**B**-*right*) presents data pooled from ≥3 independent experiments.

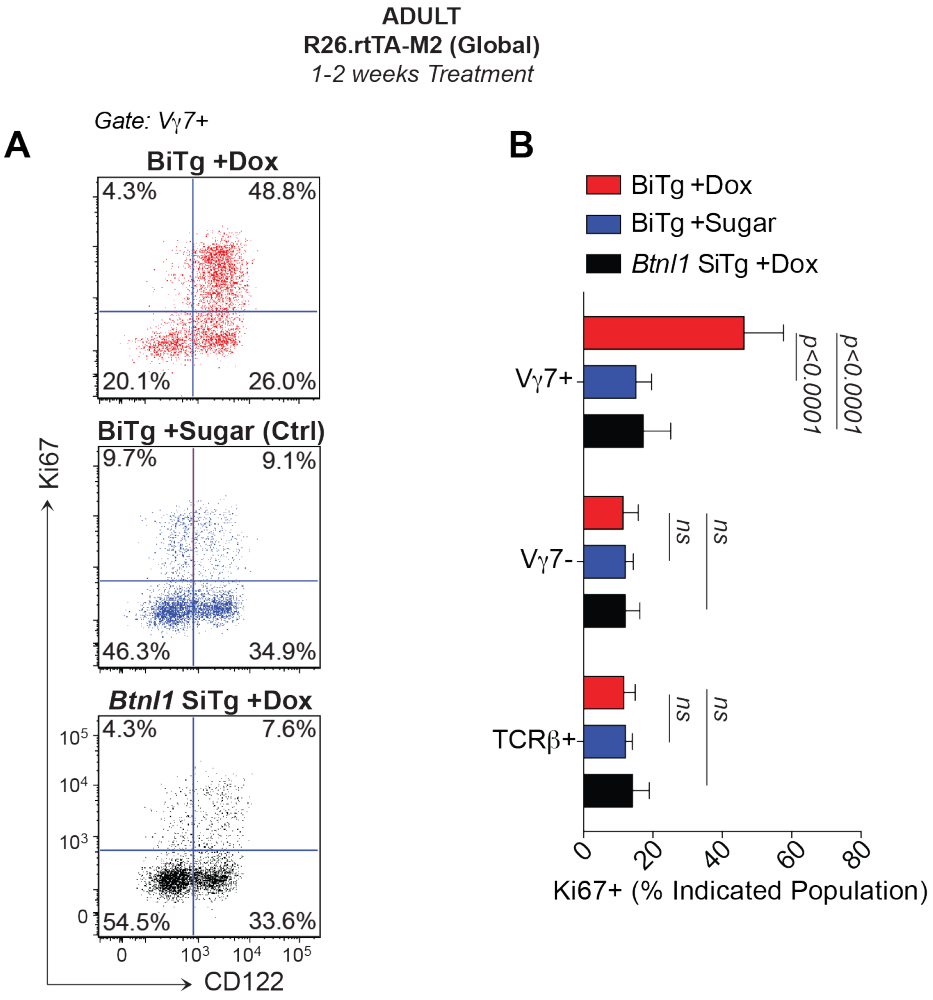

Figure 5.8 IEL phenotype in Doxycycline-treated adult Bi-transgenic mice

(**A-B**) 7-13 week old adult *Btnl1*$^{-/-}$ SiTg and BiTg mice were treated with Dox-water (1mg/ml Dox; 2% sucrose) or Ctrl-water (2% sucrose) for 1-2 weeks and analysed by flow cytometry. (**A**) CD122 and Ki67 expression in Vγ7^{+} IEL. (**B**) Ki67 expression in IEL subsets (sugar➔*n=5;* SiTg➔*n=14*; BiTg➔*n=9*). Panels include data that are representative of (**A**) and pooled (**B**) from ≥3 independent experiments

5.3.3 Villin-specific *Btnl1* induction elicits selective stimulation and phenotypic rescue of Vγ7$^+$ IEL

Having demonstrated that global *Btnl1* induction could achieve selective phenotypic changes in Vγ7$^+$ IEL *in vivo*, we next tested whether local villin-specific *Btnl1* expression could achieve similar results (**Figure 5.6**). The villin promoter is active in enterocytes along the length of the small and large intestine, in the proximal tubules of the kidney and in a small population of cells in the stomach wall (Roth et al., 2009). To compare this system with our previous experiments, we treated adult (W7-W13) BiTg mice and littermate controls with Dox or Ctrl water for 1-2 weeks before analysis.

Vγ7$^+$ IEL recovered from Dox-treated BiTg mice were uniformly Lag3$^+$ and mostly CD22^{HI}Thy1^{LO}, whereas those recovered from ctrl-treated BiTg littermates were mostly CD122^{LO} and a greater proportion were Lag3$^-$ and Thy1$^+$. Hence, villin-specific *Btnl1* expression was sufficient to elicit selective phenotypic changes in Vγ7$^+$ IEL (**Figure 5.9A**). In agreement with our previous findings, CD122^{HI} Vγ7$^+$ IEL from BiTg mice selectively up-regulated Ki67 in response to Dox-treatment, indicating they had been stimulated out of quiescence (**Figure 5.9B**). Thus, ~40% of Vγ7$^+$ IEL from Dox-treated BiTg mice expressed both CD122 and Ki67 whereas <10% of Vγ7$^+$ IEL from ctrl-treated BiTg and Dox-treated SiTg mice were found to do so. Such stimulation was specific to the Vγ7$^+$ IEL compartment, ~40% of which expressed Ki67 in Dox-treated BiTg mice compared to ~10% of TCRβ$^+$ and Vγ7$^-$ γδ IEL. While there were no Dox-dependent changes in Ki67 expression amongst TCRβ$^+$ or Vγ7$^-$ γδ IEL, there was a Dox-independent 10-20% increase in Ki67 expression in some ctrl-treated BiTg mice (**Figure 5.9B**). Given these data, we concluded that villin-specific *Btnl1* induction was sufficient to drive phenotypic rescue of Vγ7$^+$ IEL *in trans*.

In spite of the Dox-dependent increase in Ki67 expression seen in Vγ7$^+$ IEL from BiTg mice, 1-2 weeks Dox-treatment had no impact on the representation of Vγ7$^+$ or of Vγ7$^+$GL2$^+$ IEL amongst γδ IEL (*data not shown*). To test whether a longer period of Dox treatment could rescue the Vγ7$^+$ IEL compartment, we Dox treated 7-13 week-old BiTg mice alongside Dox-treated SiTg and ctrl-treated BiTg littermates

for a 3-4 week period. However, there was no significant increase in the representation or absolute cell counts of $V\gamma7^+$ or $V\gamma7^+GL2^+$ IEL in Dox-treated BiTg relative to ctrl-treated BiTg and Dox-treated SiTg mice (**Figure 5.10**). Hence, while villin-specific *Btnl1* induction in adult mice (W7-13) was sufficient to achieve selective phenotypic rescue and stimulate $V\gamma7^+$ IEL *in vivo*, it did not numerically rescue this signature IEL compartment. We therefore concluded that *Btnl1* expression could elicit phenotypic transition of $CD122^{LO}Thy1^+$ $V\gamma7^+$ IEL into $CD122^{HI}Thy1^-$ IEL while not promoting detectable expansion.

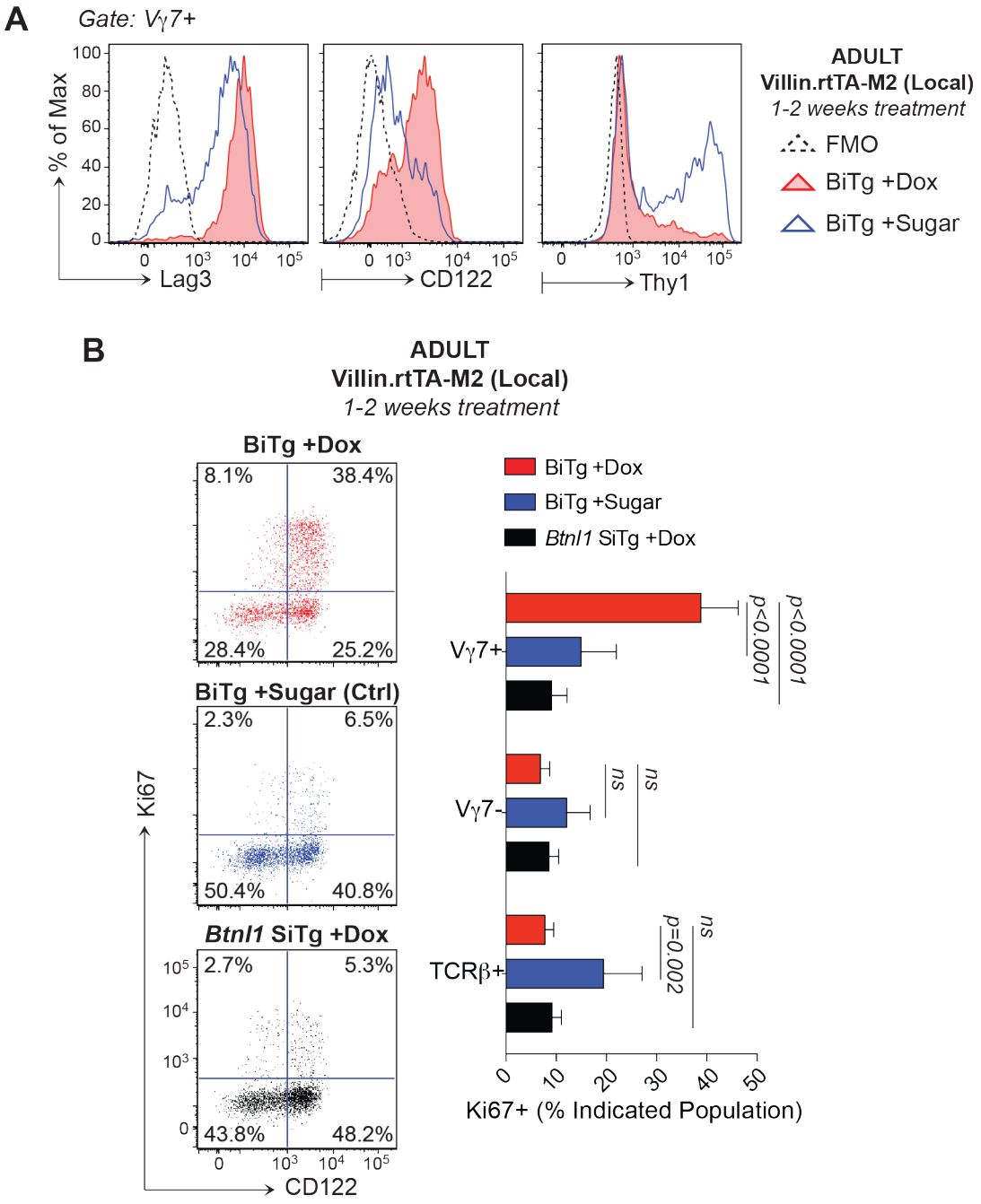

Figure 5.9 IEL phenotypes following villin-specific induction of *Btnl1* in Bi-transgenic adults

(**A-B**) 7-13 week old adult *Btnl1*$^{-/-}$ SiTg and BiTg mice were treated with Dox-water (1mg/ml Dox; 2% sucrose) or Ctrl-water (2% sucrose) for 1-2 weeks and analysed by flow cytometry. (**A**) Cell surface phenotypes of Vγ7^{+} IEL in Ctrl- *vs.* Dox-treated *Btnl1*$^{-/-}$ BiTg mice (*n*≥*5*). (**B**) *Left:* CD122 and Ki67 expression in Vγ7^{+} IEL. *Right:* Ki67 expression (*n*≥*5*). Panel (**A**) is representative of ≥2 independent experiments. Panel (**B**) contains data pooled from ≥3 independent experiments.

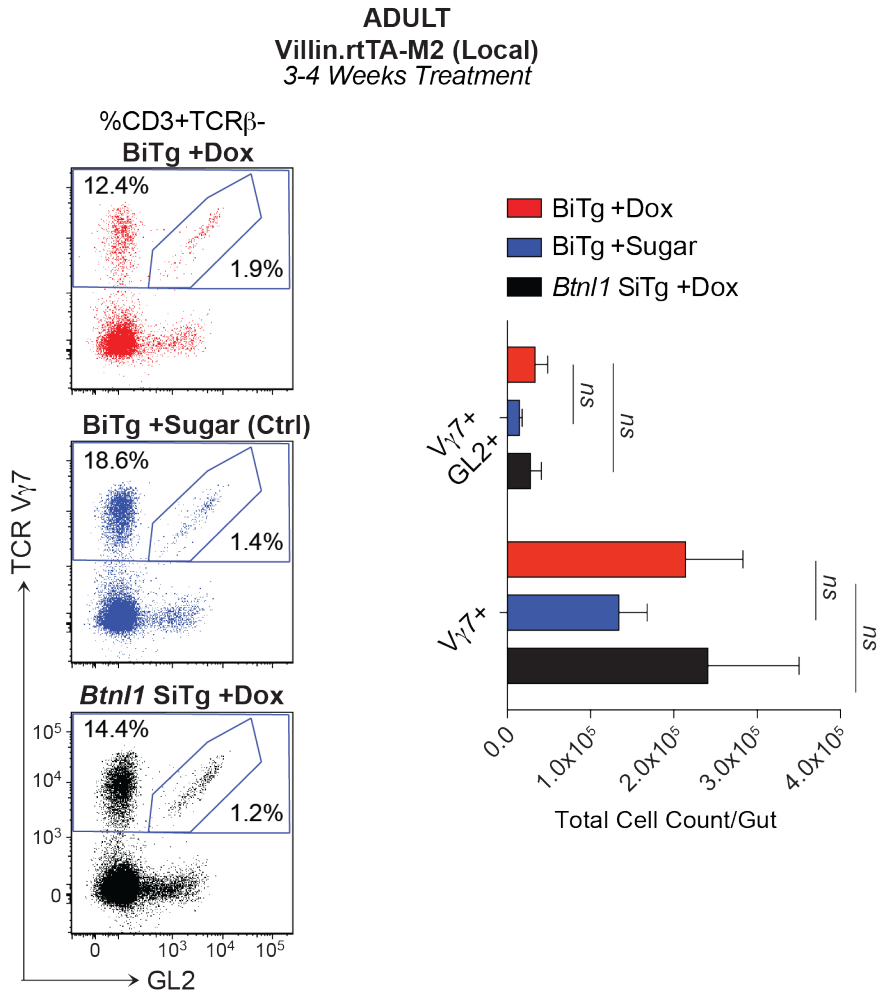

Figure 5.10 γδ IEL composition following villin-specific induction of *Btnl1* in Bi-transgenic adults

7-13 week old adult *Btnl1*$^{-/-}$ SiTg and BiTg mice were treated with Dox-water (1mg/ml Dox; 2% sucrose) or Ctrl-water (2% sucrose) for 3-4 weeks and analysed by flow cytometry. γδ IEL composition (*Left*) and absolute cell counts (*Right*) (Ctrl water➔*n=3;* Dox water➔*n≥6*). *Left* panel presents data pooled from 3 independent experiments. Statistical significance determined using Holm-Sidak method.

5.3.4 Neonatal Villin-specific *Btnl1* induction is sufficient to elicit both phenotypic and numerical rescue of Vγ7$^+$ IEL

As *Btnl1* induction in adult mice failed to rescue the expansion of signature Vγ7$^+$ IEL, we sought to analyse the impact of villin-specific *Btnl1* induction in BiTg pups, where its expression would overlap with the temporal window in which Vγ7$^+$ achieve representational dominance amongst γδ IEL (**Figure 3.1B; 3.6A**). To do this, we commenced Dox-treatment of nursing females at post-natal D7 or of weanling litters at D21. Analysis was performed by flow cytometry of IEL recovered from Dox-treated mice when they reached 5-6 weeks of age. All animals were blindly treated with Dox and genotyping was performed retrospectively.

Villin-specific *Btnl1* induction in BiTg pups elicited an increase in the representation of Vγ7$^+$ IEL from ~20% to ~50% of γδ IEL (*p<0.0001*), and an increase in the representation of Vγ7$^+$GL2$^+$ IEL from <5% to ~10% (*p<0.0001*), relative to littermate controls (**Figure 5.11A**). Moreover, this representational increase was accompanied by significant phenotypic changes. Dox-treated BiTg mice phenocopied untreated 28-35 day-old WT mice as >95% of Vγ7$^+$ IEL were CD8α$^+$, Lag3$^+$, CD24$^-$ and CD5$^-$, ~90% were Thy1$^-$ and >75% were CD122$^+$. By contrast Dox-treated SiTg mice phenocopied Dox-treated *Btnl1*$^{-/-}$ mice as ~75% expressed CD8α; ~60% expressed lag3; ~50-60% expressed CD122; ~40% expressed Thy1; ~15% expressed CD24; and ~20% expressed CD5 (**Figure 5.11B**). Taken together, these data show that re-introducing *Btnl1* expression in gut epithelium is sufficient to drive both expansion and phenotypic maturation of Vγ7$^+$ IEL in *trans* in neonatal (D7-21) but not adult (>W7) BiTg mice.

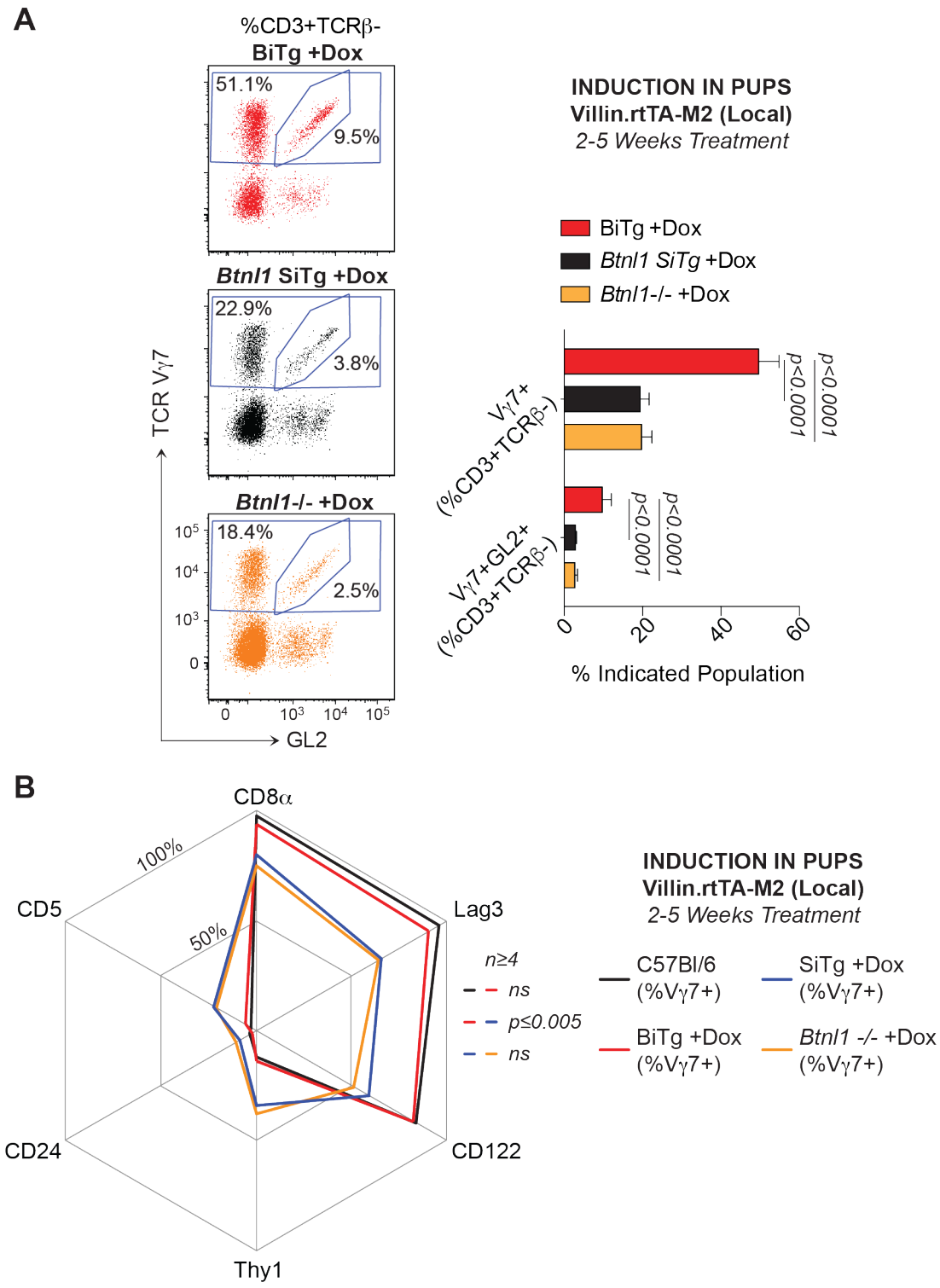

Figure 5.11 Villin-specific induction of *Btnl1* transgene in Bi-transgenic pups

(**A-B**) 7-21 day-old *Btnl1*$^{-/-}$ mixed-transgenic litters were blindly treated with Dox-water (1mg/ml Dox; 2% sucrose) for 2-5 weeks and analysed by flow cytometry. Genotyping was performed retrospectively. (**A**) γδ IEL composition (**B**) Surface phenotypes of W4-5 C57Bl/6 mice *vs.* Dox-treated mixed transgenic litters (SiTg➔*n=4; Rest*➔*n≥6*). Radar plot displays mean values. Panels (**A, B**) present data pooled from ≥3 experiments.

5.4 Conclusion

Our studies show that *Btnl1* mediates its selective impacts upon Vγ7$^+$ IEL in *trans* from the small intestinal epithelium. *Btnl1*-deficient enterocytes are thus incapable of supporting the phenotypic maturation and expansion of signature small intestinal Vγ7$^+$ IEL as they infiltrate the neonatal gut. Consequently, *Btnl1*$^{-/-}$ deficient animals carry a much-depleted Vγ7$^+$ IEL compartment, enriched for cells expressing an 'immature' CD122^{LO}Thy1$^+$Lag3$^-$CD5$^+$CD24$^+$ cell surface phenotype. This 'immature' phenotype is reminiscent of pre-selection DETC in *Skint1*-mutant mice (Lewis et al., 2006) and of putative Vγ7$^+$ IEL precursors that are enriched for in WT mice at D14 (**Figure 3.3A-C**). Therefore, it is possible that *Btnl1*$^{-/-}$ mice harbour a small compartment of putative 'immature' Vγ7$^+$ IEL precursors into their adulthood.

Consistent with this, acute induction of *Btnl1* expression in the small intestinal epithelium of adult (W7+) *Btnl1*$^{-/-}$ mice was sufficient to selectively elicit phenotypic change in the majority of 'residual' Vγ7$^+$. That such phenotypic changes in adult BiTg mice took place in the absence of detectable expansion supports the notion that *Btnl1* elicits a true phenotypic transition. However, it is not definitive proof of a precursor-product relationship. Whereas *Btnl1* induction in adults was associated with phenotypic change alone, its induction in BiTg pups (D7-D21) was associated with both expansion and phenotypic maturation. Given this, we conclude that enterocyte-expressed *Btnl1* elicits extrathymic phenotypic maturation and numerical expansion of Vγ7$^+$ IEL but that these effects are highly separable, with numerical expansion being confined to a developmental window within the first 5 post-natal weeks.

Having established that transgenic expression of *Btnl1* can elicit gain-of-function effects and rescue extrathymic Vγ7$^+$ IEL maturation ± expansion, we proceeded to investigate whether *Btnl1* can elicit similar gain-of-function effects *in vitro.*

Chapter 6. The Mechanism of *Btnl1* Activity

6.1 Introduction

The specificity of enterocyte-expressed *Btnl1* for Vγ7$^+$ IEL could imply that this molecule acts *via* a TCR-dependent pathway. Indeed, there is a strong precedent for BTN family members to regulate $\gamma\delta$TCR-dependent or -associated processes, with BTN3 regulating human Vγ9Vδ2$^+$ T cell activation and *Skint1* regulating murine DETC selection (Barbee et al., 2011; Boyden et al., 2008; Harly et al., 2012; Sandstrom et al., 2014; Turchinovich and Hayday, 2011). To further explore whether *Btnl1* may exert its impact on Vγ7$^+$ IEL *via* a TCR-associated pathway, it was necessary to establish a system in which *Btnl1* could elicit gain-of-function effects on Vγ7$^+$ IEL *in vitro.*

A recent study demonstrated that primary small intestinal enterocytes constitutively harbour *Btnl1* in complex with *Btnl6* (Lebrero-Fernández et al., 2016). Furthermore, the same study reported that *Btnl1* expressed together with *Btnl6* in MODE-K cells (Vidal et al., 1993) could preferentially elicit cell division in Vγ7$^+$ IEL that had previously undergone a 2 week expansion protocol *in vitro* (Lebrero-Fernández et al., 2016). The expansion protocol employed by this study has also been used by other studies of intestinal IEL biology (Bas et al., 2011; Swamy et al., 2015) and involves 48hrs of direct TCR stimulation in the presence of IL-2, IL-3, IL-4 and IL-15, followed by 12 days of culture in media supplemented with IL-2 alone. Given that such stimulation carries the potential to alter the composition and/or responsiveness of cultured T cells, it is not clear to what extent 'expanded' IEL are representative of IEL *in vivo*. To avoid this potential confounding issue in our studies we tested gain of function effects of MODE-K.*Btnl* transductants on intestinal IEL directly *ex vivo* in the absence of prior or concomitant TCR stimulation.

MODE-K cells are derived from proximal small intestinal epithelial cells of 2-week old germ-free mice that were cultured *in vitro* and immortalized by retroviral transduction of the large T gene of SV40 (Vidal et al., 1993). These cells express negligible levels of *Btnl1*, *Btnl4* and *Btnl6* and are insensitive to contact-mediated inhibition but do retain some features that are characteristic of intestinal epithelial

cells (Bas et al., 2011). For example, MODE-K cells adhere to plastic and form elongated cellular structures with stubby cytoplasmic protrusions that resemble microvilli (Vidal et al., 1993). MODE-K cells also retain expression of villin and cytokeratin 18, that are expressed in intestinal enterocytes and in glandular epithelial cells of the digestive tract, respectively (Vidal et al., 1993). As MODE-K cells retain some features of intestinal epithelium while lacking *Btnl1, Btnl4* and *Btnl6* expression, they provide a highly appropriate platform for *Btnl* gene gain-of-function assays.

Our previous studies have shown that enterocyte expression of *Btnl1* selectively elicits a number of phenotypic changes in $V\gamma7^+$ IEL *in vivo* (see Chapter 5). Prominent amongst these are the up-regulation of CD122 and down-regulation of CD24, both of which also occur during *Skint1*-mediated DETC selection (in the thymus) and during thymic agonist selection of $\alpha\beta$ thymocytes (Hanke et al., 1994; Lewis et al., 2006; McDonald et al., 2014; Narayan et al., 2012; Oh-hora et al., 2013). *In vitro*, the only systems in which *Skint1*-mediated selection of DETC progenitors has been rescued are FTOC and re-aggregate thymic organ cultures (RTOC) (Barbee et al., 2011; Turchinovich and Hayday, 2011). While murine bone marrow stroma-derived OP9 cells expressing delta-like 1 (OP9-DL1) can support the development of many $\alpha\beta$ and $\gamma\delta$ T cell lineages, OP9-DL1 cells transduced with *Skint1* have historically not been able to rescue *Skint1*-mediated selection outside of a RTOC (Barbee et al., 2011). Hence, it was likely that MODE-K.*Btnl* transductants would not be able to recapitulate the phenotypic changes (e.g. CD122 up-regulation) associated with *Btnl1*-mediated selection *in vivo*. We therefore had to broaden our repertoire of read-outs for gain-of-function effects.

One read-out employed by Lebrero-Fernandez, et al., (2016) was up-regulation of the IL2-receptor-α (IL2Rα) sub-unit (CD25), which is a robustly characterized consequence of TCR-mediated T cell activation but not of TCR-mediated agonist selection (Depper et al., 1984; Hanke et al., 1994; Kim and Leonard, 2002). Up-regulation of CD25 is detectable within ~6hrs of TCR engagement and has been shown to occur during TCR agonist antibody stimulation of DETC in a LAT-dependent manner (B. Zhang et al., 2015). TCR-driven up-regulation of CD25 is also thought to be an important event at the beginning of the 14-day intestinal IEL expansion protocol as it enhances IEL responsiveness to IL-2 cytokine *in vitro* (Bas

et al., 2011; Lebrero-Fernández et al., 2016; Swamy et al., 2015). As intestinal IEL do not express CD25 directly *ex vivo* (Denning et al., 2007), its up-regulation in a gain-of-function assay would be a sensitive read-out associated with TCR-mediated T cell activation. Additional read outs that may accompany up-regulation of CD25 include down-regulation of the TCR and down-regulation of CD122, which is selectively shuttled for proteasomal degradation during cytokine-driven IL-2 receptor internalisation (Hémar et al., 1995; Kim and Leonard, 2002; Yu and Malek, 2000).

Given BTN3 is known to regulate the antigen-driven TCR-dependent activation of $V\gamma9V\delta2^+$ T cells (Harly et al., 2012; Rhodes et al., 2015; Sandstrom et al., 2014), we investigated whether *Btnl1* expressed by MODE-K cells could similarly regulate the activation of signature $V\gamma7^+$ IEL. All gain-of-function assays were performed in the presence of IL-2, IL-3, IL-4 and IL-15 to maximise IEL viability during culture. Our gain-of-function read-outs included expression of CD25, CD122 and cell surface TCR (by anti-CD3).

6.2 Regulation of cell surface of *Btnl1, Btnl4* and *Btnl6* expression in MODE-K cells

Skint1 protein is poorly detectable at the cell surface, even when over-expressed in Human Embryonic Kidney (HEK)-293T cells (Barbee et al., 2011). Btnl6 is also poorly expressed at the cell surface of MODE-K cell transductants but can traffic to the cell membrane when in complex with Btnl1 (Lebrero-Fernández et al., 2016). To investigate the intracellular trafficking of Btnl1, MODE-K cells were transfected with of N-terminally tagged *Btnl* cDNA (FLAG-*Btnl1*, HIS-*Btnl4* and HA-*Btnl6*) individually, or in pairs. By flow cytometric analysis, Btnl1 cell surface expression was found to be greatly enhanced by co-expression of Btnl6 or Btnl4 (MFI increased from 333 to >1300). Likewise, cell surface Btnl6 expression was dependent on co-expressed Btnl1 (MFI increased from <200 to >1500), whereas there was no evidence of collaboration between Btnl6 and Btnl4 (**Figure 6.1**). Thus, the cell surface trafficking of a given Btnl molecule appeared to be tightly regulated, if not dependent upon co-expression of a specific, closely related Btnl isoform.

Given that *Btnl4*$^{-/-}$ mice displayed no detectable IEL phenotype (**Figure 4.5A**) and that *Btnl1* and *Btnl6* were previously shown to stimulate IEL *in vitro* and form heterodimers *in vivo* (Lebrero-Fernández et al., 2016), we tested the impact of Btnl1 and/or Btnl6 expressed in stably transduced MODE-K cells following overnight co-culture with intestinal IEL.

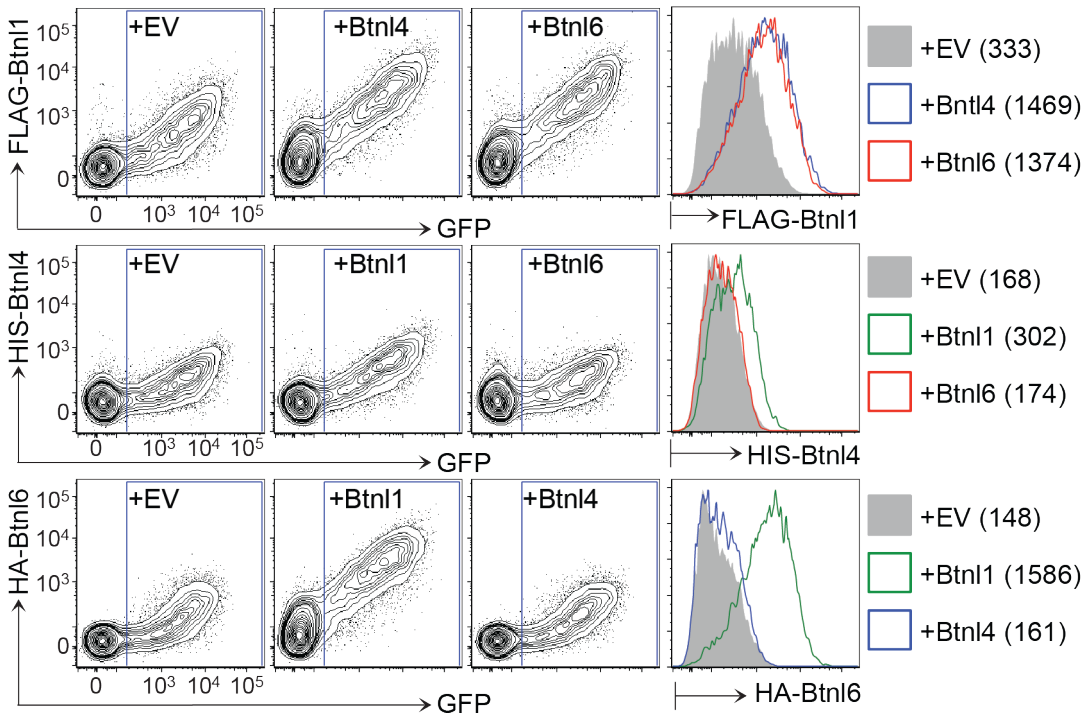

Figure 6.1 Cell surface Btnl expression in transfected MODE-K cells

Cell surface expression of FLAG-Btnl1, HIS-Btnl4 or FLAG-Btnl6 co-transfected in MODE-K cells. Constructs contained a tagged-Btnl linked to a GFP reported *via* an internal ribosome entry site (IRES). Histogram overlays show the expression of each BTNL after gating on GFP+ cells (numbers in brackets indicate geometric mean fluorescence intensity, gMFI). Cell lines were produced and analysed by Dr Vantourout.

6.3 The impact of MODE-K cells co-expressing Btnl1 and Btnl6 on intestinal IEL

6.3.1 Co-expression of Btnl1 and Btnl6 renders MODE-K cells capable of stimulating Vγ7$^+$ IEL

Overnight co-culture with MODE-K cells transduced with empty vectors (MODE-K.EV), Btnl1 (MODE-K.L1) or Btnl6 (MODE-K.L6) was associated with CD25 up-regulation in a small proportion (≤8%) of all IEL. However, MODE-K cells co-expressing Btnl1 and Btnl6 (MODE-K.L1+6), elicited a significant up-regulation of CD25 specifically in 15-30% of signature Vγ7$^+$ IEL (**Figure 6.2**). Relative to co-culture with MODE-K.EV, co-culture with MODE-K.L1+6 but not MODE-K.L1 or MODE-K.L6 was associated with a 2-8-fold increase in the proportion of Vγ7$^+$ cells expressing CD25 (*p<0.0001*). By contrast, there was no MODE-K.L1+6-dependent increase in CD25 expression amongst TCRβ^+ or Vγ7$^-$ $\gamma\delta$ IEL and there was no variation in its induction amongst IEL that had been co-cultured with MODE-K.EV relative to MODE-K.L1 or MODE-K.L6 (**Figure 6.2**). Concomitant expression of Btnl1 and Btnl6 therefore rendered MODE-K cells capable of selectively stimulating signature intestinal Vγ7$^+$ IEL *in vitro*. Given the lack of variation in the impact of MODE-K.EV relative to MODE-K.L1 or MODE-K.L6, our follow up studies exclusively employed MODE-K.EV as negative controls.

CD25 up-regulation downstream of TCR engagement can be detected within 6 hours (Depper et al., 1984; Kim and Leonard, 2002; Reinherz et al., 1982) and is often associated with down-regulation of the TCR (José et al., 2000) and CD122 (Hémar et al., 1995; Yu and Malek, 2000). To test whether MODE-K.L1+6 could elicit these changes in Vγ7$^+$ cells, we analysed CD25 expression by flow cytometry after 4 and 6 hours of co-culture with MODE-K.L1+6. We also assessed cell surface TCR (by anti-CD3) and CD122 expression in Vγ7$^+$ IEL following overnight co-culture with MODE-K.L1+6. CD25 expression was detectable on ~5.5% and ~2% of Vγ7$^+$ IEL following 6 hours of co-culture with MODE-K.L1+6 and MODE-K.EV, respectively (*p<0.0001*) (**Figure 6.3A**). Furthermore, cells that up-regulated CD25 were found to down-regulate TCR (detected by anti-CD3) and CD122

expression (**Fignre 6.3B, C**). Hence, the impact of MODE-K.L1+6 on $V\gamma7^+$ IEL evoked both the kinetics and the phenotypic consequences of TCR stimulation.

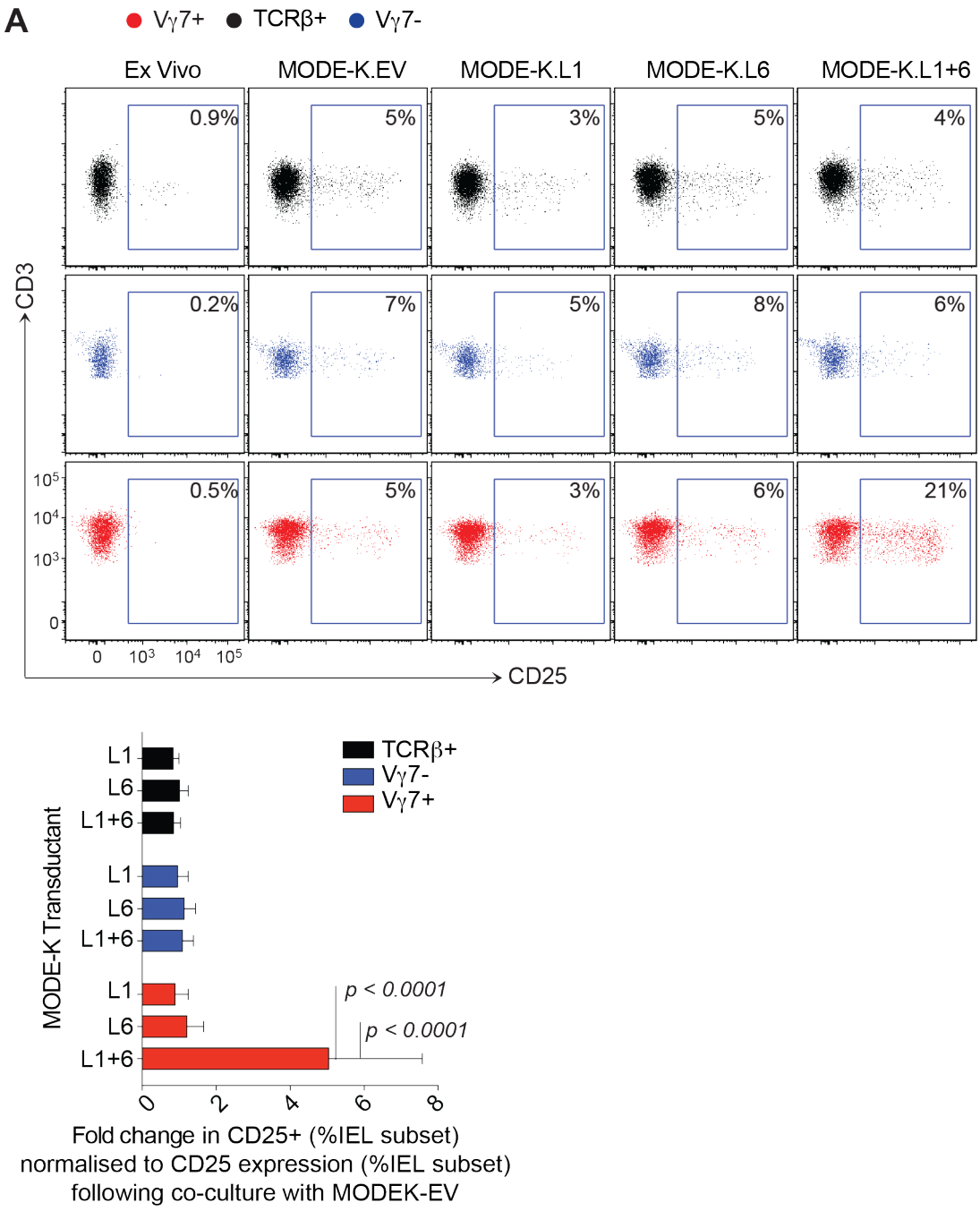

Figure 6.2 Primary intestinal IEL co-cultured with MODE-K transductants

Upper: Primary small intestinal IEL from week (W)3-6 mice cultured overnight with MODE-K cells transduced with constructs expressing either an empty vector (EV), *Btnl1* (L1), *Btnl6* (L6) or *Btnl1+6* (L1+6) analysed by flow cytometry for CD25 expression (*n=21*). *Lower:* Fold change in %CD25+ cells in the indicated IEL subsets following overnight co-culture with the indicated MODE-K transducants, normalised to %CD25+ cells following co-culture with MODE-K EV. (*n=21*). Data are representative of ≥5 independent experiments

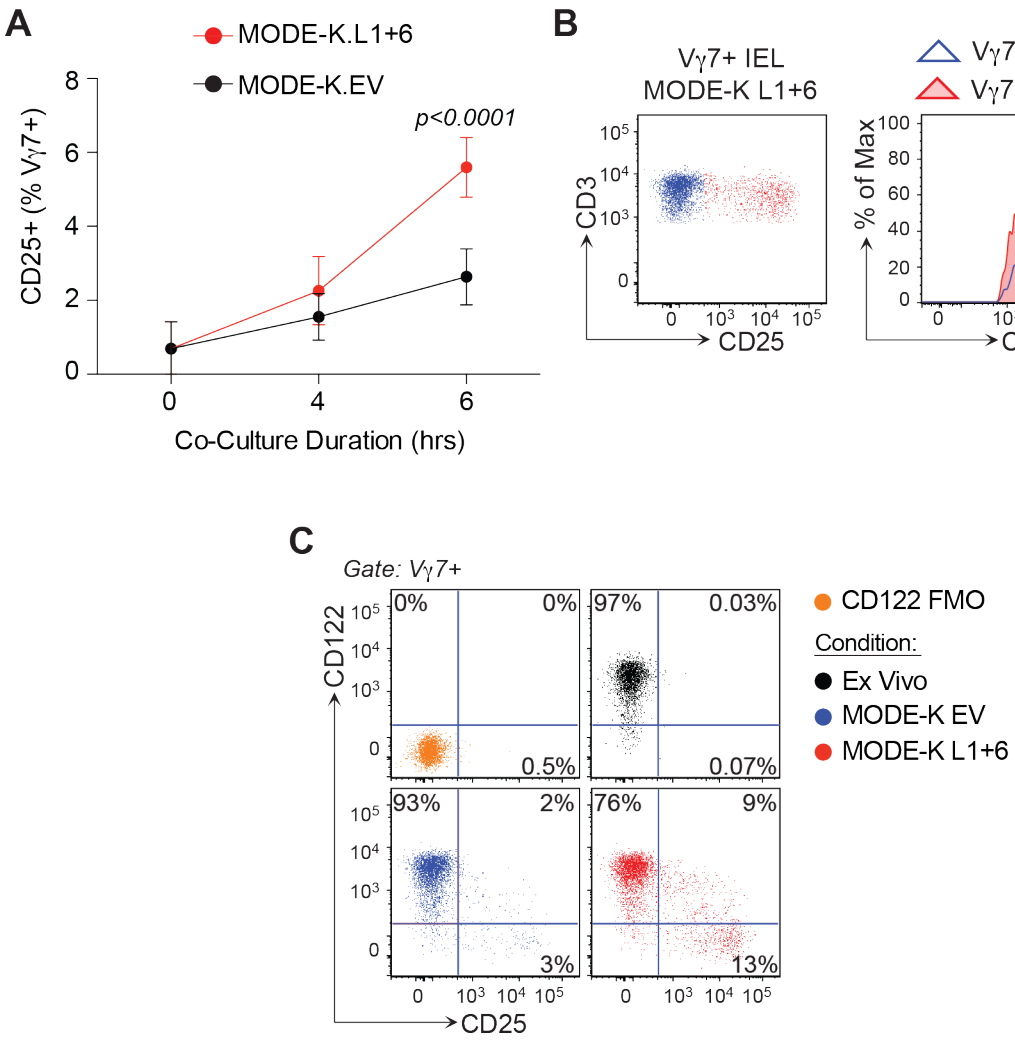

Figure 6.3 Vγ7^{+} IEL stimulation during co-culture with MODE-K transductants

A) Primary small intestinal IEL from W3-4 mice cultured for the indicated times with MODE-K cells transduced with constructs expressing an empty vector (EV) *vs. Btnl1+Btnl6* (L1+6) (*n=7*). **B)** CD3 expression in Vγ7+CD25+ *vs.* Vγ7+CD25- IEL following overnight co-culture with MODE-K.L1+6 (*n=21*). **C)** CD122 *vs.* CD25 expression on Vγ7+ cells from W3-5 mice following overnight co-culture with the indicated MODE-K transductants (*n=21*). Panels (**B,C**) are representative of ≥5 independent experiments. Panel (**A**) includes data pooled from 2 independent experiments

6.3.2 Cell-to-cell proximity with MODE-K.L1+6-cells is necessary and sufficient to elicit Vγ7$^+$ IEL stimulation

As previously discussed (see Chapter 1), cell-to-cell contact with a BTN3-expressing pAgPC is both necessary and sufficient to elicit TCR-dependent activation of human Vγ9$^+$Vδ2$^+$ T cells (Karunakaran and Herrmann, 2014). To test whether MODE-K.L1+6 were sufficient to elicit CD25 up-regulation on Vγ7$^+$ IEL, in the absence of any other cell subset, we performed overnight co-cultures using Vγ7$^+$ IEL that had previously been positively sorted by flow cytometry. While positive sorting of TCRVγ7$^+$ cells was associated with increased background induction of CD25 during co-culture with MODE-K.EV (6-7%), this did not obscure the >2-fold increase in CD25-expressing Vγ7$^+$ IEL following co-culture with MODE-K.L1+6 (**Figure 6.4A**). Hence, the MODE-K.L1+6-driven stimulation of Vγ7$^+$ IEL did not depend on any other cell-types.

To test whether Vγ7$^+$ IEL stimulation was contingent on their proximity to MODE-K transductants, we compared CD25 expression on IEL cultured in direct contact with the MODE-K monolayer, or sequestered in a suspended trans-well. Consistent with cell-to-cell proximity being important, <5% of Vγ7$^+$ IEL up-regulated CD25 when sequestered from MODE-K.EV and this did not change during sequestered co-culture with MODE-K.L1+6 (**Figure 6.4B**, *black bars*). While CD25 expression could be rescued by culturing IEL in direct contact with the monolayer (**Figure 6.4B**, *red and yellow bars*), it could not be rescued in sequestered IEL by additionally including IEL beneath the trans-well in contact with the MODE-K.L1+6 monolayer (**Figure 6.4B,** *yellow and blue bars*). Thus, we concluded that Vγ7$^+$ IEL stimulation was contingent on their cell-to-cell proximity to MODE-K.L1+6 cells and that soluble mediators produced by MODE-K.L1+6, or by CD25$^+$Vγ7$^+$ cells were insufficient to *trans*-activate sequestered T cells. In summary, cell-to-cell contact with MODE-K.L1+6 was both sufficient and necessary to elicit Vγ7$^+$ IEL stimulation.

6.3.3 Co-culture with MODE-K.L1+6 elicits weak T cell activation

MODE-K.L1+6-dependent stimulation of Vγ7$^+$ IEL *in vitro* induced down-regulation of cell surface TCR, CD122 and up-regulation of CD25. This phenotype is more

associated with T cell 'activation', rather than agonist selection, particularly as the latter induces up-regulation of CD122. To check for other consequences of putative IEL activation, we assayed 48hr co-culture supernatants for 36 cytokines in a luminex assay. Co-cultures that included γδ IEL (isolated from WT and TCRβ$^{-/-}$ mice) displayed MODE-K.L1+6-dependent increases in IFNγ (~2-fold; *p≤0.04*), GM-CSF (1.2 to 1.5-fold; *p≤0.002*), and CCL4 (~1.3-fold; *p≤0.02*), three typical effector molecules of intestinal IEL (**Figure 6.5**) (Hayday et al., 2001; Malinarich et al., 2010; Shires et al., 2001). By contrast, MODE-K.L1+6-dependent increases in cytokine production were not observed in co-cultures lacking γδ IEL (from TCRδ$^{-/-}$ mice), although these were associated with greater background levels of IFNγ production irrespective of co-culture condition. Hence, ≤150pg/ml IFNγ was detected following co-culture of TCRδ$^{-/-}$ with MODE-K.EV, relative to <50pg/ml, which was detected following co-culture of WT or TCRβ$^{-/-}$ IEL. We therefore concluded that weak γδ IEL activation may be occurring *in vitro* during co-culture with MODE-K.L1+6.

Taken together, these data attest to a specific cell-cell interaction taking place between Vγ7^{+} IEL and MODE-K cells *in vitro*. This interaction was dependent on MODE-K expression of Btnl1+Btnl6 and may have elicited weak T cell activation, possibly *via* a TCR-dependent pathway.

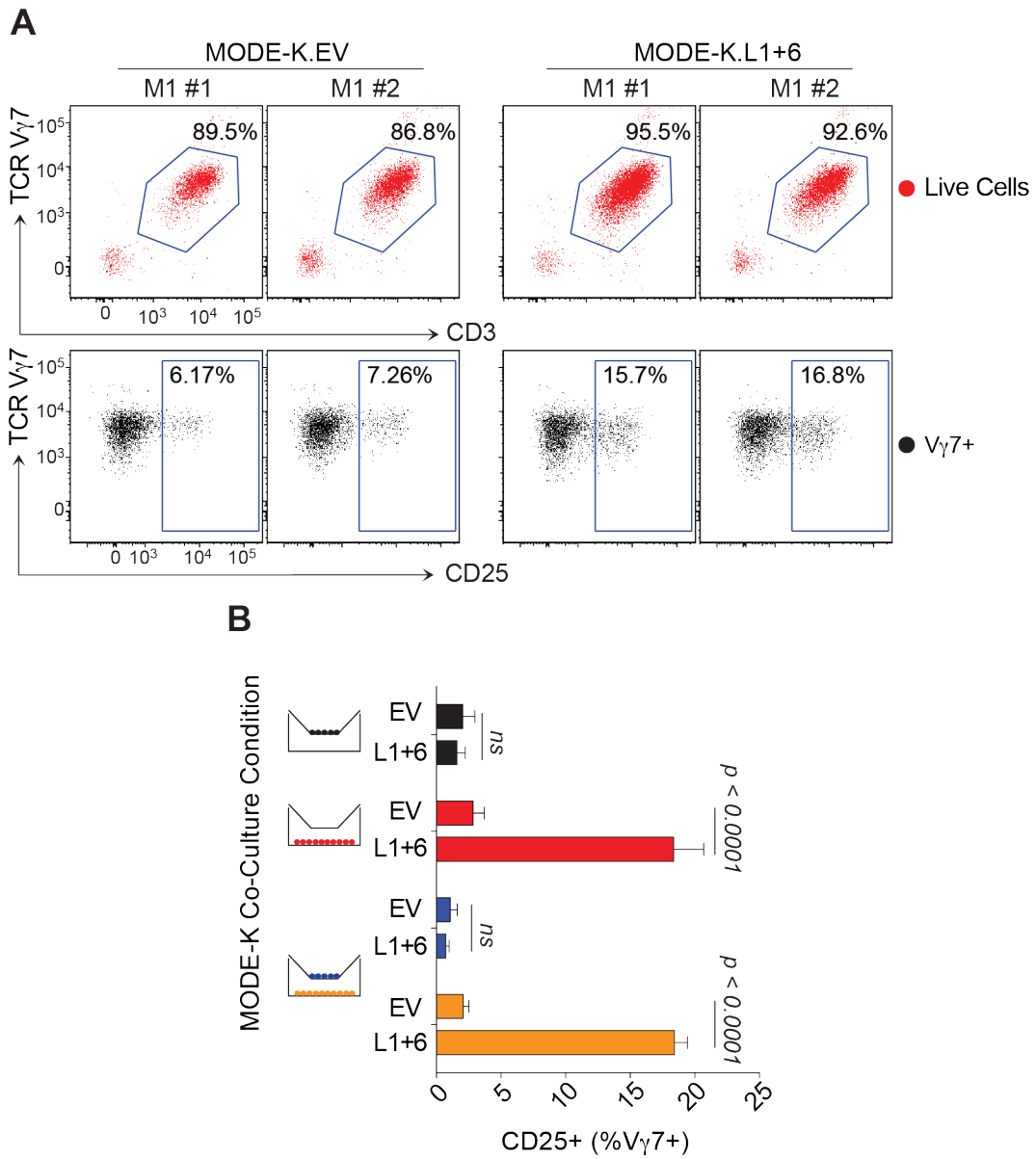

Figure 6.4 Contact dependency during IEL:MODE-K co-culture

A) CD25 expression in positively FACS-sorted Vγ7+ IEL from W3-5 mice cultured overnight with MODE-K cells expressing EV *vs.* L1+6 (*n=4*). *Upper:* Purity of positively sorted $V\gamma7^{+}$ IEL. *Lower:* CD25 expression after overnight co-culture with indicated MODE-K transductant. **B)** Mean CD25 expression in $V\gamma7^{+}$ IEL from W3-5 mice following the indicated overnight trans-well culture conditions (blue/black➔segregated; red/yellow➔in contact) (*n=3*). Panels are each representative of ≥2 independent experiments. Data in panel (**B**) provided by Dr Roberts.

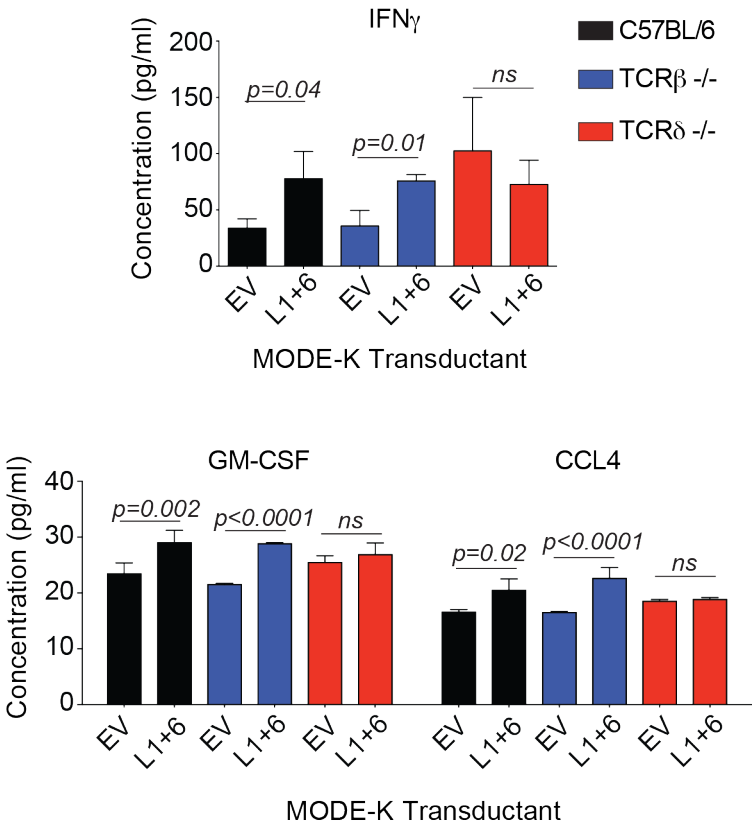

Figure 6.5 Cytokine production over 48 hours of IEL:MODE-K co-culture

IEL were isolated from 4 week-old mice of the indicated genotypes and co-cultured with the indicated MODE-K transductants for 48hrs. Supernatants were harvested and analysed by luminex assay for the presence of 36 cytokines, chemokines and growth factors (*n=3*). Data are representative of 1 experiment.

6.4 Molecular impact of co-culture with MODE-K.L1+6

6.4.1 Co-culture with MODE-K.L1+6 induces transcription at the *Nr4a1* gene locus amongst CD25$^+$Vγ7$^+$ IEL

Expression of *Nr4a1* (Nur77) marks one of the earliest transcriptional events downstream of TCR engagement in peripheral T cells and in thymocytes (Osborne et al., 1994; Winoto and Littman, 2002). This transcription factor is a member of the steroid-thyroid hormone receptor superfamily and is believed to be important for thymic negative selection (Winoto and Littman, 2002; Zhou et al., 1996), although mice deficient for Nur77 alone display no obvious defects in this process (S. L. Lee et al., 1995). Whereas the non-redundant functions of Nur77 in T cells and thymocytes are poorly defined, its transcriptional regulation is relatively well characterized and strongly associated with TCR-dependent calcium signalling (Feske et al., 2001; Winoto and Littman, 2002). Unlike CD69, the up-regulation of Nur77 is not induced by inflammatory stimuli and is thus considered to be a more specific read-out for TCR-associated intracellular signalling pathways. Because of this, the Nur77.*gfp* mouse that encodes a GFP reporter at the *Nr4a1* gene locus has been widely adopted to study developmental TCR signalling in iNKT cells and TCRβ^+CD8$\alpha\alpha^+$ IEL (Hogquist and S. C. Jameson, 2014; McDonald et al., 2014; Moran et al., 2011).

To test whether co-culture with MODE-K.L1+6 induced transcription at the *Nr4a1* gene locus, flow cytometric analysis was performed on primary IEL that had been recovered from W3-5 Nur77.*gfp* mice and cultured overnight on monolayers of MODE-K.EV or MODE-K.L1+6. Directly *ex vivo*, ~20% of TCRβ^+, ~36% of Vγ7$^-$ and ~28% of Vγ7$^+$ IEL expressed detectable levels of GFP. Irrespective of whether IEL were cultured with MODE-K.EV *versus* MODE-K.L1+6, GFP expression decreased to ~7% of TCRβ^+ and <25% of Vγ7$^-$ $\gamma\delta$ IEL (**Figure 6.6A**). By contrast, while co-culture with MODE-K.EV saw GFP expression amongst Vγ7$^+$ IEL drop from ~28% to <10%, co-culture with MODE-K.L1+6 was associated with an increase in GFP expression, such that ~34% of Vγ7$^+$ IEL were GFP$^+$ (**Figure 6.6A**). Thus, the selective interactions taking place between MODE-K.L1+6 and Vγ7$^+$ IEL *in vitro*

were sufficient to sustain and enhance transcription at the TCR-associated immediate early *Nr4a1* gene locus.

GFP expression was detectable in ~100% of $V\gamma7^{+}CD25^{+}$ cells following co-culture with MODE-K.L1+6 but only ≤50% of $V\gamma7^{+}$ IEL that up-regulated CD25 during co-culture with MODE-K.EV. Moreover, ≤50% of 'background' CD25-expression amongst $TCR\beta^{+}$ and $V\gamma7^{-}$ γδ IEL was associated with concomitant GFP-expression, irrespective of co-culture condition (**Figure 6.6A**). These data suggested that the induction of CD25 amongst $V\gamma7^{+}$ IEL that had been stimulated by MODE-K.L1+6 was uniquely driven *via* a TCR-associated pathway that elicited transcription at the *Nr4a1* gene locus. In support of this notion, $CD122^{-}CD25^{+}GFP^{+}$ cells were observed in ~7.5% of $V\gamma7^{+}$ IEL that had been cultured with MODE-K.L1+6 cells, relative to only ~1% of $V\gamma7^{+}$ IEL that had been cultured with MODE-K.EV (**Figure 6.6B**). We therefore concluded that CD25 up-regulation amongst $V\gamma7^{+}$ IEL co-cultured with MODE-K.L1+6 was uniquely linked to a TCR-associated pathway, whereas background CD25 induction was not.

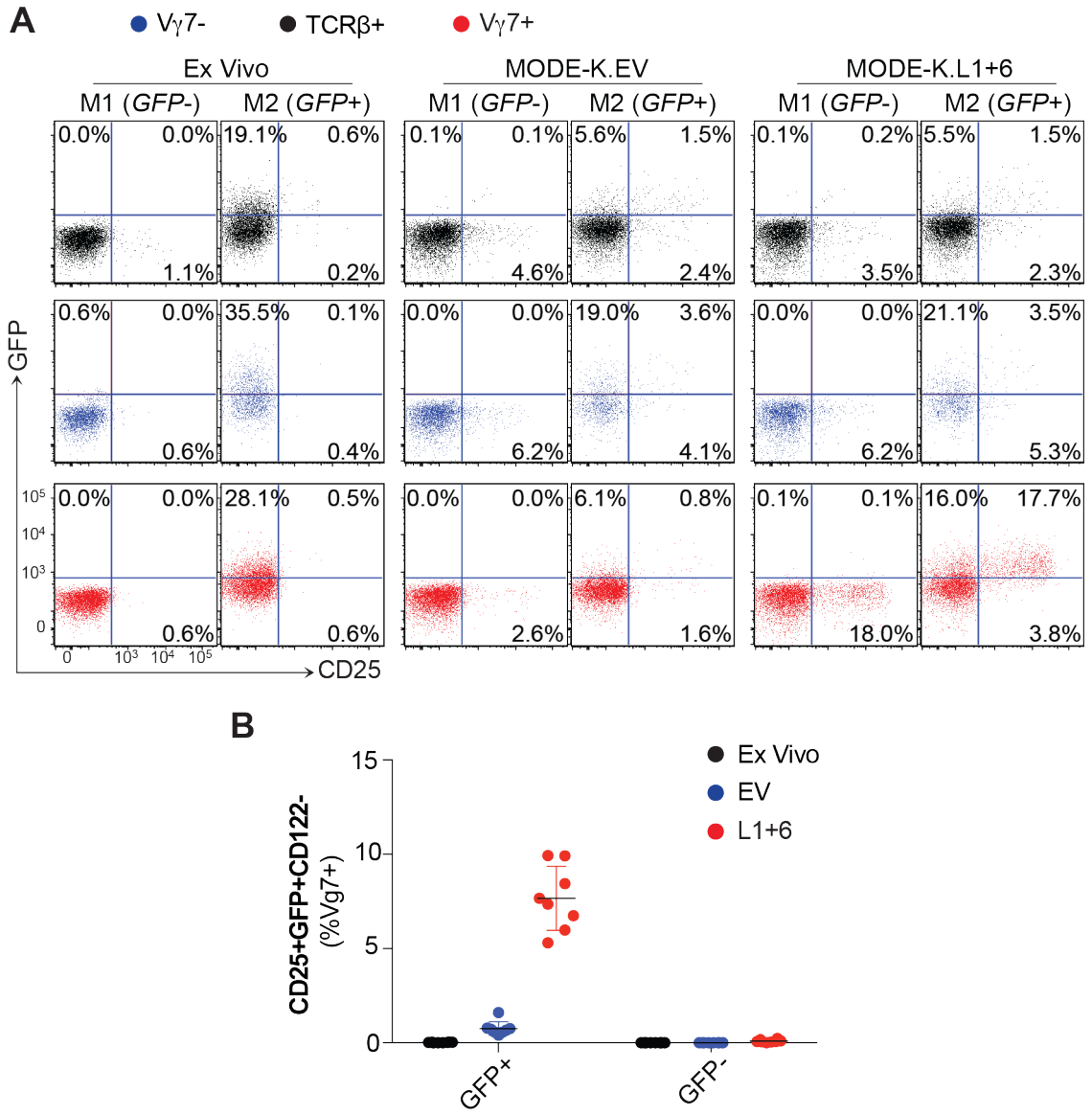

Figure 6.6 IEL from Nur77.gfp mice co-cultured with MODE-K transductants

A) GFP and CD25 expression in small intestinal IEL isolated from W3-5 Nur77.gfp mice *ex vivo* or following overnight co-culture with MODE-K expressing EV *vs.* L1-6 (*n=8*). **B)** %$V\gamma7^{+}$ cells from Nur77.gfp *versus* WT mice that were simultaneously $CD25^{+}$ GFP^{+} $CD122^{-}$ following overnight co-culture with the indicated MODE-K transductants. Panels (**A**) are representative of and include data pooled (**B**) from 2 independent experiments.

6.4.2 Stimulation with TCR agonist antibody elicits CD25 up-regulation in intestinal IEL

To verify whether direct TCR cross-linking could elicit CD25 expression amongst intestinal IEL recovered from W3-6 mice, freshly recovered cells were stimulated overnight on plate-bound anti-CD3 (10μg/ml) and analysed by flow cytometry. While TCR-stimulation elicited CD25 expression in ~10% of Vγ7$^+$ IEL, this effect was smaller than that seen for TCRβ$^+$ IEL (~20% CD25+) and Vγ7$^-$ IEL (~40% CD25+) (**Figure 6.7A**). Furthermore, it was also smaller than the ~20% of Vγ7$^+$ IEL that up-regulated CD25 in response to co-culture with MODE-K.L1+6 (**Figure 6.7B**). By contrast, 'residual' Vγ7$^+$ IEL from *Btnl1*$^{-/-}$ mice displayed greatly enhanced responsiveness to TCR stimulation with ~30% of cells up-regulating CD25 (**Figure 5.7B**). Consistent with their capacity to respond to the acute up-regulation of *Btnl1 in vivo* (See chapter 5), residual Vγ7$^+$ from *Btnl1*$^{-/-}$ mice could also respond to MODE-K.L1+6 *in vitro*. However, by contrast to their enhanced responsiveness to direct TCR cross-linking, their up-regulation of CD25 following co-culture with MODE-K.L1+6 was comparable to that seen in Vγ7$^+$ cells from WT mice, with ~20% of cells up-regulating CD25 (**Figure 5.7B**). Thus, although anti-CD3 stimulation could elicit CD25 up-regulation in all IEL subsets, the responsiveness of Vγ7$^+$ IEL to direct TCR cross-linking was attenuated in cells that had previously encountered *Btnl1 in vivo*. By contrast, prior exposure to *Btnl1 in vivo* had no effect on the responsiveness of Vγ7$^+$ IEL to co-culture with MODE-K.L1+6.

To test whether TCR-associated signalling components were required for MODE-K.L1+6-driven stimulation, co-cultures were supplemented with PP2, an inhibitor of Src-family kinases (SFK) or its negative control, PP3. SFKs act proximally to TCR triggering and are responsible for phosphorylating ITAM domains on the cytoplasmic tails of CD3. When such phosphorylation is inhibited, the TCR complex is unable to recruit intracellular Syk-family kinases and TCR signal cannot be propagated (P. E. Love and Hayes, 2010; Smith-Garvin et al., 2009). Consistent with SFK activity being critical for Vγ7$^+$ IEL stimulation, supplementation of the co-culture with PP2 but not PP3 reduced the proportion of Vγ7$^+$ IEL up-regulating CD25 during co-culture with MODE-K.L1+6 by ~90% (**Figure 6.8**). By contrast,

PP2 had no effect on background induction of CD25 during co-culture with MODE-K.EV. Taken together, these data support the hypothesis that MODE-K can elicit Btnl1+Btnl6-dependent stimulation of $V\gamma7^+$ IEL *via* a TCR-*associated* molecular pathway. Furthermore, they suggest that background CD25 expression is independent of SFK and thus occurs independently of TCR signalling.

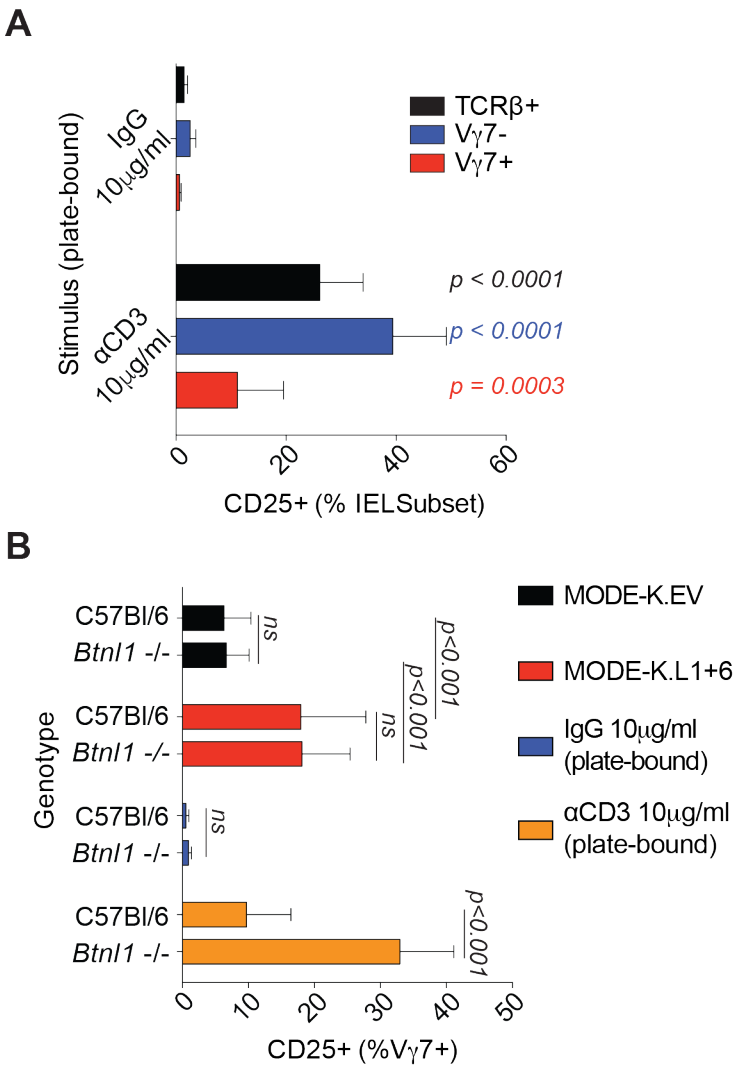

Figure 6.7 Direct TCR stimulation of 1^0 intestinal IEL and IEL co-cultured with MODE-K transductants

A) CD25 expression in primary IEL from WT W3-6 mice treated overnight with plate-bound αCD3 (10mg/ml) or IgG isotype control (*n*≥*12*). **B)** Mean CD25 expression on $V\gamma7^+$ IEL from W3-5 WT *vs* *Btnl1*-/- mice following the indicated overnight culture conditions (*n*=7; IgG/αCD3 at 10μg/ml plate-bound). Panels (**A,B**) include data pooled from ≥3 independent experiments.

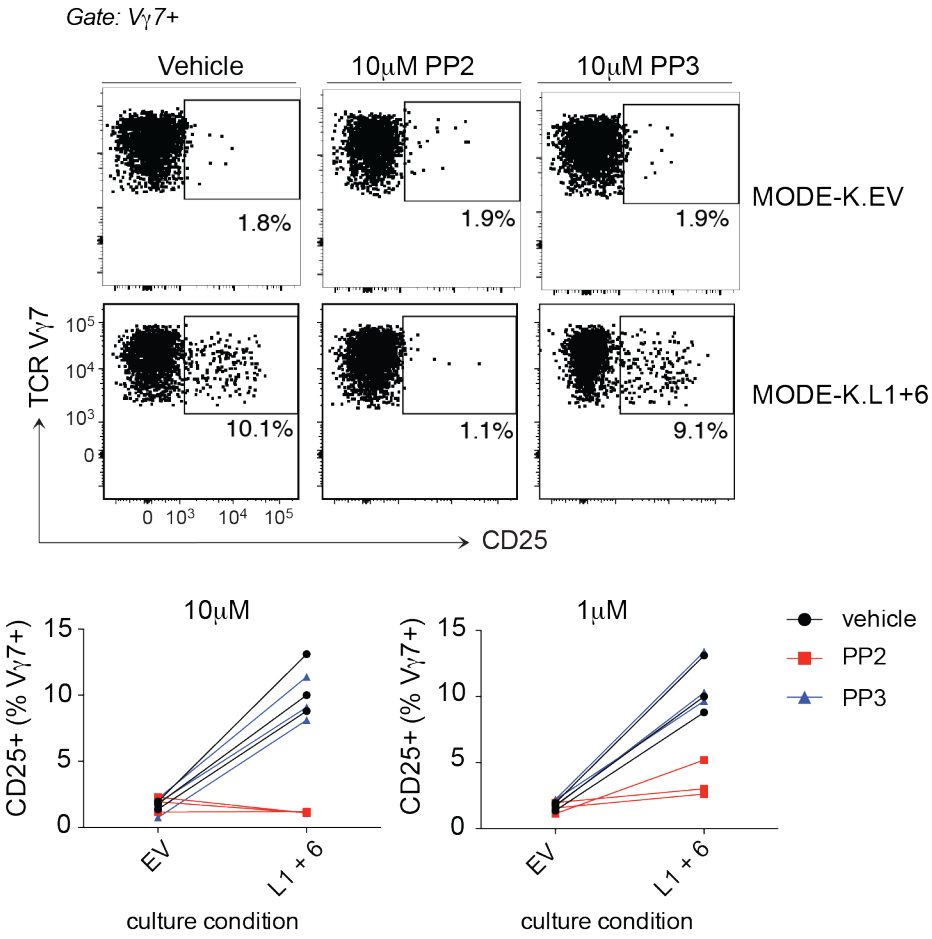

Figure 6.8 IEL:MODE-K co-cultures in the presence of signalling inhibitors

CD25 expression in primary Vγ7$^+$ IEL from W4 mice treated with PP2, PP3 or vehicle and co-cultured overnight with the indicated MODE-K transductants. Values above graphs correspond to the concentration of PP2 or PP3 that was used. *Upper:* Representative plots following co-culture. *Lower:* two different concentrations of PP2/PP3. Data are representative of 1 experiment. Data provided by Dr Roberts.

6.4.3 Conclusion

These studies have demonstrated that MODE-K cells expressing Btnl1 together with Btnl6 are sufficient to elicit selective stimulation of co-localised Vγ7$^+$ IEL, giving rise to several of the same consequences as TCR-mediated T cell activation. These consequences include up-regulation of CD25, enhanced transcription at the *Nr4a1* gene locus and down-regulation of the TCR (by anti-CD3) and of CD122. Consistent with its putative induction downstream of TCR signal, the up-regulation of CD25 was highly sensitive to SFK inhibition by PP2. By contrast, background induction of CD25 during co-culture with MODE-K.EV was not sensitive to PP2-mediated inhibition and was also not strongly associated with active transcription at the *Nr4a1* gene locus. We therefore conclude that MODE-K.L1+6 cells are able to selectively activate a TCR-associated response-pathway in intestinal Vγ7$^+$ IEL.

Our studies have also shown that selective interactions with *Btnl1*-expressing enterocytes *in vivo* may attenuate the responsiveness of Vγ7$^+$ IEL to direct TCR stimulation *ex vivo*. Thus, relative to Vγ7$^+$ IEL from WT mice, a greater proportion of 'residual' Vγ7$^+$ IEL from *Btnl1*$^{-/-}$ mice up-regulated CD25 in response to direct TCR cross-linking. By contrast, the responsiveness of Vγ7$^+$ IEL from WT and *Btnl1*$^{-/-}$ mice to stimulation by MODE-K.L1+6 was not significantly different. The comparable responsiveness of Vγ7$^+$ IEL from WT and *Btnl1*$^{-/-}$ mice to MODE-K.L1+6-mediated stimulation *in vitro* is consistent with their capacity to respond to *Btnl1 in vivo* (see chapter 5) and further supports the notion that CD122^{LO} Vγ7$^+$ IEL in *Btnl1*$^{-/-}$ mice are precursors to signature CD122^{HI} Vγ7$^+$ IEL in WT mice.

Given these collective observations, we conclude that MODE-K.L1+6 can elicit selective stimulation of Vγ7$^+$ IEL, *via* the engagement of cell surface receptors, which may include the Vγ7$^+$ TCR.

Chapter 7. Discussion

Up to this point, the discovery of *Skint1* had provided a singular insight into how organ-specific products of epithelial cell differentiation may actively regulate γδ IEL composition (Barbee et al., 2011; Lewis et al., 2006). However, as *Skint* genes are mostly expressed in the skin and thymus, and neither *Skint* nor DETC are conserved in humans, the generality of this pathway was unclear (Boyden et al., 2008). The aim of this thesis was to determine whether *Skint1*-mediated regulation of DETC composition is exceptional, or whether it represents a generalizable mechanism by which epithelia regulate the composition of local intraepithelial γδ T cell compartments.

To investigate this, we characterized the phenotypic maturation of signature small intestinal Vγ7$^+$ IEL and found evidence to suggest that this occurred *via* an extrathymic pathway. This pathway exhibited key parallels with *Skint1*-mediated DETC selection and was found to be dependent on enterocyte-expressed *Btnl1*, a gene that is closely related to *Skint1* (see Chapter 1). Consistent with the extrathymic nature of this pathway, the impact of *Btnl1* was mediated within the gut and its transgenic expression in small intestinal enterocytes was sufficient to rescue phenotypic transition and expansion of Vγ7$^+$ IEL *in vivo*. To study the mechanism through which *Btnl1* acts, we developed a gain-of-function system *in vitro* and showed that Btnl1 can co-operate with Btnl6 to stimulate Vγ7$^+$ IEL *via* a TCR-associated pathway. In summary, our studies firmly establish that *Skint1*-mediated DETC selection is one example of a general mechanism employed by epithelia to establish and maintain the signature γδ IEL composition. Furthermore, they provide additional evidence to support the notion that Btnl molecules influence IEL composition through the selective activation of TCR-associated signalling pathways.

7.1 Hallmarks of signature small intestinal γδ IEL

Consistent with their status as the signature small intestinal γδ IEL subset, Vγ7$^+$ IEL selectively displayed a mature cell surface phenotype that resembled both *Skint1*-selected DETC and/or agonist-selected TCRβ$^+$CD8αα$^+$ IEL (**Table 7.1**). This

included uniformly high expression of CD122, TCR, TIGIT, CD69 and Lag3; their expression of the CD8$\alpha\alpha^+$ homodimer; and their lack of cell surface Thy1 and CD5.

Table 1 Surface phenotypes of DETC and intestinal IEL subsets

Expression levels presented as high (+++); moderate (++); low (+); mostly negative +/-); and negative (-). Data for V$\gamma7^+$ and V$\gamma7^-$ IEL are presented in thesis results chapters. Data for TCRβ^+CD8$\alpha\alpha^+$/CD8$\alpha\beta^+$ IEL and DETC are compiled from our unpublished data and are corroborated by several studies (Denning et al., 2007; Gangadharan et al., 2006; Klose et al., 2014; Lewis et al., 2006; Mayans et al., 2014; McDonald et al., 2014; Payer et al., 1991; 1995; 1994; Pennington et al., 2003; 2006; Sumaria et al., 2011; Turchinovich and Hayday, 2011).

IEL subset	CD122	TIGIT	TCR	CD8$\alpha\alpha$	Lag3	CD5	Thy1	CD69
V$\gamma7^+$	+++	+++	+++	+++	+++	-	+/-	+++
DETC	+++	+++	+++	-	+++	-	++	+++
TCRβ^+CD8$\alpha\alpha^+$	+++	+++	+	+++	+++	-	+/-	+++
V$\gamma7^-$ (CD3$^+$TCRβ^-)	+/-	+/-	++	++	+/-	+/-	+/-	++
TCRβ^+CD8$\alpha\beta^+$	+/-	+/-	+	+/-	+/-	+++	+++	++

7.1.1 Dependency on IL-15 signalling

Of these phenotypic markers, CD122 (IL-2/-15Rβ) is one of the most critical components of DETC and intestinal IEL biology. High expression of CD122 by DETC, TCRβ$^+$CD8αα$^+$ and Vγ7$^+$ IEL confers sensitivity to IL-15, which is constitutively produced by epithelial cells and is critically required for their long-term maintenance (De Creus et al., 2002; Kawai et al., 1998; Lai et al., 2008; Lodolce et al., 1998; Ma et al., 2009; Schluns et al., 2004). By contrast, intestinal Vγ1$^+$ and TCRβ$^+$CD8αβ$^+$ T_{RM} IEL express low levels of CD122, and accordingly, are not dependent on IL-15-signalling for their reconstitution in bone marrow chimeras (Schenkel et al., 2016; Schluns et al., 2004; Sheridan et al., 2014). Thus, a dependency on IL-15 signalling differentiates signature IEL compartments, including DETC, Vγ7$^+$ and TCRβ$^+$CD8αα$^+$ IEL from other populations of co-localised intestinal or dermal γδ or αβ T cells.

The developmental up-regulation of CD122 is classically associated with agonist selection and has been shown to occur in αβ or γδ thymocytes following agonist ligand engagement (Hanke et al., 1994; Jensen et al., 2008; McDonald et al., 2014; Muñoz-Ruiz et al., 2016; Oh-hora et al., 2013). Indeed, intraperitoneal injection of TCR agonist antibody in adult mice has recently been shown to elicit a significant increase in representation of CD122^{HI}NK1.1$^+$ γδ thymocytes (Muñoz-Ruiz et al., 2016). Moreover, DETC up-regulate CD122 along with their TCR during *Skint1*-mediated selection, which is thought to involve a TCR-associated pathway (Lewis et al., 2006; Turchinovich and Hayday, 2011). Assuming the level of CD122 expression correlates with sensitivity to IL-15, selective up-regulation of CD122 amongst *Btnl*- or agonst-selected IEL subsets could confer a selective survival advantage to these cells, enabling them to preferentially thrive in their respective epithelial microenvironments.

7.1.2 Inhibitory co-receptors

Signature Vγ7$^+$ IEL were also characterized by their constitutively high expression of several co-inhibitory receptors including the CD8αα homodimer, Lag3 and TIGIT, all of which have been shown to be up-regulated on αβ T cells during antigen

dependent activation (Y. Huang et al., 2011; Joller et al., 2011; Mucida et al., 2013; Reis et al., 2014; 2013; Triebel et al., 1990). Lag3 and TIGIT are additionally up-regulated during thymic agonist selection and are highly expressed in the periphery by agonist-selected $CD4^+$ regulatory T cells (C.-T. Huang et al., 2004; Joller et al., 2014; Oh-hora et al., 2013). The precise mechanisms by which these co-inhibitory receptors attenuate T cell activation are not fully understood but their ligands are often expressed in the small intestinal epithelium, either at the steady state or during inflammation.

CD8$\alpha\alpha$ binds mouse thymus leukaemia antigen (TLA), a non-classical MHC class I molecule, which is constitutively expressed by thymic epithelium and intestinal epithelium and can be induced on activated APCs (Y. Huang et al., 2011; Leishman et al., 2001). The CD8$\alpha\alpha$ homodimer is believed to repress T cell activation and has been shown to promote T cell survival in the context strong TCR signaling (Cheroutre and Lambolez, 2008; Gangadharan et al., 2006; Y. Huang et al., 2011; Madakamutil et al., 2004). TIGIT is a member of the Ig superfamily and may regulate T cell activation intrinsically by recruiting phosphatases to its cytoplasmic immunoreceptor tyrosine-based inhibitory (ITIM) motif (Anderson et al., 2016). TIGIT competes with DNAM-1, a positive co-stimulator of lymphocyte activation, for the engagement of poliovirus receptor (PVR), which is expressed in the gastro-intestinal tract (Anderson et al., 2016; Chan et al., 2014; Uhlen et al., 2015). Lag3 is structurally similar to CD4 and has been shown to engage both MHC class II or LSECtin (CLEC4G), although it is not yet clear which of these interactions are responsible for its repressor function *in vivo* (Huard et al., 1995; Xu et al., 2014). Nonetheless, MHC class II expression can be induced on small intestinal epithelial cells by IFNγ signaling, whereas LSEctin is highly expressed in the hepatobilliary system and in melanoma but is relatively understudied in the small intestine (Büning et al., 2005; Xu et al., 2014). Thus, it is possible that all these co-inhibitory receptors are constitutively and/or inducibly engaged to increase the threshold for IEL activation.

High activation thresholds may be critical to maintain the 'activated-yet-resting' state of intestinal IEL that are thought to harbour considerable cytolytic potential (Fahrer et al., 2001; Shires et al., 2001). Intestinal $\gamma\delta$ IEL constitutively express high levels of granzyme (Gzm)A and GzmB, which can induce apoptosis upon entry into

target cells (Beresford et al., 1999); and FasL, which induces apoptosis of target cells upon engagement of Fas (Fahrer et al., 2001; Nagata and Golstein, 1995; Shires et al., 2001). Given that agonist-selected IEL are thought to be self-reactive, constitutive inhibition may be critical to prevent their inappropriate activation in the absence of overt challenge (Cheroutre et al., 2011; Hayday et al., 2001; Rocha et al., 1991). Moreover, as many of these inhibitory co-receptors are also shared by DETC but not by other tissue-resident γδ or αβ T cell subsets, they may represent a generalizable form of T cell regulation employed by the intraepithelial gatekeepers of the lymphoid-stress surveillance response.

7.1.3 Extrathymic maturation

Whereas DETC progenitors acquire their mature cell surface phenotype across a *Skint1*-dependent checkpoint in the embryonic thymus (Lewis et al., 2006; Turchinovich and Hayday, 2011), our studies found no evidence for intra-thymic maturation of Vγ7$^+$ or Vγ7$^+$GL2$^+$ cells during the first 8 post-natal weeks. Instead, we identified a putative developmental checkpoint for these signature T cells in the small intestinal epithelium between postnatal D14 and D21. This checkpoint was associated with significant phenotypic change and selective expansion of Vγ7$^+$ IEL, such that their representation amongst γδ IEL increased by 1.5- to 4-fold during this time. Furthermore, transition through this checkpoint occurred independently of the thymus, most secondary lymphoid organs, the microbiome and diet-derived protein, evoking *Skint1*-mediated DETC selection and MHC-mediated selection of αβ T cells in the thymus.

A notable difference between our data regarding the extra-thymic maturation of Vγ7$^+$ IEL and the intra-thymic maturation of DETC is that we were not able to demonstrate a time point at which 100% of Vγ7$^+$ IEL carried an immature cell surface phenotype. Instead, we found that at D14-D17, Vγ7$^+$ IEL displayed a bi-modal distribution in cell surface phenotype, with an enrichment in 'immature' CD122^{lo}Thy1$^+$ putative precursor cells. Although post-natal D14 was the earliest time-point at which these cells could be reliably recovered in sufficient numbers for flow cytometric analysis, it is likely that Vγ7$^+$ begin their infiltration of the small intestinal epithelium at an earlier time point (Kuo et al., 2001), which would allow a

significant proportion of cells to have attained phenotypically maturity ($CD122^{hi}Thy1^{-}$) by the time of our analysis.

Our phenotypic profiling of putative $V\gamma7^{+}$ precursor cells demonstrated that they carried a $TCR^{LO}TIGIT^{LO}Lag3^{-}CD24^{+}CD5^{+}CD8\alpha^{-}$ cell surface phenotype that was reminiscent of pre-selection DETC and of $V\gamma7^{+}$ thymocytes and importantly, did not overlap with the phenotype of their 'mature' $V\gamma7^{+}$ IEL counterparts (see table 1) (Lewis et al., 2006; Turchinovich and Hayday, 2011). The expression of CD24 on putative intestinal precursor cells was particularly surprising, as it is conventionally associated with $\gamma\delta$ and $\alpha\beta$ thymocyte maturation (Narayan et al., 2012). Thus, by multiple phenotypic criteria, the putative precursor population we have characterised evokes a pre-selection DETC or 'immature' $\gamma\delta$ thymocyte population.

Consistent with this, several genes that are up- or down-regulated across the *Skint1* selection checkpoint were similarly up- or down-regulated in 'mature' $CD122^{HI}$ $V\gamma7^{+}$ IEL relative to 'immature' $CD122^{LO}V\gamma7^{+}$ IEL. Up-regulated genes included *Tbx21* (T-bet), which is known to be critical for the development of $\gamma\delta$ and $\alpha\beta$ $CD8\alpha\alpha^{+}$ IEL (Klose et al., 2014; Kwong and Lazarevic, 2014); *Xcl1*, which is highly expressed by intestinal IEL and is produced by DETC (Boismenu et al., 1996; Lei and Takahama, 2012; Shires et al., 2001); and *Tnfrsf9* (4-1bb), which is a positive co-stimulatory receptor for T cell activation that is known to be up-regulated during TCR engagement (S. J. Lee et al., 2013). Down-regulated genes include *Bcl11b*, *Sox13, Sox4* and *Rorc,* all of which play important roles during $\gamma\delta$ thymocyte differentiation (Gray et al., 2013; Kang and Malhotra, 2015; Kueh et al., 2016; Malhotra et al., 2013; Turchinovich and Hayday, 2011); and are particularly important for the development of IL-17 producing $\gamma\delta$ T cells (**Figure 1.5**) (Gray et al., 2013; Malhotra et al., 2013; Turchinovich and Pennington, 2011). This comparative gene expression analysis is the first of its kind for $V\gamma7^{+}$ cells, as previous studies have been unable to identify 'mature' and 'immature' counterparts co-localised within the same organ (e.g. the thymus) (Narayan et al., 2012). As both *Skint1*-mediated DETC selection, and intestinal $V\gamma7^{+}$ IEL maturation were associated with similar changes in gene expression, these data suggested similar intracellular pathways were being activated across the two developmental checkpoints.

While our data are consistent with a model in which CD122^{lo}Thy1^{hi} Vγ7^{+} IEL mature into their CD122^{hi}Thy1^{lo} counterparts, our work has not confirmed that a true precursor-product relationship exists between these two populations. To address this, future studies should seek to adopt lineage-tracing methods to map out the development pathway of these cells. An initial approach could be to adoptively transfer cell trace violet-loaded $\gamma\delta$ thymocytes, which uniformly display an 'immature' cell surface phenotype, into an adult lympho-depleted host. By labelling these cells, one could track their infiltration into the gut and correlate cycles of cell division with changes in the expression of CD122 and Thy1.

7.2 The biological impact of *Btnl1 in vivo*

Consistent with our hypothesis, our analysis of *Btnl1*- and *Btnl4*-deficient mice has demonstrated that *Btnl1* but not *Btnl4* is a critical determinant for signature Vγ7^{+} IEL. *Btnl1*$^{-/-}$ mice displayed a ~90% depletion of signature small intestinal Vγ7^{+} IEL. The lymphodepletion associated with *Btnl1*-deficiency was highly specific to the Vγ7^{+} IEL compartment as *Btnl1*$^{-/-}$ mice displayed no depletion in other intestinal $\gamma\delta$ IEL (e.g. Vγ1^{+} and Vγ4^{+}), and likewise displayed no alterations in systemic T cell, B cell and myeloid cell composition. Moreover, *Btnl1*-deficiency had no impact on the abundance or cell surface phenotype of Vγ7^{+} thymocytes. Thus, *Btnl1* is a critical extrathymic regulator of intestinal $\gamma\delta$ IEL composition. These data further substantiate previous reports showing *Btnl1*, *Btnl4* and *Btnl6* to be exclusively highly expressed in small intestinal enterocytes (Bas et al., 2011). Furthermore, they extend the paradigm of *Skint1*-mediated DETC selection to other epithelial tissues, suggesting it represents a generalizable mechanism of regulating $\gamma\delta$ IEL composition.

In the absence of *Btnl1*, Vγ7^{+} IEL failed to uniformly acquire their mature cell surface phenotype and failed to selectively expand *in situ*. Hence, the severely depleted 'residual' Vγ7^{+} IEL compartment of *Btnl1*$^{-/-}$ mice was enriched for cells carrying an 'immature' CD122^{LO}TIGIT^{LO}Thy1^{+}CD8α^{-}Lag3^{-}CD24^{+}CD5^{+} cell surface phenotype reminiscent of Vγ7^{+} thymocytes; 'immature' Vγ7^{+} IEL from D14-D17 WT mice; and pre-selected DETC-progenitors (Lewis et al., 2006). 'Residual' Vγ7^{+} IEL also displayed a significantly reduced rate of thymidine analogue incorporation at

D28 and a smaller proportion of cells expressed Ki67 at every time point analysed between D14 to W7. Given that haematopoietic expression of *Btnl1* was dispensable for Vγ7$^+$ IEL development, we concluded that enterocyte-expressed *Btnl1* acted in *trans* to drive the extrathymic maturation and expansion of Vγ7$^+$ IEL. Thus, the depletion in Vγ7$^+$ IEL from *Btnl1*$^{-/-}$ mice was at least partly caused by a failure of *Btnl1*-deficient enterocytes to support the neonatal maturation and expansion of this signature intestinal immune compartment.

7.2.1 Some Vγ7$^+$ IEL in *Btnl1*$^{-/-}$ mice attain 'mature' CD122^{HI} status

A key difference between the impact of *Btnl1* and *Skint1* on signature IEL compartments is that *Skint1*-mediated selection initially takes place in the thymus, whereas *Btnl1*-mediated selection takes place peripherally in the small intestinal epithelium (Lewis et al., 2006; Turchinovich and Hayday, 2011). Consequently, DETC progenitors in *Skint1*-mutant mice display developmental defects in the thymus and fail to home to the skin, whereas putative Vγ7$^+$ IEL precursors in *Btnl1*$^{-/-}$ mice infiltrate the small intestinal epithelium but fail to mature and expand *in situ* (Barbee et al., 2011; Boyden et al., 2008; Jin et al., 2010). Although Vγ7$^+$ IEL are highly depleted in the absence of *Btnl1*, our data do show that a proportion of Vγ7$^+$ IEL in *Btnl1*$^{-/-}$ mice are able to attain a CD122^{HI}Thy1^{LO} cell surface phenotype, reminiscent of their 'mature' counterparts in WT mice (see Chapter 5). Assuming Vγ7$^+$ IEL in WT mice universally acquire their mature cell surface phenotype in the gut, the up-regulation of CD122 in *Btnl1*-deficient animals must be occurring *via* an alternative pathway and there are various possibilities in this regard.

Firstly, in the absence of *Btnl1*, it is possible that *Btnl4* and/or *Btnl6* could elicit some degree of phenotypic maturation in a proportion Vγ7$^+$ IEL *in vivo*. Alternatively, it is possible that a proportion of 'residual' Vγ7$^+$ IEL are still able to engage other cell surface molecules on enterocytes that are sufficient to induce their maturation. For example, ~1% of mouse γδ T cells including Vγ7$^+$ IEL can engage non-classical MHC class Ib molecules (T10/T22) *via* their TCRδ CDR3 (Adams et al., 2008; 2005; Chien and Konigshofer, 2007; Crowley et al., 2000; Shin et al., 2005). T10 and T22 are constitutively expressed in small intestinal enterocytes of C57Bl/6 but not β2M$^{-/-}$ mice and their engagement has previously been shown to up-regulate

CD122 *in vivo* (Jensen et al., 2008; 2009). In addition, the gut microenvironment is rich in several cytokines that may be able to elicit some degree of phenotypic maturation independently of *Btnl1*. IL-15 is constitutively produced by epithelial cells and has been shown to drive up-regulation of T-bet and CD8αα and down-regulation of CD5 in thymic precursors of TCRβ$^+$CD8αα$^+$ *in vitro* (Klose et al., 2014). Likewise, TGFβ and retinoic acid have been shown to promote up-regulation of CD8αα expression on αβ T cells *in vivo* and *in vitro* (Konkel et al., 2011; Reis et al., 2014; 2013).

Phenotypic maturation independent of TCR agonist engagement has been reported to occur in αβ T cells during systemic lymphopaenia. Specifically, when naïve CD8αβ T cells are adoptively transferred into a lymphopaenic host, they have been shown to transiently acquire a 'memory-like' CD122^{HI}CD44$^+$ cell surface phenotype and slowly proliferate until they fill the available niche (Goldrath et al., 2000). Given that the neonatal gut grows particularly rapidly at the time of weaning, it is possible that the small intestinal IEL niche enters a transient lymphopaenic state, which could theoretically drive phenotypic maturation and slow proliferation of 'residual' Vγ7$^+$ IEL in a *Btnl1*-independent manner. While there are several potential mechanisms that could co-operate to drive the phenotypic maturation of Vγ7$^+$ IEL *in vivo*, it is important to emphasize that in the absence of *Btnl1,* the intestinal cytokine *milleu*, other Butyrophilin-like molecules and any other alternative ligands for cell surface receptors are wholly insufficient to sustain the extrathymic development and expansion of Vγ7$^+$ IEL.

7.2.2 Loss of Vγ7$^+$ IEL is compensated for by TCRβ$^+$CD8αα$^+$ IEL

Whereas loss of signature DETC in *Skint1*-mutant mice is compensated by an increase in polyclonal epidermal γδ T cells, loss of Vγ7$^+$ IEL in *Btnl1*$^{-/-}$ mice is mostly compensated for by an expansion of TCRβ$^+$CD8αα$^+$ IEL (Barbee et al., 2011; Boyden et al., 2008; Lewis et al., 2006). TCRβ$^+$CD8αα$^+$ IEL share a similar gene expression profile to bulk γδ IEL, display a similar cell surface phenotype to Vγ7$^+$ IEL (Table 1) but are thought to require thymic agonist selection for their development (Denning et al., 2007; Gangadharan et al., 2006; Lambolez et al., 2005; Mayans et al., 2014; McDonald et al., 2014; Oh-hora et al., 2013; Pennington

et al., 2003). Notably, the expansion of TCRβ$^+$CD8αα$^+$ IEL was not the root cause of Vγ7$^+$ IEL depletion in *Btnl1*$^{-/-}$ mice as this phenotype was replicated in athymic NU/NU.*Btnl1*$^{-/-}$ mice that lack most αβ IEL. Instead, these two phenotypically similar populations are known to preferentially compensate for each other's deficiency *in vivo*. Thus, TCRβ$^+$CD8αα$^+$ cells preferentially expand to compensate for γδ IEL deficiency in TCRδ$^{-/-}$ mice; and γδ IEL, which are mostly Vγ7$^+$, likewise expand to compensate for αβ IEL depletion in β2m$^{-/-}$ mice (Fujiura et al., 1996; Gapin et al., 1999; Park et al., 1999).

The capacity for these two IEL subsets to preferentially compensate for each other may be due to their selective concentration in the proximal small intestine (H. Suzuki et al., 2002); their expression of the CD8αα homodimer, which reduces activation-induced cell death (Cheroutre and Lambolez, 2008; Gangadharan et al., 2006; Y. Huang et al., 2011); and/or their selective expression of counter-receptors for enterocyte determinants such as *Btnl1* for Vγ7$^+$ IEL. Indeed, such determinants for TCRβ$^+$CD8αα$^+$ IEL could include non-classical MHC class Ib molecules such as Qa-2, which would explain their deficiency in β2m$^{-/-}$ mice (G. Das et al., 2000).

The similarities in gene expression profile, anatomical distribution and cell surface phenotype of Vγ7$^+$ and TCRβ$^+$ IEL raises the question of whether these cells can functionally compensate for each other's absence. Whereas the study of DETC has greatly benefited from Vγ5$^{-/-}$Vδ1$^{-/-}$ and *Skint1*-mutant mice that lack canonical DETC (Dalessandri et al., 2016; Lewis et al., 2006; Strid et al., 2011; 2008), there are no Vγ7$^{-/-}$ mice. As such, very few studies have clearly attributed the gastro-intestinal consequences of γδ T cell-deficiency (in TCRδ$^{-/-}$ mice) to Vγ7$^+$ IEL. In this regard, the *Btnl1*$^{-/-}$ mouse provides the first opportunity to characterize the critical and non-redundant contribution of Vγ7$^+$ IEL to small intestinal physiology. By administering inflammatory, carcinogenic or infectious challenges to *Btnl1*$^{-/-}$ and TCRδ$^{-/-}$ mice in parallel, one should be able to pull out shared phenotypes that are direct consequences of signature intestinal γδ IEL deficiency (rather than an indirect consequence of systemic γδ T cell- or *Btnl1*-deficiency). Such studies are now on-going and alongside studies of DETC, should help to define the critical contributions that these evolutionarily conserved immune cell populations make to host physiology.

7.2.3 A temporal window for small intestinal *Btnl1* activity

To test whether enterocyte-expressed *Btnl1* could rescue the extrathymic maturation of signature Vγ7$^+$ IEL in *Btnl1*$^{-/-}$ mice, we developed an inducible transgenic system to re-introduce *Btnl1* expression globally (R26-rtTA2-M2) or locally to intestinal enterocytes (villin-rtTA2-M2). Using this system we demonstrated that enterocyte expression of *Btnl1* within the first 5 post-natal weeks was sufficient to rescue both the phenotypic maturation and numerical expansion of Vγ7$^+$ and Vγ7$^+$GL2$^+$ IEL. These data confirmed that the impact of *Btnl1* is indeed mediated *in trans* from small intestinal enterocytes and strongly support the notion that its expression is key to determining the lifelong composition and phenotype of intestinal $\gamma\delta$ IEL.

Interestingly, the capacity for enterocyte-expressed *Btnl1* to elicit phenotypic change and numerical expansion was highly separable, with expansion being confined to a developmental window within the first 5 post-natal weeks. Hence, while induction of *Btnl1* expression in adult (W7-W13) BiTg mice was associated with phenotypic changes such as up-regulation of CD122, Lag3 and Ki67, this was not accompanied by numerical expansion. Similar observations were also made after an extended period of *Btnl1* induction (3-4 weeks). Given that phenotypic changes occurred in absence of detectable expansion, these data support the notion that *Btnl1* elicits true phenotypic maturation of putative CD122^{LO}Thy1$^+$ Vγ7$^+$ IEL precursors, rather than just expanding a subset of cells that were CD122^{HI}Thy1$^-$ to begin with.

The failure of *Btnl1* to expand 'residual' Vγ7$^+$ IEL in adult mice could be due to lack of available space within the small intestinal epithelial niche, which has instead been occupied by TCRβ^+CD8$\alpha\alpha^+$ IEL ('niche hypothesis'). In this scenario, Vγ7$^+$ cells may enter but not complete the cell cycle, or they divide but their daughter cells fail to 'embed' or adhere to available space. Alternatively, it is possible that IEL expansion requires a specific additional factor that is exclusively present in the neonatal gut ('neonatal factor hypothesis'). However, the full reconstitution of Vγ7$^+$ IEL from donor bone marrow in irradiated TCR$\delta^{-/-}$ adult mice makes the 'neonatal factor hypothesis' less likely. Given that such reconstitution occurs in bone marrow chimeras, perhaps the irradiation conditions the small intestinal epithelium in such

a way that enables full recovery of γδ IEL compartments. To test this, one could assess Vγ7^{+} IEL reconstitution in BiTg mice following irradiation, bone marrow transfer and simultaneous induction of *Btnl1*.

Should the data acquired from these experiments support a 'niche hypothesis', further efforts should be made to dissect how the size of this niche may be regulated at the steady state, during inflammation and during recovery. Such studies may have profound implications for human pathology, as over-expansion of intestinal intraepithelial γδ T cells is associated with mucosal γδ T cell lymphomas, which show a particularly aggressive clinical course (Gaulard et al., 2003); and with coeliac disease, where expansion of γδ IEL has been proposed as a fast and accurate diagnostic test (Fernández-Bañares et al., 2014; Leon et al., 2002). In this context, the implication of *Btnl*-gene products in driving IEL expansion, and up-regulation of CD122 merits their study in the context of small intestinal enteropathy, where IL-15 signalling is thought to promote IEL cytotoxicity and contribute to villus atrophy (Hüe et al., 2004).

7.2.4 Implications for extrathymic development

As discussed (see Chapter 1), several studies have suggested that intestinal γδ IEL develop extrathymically. This is because they are still detectable in athymic NU/NU mice (Guy-Grand et al., 1991); because their development is rescued in IL-7$^{-/-}$ mice by enterocyte-specific transgenic expression of IL-7 (Laky et al., 2000); and because TN cryptopatch lymphoid precursor cells can give rise to γδ IEL when adoptively transferred into thymectomized immunodeficient hosts (Saito et al., 1998). However, the role for extrathymic development in euthymic mice was contested by studies that have failed to detect significant *Rag* expression in cryptopatches (Guy-Grand et al., 2003); and by studies that have dismissed the role of cryptopatches altogether (G. Eberl and Littman, 2004; Guy-Grand et al., 2013). Albeit both of these arguments were in and of themselves later contested by proponents of extrathymic development (Ishikawa et al., 2007; Naito et al., 2008). Thus, this issue has remained unresolved for several years and most recent studies have not focussed on this developmental question (Hayday and Gibbons, 2008).

While our study has not addressed the anatomical location where TCR rearrangement takes place, we have identified *Btnl1* as an extrathymic intestinal selecting element. We thus propose that depending on context (e.g. euthymic *vs* athymic mice), TCR rearrangements may take place intra- or extra-thymically (or both). However, once the Vγ7$^+$ TCR is assembled, the selection of these T cells takes place outside of the thymus, during their selective interactions with *Btnl1*-expressing small intestinal enterocytes (**Figure 7.1**). As the gut clearly has some capacity to support lymphopoiesis (Laky et al., 2000), extrathymic selection would enable the development and maintenance of this critical immune compartment in the absence of continued thymic output. Such a pathway may be necessary to replenish Vγ7$^+$ IEL in later life when the thymus has undergone involution; and may be necessary to avoid negative selection in the adult thymus, as has been reported in mice rendered transgenic for self-reactive $\gamma\delta$ TCRs (Lin et al., 1999). Hence, extrathymic selection may provide an important pathway for the lifelong maintenance of signature intestinal $\gamma\delta$ IEL and merits further analysis.

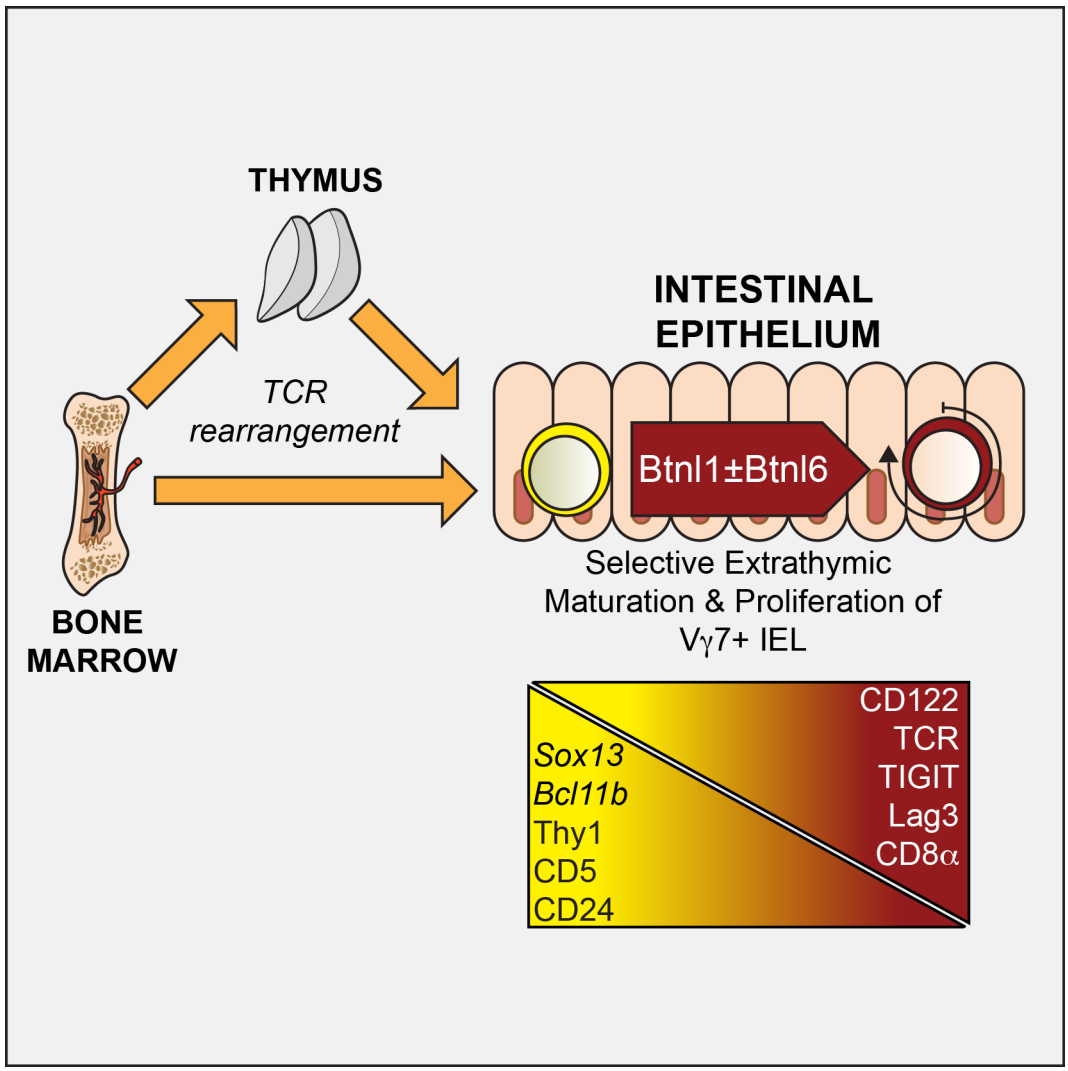

Figure 7.1 Model for the development of a signature Vγ7$^+$ IEL compartment

Development - Phenotypically immature Vγ7$^+$ IEL precursors home to the small intestinal epithelium after TCR rearrangement, which in a young euthymic mouse may/may not occur in the thymus (G. Eberl and Littman, 2004); and in athymic mice or in elderly mice after thymic involution, may take place extrathymically in lymphoid organs such as cryptopatches, PP or MLN (Guy-Grand et al., 2003; Kanamori et al., 1996; Lambolez et al., 2002; Saito et al., 1998). Upon arrival at the small intestinal epithelium, Vγ7$^+$ IEL progenitors engage in *Btnl1*-dependent interactions with villus enterocytes, which enables them to attain phenotypic maturity and representational predominance by postnatal W3, which roughly coincides with the time of weaning.

Maintenance - Following perturbation to the small intestinal epithelium, this pathway may be necessary to enable full reconstitution of the signature Vγ7$^+$ IEL compartment. Such reconstitution could be mediated by selective expansion of locally resident Vγ7+ cells and/or by selective maturation and expansion of newly arrived Vγ7$^+$ IEL precursors.

7.3 Mechanism of *Btnl1*-mediated selection

The remarkable specificity of *Btnl1* for Vγ7$^+$ IEL suggested that the extrathymic selection of these cells was being driven *via* a TCR-associated pathway. Consistent with this, we showed that *Btnl1* expressed together with *Btnl6* rendered MODE-K cells capable of selectively stimulating Vγ7$^+$ IEL *in vitro*, eliciting several consequences conventionally associated with TCR-mediated activation. These included up-regulation of CD25, enhanced transcription at the *Nr4a1* gene locus and down-regulation of the TCR and CD122 (Hémar et al., 1995; José et al., 2000; Kim and Leonard, 2002; Yu and Malek, 2000). Stimulation of Vγ7$^+$ IEL was dependent on cell-to-cell contact and was still detectable after Vγ7$^+$ IEL had been purified by flow cytometry prior to co-culture. Furthermore, stimulation of Vγ7$^+$ IEL was detectable within 6 hours of co-culture. Although a small proportion of Vγ7$^+$ IEL up-regulated CD25 in a Btnl1+Btnl6-independent manner during co-culture with MODE-K.EV, this was mostly not associated with transcription at the *Nr4a1* locus and could not be inhibited by PP2, suggesting it was driven *via* an alternative or TCR-independent pathway. Indeed, low-level background CD25 up-regulation was observed within every IEL subset irrespective of TCR chain usage during overnight co-cultures. Thus, MODE-K.L1+6 cells were both necessary and sufficient to elicit putative TCR-mediated stimulation of Vγ7$^+$ IEL *in vitro*.

7.3.1 Cell surface trafficking of *Btnl* gene products

Previous studies have shown that the cell surface expression of *Skint1* is very tightly regulated but is critically required for DETC maturation (Barbee et al., 2011; Salim et al., 2016). Consistent with this, phenotypic maturation of DETC was shown to be inhibited by adding soluble anti-Skint1-IgV blocking antibody to FTOC (Salim et al., 2016). Although our experiments have not demonstrated an absolute requirement for cell surface expression of Btnl1 or Btnl6 during IEL stimulation, we have shown that cell surface trafficking of these proteins is also tightly regulated and in the case of Btnl6, is dependent on co-expression of Btnl1. Given that MODE-K cells expressing Btnl1 or Btnl6 alone were unable to elicit stimulation of Vγ7$^+$ IEL, it is possible that their heterodimerization and cell surface trafficking are critical for their impact *in vitro*. Furthermore, s Btnl1 reportedly exists in complex

with Btnl6 in primary enterocytes, it is possible that its impact on Vγ7$^+$ IEL *in vivo* is similarly mediated in co-operation with Btnl6 (Lebrero-Fernández et al., 2016). If so, we would expect *Btnl6*$^{-/-}$ mice to phenocopy *Btnl1*$^{-/-}$ mice with respect to Vγ7$^+$ IEL depletion. To test this, *Btnl6*$^{-/-}$ mice are currently in the pipeline being bred to homozygosity.

The capacity for Btnl1+Btnl6 to regulate Vγ7$^+$ T cell selection *in vivo* and weak T cell activation *in vitro* evokes provocative comparisons with MHC, which directly engage TCRs to mediate both of these processes in αβ T cells. However, in the absence of TCR binding data for Btnl1 and Btnl6, we cannot conclude that these molecules are directly engaging the Vγ7$^+$ TCR. Indeed, as members of the B7 superfamily it is still possible that *Btnl/Skint* gene products serve as subset-specific co-stimulators that are necessary but insufficient for TCR activation. If this were the case, they would represent the first co-stimulators to engage lymphocyte counter-receptors that segregate according to TCR variable chain usage (e.g. with Vγ7$^+$ but not Vγ7$^-$ intestinal IEL). That notwithstanding, both models are consistent with Btnl1 and Btnl6 regulating Vγ7$^+$ IEL activation *in vitro* and Vγ7$^+$ IEL selection *in vivo*, *via* a TCR-associated pathway.

In an alternative model, it is still possible that Btnl1+Btnl6 are necessary for the recruitment of additional protein(s) that mediate TCR engagement. Such an 'indirect' model for TCR stimulation was recently proposed for BTN3A1, which is unable to present pAg when over-expressed in hamster CHO cells in the absence of factors encoded in human chromosome 6 (so called 'factor X') (Karunakaran and Herrmann, 2014; Riaño et al., 2014). However, as chromosome 6 also contains BTN3A2 and BTN3A3, it is unclear whether this phenotype is due to an absence of heterodimerization, or whether there is a critical non-BTN3 gene encoded within the chromosome. This will need to be clarified because when any one of the three BTN3 isoforms is knocked down in a human pAgPC, its capacity to activate Vγ9$^+$Vδ2$^+$ T cells is significantly compromised (Rhodes et al., 2015). Thus, the mechanisms by which BTN/Btnl molecules exert their selective impacts on discreet subsets of γδ T cells is poorly understood and requires further research.

To better characterise the mechanism of Btnl1+Btnl6-mediated Vγ7$^+$ IEL stimulation, the next logical step would be to determine the importance of TCR specificity in

these selective interactions. This could be tested by purifying CD25$^+$ MODE-K.L1+6-responsive Vγ7$^+$ T cells and determining their TCR chain pairing by single cell PCR. TCRs cloned from 'responder' cells could then be tested for their capacity to confer MODE-K.L1+6-responsiveness to cell lines (e.g. Jurkat [human]; BWZ.36 [murine]) expressing TCR signal reporter constructs (e.g. luciferase downstream of IL-2 promoter (Dolmetsch et al., 1998)). If this approach is successful, targeted mutagenesis should be employed to determine which region of the Vγ7$^+$ TCR is most important for regulating their responsiveness to MODE-K.L1+6 (e.g. the Vδ chain *versus* Vγ7; or the CDR3 *versus* CDR2 or CDR1). To follow up these studies *in vivo*, 'responsive' and 'non-responsive' Vγ7$^+$ TCRs can be transduced into donor bone marrow to compare their capacity to support Vγ7$^+$ IEL development in an irradiated host. Similar experiments were recently performed to compare the lineage commitment of thymocytes expressing transgenic TCRs cloned from TCRβ^+CD8$\alpha\alpha^+$ *versus* TCRβ^+CD8$\alpha\beta^+$ IEL (Mayans et al., 2014; McDonald et al., 2014).

7.3.2 TCR hypo-responsiveness

Our data suggest that *Btnl1*-mediated selection *in vivo* may be associated with attenuation of TCR responsiveness, in a striking phenocopy of *Skint1*-selection of DETC progenitors (Wencker et al., 2013). Specifically, we showed that TCR agonist antibody stimulation could elicit CD25 up-regulation in a greater proportion of Vγ7$^+$ IEL that were recovered from *Btnl1*$^{-/-}$ mice, relative to those recovered from age-matched WT controls. TCR hypo-responsiveness has previously been reported for TCRβ^+CD8$\alpha\alpha^+$ IEL and for CD8$\alpha\alpha^+$ $\gamma\delta$ IEL but had not been specifically attributed to the Vγ7$^+$ compartment (Malinarich et al., 2010; Wencker et al., 2013). Our data suggest this may be the case as non-Btnl1-selected Vγ7$^-$ $\gamma\delta$ IEL were significantly more responsive to TCR agonist antibody stimulation than Vγ7$^+$ IEL from the same WT mouse.

Hypo-responsiveness to TCR stimulation is considered to be a key feature of IEL biology and has been suggested to represent a mechanism by which *innate-like* T cells developmentally accommodate their *innate* response mode(s) (Wencker et al., 2013). In DETC, hyporesponsiveness may be necessary to prevent their

inappropriate activation during the steady state, where they have been shown to constitutively engage keratinocytes forming contacts that are enriched in TCR, phospho-tyrosine, phosphoCD3ζ, and phospho-Zap70, suggestive of steady-state TCR signalling (Chodaczek et al., 2012). Such contacts are highly dependent on TCR specificity, may be responsible for driving DETC expansion in neonatal mice (Aono et al., 2000; Hara et al., 2000; Payer et al., 1991) and our unpublished data suggest they are highly dependent on *Skint1,* which is constitutively expressed by suprabasal keratinocytes (Boyden et al., 2008).

Given what we know about DETC biology, it is possible that Vγ7$^+$ IEL also engage villus enterocytes in *Btnl1*- and TCR-dependent points of contacts, which may drive their constitutive expression of chemokines and cytolytic effector molecules (Shires et al., 2001). Such *Btnl1*-dependent contacts may also be responsible for the pre-existing GFP expression observed in Vγ7$^+$ IEL freshly recovered from Nur77.gfp mice. Although we have not provided formal proof of these contacts *in vivo*, our observation that baseline GFP expression Vγ7$^+$ IEL is mostly lost during overnight co-culture with MODE-K.EV but is re-induced when cells are cultured with MODE-K.L1+6 is consistent with this model. Indeed, co-culture with MODE-K.L1+6 was uniquely associated with eliciting a CD25$^+$GFP$^+$CD122^{LO} cell surface phenotype amongst Vγ7$^+$ IEL. If constitutive TCR signalling occurs in both DETC and Vγ7$^+$ IEL, it may be that attenuation of TCR responsiveness is necessary to prevent inappropriate activation of Vγ7$^+$ IEL in the absence of challenge.

How attenuation of TCR responsiveness is achieved is poorly understood but could feasibly involve the *Btnl1*-dependent up-regulation of co-inhibitory receptors (**Table 7.1**). As the contribution of these co-inhibitory receptors to IEL biology is generally poorly understood, future work should seek to analyse the consequences of co-inhibitory receptor deficiency during specific challenges to the skin (e.g. UV irradiation) or to the small intestinal epithelium (e.g. low dose methotrexate (Aparicio-Domingo et al., 2015)). In particular, it will be important for these studies to use conditional knock-out systems, such as the TCRδ-CRE and the Villin-CRE to assess the consequence(s) of co-inhibitory receptor deficiency in γδ T cells, alongside the consequence(s) of counter-receptor deficiency in the epithelium (Roth et al., 2009; B. Zhang et al., 2015). Data from these studies would be highly clinically relevant as many such receptors are targets for pharmacological blockade

in clinic (Anderson et al., 2016). In this regard, it will also be interesting to see if their use in clinical trials is associated with specific gastrointestinal or cutaneous inflammatory side-effects.

7.3.3 Putative regulatory role of the B30.2 domain

As members of the *BTN/Btn* gene family, *Btnl1* and *Btnl6* both contain a cytoplasmic B30.2 (PRY/SPRY) domain (see Chapter 1). B30.2 domains are also found on TRIM proteins, where they are believed to regulate TRIM function by binding endogenous or exogenous molecules. For example, rhesus TRIM5α B30.2 engages HIV capsid protein and targets it for proteasomal degradation, whereas TRIM21 B30.2 serves as an intracellular F_c receptor that activates *innate* intracellular neutralization pathways upon engagement of IgG-opsonised viral particles (Mische et al., 2005; Pertel et al., 2011; Rhodes and Trowsdale, 2007). Likewise, the B30.2 domain of *BTN1a1/Btn1a1*, the prototypic founder of the *BTN/Btn* gene family, engages intracellular xanthene oxidoreductase to promote milk fat globule secretion from lactating mammary gland epithelial cells (Franke et al., 1981; Jeong et al., 2009; Ogg et al., 2004). Thus it is possible that the biological activity of *BTN/Btn/BTNL/Btnl* gene products is also regulated by their engagement of cytosolic factors *via* their intracellular B30.2 domains.

In support of this hypothesis BTN3A1 is believed to regulate the TCR-dependent activation of human circulating $V\gamma9^+V\delta2^+$ T cells by binding intracellular phospho-antigens (IPP/HMBPP) that are intermediary products of isoprenoid synthesis (Harly et al., 2012; Karunakaran and Herrmann, 2014; Rhodes et al., 2015; Sandstrom et al., 2014). Such pAgs accumulate endogenously in APCs during viral infection or cellular transformation, but may also be exogenously derived from microbial metabolism (H. Das et al., 2001; M. Eberl et al., 2003; Gober et al., 2003). Thus, this pathway links the engagement of an *innate* germline-encoded PRR domain (B30.2) to the activation of an adaptive (albeit *innate*-like) lymphocyte *via* its RAG-rearranged T cell receptor. While direct binding between BTN3 and the TCR has not been reproducibly demonstrated (Sandstrom et al., 2014; Vavassori et al., 2013), it is believed engagement of the intracellular B30.2 domain elicits conformational changes in the extracellular IgC/IgV domain that enable it to engage a lymphocyte counter-receptor (Sebestyen et al., 2016). Given these data

regarding BTN3, it is tempting to speculate that Btnl1+Btnl6 mediate $V\gamma7^+$ IEL selection *in vivo* or $V\gamma7^+$ IEL stimulation *in vitro via* a TCR-dependent pathway that is regulated by engagement of the B30.2 domain.

Future studies should therefore seek to better understand the role of B30.2 domains in regulating the activity of Btnl1+Btnl6. Based on what has been published regarding BTN3A1 (Rhodes et al., 2015; Sandstrom et al., 2014; Sebestyen et al., 2016), we would predict that deleting or mutating the B30.2 domain of *Btnl1* and/or *Btnl6* would abrogate the capacity of MODE-K.L1+6 to activate $V\gamma7^+$ IEL *in vitro*. Should this be demonstrated, the more challenging task will be to identify the nature of the molecule that engages the B30.2 domains of Btnl1+Btnl6. This could be a protein (e.g. XOR for Btn1a1), or a low molecular mass metabolite (e.g. pAg from isoprenoid synthesis for BTN3A1). It may or may not engage Btnl1+Btnl6 together as a heterodimer and may also regulate their cell surface trafficking. Whichever the answer, the MODE-K cell transductants presented in this thesis will certainly prove useful in testing the hypothesis and in providing a platform for further studies *in vivo*.

Ultimately, defining the molecular regulator(s) of Btnl1+Btnl6 activity *in vitro* will provide us with a better understanding of the biological context in which these proteins function *in vivo*. Such studies may additionally help to explain why γδ IEL composition is regulated by organ-specific *Btnl* gene-products, rather than by pan-epithelial molecules. In this regard, while it is interesting that the initial impact of *Btnl1 in vivo* overlaps with the time of weaning, our experiments using inducible transgenic mice and bone marrow transfer studies suggest that the capacity to elicit stimulation of $V\gamma7^+$ IEL persists into adulthood. To investigate the impact of weaning, we have tried to wean mice earlier than D21 but found that this did not accelerate $V\gamma7^+$ IEL maturation (*data not shown*). Recently it was suggested that Btnl1 protein is only detectable by immunohistochemistry from postnatal D14, which could explain the kinetics of $V\gamma7^+$ IEL maturation we observed *in vivo* (Lebrero-Fernández and Bas-Forsberg, 2016). As we now have our own *Btnl1*-specific monoclonal antibody, we can try to replicate some of these studies using the *Btnl1*$^{-/-}$ mouse as a negative control.

An additional consideration that should not be ignored is the possibility that the B30.2 domains of *Btnl1* and *Btnl6* signal back into the epithelial cells that display them (Bas et al., 2011). Such signals may or may not be dependent on interaction with Vγ7$^+$ IEL and may constitutively regulate epithelial cell function or attenuate its response to inflammation. Evidence for the latter was provided by the finding that overexpressed *Btnl1* can alter the MODE-K cell response to IFNγ (Bas et al., 2011). However, this has not been tested in primary enterocytes *in vitro* or *in vivo* as we have not had the appropriate tools. Together, the *Btnl1*$^{-/-}$ and inducible BiTg mice presented in this thesis provide these tools and future studies will investigate this potential biology.

In summary, we believe that future studies of these genes should strive to identify:

a) The non-redundant contributions of Vγ7$^+$ IEL to host physiology.
b) The role of TCR specificity in *Btnl*-driven Vγ7$^+$ IEL stimulation *in vitro/in vivo*.
c) The biological context in which *Btnl* gene products function *in vivo* and *in vitro*, along with the molecule(s) that regulates this function.
d) Whether *Btnl* gene products directly influence epithelial cell biology *in vivo* and whether these impacts depend on constitutive or stress-inducible interactions with signature γδ IEL.

7.4 Outlook: Potential Implications for human health

7.4.1 Btnl3 and Btnl8 regulate human intestinal γδ T cells

Btnl1, *Btnl4*, and *Btnl6* are each encoded in an amplicon that lies adjacent to *Btnl2* on mouse chromosome 17. While no equivalent amplicon is found adjacent to human *BTNL2*, there is an amplicon encoding *BTNL8* and *BTNL3* adjacent to *BTNL9* on human chromosome 5 (**Figure 7.2**). *BTNL3* and *BTNL8* are highly expressed In the human gastrointestinal tract (Uhlen et al., 2015), particularly within EpCAM$^+$ epithelial cells, suggesting they may fulfil a similar biological function to murine *Btnl1* and *Btnl6* (Di Marco Barros et al., 2016). Indeed, our recent studies of BTNL3 and BTNL8 suggest that their trafficking to the cell surface is also highly regulated and requires concomitant expression of both molecules. While we were unable to test the developmental dependence of human gut γδ T cells on intestinal BTNL3 (L3) and BTNL8 (L8), we have tested whether expression

of these molecules renders human embryonic kidney (HEK293T) cells capable of activating primary human gut-derived γδ T cells *in vitro*.

These studies have revealed a striking conservation of biological function across human and mouse organ-specific *BTNL/Btnl* molecules in that they can selectively regulate signature organ-specific γδ T cell subsets. Specifically, we found that human gut-derived T cells that are stained with antibodies specific for TCRVγ2/3/4, but not with antibodies specific for Vγ5/3, Vγ8, or Vγ9, selectively down-regulate cell surface TCR and up-regulate CD25 during co-culture with HEK293T.L3+8 (but not during co-culture with HEK293T.EV, HEK293.L3 or HEK293.L8) (Di Marco Barros et al., 2016). Amplification and sequencing of TCRVγ chains among HEK293T.L3+8-responsive T cells identified a high prevalence of Vγ4 genes, suggesting that human $V\gamma4^+$ cells selectively responded to co-culture with HEK293T.L3+8. Emphasizing the specificity of this response to gut-derived γδ T cells, skin-derived γδ T cells, which showed bias towards Vγ3 expression, did not respond to HEK293T.L3+8. In conclusion, human intestinal epithelial *BTNL* genes appear to selectively regulate local intestinal γδ T cells expressing a particular TCRVγ-chain. These data demonstrate that human organ-specific *BTNL* molecules could similarly regulate the lifelong composition of human organ-specific γδ T cell compartments, with potential implications for human health. Future studies should therefore seek to determine whether BTNL3 and BTNL8 show up- or down-regulation in human intestinal pathology that is associated with over-expansion of γδ IEL (e.g. Coeliac disease and mucosal γδ T cell lymphoma).

7.4.2 Genetic associations of BTNs with disease

There is significant interest in the putative role of Butyrophilin(-like) genes in the regulation of systemic immune responses (Abeler-Dörner et al., 2012; Arnett and Viney, 2014; Rhodes et al., 2016). In particular, *BTNL2* has drawn significant attention to the extended BTN gene family because of its genetic association with human inflammatory diseases including sarcoidosis and ulcerative colitis (Pathan et al., 2009; Valentonyte et al., 2005). To investigate the biology underlying these associations, several studies have tested the impact recombinant Fc fusion peptides of several different BTN/Btn and BTNL/Btnl proteins, on the activation of

αβ T cells *in vitro*. Using this approach, several studies have concluded that Butyrophilin(-like) molecules modulate TCR-driven activation of αβ T cells *in vitro* and may bind to the cell surface of activated but not resting αβ T cells, which is indicative of an activation-induced counter receptor (Ammann et al., 2013; Arnett et al., 2007; Nguyen et al., 2006; Sarter et al., 2016; Smith et al., 2010; Yamazaki et al., 2010). Consistent with an immunoregulatory role for one of these proteins, *Btn2A2*$^{-/-}$ mice are reported to display worse clinical scores during experimental allergic encephalitis and a reduced rate of tumour growth *in vivo* (Sarter et al., 2016). The mechanism by which this immunoregulatory impact is mediated is not well understood but is thought to involve induction of $CD4^+$ regulatory T cells.

Aside from Btn2A1, which may regulate T cell activation by engaging DC-SIGN on APCs (Malcherek et al., 2007), no counter receptor has been identified for any other butyrophilin(-like) molecule. Thus, the mechanism by which αβ T cell activation may be regulated by these proteins *in vitro* or *in vivo* remains very poorly defined. Furthermore, as studies have largely used Fc fusion peptides of single butyrophilin(-like) molecules to test their function *in vitro*, it is unclear whether the reported immunoregulatory effects are physiological for proteins that may depend on heterodimerization for their function. In this regard, the study of *BTN/Btnl* genes in the regulation of γδ T cell development and activation has arguably identified the only physiological context(s) in which these proteins may function *in vivo*. Given that *Skint1*, BTN3A1/2/3, *Btnl1/6* and BTNL3/8 are all directly implicated in the regulation of γδ T cell responses, it is tempting to speculate that the primary function of this gene family is to regulate discreet subsets of γδ T cells (**Figure 7.3**). Indeed, γδ T cell deficiency is often associated with exaggerated αβ T cell-mediated inflammatory responses (Hayday et al., 2000). Thus, it will be imperative for any future study of butyrophilin(-like)-deficiency *in vivo* to rule out the possibility that a γδ T cell compartment has been selectively ablated. Moreover, pathologies that have been genetically associated with members of the extended BTN gene family should be thoroughly assessed for potential γδ T cell involvement.

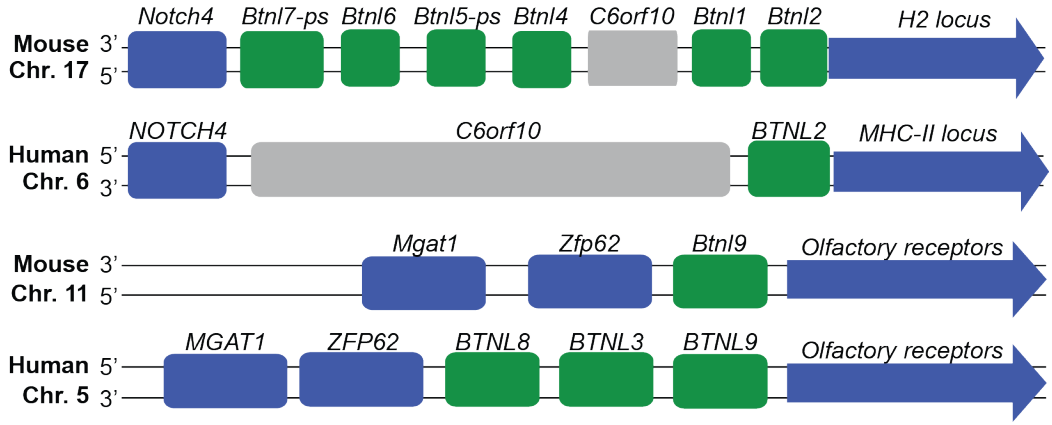

Figure 7.2 Schematic of mouse and human *BTNL2/Btnl2* and *BTNL9/Btnl9* gene loci

Btnl1, *Btnl4*, and *Btnl6* are encoded in an amplicon adjacent to *Btnl2* on mouse chromosome 17. *BTNL8* and *BTNL3* are encoded in an amplicon adjacent to *BTNL9* on human chromosome 5. Schematic provided by Dr Vantourout.

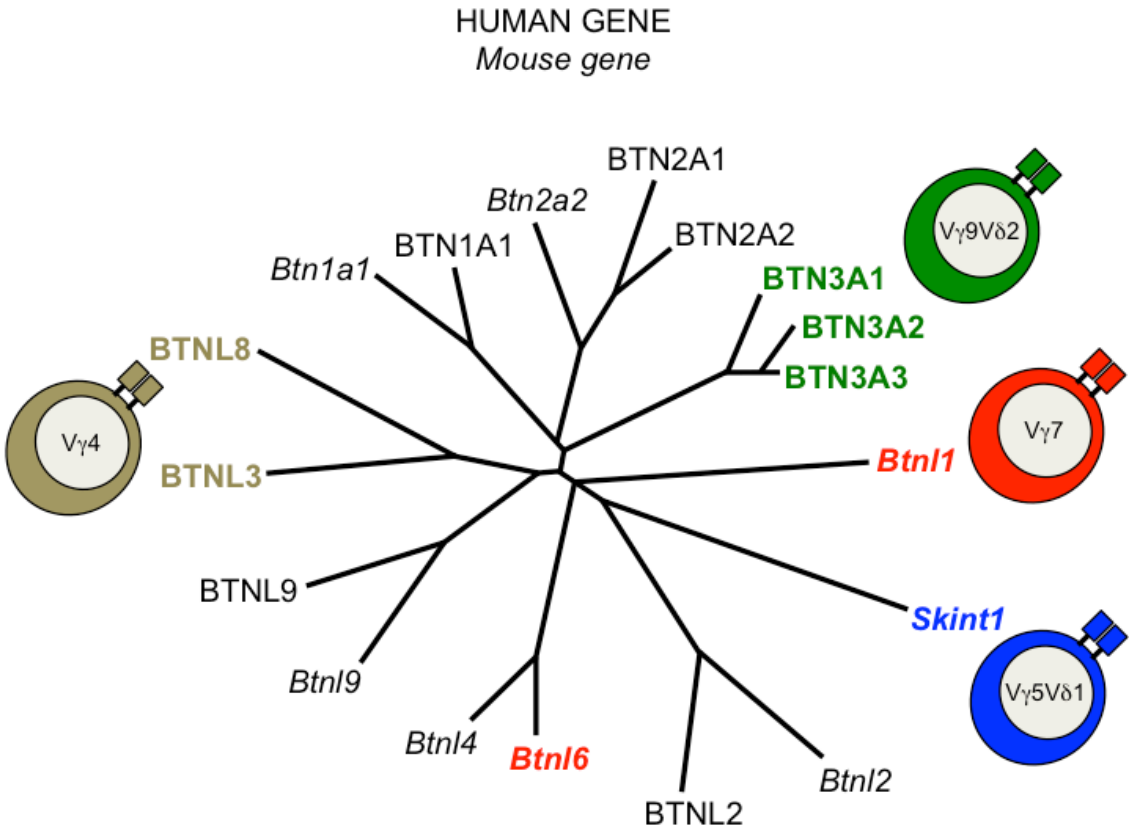

Figure 7.3 The emerging role of Butyrophilins in the regulation of γδ T cells

Phylogenetic tree of Butyrophilin gene family and the associated γδ T cell subsets they regulate. Adapted from: (Abeler-Dörner et al., 2012).

7.4.3 On the regulation of T cell composition and implications for cancer

The capacity of a non-lymphoid barrier tissue to actively regulate the composition of its locally resident lymphocyte compartment has profound implications for tumour immunosurveillance and auto-inflammatory disease; as such cells may ameliorate or exacerbate pathology. Indeed, histological data concerning the composition of lymphocytes infiltrating solid tumours has been shown to correlate with clinical outcomes (Fridman et al., 2012; Mlecnik et al., 2011) and has led to calls for histological 'immune scores' to be adopted for human tumour classification (Jerome Galon et al., 2012). Likewise, it is conceivable the composition of tumour-infiltrating lymphocytes could influence the efficacy of novel checkpoint inhibition therapies that are being trialled across a range of malignancies (Ansell et al., 2015; Hamid et al., 2013; Pardoll, 2012; Robert et al., 2015; Schadendorf et al., 2015; Weber et al., 2015; Wolchok et al., 2013).

Over recent years, γδ T cells have attracted considerable attention because of their capacity to rapidly respond to dysregulated or 'stressed' self, *via* the LSSR (Hayday, 2009). Indeed, tumour-associated γδ T cell gene expression signatures were recently reported to be the single greatest correlate with overall survival in an unbiased bioinformatics analysis of gene expression data across ~18,000 human tumours (Gentles et al., 2015). This thesis has presented genetic evidence to support the hypothesis that epithelial cells actively regulate the composition of their local lymphocyte compartments *via* their expression of organ-specific *Btnl* gene products. Given that most tumours derive from epithelial tissue, it is possible that regulators of immune composition may be up- or down-regulated according to what confers the greatest survival advantage to the tumour cell. Taking this into consideration, future analyses of tumour gene expression datasets should strive to characterize the landscape of Butyrophilin(-like) gene expression, to see if this shows any favourable correlation with the reported prognostic indicator of γδ T cell infiltration for overall survival.

7.5 Conclusion

In this thesis, we sought to determine how the lifelong composition of signature γδ IEL compartments are established and maintained. In particular, we investigated whether *Skint1*-mediated DETC selection was an exceptional mechanism, or whether closely related *Btnl* gene products similarly regulate the composition of other signature γδ IEL. From these studies, it is now clear that the development of the two signature murine γδ IEL compartments studied in any detail (DETC and intestinal Vγ7$^+$ IEL) is in both cases driven by organ-specific, epithelial expression of butyrophilin-like genes, *Skint1* and *Btnl1*(+*Btnl6*), respectively. These data provide the first demonstration that *Skint1*-mediated DETC selection is a generalizable mechanism by which *Btnl* products of epithelial cell differentiation serve to regulate the lifelong composition of local γδ IEL. Thus, *Btnl* gene products are the master regulators of intraepithelial γδ T cell composition.

Through the analysis of WT pups, *Btnl1*-deficient mice, and inducible *Btnl1* transgenic mice, at least some of the consequences of epithelial *Btnl1/Skint1*-mediated selection of IEL are now clear. First and foremost, 'selected' γδ T cells up-regulate the IL-15Rβ (CD122) that is essential for the cells' steady-state maintenance in small intestinal epithelium and epidermis. They also up-regulate the TCR and up-regulate several co-inhibitory receptors (e.g. TIGIT, Lag3), which most likely serves to limit IEL responsiveness to signalling *via* the TCR. Selected IEL proliferate, and suppress the expression of genes, notably *Sox13, Sox4, Rorc,* and *Bcl11b* that are commonly associated with the development γδ17 cells. These effects of *Skint1* and *Btnl1* coupled with their fine specificity for cells expressing defined TCRs results in the rapid emergence of signature T cell compartments uniquely associated with defined anatomical sites.

Adopting a gain-of-function approach *in vitro*, we provided compelling evidence to support the notion that Btnl1 elicits Vγ7$^+$ TCR-dependent events in co-operation with Btnl6 when co-expressed in MODE-K cells. Such heterodimerization has been shown to occur in primary enterocytes and could also be involved in *Skint1*-mediated DETC selection and/or BTN3-mediated activation of human Vγ9$^+$Vδ2$^+$ T cells. Peptide:MHC complexes are known to have the capacity to elicit several

potential impacts on developing αβ T cells These include positive and negative selection of αβ thymocytes, 'agonist selection' of regulatory T cells, and the activation or anergy of peripheral αβ T cell subsets. Throughout this thesis, we provide genetic evidence that Btnl1 drives the intestinal selection of Vγ7$^+$ IEL *in vivo* and cell biological evidence that Btnl1+Btnl6 drives Vγ7$^+$ IEL activation *in vitro*. While our data do not demonstrate a direct interaction between Btnl1+Btnl6 and the Vγ7$^+$ TCR, they do demonstrate the capacity for Btnl1+Btnl6-mediated stimulation to elicit several consequences of TCR signalling, as was previously reported for *Skint1*-mediated selection.

An exception to the parallels between *Skint1*- and *Btnl1*-mediated IEL selection is that the impact of *Skint1* is initially mediated in the thymus, whereas that of *Btnl1* is mediated in the gut. By demonstrating that enterocyte expression of *Btnl1 in vivo* drives selective phenotypic maturation and expansion of Vγ7$^+$ IEL in BiTg mouse pups, we have established that the signature small intestinal γδ IEL compartment is shaped extrathymically, irrespective of where TCR rearrangement takes place. Thus, we are able to reconcile many conflicting reports and our data provide the foundations to resolve a long-standing debate.

In conclusion, this thesis has provided a compelling answer to the question set out in its objective. Namely, that *Skint1*-mediated DETC selection is not exceptional and is likely to represent an evolutionarily conserved mechanism by which epithelia actively regulate the composition of their signature γδ IEL compartment. In answering this question, we have comprehensively described new experimental systems (e.g. *Btnl1*$^{-/-}$ mice, BiTg mice, MODE-K transductants) that will undoubtedly prove to be invaluable in future studies of Vγ7$^+$ IEL function; and in future investigations regarding the mechanism of Btnl1+Btnl6-mediated Vγ7$^+$ IEL stimulation. The conservation of BTNL3+8-mediated subset-specific stimulation of human intestinal γδ T cells (Di Marco Barros et al., 2016) heralds an exciting new chapter in human γδ T cell biology and brings us that little bit closer to defining the critical contribution of these enigmatic cells to mouse and human immunity.

Chapter 8. Appendix

8.1 Buffers

Phosphate Buffered Saline (Gibco - 14190-094)

Hank's balanced salt solution (Gibco - 14175-095)

20X SSC

800ml H_2O

175.3g NaCl

88.2 sodium citrate-$2H_2O$

pH to 7.0 with HCl

Top up to 1L with H_2O

10% Sodium Dodecyl Sulfate (SDS)

Dissolve 100g SDS crystals in 900ml H_2O, heat to 68^{o}C

pH to 7.2 with HCl

Top up to 1L with milliQ water

0.5M EDTA

186.12g EDTA (Fisher Scientific)

pH to 8 with sodium hydroxide

Top up to 1L with water.

70% ethanol

70% Ethanol (Sigma)

30% MilliQ water

RPMI:DTT solution

RPMI 1640 (Gibco)

10% FCS (Gibco)

5ml Penicillin/Streptomycin (Sigma; [net] = 0.1mg/ml strep/100 units/ml pen)

10mM DTT

IEL recovery medium

RPMI 1640 (Gibco)

10% FCS (Gibco)

5ml Penicillin/Streptomycin (0.1mg/ml strep; 100 units/ml pen)

Complete RPMI

RPMI 1640 (Gibco)

10% FCS (Gibco)

5ml Penicillin/Streptomycin (Sigma; [net] = 0.1mg/ml strep; 100 units/ml pen)

12.5ml 1M HEPES (Gibco)

5ml 100X Non-essential amino acids (Invitrogen)

5ml 100X Sodium pyruvate (Gibco)

1ml 50mM β mercapto-ethanol (Gibco)

IL-2 (10U/ml), IL-15 (10 ng/ml) (Immunotools), IL-3 (100U/ml), IL-4 (200U/ml) (R&D).

F2.67 hybridoma culture medium

DMEM +glutamine/+glucose/+pyruvate (Gibco)

5% FCS (Gibco)

5ml 100X Non-essential amino acids (Invitrogen)

5ml Penicillin/Streptomycin (Sigma; [net] = 0.1mg/ml strep; 100 units/ml pen)

1ml 50mM β mercapto-ethanol (Gibco)

MODE-K Culture medium

DMEM +glucose/+glutamine/+pyruvate (Gibco)

10% FCS (Gibco)

5ml Penicillin/Streptomycin (Sigma; [net] = 0.1mg/ml strep/100 units/ml pen)

1:100 Hygromycin (Invitrogen; [net] = 0.5mg/ml)

Puromycin (Sigma; [net] = 200ng/ml)

Percoll 100% stock solution

90ml Percoll (GE Healthcare)

10ml 10X PBS

Percoll 80%

80% Percoll (100% stock solution)

20% PBS

Percoll 40%

40% Percoll (100% stock solution)

60% PBS

Percoll 20%

20% Percoll (100% stock solution)

80% PBS

FACS buffer

PBS

0.5% Bovine serum albumin

2mM EDTA

Tail buffer

40mM Tris, pH8

25mM EDTA, pH8

100mM NaCl

1% sodium dodwSDS

Add 15μl (10mg/ml) Proteinase K (Sigma) to 360μl tail buffer at time of use

Southern blot buffers

Depurination buffer

0.25M HCl

Denaturation buffer

1.5M NaCl
0.5M NaOH

Neutralization buffer

1.5M NaCl

0.5M Tris
pH 7.5

1x Maleic acid buffer

0.1M Maleic Acid
0.15M NaCl
pH 7.5

Post Hyb Wash I

2x SSC
0.1% SDS

Post Hyb Wash II

0.1% SSC
0.1% SDS

Blocking buffer (10X)

Dissolve blocking reagent to a final concentration of 10% in Maleic acid buffer. Bring to 1X by diluting 10X solution in Maleic acid buffer at time of use.

Washing buffer

Maleic acid buffer + 0.3% tween

Buffers for gut whole mount staining (Confocal)

Washing Buffer

PBS

0.5% BSA

Zamboni's fixative

PBS

1% PFA

15% Picric acid solution

pH to 7.3

Block A:

5% normal goat serum

0.5% BSA

0.4% Triton X-100

in PBS

(make fresh)

Block B:

100 ug/ml Rat gamma-globulin
0.5% BSA

0.4% Triton X-100

in PBS

(make fresh)

8.2 Antibodies, cytokines, chemicals, materials and kits

Antibodies		
CD3 APC Cy7 (17A2)	BioLegend	Cat#:100222
CD3 PerCPCy5.5 (145-2C11)	BioLegend	Cat#:100328
TCRβ Brilliant Violet 421 (H57-597)	BioLegend	Cat#:109229
TCRβ APC (H57-597)	BioLegend	Cat#:109212
CD122 PE (TMβ1)	BioLegend	Cat#:123209
CD122 Brilliant Violet 421 (TMβ1)	BD	Cat#:562960
CD122 APC (TMβ1)	BioLegend	Cat#:123213
TIGIT PE (GIGD7)	eBiosciences	Cat#:12-9501-82
CD45RB APC Cy7 (C363-16A)	BioLegend	Cat#:C363-16A
Thy1.2 Brilliant Violet 510 (53-2.1)	BioLegend	Cat#:140319
Lag3 PerCP-efluor 710 (C9B7W)	eBioscience	Cat#:46-2231-80
CD5 PE (53-7.3)	BD Pharmingen	Cat#:553023
CD24 FITC (M1/69)	eBiosciences	Cat#:11-0242-81
CD24 PECy7 (M1/69)	BD Pharmingen	Cat#:560536
CD8α PECy7 (53-6.7)	BioLegend	Cat#:100722
TCR Vδ4 FITC (GL-2)	BD	Cat#:552143
TCR Vδ4 PE (GL-2)	BioLegend	Cat#:134905
CD8β PerCpCy5.5 (YTS156.7.7)	BioLegend	Cat#:126609
CD25 PerCpCy5.5 (PC61)	BioLegend	Cat#:102030
CD69 PECy7 (H1.2F3)	BioLegend	Cat#:104512
CCR9 PECy7 (CW-1.2)	BioLegend	Cat#:128711
CD44 PECy7 (IM7)	BioLegend	Cat#:103030
TCRVγ7 (F2.67)	Institut Pasteur Pablo Pereira	N/A
TCRVγ1 APC (2.11)	BioLegend	Cat#:141107
TCRVγ4 APC (UC3-10A6)	BioLegend	Cat#:137708
TCRδ BV421 (GL3)	BioLegend	Cat#:118119
Ki67 FITC (B56/MOPC-21)	BD Pharmingen	Cat#:556026
CD45 Qdot 605 (30-F11)	eBiosciences	Cat#:93-0451-42
CD5 Brilliant Violet 510 (53-7.3)	BD	Cat#:563069
TCRδ PeCy7 (GL3)	BioLegend	Cat#:118124
CD161/NK1.1 Brilliant Violet 650 (PK136)	BioLegend	Cat#:108735
CD4 Brilliant Violet 786 (GK1.5)	BD	Cat#:563331
CD8α AlexaFluor 700 (53-6.7)	BD	Cat#:557959
CD25 APC (PC61)	BD	Cat#:557192
GITR PE (DTA-1)	BD	Cat#:558119
CD44 FITC (IM7)	BD	Cat#:553133
CD62L PerCP-Cy5.5 (MEL-14)	BD	Cat#:560513
KLRG1 BV421 (2F1)	BD	Cat#:562897
CD11c BV786 (HL3)	BD	Cat#:563735
CD11b BV510 (M1/70)	BioLegend	Cat#:101245

F4/80 PerCPCy5.5 (BM8)	BioLegend	Cat#:123128
Ly6G APC (1A8)	BD	Cat#:560599
Ly6C AlexaFluor 700 (AL-21)	BD	Cat#:561237
CD103 PE (M290)	BD	Cat#:557495
CD317 Brilliant Violet 650 (927)	BioLegend	Cat#:127019
MHCII/IA/IE FITC (2G9)	BD	Cat#:553623
CD86 Pe-Cy7 (GL1)	BD	Cat#:560582
CD3 Brilliant Violet 421 (145-2C11)	BD	Cat#:562600
CD19 Brilliant Violet 421 (1D3)	BD	Cat#:562701
CD161/NK1.1 (lin) Brilliant Violet 421 (PK136)	BioLegend	Cat#:108735
IgG1 PE (A85-1)	BD	Cat#:550083
B220 (CD45R) AlexaFluor 700 (RA3-6B2)	BD	Cat#:557957
IgM Brilliant Violet 786 (R6-60.2)	BD	Cat#:564028
IgD PerCPCy5.5 (11-26c.2a)	Biolegend	Cat#:405710
GL-7 AlexaFluor 647 (GL7)	BD	Cat#:561529
CD95 PECy7 (Jo2)	BD	Cat#:557653
CD138 Brilliant Violet 650 (281-2)	BioLegend	Cat#:142517
CD21/35 FITC (7G6)	BD	Cat#:553818
CD23 Brilliant Violet 421 (B-ly6)	BD	Cat#:563929
DYKDDDDK-PE (Flag)	BioLegend	Cat#:627310
DYKDDDDK-APC (Flag)	BioLegend	Cat#:627308
HA-DyLight 650	Thermo Fisher	Cat#:26183-D650
6x-Histidine-PE	Abcam	Cat#:Ab72467
LEAF-P. Hamster IgG Isotype Control (HTK888)	Biolegend	Cat#:400933
LEAF-P. anti-mouse CD3-e (2C11)	Biolegend	Cat#:100331
CD3-*uncongjugated* (17A2)	eBioscience	Cat#:16-0032-85
Goat anti-Rat IgG Alexa Fluor 555	ThermoFisher	Cat#:A-21434
Cytokines		
IL-2	Immunotools	Cat#:12340024
IL-15	Immunotools	Cat#:12340155
IL-3	R&D Systems	Cat#:403-mL
IL-4	R&D Systems	Cat#:404-mL
Chemicals, Enzymes, Media		
Dulbecco's phosphate buffered saline (PBS)	Gibco	Cat#:14190-094
Hank's balanced salt solution (HBSS)	Gibco	Cat#:14175-095
RPMI medium 1640	Gibco	Cat#:21875-034
Foetal calf serum (FCS)	Gibco	Cat#:10270-106
Penicillin-Streptomycin (PenStrep)	Sigma	Cat#:P4333
EDTA	Fisher Scientific	Cat#:D/0700/53
HEPES	Gibco	Cat#:15630-056
Non-essential amino acids (NEAA)	Invitrogen	Cat#:11140
β mercapto-ethanol (50mM)	Gibco	Cat#:31350-010
β mercapto-ethanol	Fisher scientific	Cat#:M/P200/05
Sodium Pyruvate	Gibco	Cat#:11360-039

DMEM	Gibco	Cat#:41966-029
Hygromycin	Invitrogen	Cat#:10687010
Puromycin	Sigma	Cat#:P8833
Percoll	GE Healthcare	Cat#:17-0891-01
DL-Dithiothreitol (DTT)	Sigma-Aldrich	Cat#:D0632
Bovine Serum Albumin	Sigma	Cat#:A4503
BrdU	Sigma-Aldrich	Cat#:B5002
Zombie NIR™ Fixable Viability Kit	Biolegend	Cat#:423106
Live/Dead Fixable Blue Dead Cell Stain Kit	Thermo Fisher	Cat#:L23105
Superscript II	Invitrogen	Cat#:18064014
Platinum SYBR Green qPCR SuperMix-UDG	Thermo Fisher	Cat#:11744500
Proteinase K	Sigma	Cat#:P2308
RedTaq DNA polymerase	Sigma	Cat#:D4309
Isopropanol	Fisher Chemical	Cat#:P/7500/PC17
Ethanol	Sigma	Cat#:32221
Accutase	PAA	Cat#:L11-007
Picric acid	Sigma	Cat#:197378
Normal goat serum	Jackson ImmunoReseach	Cat#:005-000-001
Triton X-100	Fisher Scientific	Cat#:T/3751/08
Rat γ globulin	Jackson ImmunoResearch	Cat#:012-000-002
Southern Blot DIG-reagents/kits		
DIG PCR Probe Synthesis Kit	Roche	Cat#:11636090910
DIG Easy Hyb	Roche	Cat#:11603558001
DIG Blocking reagent	Roche	Cat#:11096176001
DIG Luminescent Detection Kit	Roche	Cat#:11363514910
DNA Molecular Weight Marker II (DIG-labelled)	Roche	Cat#:11218590910
Other Kits		
Click-iT EdU Alexa Fluor 647 Flow Cytometry Assay Kit	Invitrogen	Cat#:A10202
Foxp3 Staining Buffer Set	eBioscience	Cat#:00-5523-00
RNAscope 2.0 HD Reagent Kit-Brown	ACD	Cat#:320497
Mouse TCS Purification System	abcam	Cat#:ab128749
EZ-Link Sulfo-NHS-LC Biotinylation Kit	Thermo Fisher	Cat#:21435
Alexa Fluor 647 protein labelling kit	Thermo Fisher	Cat#:A20173
KAPA Stranded RNA-seq Kit with RiboErase (HMR)	Roche	Cat#:07962282001
RNeasy Plus Micro Kit	Qiagen	Cat#:74034
RNeasy Mini Kit	Qiagen	Cat#:74104

Misellaneous Items		
LS-Columns	Mitlenyi Biotech	Cat#:130-042-401
Red Blood Cell Lysis Buffer	Sigma	Cat#:R7757
V-bottom 96-well plate	Fisherbrand	Cat#:FB56414
U-bottom 96-well plate	Corning	Cat#:353077
24-well transwell plate	Corning	Cat#:CLS3452
48-well plate	Corning	Cat#:CLS3548

8.3 Spleen and Mesentric lymph node immunophenotyping panels

T Cells	
Population	**Description by markers**
Total T cells	CD45+ , CD5+ , TCRδ+ or CD4+ or CD8+
Total γδ T cells	CD45+ , TCRδ+,
Effector γδ T cells	CD45+ , TCRδ+ , CD44+ , CD62L-
Resting γδ T cells	CD45+ , TCRδ+ , CD62L+
KLRG1+ γδ T cells	CD45+ , TCRδ+ , KLRG1+
CD5+ γδ T cells	CD45+ , TCRδ+ , CD5+
Total αβ T cells	CD45+ , CD5+ , TCRδ- , CD4+ or CD8+
Total CD8+ T cells	CD45+ , CD5+ , TCRδ- , CD4- , CD8+
Effector CD8+ T	CD45+ , CD5+ , TCRδ- , CD4- , CD8+ , CD44+, CD62L-
Resting CD8+ T	CD45+ , CD5+ , TCRδ- , CD4- , CD8+ , CD44+ , CD62L+
Naive CD8+ T cells	CD45+ , CD5+ , TCRδ- , CD4- , CD8+ , CD44- , CD62L+
KLRG1+ CD8+ T	CD45+ , CD5+ , TCRδ- , CD4- , CD8+, KLRG1+
Total CD4+ T cells	CD45+ , CD5+ , TCRδ- , CD4+ , CD8-
CD4+ T helper cells	CD45+ , CD5+ , TCRδ- , CD4+ , CD8- , CD25- , GITR-
Effector CD4+ T	CD45+ , CD5+ , TCRδ- , CD4+ , CD8- , CD25- , GITR- ,
Resting CD4+ T	CD45+ , CD5+ , TCRδ- , CD4+ , CD8-, CD25- , GITR- , CD62L+
KLRG1+ CD4+ T	CD45+ , CD5+ , TCRδ- , CD4+ , CD8- , CD25- , GITR- ,
Total Tregs	CD45+ , CD5+ , TCRδ- , CD4+ , CD8- , CD25+ , GITR+
Effector Tregs	CD45+ , CD5+ , TCRδ- , CD4+ , CD8- , CD25+ , GITR+ ,
Resting Tregs	CD45+ , CD5+ , TCRδ- , CD4+ , CD8- , CD25+ , GITR+ ,
KLRG1+ Tregs	CD45+ , CD5+ , TCRδ- , CD4+ , CD8- , CD25+ , GITR+ ,
NKT cells	
Total NKT cells	CD45+ , CD5+ , TCRδ- , CD161+
Total CD4- NKT cells	CD45+ , CD5+ , TCRδ- , CD161+ , CD4-
Effector CD4- NKT	CD45+ , CD5+ , TCRδ- , CD161+ , CD4- , CD44+ , CD62L-
Resting CD4- NKT	CD45+ , CD5+ , TCRδ- , CD161+ , CD4- , CD62L+
KLRG1+ CD4- NKT	CD45+ , CD5+ , TCRδ- , CD161+ , CD4- , KLRG1+
Total CD4+ NKT	CD45+ , CD5+ , TCRδ- , CD161+ , CD4+
Effector CD4+ NKT	CD45+ , CD5+ , TCRδ- , CD161+ , CD4+ , CD44+ , CD62L-
Resting CD4+ NKT	CD45+ , CD5+ , TCRδ- , CD161+ , CD4+ , CD62L+
KLRG1+ CD4+ NKT	CD45+ , CD5+ , TCRδ- , CD161+ , CD4+ , KLRG1+
NK cells	
Total NK cells	CD45+ , CD5- , TCRδ- , CD4- , CD8- , CD161+
Effector NK cells	CD45+ , CD5- , TCRδ- , CD4- , CD8- , CD161+ , CD44+ ,
Resting NK cells	CD45+ , CD5- , TCRδ- , CD4- , CD8- , CD161+ , CD62L+
KLRG1+ NK cells	CD45+ , CD5- , TCRδ- , CD4- , CD8- , CD161+ , KLRG1+

B cells	
Total B cells	CD45+ ,B220+ , CD138-
B1a cells	CD45+ ,B220+, CD138- , CD5+
Total B2 cells	CD45+ ,B220+, CD138- , CD5-
Marginal zone B cells	CD45+ ,B220+, CD138- , CD5- , GL-7- , CD95- , IgM+ , IgG- , CD21high , CD23+
Transitional 1 B cells	CD45+ ,B220+, CD138- , CD5- , GL-7- , CD95- , IgM+ , IgG- , CD21- , CD23-
Transitional 2 B cells	CD45+ ,B220+, CD138- , CD5- , GL-7- , CD95- , IgM+ , IgG- , CD21- , CD23+
Follicular B cells	CD45+ ,B220+, CD138- , CD5- , GL-7- , CD95- , IgM+ , IgG- , CD21low , CD23+
Plasma cells	CD45+ B220low , CD138+
Memory B cells	CD45+ ,B220+, CD138- , CD5- , GL-7- , CD95- , IgM- , IgG+
Germinal centre B	CD45+ ,B220+, CD138- , CD5- , GL7+ , CD95+
Early germinal	CD45+ ,B220+, CD138- , CD5- , GL7+ , CD95+ , IgM+ , IgG-
Late germinal centre	CD45+ ,B220+, CD138- , CD5- , GL7+ , CD95+ , IgM- , IgG+
Myeloid	
Total myeloid cells	CD19- , CD3-, NK1.1-,
Macrophages	CD19- , CD3-, NK1.1-, F4/80+ , CD11blow
Granulocytes	CD19- , CD3-, NK1.1-, F4/80- , Ly6C+ , Ly6G+ , CD11b+
Monocytes	CD19- , CD3-, NK1.1-, F4/80- , Ly6C+ , Ly6G- , CD11b+
Eosinophils	CD19- , CD3-, NK1.1-, F4/80- , Ly6C+ , Ly6G-
Total dendritic cells	CD19- , CD3-, NK1.1-, F4/80- , Ly6C- , Ly6G-
Plasmacytoid DC	CD19- , CD3-, NK1.1-, F4/80- , Ly6C+ , Ly6G- , CD317+
Conventional DC	CD19- , CD3-, NK1.1-, F4/80- , Ly6G- , CD11c+ , MHCII+
CD11b type cDC	CD19- , CD3-, NK1.1-, F4/80- , Ly6G- , CD11c+ , MHCII+ , CD11b+
CD8a type cDC	CD19- , CD3-, NK1.1-, F4/80- , Ly6G- , CD11c+ , MHCII+ , CD11b-, CD86+
CD103+ CD8 type cDC	CD19- , CD3-, NK1.1-, F4/80- , Ly6G- , CD11c+ , MHCII+ , CD11b- ,CD86+, CD103+

Reference List

Abeler-Dörner, L., Swamy, M., Williams, G., Hayday, A.C., Bas, A., 2012. Butyrophilins: an emerging family of immune regulators. Trends in Immunology 33, 34–41.

Adams, E.J., Chien, Y.-H., Garcia, C., 2005. Structure of a γδ T Cell Receptor in Complex with the Nonclassical MHC T22. Science 308, 227–231.

Adams, E.J., Strop, P., Shin, S., Chien, Y.-H., Garcia, K.C., 2008. An autonomous CDR3δ is sufficient for recognition of the nonclassical MHC class I molecules T10 and T22 by γδ T cells. Nature immunology 9, 777–784.

Afrache, H., Gouret, P., Ainouche, S., Pontarotti, P., Olive, D., 2012. The butyrophilin (BTN) gene family: from milk fat to the regulation of the immune response. Immunogenetics 64, 781–794.

Almeida, F.F., Tenno, M., Brzostek, J., Li, J.L., Allies, G., Hoeffel, G., See, P., Ng, L.G., Fehling, H.J., Gascoigne, N.R.J., Taniuchi, I., Ginhoux, F., 2015. Identification of a novel lymphoid population in the murine epidermis. Nature Scientific Reports 5, 1–17.

Ammann, J.U., Cooke, A., Trowsdale, J., 2013. Butyrophilin Btn2a2 Inhibits TCR Activation and Phosphatidylinositol 3-Kinase/Akt Pathway Signaling and Induces Foxp3 Expression in T Lymphocytes. The Journal of Immunology 190, 5030–5036.

Anderson, A.C., Joller, N., Kuchroo, V.K., 2016. Lag-3, Tim-3, and TIGIT: Co-inhibitory Receptors with Specialized Functions in Immune Regulation. Immunity 44, 1–16.

Ansell, S.M., Lesokhin, A.M., Borrello, I., Halwani, A., Scott, E.C., Gutierrez, M., Schuster, S.J., Millenson, M.M., Cattry, D., Freeman, G.J., Rodig, S.J., Chapuy, B., Ligon, A.H., Zhu, L., Grosso, J.F., Kim, S.Y., Timmerman, J.M., Shipp, M.A., Armand, P., 2015. PD-1 Blockade with Nivolumab in Relapsed or Refractory Hodgkin's Lymphoma. New England Journal of Medicine 372, 311–319.

Aono, A., Enomoto, H., Yoshida, N., Yoshizaki, K., Kishimoto, T., Komori, T., 2000. Forced expression of terminal deoxynucleotidyl transferase in fetal thymus resulted in a decrease in γδ T cells and random dissemination of Vγ3Vδ1 T cells in skin of newborn but not adult mice. Immunology 99, 498–497.

Aparicio-Domingo, P., Romera-Hernandez, M., Karrich, J.J., Cornelissen, F., Papazian, N., Lindenbergh-Kortleve, D.J., Butler, J.A., Boon, L., Coles, M.C., Samsom, J.N., Cupedo, T., 2015. Type 3 innate lymphoid cells maintain intestinal epithelial stem cells after tissue damage. Journal of Experimental Medicine 212, 1783–1791.

Arnett, H.A., Escobar, S.S., Gonzalez-Suarez, E., Budelsky, A.L., Steffen, L.A., Boiani, N., Zhang, M., Siu, G., Brewer, A.W., Viney, J.L., 2007. BTNL2, a Butyrophilin/B7-Like Molecule, Is a Negative Costimulatory Molecule Modulated in Intestinal Inflammation. The Journal of Immunology 178, 1523–1533.

Arnett, H.A., Viney, J.L., 2014. Immune modulation by butyrophilins. Nature Reviews Immunology 14, 559–569.

Asarnow, D.M., Kuziel, W.A., Bonyhadi, M., Tigelaar, R.E., Tucker, P.W., Allison, J.P., 1988. Limited diversity of gamma delta antigen receptor genes of Thy-1+ dendritic epidermal cells. Cell 55, 837–847.

Azzam, H.S., DeJarnette, J.B., Huang, K., Emmons, R., Park, C.S., Sommers, C.L., El-Khoury, D., Shores, E.W., Love, P.E., 2001. Fine Tuning of TCR Signaling by CD5. The Journal of Immunology 166, 5464–5472.

Baldwin, T.A., Hogquist, K.A., Jameson, S.C., 2004. The fourth way? Harnessing aggressive tendencies in the thymus. The Journal of Immunology 173, 6515–6520.

Banchereau, J., Steinman, R.M., 1998. Dendritic cells and the control of immunity. Nature 392, 245–252.

Bandeira, A., Mota-Santos, T., Itohara, S., Degermann, S., Heusser, C., Tonegawa, S., Coutinho, A., 1990. Localization of γ/δ T cells to the intestinal epithelium is independent of normal microbial colonization. Journal of Experimental Medicine 172, 239–244.

Barbee, S.D., Woodward, M.J., Turchinovich, G., Mention, J.-J., Lewis, J.M., Boyden, L.M., Lifton, R.P., Tigelaar, R., Hayday, A.C., 2011. Skint-1 is a highly specific, unique selecting component for epidermal T cells. Proc Natl Acad Sci USA 108, 3330–3335.

Bas, A., Swamy, M., Abeler-Dörner, L., Williams, G., Pang, D.J., Barbee, S.D., Hayday, A.C., 2011. Butyrophilin-like 1 encodes an enterocyte protein that selectively regulates functional interactions with T lymphocytes. Proc Natl Acad Sci USA 108, 4376–4381.

Beresford, P.J., Xia, Z., Greenberg, A.H., Lieberman, J., 1999. Granzyme A loading induces rapid cytolysis and a novel form of DNA damage independently of caspase activation. Immunity 10, 585–594.

Berndt, A., Pieper, J., Methner, U., 2006. Circulating γδ T Cells in Response to Salmonella enterica Serovar Enteritidis Exposure in Chickens. Infection and Immunity 74, 3967–3978.

Boismenu, R., Havran, W.L., 1994. Modulation of epithelial cell growth by intraepithelial γδ T cells. Science 266, 1253–1255.

Bonneville, M., Itohara, S., Krecko, E.G., Mombaerts, P., Ishida, I., Katsuki, M., Berns, A., Farr, A.G., Janeway, C.A., Tonegawa, S., 1990. Transgenic mice demonstrate that epithelial homing of γ/δ T cells is determined by cell lineages independent of T cell receptor specificity. Journal of Experimental Medicine 171, 1015–1026.

Borst, J., van de Griend, R.J., van Oostveen, J.W., Ang, S.L., Melief, C.J., Seidman, J.G., Bolhuis, R.L., 1987. A T-cell receptor γ/CD3 complex found on cloned functional lymphocytes. Nature 325, 683–688.

Boyden, L.M., Lewis, J.M., Barbee, S.D., Bas, A., Girardi, M., Hayday, A.C., Tigelaar, R.E., Lifton, R.P., 2008. Skint1, the prototype of a newly identified immunoglobulin superfamily gene cluster, positively selects epidermal γδ T cells. Nature Genetics 40, 656–662.

Brenner, M.B., McLean, J., Dialynas, D.P., Strominger, J.L., Smith, J.A., Owen, F.L., Seidman, J.G., Ip, S., Rosen, F., Krangel, M.S., 1986. Identification of a putative second T-cell receptor. Nature 322, 145–149.

Büning, J., Schmitz, M., Repenning, B., Ludwig, D., Schmidt, M.A., Strobel, S., Zimmer, K.-P., 2005. Interferon-γ mediates antigen trafficking to MHC class II-positive late endosomes of enterocytes. European Journal of Immunology 35, 831–842.

Capone, M., Lees, R.K., Finke, D., Ernst, B., Meerwijk, J.P.M.V., MacDonald, H.R., 2003. Selective absence of CD8+ TCRαβ+ intestinal epithelial cells in transgenic mice expressing β2-microglobulin-associated ligands exclusively on thymic cortical epithelium. European Journal of Immunology 33, 1471–1477.

Carding, S.R., Egan, P.J., 2002. γδ T Cells: Functional Plasticity and Heterogeneity. Nature Reviews Immunology 2, 336–345.

Chan, C.J., Martinet, L., Gilfillan, S., Souza-Fonseca-Guimaraes, F., Chow, M.T., Town, L., Ritchie, D.S., Colonna, M., Andrews, D.M., Smyth, M.J., 2014. The receptors CD96 and CD226 oppose each other in the regulation of natural killer cell functions. Nature immunology 15, 431–438.

Chen, H., Kshirsagar, S., Jensen, I., Lau, K., Covarrubias, R., Schluter, S.F., Marchalonis, J.J., 2009. Characterization of arrangement and expression of the T cell receptor γ locus in the sandbar shark. Proc Natl Acad Sci USA 106, 8591–8596.

Chennupati, V., Worbs, T., Liu, X., Malinarich, F.H., Schmitz, S., Haas, J.D., Malissen, B., Forster, R., Prinz, I., 2010. Intra- and Intercompartmental Movement of γδ T Cells: Intestinal Intraepithelial and Peripheral γδ T Cells Represent Exclusive Nonoverlapping Populations with Distinct Migration Characteristics. The Journal of Immunology 185, 5160–5168.

Cheroutre, H., Lambolez, F., 2008. Doubting the TCR Coreceptor Function of CD8αα. Immunity 28, 149–159.

Cheroutre, H., Lambolez, F., Mucida, D., 2011. The light and dark sides of intestinal intraepithelial lymphocytes. Nature Reviews Immunology 11, 445–456.

Chien, Y.H., Konigshofer, Y., 2007. Antigen recognition by γδ T cells. Immunological Reviews. 215, 46–58.

Chodaczek, G., Papanna, V., Zal, M.A., Zal, T., 2012. Body-barrier surveillance by epidermal γδ TCRs. Nature immunology 13, 272–282.

Ciofani, M., Zúñiga-Pflücker, J.C., 2010. Determining γδ versus αβ T cell development. Nature Reviews Immunology 10, 657–663.

Connor, K., Aylward, L., 2007. Human Response to Dioxin: Aryl Hydrocarbon Receptor (AhR) Molecular Structure, Function, and Dose-Response Data for Enzyme Induction Indicate an Impaired Human AhR. Journal of Toxicology and Environmental Health, Part B 9, 141–171.

Crowley, M.P., Fahrer, A.M., Baumgarth, N., Hampl, J., Gutgemann, I., Teyton, L., Chien, Y., 2000. A population of murine γδ T cells that recognize an inducible MHC class Ib molecule. Science 287, 314–316.

Dalessandri, T., Crawford, G., Hayes, M., Seoane, R.C., Strid, J., 2016. IL-13 from intraepithelial lymphocytes regulates tissue homeostasis and protects against carcinogenesis in the skin. Nature Communications 7, 1–12.

Dalton, J.E., Cruickshank, S.M., Egan, C.E., Mears, R., Newton, D.J., Andrew, E.M., Lawrence, B., Howell, G., Else, K.J., Gubbels, M.J., Striepen, B., Smith, J.E., White, S.J., Carding, S.R., 2006. Intraepithelial γδ+ Lymphocytes Maintain the Integrity of Intestinal Epithelial Tight Junctions in Response to Infection. Gastroenterology 131, 818–829.

Das, G., Gould, D.S., Augustine, M.M., Fragoso, G., Scitto, E., Stroynowski, I., Van Kaer, L., Schust, D.J., Ploegh, H., Janeway, C.A., 2000. Qa-2-dependent selection of CD8α/α T cell receptor α/β+ cells in murine intestinal intraepithelial lymphocytes. Journal of Experimental Medicine. 192, 1521–1528.

Das, H., Wang, L., Kamath, A., Bukowski, J.F., 2001. Vγ2Vδ2 T cell receptor-mediated recognition of aminobisphosphonates. Blood 98, 1616–1618.

Davis, M.M., Bjorkman, P.J., 1988. T-cell antigen receptor genes and T-cell recognition. Nature 334, 395–402.

De Creus, A., Van Beneden, K., Stevenaert, F., Debacker, V., Plum, J., Leclercq, G., 2002. Developmental and functional defects of thymic and epidermal Vγ3 cells in IL-15-deficient and IFN regulatory factor-1-deficient mice. J. Immunol. 168, 6486–6493.

Denning, T.L., Granger, S., Mucida, D., Graddy, R., Leclercq, G., Zhang, W., Honey, K., Rasmussen, J.P., Cheroutre, H., Rudensky, A.Y., Kronenberg, M., 2007. Mouse TCRαβ+CD8αα Intraepithelial Lymphocytes Express Genes That Down-Regulate Their Antigen Reactivity and Suppress Immune Responses. The Journal of Immunology 178, 4230–4239.

Depper, J.M., Leonard, W.J., Krönke, M., Noguchi, P.D., Cunningham, R.E., Waldmann, T.A., Greene, W.C., 1984. Regulation of interleukin 2 receptor expression: effects of phorbol diester, phospholipase C, and reexposure to lectin or antigen. The Journal of Immunology 133, 3054–3061.

Di Marco Barros, R., Roberts, N.A., Dart, R.J., Vantourout, P., Jandke, A., Nussbaumer, O., Deban, L., Cipolat, S., Hart, R., Iannitto, M.L., Laing, A., Spencer-Dene, B., East, P., Gibbons, D., Irving, P.M., Pereira, P., Steinhoff, U., Hayday, A., 2016. Epithelia Use Butyrophilin-like Molecules to Shape Organ-Specific γδ T Cell Compartments. Cell 167, 1–16.

Dimova, T., Brouwer, M., Gosselin, F., Tassignon, J., Leo, O., Donner, C., Marchant, A., Vermijlen, D., 2015. Effector Vγ9Vδ2 T cells dominate the human fetal γδ T-cell repertoire. Proc Natl Acad Sci USA 112, E556–E565.

Dolmetsch, R.E., Xu, K., Lewis, R.S., 1998. Calcium oscillations increase the efficiency and specificity of gene expression. Nature 392, 933–936.

Dudley, E.C., Girardi, M., Owen, M.J., Hayday, A.C., 1995. αβ and γδ T cells can share a late common precursor. Current Biology 5, 659–669.

Eberl, G., 2005. Inducible lymphoid tissues in the adult gut: recapitulation of a fetal developmental pathway? Nature Reviews Immunology 5, 413–420.

Eberl, G., Littman, D.R., 2004. Thymic origin of intestinal αβ T cells revealed by fate mapping of RORγt+ cells. Science 305, 248–251.

Eberl, M., Hintz, M., Reichenberg, A., Kollas, A.-K., Wiesner, J., Jomaa, H., 2003. Microbial isoprenoid biosynthesis and human γδ T cell activation. FEBS Letters 544, 4–10.

Edelblum, K.L., Singh, G., Odenwald, M.A., Lingaraju, A., Bissati, El, K., McLeod, R., Sperling, A.I., Turner, J.R., 2015. γδ Intraepithelial Lymphocyte Migration Limits Transepithelial Pathogen Invasion and Systemic Disease in Mice. Gastroenterology 148, 1417–1426.

Fan, X., Rudensky, A.Y., 2016. Hallmarks of Tissue-Resident Lymphocytes. Cell 164, 1198–1211.

Fernandez-Salguero, P., Pineau, T., Hilbert, D.M., McPhail, T., Lee, S.S., Kimura, S., Nebert, D.W., Rudikoff, S., Ward, J.M., Gonzalez, F.J., 1995. Immune system impairment and hepatic fibrosis in mice lacking the dioxin-binding Ah receptor. Science 268, 722–726.

Fernández-Bañares, F., Carrasco, A., García-Puig, R., Rosinach, M., González, C., Alsina, M., Loras, C., Salas, A., Viver, J.M., Esteve, M., 2014. Intestinal Intraepithelial Lymphocyte Cytometric Pattern Is More Accurate than Subepithelial Deposits of Anti-Tissue Transglutaminase IgA for the Diagnosis of Celiac Disease in Lymphocytic Enteritis. PLoS ONE 9, e101249.

Feske, S., Giltnane, J., Dolmetsch, R., Staudt, L.M., Rao, A., 2001. Gene regulation mediated by calcium signals in T lymphocytes. Nature immunology 2, 316–324.

Fouchier, R.A., Meyer, B.E., Simon, J.H., Fischer, U., Malim, M.H., 1997. HIV-1 infection of non-dividing cells: evidence that the amino-terminal basic region of the viral matrix protein is important for Gag processing but not for post-entry nuclear import. The EMBO Journal 16, 4531–4539.

Franke, W.W., Heid, H.W., Grund, C., Winter, S., Freudenstein, C., Schmid, E., Jarasch, E.-D., Keenan, T.W., 1981. Antibodies to the major insoluble milk fat globule membrane-associated protein: specific location in apical regions of lactating epithelial cells. The journal of cell biology 89, 485–494.

Fridman, W.H., Pagès, F., Sautès-Fridman, C., Galon, J., 2012. The immune contexture in human tumours: impact on clinical outcome. Nature Reviews Cancer 12, 298–306.

Fujiura, Y., Kawaguchi, M., Kondo, Y., Obana, S., Yamamoto, H., Nanno, M., Ishikawa, H., 1996. Development of CD8 alpha alpha+ intestinal intraepithelial T cells in beta 2-microglobulin-and/or TAP1-deficient mice. The Journal of Immunology 156, 2709–2715.

Fütterer, A., Mink, K., Luz, A., Kosco-Vilbois, M.H., Pfeffer, K., 1998. The lymphotoxin β receptor controls organogenesis and affinity maturation in peripheral lymphoid tissues. Immunity 9, 59–70.

Gangadharan, D., Lambolez, F., Attinger, A., Wang-Zhu, Y., Sullivan, B.A., Cheroutre, H., 2006. Identification of Pre- and Postselection TCRαβ+ Intraepithelial Lymphocyte Precursors in the Thymus. Immunity 25, 631–641.

Gapin, L., Cheroutre, H., Kronenberg, M., 1999. Cutting edge: TCRαβ+ CD8αα+ T cells are found in intestinal intraepithelial lymphocytes of mice that lack classical MHC class I molecules. The Journal of Immunology 163, 4100–4101.

Gaulard, P., Belhadj, K., Reyes, F., 2003. γδ T-cell lymphomas. Seminars in Hematology 40, 233–243.

Gentles, A.J., Newman, A.M., Liu, C.L., Bratman, S.V., Feng, W., Kim, D., Nair, V.S., Xu, Y., Khuong, A., Hoang, C.D., Diehn, M., West, R.B., Plevritis, S.K., Alizadeh, A.A., 2015. The prognostic landscape of genes and infiltrating immune cells across human cancers. Nat Med 21, 938–945.

Germain, R.N., 2002. T-cell development and the CD4–CD8 lineage decision. Nature Reviews Immunology 2, 309–322.

Girardi, M., Lewis, J., Glusac, E., Filler, R.B., Geng, L., Hayday, A.C., Tigelaar, R.E., 2002. Resident skin-specific γδ T cells provide local, nonredundant regulation of cutaneous inflammation. Journal of Experimental Medicine. 195, 855–867.

Girardi, M., Oppenheim, D.E., Steele, C.R., Lewis, J.M., Glusac, E., Filler, R., Hobby, P., Sutton, B., Tigelaar, R.E., Hayday, A.C., 2001. Regulation of cutaneous malignancy by γδ T cells. Science 294, 605–609.

Gober, H.-J., Kistowska, M., Angman, L., Jenö, P., Mori, L., De Libero, G., 2003. Human T Cell Receptor γδ Cells Recognize Endogenous Mevalonate Metabolites in Tumor Cells. Journal of Experimental Medicine 197, 163–168.

Godfrey, D.I., Uldrich, A.P., McCluskey, J., Rossjohn, J., Moody, D.B., 2015. The burgeoning family of unconventional T cells. Nature immunology 16, 1114–1123.

Goldrath, A.W., Bevan, M.J., 1999. Selecting and maintaining a diverse T-cell repertoire. Nature 402, 255–262.

Goldrath, A.W., Bogatzki, L.Y., Bevan, M.J., 2000. Naive T cells transiently acquire a memory-like phenotype during homeostasis-driven proliferation. Journal of Experimental Medicine 192, 557–564.

Gray, E.E., Ramírez-Valle, F., Xu, Y., Wu, S., Wu, Z., Karjalainen, K.E., Cyster, J.G., 2013. Deficiency in IL-17-committed Vγ4+ γδ T cells in a spontaneous Sox13-mutant CD45.1+ congenic mouse substrain provides protection from dermatitis. Nature immunology 14, 584–592.

Gray, E.E., Suzuki, K., Cyster, J.G., 2011. Cutting Edge: Identification of a Motile IL-17-Producing γδ T Cell Population in the Dermis. The Journal of Immunology 186, 6091–6095.

Groh, V., Bahram, S., Bauer, S., Herman, A., Beauchamp, A., Spies, T., 1996. Cell stress-regulated human major histocompatibility complex class I gene expressed in gastrointestinal epithelium. Proc Natl Acad Sci USA, pp. 12445–12450.

Guo, L., Junttila, I.S., Paul, W.E., 2012. Cytokine-induced cytokine production by conventional and innate lymphoid cells. Trends in Immunology 33, 598–606.

Guy-Grand, D., Azogui, O., Celli, S., Darche, S., Nussenzweig, M.C., Kourilsky, P., Vassalli, P., 2003. Extrathymic T Cell Lymphopoiesis: Ontogeny and

Contribution to Gut Intraepithelial Lymphocytes in Athymic and Euthymic Mice. Journal of Experimental Medicine 197, 333–341.

Guy-Grand, D., Cerf-Bensussan, N., Malissen, B., Malassis-Seris, M., Briottet, C., Vassalli, P., 1991. Two gut intraepithelial CD8+ lymphocyte populations with different T cell receptors: a role for the gut epithelium in T cell differentiation. Journal of Experimental Medicine. 173, 471–481.

Guy-Grand, D., Vassalli, P., Eberl, G., Pereira, P., Burlen-Defranoux, O., Lemaitre, F., Di Santo, J.P., Freitas, A.A., Cumano, A., Bandeira, A., 2013. Origin, trafficking, and intraepithelial fate of gut-tropic T cells. Journal of Experimental Medicine 210, 1839–1854.

Haas, J.D., Ravens, S., Düber, S., Sandrock, I., Oberdörfer, L., Kashani, E., Chennupati, V., Föhse, L., Naumann, R., Weiss, S., Krueger, A., Förster, R., Prinz, I., 2012. Development of Interleukin-17-Producing γδ T Cells Is Restricted to a Functional Embryonic Wave. Immunity 37, 48–59.

Haks, M.C., Lefebvre, J.M., Lauritsen, J.P.H., Carleton, M., Rhodes, M., Miyazaki, T., Kappes, D.J., Wiest, D.L., 2005. Attenuation of γδTCR Signaling Efficiently Diverts Thymocytes to the αβ Lineage. Immunity 22, 595–606.

Hamid, O., Robert, C., Daud, A., Hodi, F.S., Hwu, W.-J., Kefford, R., Wolchok, J.D., Hersey, P., Joseph, R.W., Weber, J.S., Dronca, R., Gangadhar, T.C., Patnaik, A., Zarour, H., Joshua, A.M., Gergich, K., Elassaiss-Schaap, J., Algazi, A., Mateus, C., Boasberg, P., Tumeh, P.C., Chmielowski, B., Ebbinghaus, S.W., Li, X.N., Kang, S.P., Ribas, A., 2013. Safety and Tumor Responses with Lambrolizumab (Anti–PD-1) in Melanoma. New England Journal of Medicine 369, 134–144.

Hanke, T., Mitnacht, R., Boyd, R., Hünig, T., 1994. Induction of interleukin 2 receptor beta chain expression by self-recognition in the thymus. Journal of Experimental Medicine. 180, 1629–1636.

Hara, H., Kishihara, K., Matsuzaki, G., Takimoto, H., Tsukiyama, T., Tigelaar, R.E., Nomoto, K., 2000. Development of dendritic epidermal T cells with a skewed diversity of γδ TCRs in Vδ1-deficient mice. J. Immunol. 165, 3695–3705.

Harly, C., Guillaume, Y., Nedellec, S., Peigne, C.M., Monkkonen, H., Monkkonen, J., Li, J., Kuball, J., Adams, E.J., Netzer, S., Dechanet-Merville, J., Leger, A., Herrmann, T., Breathnach, R., Olive, D., Bonneville, M., Scotet, E., 2012. Key implication of CD277/butyrophilin-3 (BTN3A) in cellular stress sensing by a major human γδ T-cell subset. Blood 120, 2269–2279.

Havran, W.L., Allison, J.P., 1988. Developmentally ordered appearance of thymocytes expressing different T-cell antigen receptors. Nature 335, 443–445.

Havran, W.L., Jameson, J.M., 2010. Epidermal T Cells and Wound Healing. The Journal of Immunology 184, 5423–5428.

Hayday, A., Gibbons, D., 2008. Brokering the peace: the origin of intestinal T cells. Mucosal Immunology 1, 172–174.

Hayday, A., Theodoridis, E., Ramsburg, E., Shires, J., 2001. Intraepithelial lymphocytes: exploring the Third Way in immunology. Nature immunology 2, 997–1003.

Hayday, A.C., 2009. γδ T Cells and the Lymphoid Stress-Surveillance Response. Immunity 31, 184–196.

Hayday, A.C., 2000. γδ cells: a right time and a right place for a conserved third way of protection. Annu. Rev. Immunol. 18, 975–1026.

Hayday, A.C., Roberts, S., Ramsburg, E., 2000. γδ cells and the regulation of mucosal immune responses. American Journal of Respiratory and Critical Care Medicine 162, S161–S163.

Hayday, A.C., Saito, H., Gillies, S.D., Kranz, D.M., Tanigawa, G., Eisen, H.N., Tonegawa, S., 1985. Structure, organization, and somatic rearrangement of T cell gamma genes. Cell 40, 259–269.

Hayes, S.M., Li, L., Love, P.E., 2005. TCR Signal Strength Influences αβ/γδ Lineage Fate. Immunity 22, 583–593.

Hein, W.R., Dudler, L., 1997. TCR γδ+ cells are prominent in normal bovine skin and express a diverse repertoire of antigen receptors. Immunology 91, 58–64.

Henry, J., Miller, M.M., Pontarotti, P., 1999. Structure and evolution of the extended B7 family. Immunology Today 20, 285–288.

Hémar, A., Subtil, A., Lieb, M., Morelon, E., Hellio, R., Dautry-Varsat, A., 1995. Endocytosis of interleukin 2 receptors in human T lymphocytes: distinct intracellular localization and fate of the receptor α, β, and γ chains. The journal of cell biology 129, 55–64.

Hirano, M., Guo, P., McCurley, N., Schorpp, M., Das, S., Boehm, T., Cooper, M.D., 2013. Evolutionary implications of a third lymphocyte lineage in lampreys. Nature 501, 435–438.

Hochedlinger, K., Yamada, Y., Beard, C., Jaenisch, R., 2005. Ectopic Expression of Oct-4 Blocks Progenitor-Cell Differentiation and Causes Dysplasia in Epithelial Tissues. Cell 121, 465–477.

Hogquist, K.A., Jameson, S.C., 2014. The self-obsession of T cells: how TCR signaling thresholds affect fate “decisions” and effector function. Nature Immunology 15, 815–823.

Holtmeier, W., Pfänder, M., Hennemann, A., Caspary, W.F., Zollner, T.M., Kaufmann, R., Caspary, W.F., 2001. The TCR δ Repertoire in Normal Human Skin is Restricted and Distinct from the TCR δ Repertoire in the Peripheral Blood. Journal of Investigative Dermatology. 116, 275–280.

Hozumi, N., Tonegawa, S., 1976. Evidence for somatic rearrangement of immunoglobulin genes coding for variable and constant regions. Proc Natl Acad Sci USA 73, 3628–3632.

Hsu, H.-C., Zhang, H.-G., Li, L., Yi, N., Yang, P.-A., Wu, Q., Zhou, J., Sun, S., Xu, X., Yang, X., Lu, L., Van Zant, G., Williams, R.W., Allison, D.B., Mountz, J.D., 2003. Age-related thymic involution in C57BL/6J × DBA/2J recombinant-inbred mice maps to mouse chromosomes 9 and 10. Genes and Immunity 4, 402–410.

Huang, C.-T., Workman, C.J., Flies, D., Pan, X., Marson, A.L., Zhou, G., Hipkiss, E.L., Ravi, S., Kowalski, J., Levitsky, H.I., Powell, J.D., Pardoll, D.M., Drake, C.G., Vignali, D.A.A., 2004. Role of LAG-3 in regulatory T cells. Immunity 21,

503–513.

Huang, Y., Park, Y., Wang-Zhu, Y., Larange, A., Arens, R., Bernardo, I., Olivares-Villagómez, D., Herndler-Brandstetter, D., Abraham, N., Grubeck-Loebenstein, B., Schoenberger, S.P., Van Kaer, L., Kronenberg, M., Teitell, M.A., Cheroutre, H., 2011. Mucosal memory CD8+ T cells are selected in the periphery by an MHC class I molecule. Nature immunology 12, 1086–1095.

Huard, B., Prigent, P., Tournier, M., 1995. CD4/major histocompatibility complex class II interaction analyzed with CD4- and lymphocyte activation gene-3 (LAG-3)-Ig fusion proteins. European Journal of Immunology. 25, 2718–2721.

Hüe, S., Mention, J.-J., Monteiro, R.C., Zhang, S., Cellier, C., Schmitz, J., Verkarre, V., Fodil, N., Bahram, S., Cerf-Bensussan, N., Caillat-Zucman, S., 2004. A direct role for NKG2D/MICA interaction in villous atrophy during celiac disease. Immunity 21, 367–377.

Inagaki-Ohara, K., Chinen, T., Matsuzaki, G., Sasaki, A., Sakamoto, Y., Hiromatsu, K., Nakamura-Uchiyama, F., Nawa, Y., Yoshimura, A., 2004. Mucosal T Cells Bearing TCRγδ Play a Protective Role in Intestinal Inflammation. The Journal of Immunology 173, 1390–1398.

Inagaki-Ohara, K., Sakamoto, Y., Dohi, T., Smith, A.L., 2011. γδ T cells play a protective role during infection with Nippostrongylus brasiliensis by promoting goblet cell function in the small intestine. Immunology 134, 448–458.

Ishida, Y., Agata, Y., Shibahara, K., Honjo, T., 1992. Induced expression of PD-1, a novel member of the immunoglobulin gene superfamily, upon programmed cell death. The EMBO Journal 11, 3887.

Ishikawa, H., Naito, T., Iwanaga, T., Takahashi-Iwanaga, H., Suematsu, M., Hibi, T., Nanno, M., 2007. Curriculum vitae of intestinal intraepithelial T cells: their developmental and behavioral characteristics. Immunological Reviews 215, 154–165.

Ismail, A.S., Severson, K.M., Vaishnava, S., Behrendt, C.L., Yu, X., Benjamin, J.L., Ruhn, K.A., Hou, B., DeFranco, A.L., Yarovinsky, F., Hooper, L.V., 2011. γδ intraepithelial lymphocytes are essential mediators of host-microbial homeostasis at the intestinal mucosal surface. Proc Natl Acad Sci USA 108, 8743–8748.

Itohara, S., Farr, A.G., Lafaille, J.J., Bonneville, M., Takagaki, Y., Haas, W., Tonegawa, S., 1990. Homing of a γδ thymocyte subset with homogeneous T-cell receptors to mucosal epithelia. Nature 343, 754–757.

Itohara, S., Mombaerts, P., Lafaille, J., Iacomini, J., Nelson, A., Clarke, A.R., Hooper, M.L., Farr, A., Tonegawa, S., 1993. T cell receptor δ gene mutant mice: independent generation of αβ T cells and programmed rearrangements of γδ TCR genes. Cell 72, 337–348.

Jack, L.J., Mather, I.H., 1990. Cloning and analysis of cDNA encoding bovine butyrophilin, an apical glycoprotein expressed in mammary tissue and secreted in association with the milk-fat globule membrane during lactation. The Journal of Biological Chemistry. 265, 14481–14486.

Jameson, J.M., Cruz, J., Costanzo, A., Terajima, M., Ennis, F.A., 2010. A role for the mevalnoate pathway in the induction of subtype cross-reactive immunity to influenza A virus by human γδ T lymphocytes. Cellular Immunology 264, 71–77.

Janeway, C.A., 1989. Approaching the asymptote? Evolution and revolution in immunology. Cold Spring Harbor symposia on quantitative biology 54, 1–13.

Janeway, C.A., Jr., Jones, B., Hayday, A., 1988. Specificity and function of T cells bearing γδ receptors. Immunology Today 9, 73–76.

Janeway, C.A., Jr., Medzhitov, R., 2002. INNATE IMMUNE RECOGNITION. Annual Review of Immunology. 20, 197–216.

Jensen, K.D.C., Shin, S., Chien, Y.-H., 2009. Cutting Edge: γδ Intraepithelial Lymphocytes of the Small Intestine Are Not Biased toward Thymic Antigens. The Journal of Immunology 182, 7348–7351.

Jensen, K.D.C., Su, X., Shin, S., Li, L., Youssef, S., Yamasaki, S., Steinman, L., Saito, T., Locksley, R.M., Davis, M.M., Baumgarth, N., Chien, Y.-H., 2008. Thymic Selection Determines γδ T Cell Effector Fate: Antigen-Naive Cells Make Interleukin-17 and Antigen-Experienced Cells Make Interferon γ. Immunity 29, 90–100.

Jeong, J., Rao, A.U., Xu, J., Ogg, S.L., Hathout, Y., Fenselau, C., Mather, I.H., 2009. The PRY/SPRY/B30.2 Domain of Butyrophilin 1A1 (BTN1A1) Binds to Xanthine Oxidoreductase: IMPLICATIONS FOR THE FUNCTION OF BTN1A1 IN THE MAMMARY GLAND AND OTHER TISSUES. Journal of Biological Chemistry 284, 22444–22456.

Jerome Galon, Franck Pages, Francesco M Marincola, Thurin, M., Trinchieri, G., Bernard A Fox, Gajewski, T.F., Paolo A Ascierto, 2012. The Immune Score as a New Possible Approach for the Classification of Cancer. Journal of Translational Medicine 10, 1–4.

Jin, Y., Xia, M., Saylor, C.M., Narayan, K., Kang, J., Wiest, D.L., Wang, Y., Xiong, N., 2010. Cutting Edge: Intrinsic Programming of Thymic γδT Cells for Specific Peripheral Tissue Localization. The Journal of Immunology 185, 7156–7160.

Jitsukawa, S., Faure, F., Lipinski, M., Triebel, F., Hercend, T., 1987. A novel subset of human lymphocytes with a T cell receptor-γ complex. Journal of Experimental Medicine. 166, 1192–1197.

Joller, N., Hafler, J.P., Brynedal, B., Kassam, N., Spoerl, S., Levin, S.D., Sharpe, A.H., Kuchroo, V.K., 2011. Cutting Edge: TIGIT Has T Cell-Intrinsic Inhibitory Functions. The Journal of Immunology 186, 1338–1342.

Joller, N., Lozano, E., Burkett, P.R., Patel, B., Xiao, S., Zhu, C., Xia, J., Tan, T.G., Sefik, E., Yajnik, V., Sharpe, A.H., Quintana, F.J., Mathis, D., Benoist, C., Hafler, D.A., Kuchroo, V.K., 2014. Treg Cells Expressing the Coinhibitory Molecule TIGIT Selectively Inhibit Proinflammatory Th1 and Th17 Cell Responses. Immunity 40, 569–581.

José, E.S., Borroto, A., Niedergang, F., Alcover, A., Alarcón, B., 2000. Triggering the TCR complex causes the downregulation of nonengaged receptors by a signal transduction-dependent mechanism. Immunity 12, 161–170.

Kadow, S., Jux, B., Zahner, S.P., Wingerath, B., Chmill, S., Clausen, B.E., Hengstler, J., Esser, C., 2011. Aryl Hydrocarbon Receptor Is Critical for Homeostasis of Invariant γδ T Cells in the Murine Epidermis. The Journal of Immunology 187, 3104–3110.

Kanamori, Y., Ishimaru, K., Nanno, M., Maki, K., Ikuta, K., Nariuchi, H., Ishikawa, H., 1996. Identification of novel lymphoid tissues in murine intestinal mucosa where clusters of c-kit+ IL-7R+ Thy1+ lympho-hemopoietic progenitors develop. Journal of Experimental Medicine. 184, 1449–1459.

Kang, J., Malhotra, N., 2015. Transcription Factor Networks Directing the Development, Function, and Evolution of Innate Lymphoid Effectors. Annual Review of Immunology 33, 505–538.

Karunakaran, M.M., Herrmann, T., 2014. The Vγ9Vδ2 T Cell Antigen Receptor and Butyrophilin-3 A1: Models of Interaction, the Possibility of Co-Evolution, and the Case of Dendritic Epidermal T Cells. Frontiers in Immunology 5, 648.

Kasamatsu, J., Sutoh, Y., Fugo, K., Otsuka, N., Iwabuchi, K., Kasahara, M., 2010. Identification of a third variable lymphocyte receptor in the lamprey. Proc Natl Acad Sci USA 107, 14304–14308.

Kawaguchi, M., Nanno, M., Umesaki, Y., Matsumoto, S., Okada, Y., Cai, Z., Shimura, T., Matsuoka, Y., Ohwaki, M., Ishikawa, H., 1993. Cytolytic activity of intestinal intraepithelial lymphocytes in germ-free mice is strain dependent and determined by T cells expressing γδ T-cell antigen receptors, in:. Presented at the Proc Natl Acad Sci USA 90, 8591–8594.

Kawai, K., Suzuki, H., Tomiyama, K., Minagawa, M., Mak, T.W., Ohashi, P.S., 1998. Requirement of the IL-2 Receptor β Chain for the Development of Vγ3 Dendritic Epidermal T Cells. Journal of Investigative Dermatology 110, 961–965.

Kazen, A.R., Adams, E.J., 2011. Evolution of the V, D, and J gene segments used in the primate γδ T-cell receptor reveals a dichotomy of conservation and diversity. Proc Natl Acad Sci USA 108, E332–E340.

Kim, H.-P., Leonard, W.J., 2002. The basis for TCR-mediated regulation of the IL-2 receptor α chain gene: role of widely separated regulatory elements. The EMBO Journal 21, 3051–3059.

Klose, C.S.N., Blatz, K., d'Hargues, Y., Hernandez, P.P., Kofoed-Nielsen, M., Ripka, J.F., Ebert, K., Arnold, S.J., Diefenbach, A., Palmer, E., Tanriver, Y., 2014. The Transcription Factor T-bet Is Induced by IL-15 and Thymic Agonist Selection and Controls CD8αα. Immunity 41, 230–243.

Konkel, J.E., Maruyama, T., Carpenter, A.C., Xiong, Y., Zamarron, B.F., Hall, B.E., Kulkarni, A.B., Zhang, P., Bosselut, R., Chen, W., 2011. Control of the development of CD8αα+ intestinal intraepithelial lymphocytes by TGF-β. Nature immunology 12, 312–319.

Kreslavsky, T., Garbe, A.I., Krueger, A., Boehmer, von, H., 2008. T cell receptor–instructed αβ versus γδ lineage commitment revealed by single-cell analysis. Journal of Experimental Medicine 205, 1173–1186.

Kueh, H.Y., Yui, M.A., Ng, K.K.H., Pease, S.S., Zhang, J.A., Damle, S.S., Freedman, G., Siu, S., Bernstein, I.D., Elowitz, M.B., Rothenberg, E.V., 2016. Asynchronous combinatorial action of four regulatory factors activates Bcl11b for T cell commitment. Nature immunology 17, 956–965.

Kuo, S., Guindy, El, A., Panwala, C.M., Hagan, P.M., Camerini, V., 2001. Differential appearance of T cell subsets in the large and small intestine of neonatal mice. Pediatric Research 49, 543–551.

Kuziel, W.A., Takashima, A., Bonyhadi, M., Bergstresser, P.R., Allison, J.P., Tigelaar, R.E., Tucker, P.W., 1987. Regulation of T-cell receptor γ-chain RNA expression in murine Thy-1+ dendritic epidermal cells. Nature 328, 263–266.

Kwong, B., Lazarevic, V., 2014. T-bet Orchestrates CD8αα IEL Differentiation. Immunity 41, 169–171.

Kyes, S., Carew, E., Carding, S.R., Janeway, C.A., Hayday, A., 1989. Diversity in T-cell receptor γ gene usage in intestinal epithelium. Proc. Natl. Acad. Sci. U.S.A. 86, 5527–5531.

Lai, Y.G., Hou, M.S., Hsu, Y.W., Chang, C.L., Liou, Y.H., Tsai, M.H., Lee, F., Liao, N.S., 2008. IL-15 Does Not Affect IEL Development in the Thymus but Regulates Homeostasis of Putative Precursors and Mature CD8 + IELs in the Intestine. The Journal of Immunology 180, 3757–3765.

Laky, K., Lefrançois, L., Lingenheld, E.G., 2000. Enterocyte expression of interleukin 7 induces development of γδ T cells and Peyer's patches. Journal of Experimental Medicine. 191, 1569–1580.

Lambolez, F., Arcangeli, M.-L., Joret, A.-M., Pasqualetto, V., Cordier, C., Santo, J.P.D., Rocha, B., Ezine, S., 2005. The thymus exports long-lived fully committed T cell precursors that can colonize primary lymphoid organs. Nature immunology 7, 76–82.

Lambolez, F., Azogui, O., Joret, A.-M., Garcia, C., Boehmer, von, H., Di Santo, J., Ezine, S., Rocha, B., 2002. Characterization of T cell differentiation in the murine gut. Journal of Experimental Medicine. 195, 437–449.

Landau, S.B., Aziz, W.I., Woodcock-Mitchell, J., and Melamede, R. (1995). Vγ (I) expression in human intestinal lymphocytes is restricted. Immunol. Invest. *24*, 947–955.

Lebrero-Fernández, C., Bas-Forsberg, A., 2016. The ontogeny of Butyrophilin-like (Btnl) 1 and Btnl6 in murine small intestine. Scientific Reports 6, 1–8.

Lebrero-Fernández, C., Bergström, J.H., Pelaseyed, T., Bas-Forsberg, A., 2016. Murine Butyrophilin-Like 1 and Btnl6 Form Heteromeric Complexes in Small Intestinal Epithelial Cells and Promote Proliferation of Local T Lymphocytes. Frontiers in Immunology 7, 7354.

Lee, S.J., Kim, Y.H., Hwang, S.H., Kim, Y.I., Han, I.S., Vinay, D.S., Kwon, B.S., 2013. 4-1BB signal stimulates the activation, expansion, and effector functions of γδ T cells in mice and humans. European Journal of Immunology. 43, 1839–1848.

Lee, S.L., Wesselschmidt, R.L., Linette, G.P., Kanagawa, O., Russell, J.H., Milbrandt, J., 1995. Unimpaired thymic and peripheral T cell death in mice lacking the nuclear receptor NGFI-B (Nur77). Science 269, 532–535.

Leeansyah, E., Loh, L., Nixon, D.F., Sandberg, J.K., 2014. Acquisition of innate-like microbial reactivity in mucosal tissues during human fetal MAIT-cell development. Nature Communications 5, 3143.

Lefrançois, L., LeCorre, R., Mayo, J., Bluestone, J.A., Goodman, T., 1990. Extrathymic selection of TCR γδ+ T cells by class II major histocompatibility complex molecules. Cell 63, 333–340.

Lefrançois, L., Olson, S., 1994. A novel pathway of thymus-directed T lymphocyte maturation. The Journal of Immunology. 153, 987–995.

Leishman, A.J., Gapin, L., Capone, M., Palmer, E., MacDonald, H.R., Kronenberg, M., Cheroutre, H., 2002. Precursors of functional MHC class I- or class II-restricted CD8αα+ T cells are positively selected in the thymus by agonist self-peptides. Immunity 16, 355–364.

Leishman, A.J., Naidenko, O.V., Attinger, A., Koning, F., Lena, C.J., Xiong, Y., Chang, H.C., Reinherz, E., Kronenberg, M., Cheroutre, H., 2001. T cell responses modulated through interaction between CD8αα and the nonclassical MHC class I molecule, TL. Science 294, 1936–1939.

Leon, F., Eiras, P., Roy, G., Camarero, C., 2002. Intestinal intraepithelial lymphocytes and anti-transglutaminase in a screening algorithm for coeliac disease. Gut 50, 740–741.

Lewis, J.M., Girardi, M., Roberts, S.J., D Barbee, S., Hayday, A.C., Tigelaar, R.E., 2006. Selection of the cutaneous intraepithelial γδ+ T cell repertoire by a thymic stromal determinant. Nature immunology 7, 843–850.

Li, B., Dewey, C., 2011. RSEM: accurate transcript quantification fromRNA-Seq data with or without a reference. BMC Bioinformatics 12, 1–16.

Li, Y., Innocentin, S., Withers, D.R., Roberts, N.A., Gallagher, A.R., Grigorieva, E.F., Wilhelm, C., Veldhoen, M., 2011. Exogenous Stimuli Maintain Intraepithelial Lymphocytes via Aryl Hydrocarbon Receptor Activation. Cell 147, 629–640.

Lin, T., Yoshida, H., Matsuzaki, G., Guehler, S.R., Nomoto, K., Barrett, T.A., Green, D.R., 1999. Autospecific γδ thymocytes that escape negative selection find sanctuary in the intestine. Journal of Clinical Investigation 104, 1297–1305.

Lodolce, J.P., Boone, D.L., Chai, S., Swain, R.E., Dassopoulos, T., Trettin, S., Ma, A., 1998. IL-15 receptor maintains lymphoid homeostasis by supporting lymphocyte homing and proliferation. Immunity 9, 669–676.

Love, M.I., Huber, W., Anders, S., 2014. Moderated estimation of fold change and dispersion for RNA-seq data with DESeq2. Genome Biol 15, 31.

Love, P.E., Hayes, S.M., 2010. ITAM-mediated Signaling by the T-Cell Antigen Receptor. Cold Spring Harbor Perspectives in Biology 2, 1–11.

Ma, L.J., Acero, L.F., Zal, T., Schluns, K.S., 2009. Trans-Presentation of IL-15 by Intestinal Epithelial Cells Drives Development of CD8αα IELs. The Journal of Immunology 183, 1044–1054.

Madakamutil, L.T., Christen, U., Lena, C.J., Wang-Zhu, Y., Attinger, A., Sundarrajan, M., Ellmeier, W., Herrath, von, M.G., Jensen, P., Littman, D.R., Cheroutre, H., 2004. CD8αα-mediated survival and differentiation of CD8 memory T cell precursors. Science 304, 590–593.

Malcherek, G., Mayr, L., Roda-Navarro, P., Rhodes, D., Miller, N., Trowsdale, J., 2007. The B7 Homolog Butyrophilin BTN2A1 Is a Novel Ligand for DC-SIGN. The Journal of Immunology 179, 3804–3811.

Malhotra, N., Narayan, K., Cho, O.H., Sylvia, K.E., Yin, C., Melichar, H., Rashighi, M., Lefebvre, V., Harris, J.E., Berg, L.J., Kang, J., Consortium5, T.I.G.P., 2013. A Network of High-Mobility Group Box Transcription Factors Programs Innate Interleukin-17 Production. Immunity 38, 681–693.

Malinarich, F.H., Grabski, E., Worbs, T., Chennupati, V., Haas, J.D., Schmitz, S., Candia, E., Quera, R., Malissen, B., Förster, R., Hermoso, M., Prinz, I., 2010. Constant TCR triggering suggests that the TCR expressed on intestinal intraepithelial γδ T cells is functional in vivo. European Journal of Immunology. 40, 3378–3388.

Mallick-Wood, C.A., Lewis, J.M., Richie, L.I., Owen, M.J., Tigelaar, R.E., Hayday, A.C., 1998. Conservation of T Cell Receptor Conformation in Epidermal γδ Cells with Disrupted Primary Vγ Gene Usage. Science 279, 1729–1733.

Martin, B., Hirota, K., Cua, D.J., Stockinger, B., Veldhoen, M., 2009. Interleukin-17-Producing γδ T Cells Selectively Expand in Response to Pathogen Products and Environmental Signals. Immunity 31, 321–330.

Masopust, D., Vezys, V., Wherry, E.J., Barber, D.L., Ahmed, R., 2006. Cutting Edge: Gut Microenvironment Promotes Differentiation of a Unique Memory CD8 T Cell Population. The Journal of Immunology 176, 2079–2083.

Matsuda, S., Kudoh, S., Katayama, S., 2001. Enhanced Formation of Azoxymethane-induced Colorectal Adenocarcinoma in γδ T Lymphocyte-deficient Mice. Japanese journal of cancer research 92, 880–885.

Matzinger, P., 2002. The danger model: a renewed sense of self. Science 296, 301–305.

McDonald, B.D., Bunker, J.J., Ishizuka, I.E., Jabri, B., Bendelac, A., 2014. Elevated T Cell Receptor Signaling Identifies a Thymic Precursor to the TCRαβ+CD4-CD8β- Intraepithelial Lymphocyte Lineage. Immunity 41, 219–229.

Melichar, H.J., Narayan, K., Der, S.D., Hiraoka, Y., Gardiol, N., Jeannet, G., Held, W., Chambers, C.A., Kang, J., 2007. Regulation of γδ versus αβ T lymphocyte differentiation by the transcription factor SOX13. Science 315, 230–233.

Mische, C.C., Javanbakht, H., Song, B., Diaz-Griffero, F., Stremlau, M., Strack, B., Si, Z., Sodroski, J., 2005. Retroviral Restriction Factor TRIM5 Is a Trimer. Journal of Virology 79, 14446–14450.

Mlecnik, B., Tosolini, M., Kirilovsky, A., Berger, A., Bindea, G., Meatchi, T., Bruneval, P., Trajanoski, Z., Fridman, W.H., Pages, F., Galon, J., 2011. Histopathologic-Based Prognostic Factors of Colorectal Cancers Are Associated With the State of the Local Immune Reaction. Journal of Clinical Oncology 29, 610–618.

Mohamed, R.H., Sutoh, Y., Itoh, Y., Otsuka, N., Miyatake, Y., Ogasawara, K., Kasahara, M., 2015. The SKINT1-Like Gene Is Inactivated in Hominoids But Not in All Primate Species: Implications for the Origin of Dendritic Epidermal T Cells 1–15.

Montufar-Solis, D., Garza, T., Klein, J.R., 2007. T-cell activation in the intestinal mucosa. Immunol. Rev. 215, 189–201.

Moran, A.E., Holzapfel, K.L., Xing, Y., Cunningham, N.R., Maltzman, J.S., Punt, J., Hogquist, K.A., 2011. T cell receptor signal strength in Treg and iNKT cell development demonstrated by a novel fluorescent reporter mouse. Journal of Experimental Medicine 208, 1279–1289.

Mucida, D., Husain, M.M., Muroi, S., van Wijk, F., Shinnakasu, R., Naoe, Y., Reis, B.S., Huang, Y., Lambolez, F., Docherty, M., Attinger, A., Shui, J.-W., Kim, G., Lena, C.J., Sakaguchi, S., Miyamoto, C., Wang, P., Atarashi, K., Park, Y., Nakayama, T., Honda, K., Ellmeier, W., Kronenberg, M., Taniuchi, I., Cheroutre, H., 2013. Transcriptional reprogramming of mature CD4+ helper T cells generates distinct MHC class II–restricted cytotoxic T lymphocytes. Nature immunology 14, 281–289.

Muñoz-Ruiz, M., Ribot, J.C., Grosso, A.R., Gonçalves-Sousa, N., Pamplona, A., Pennington, D.J., Regueiro, J.R., Fernández-Malavé, E., Silva-Santos, B., 2016. TCR signal strength controls thymic differentiation of discrete proinflammatory γδ T cell subsets. Nature immunology 17, 721–727.

Naito, T., Shiohara, T., Hibi, T., Suematsu, M., Ishikawa, H., 2008. RORγt is dispensable for the development of intestinal mucosal T cells. Mucosal Immunology 1, 198–207.

Narayan, K., Sylvia, K.E., Malhotra, N., Yin, C.C., Martens, G., Vallerskog, T., Kornfeld, H., Xiong, N., Cohen, N.R., Brenner, M.B., Berg, L.J., Kang, J., IGPC, 2012. Intrathymic programming of effector fates in three molecularly distinct γδ T cell subtypes. Nature Immunology 13, 511–518.

Nguyen, T., Liu, X.K., Zhang, Y., Dong, C., 2006. BTNL2, a Butyrophilin-Like Molecule That Functions to Inhibit T Cell Activation. The Journal of Immunology 176, 7354–7360.

Nitahara, A., Shimura, H., Ito, A., Tomiyama, K., Ito, M., Kawai, K., 2006. NKG2D Ligation without T Cell Receptor Engagement Triggers Both Cytotoxicity and Cytokine Production in Dendritic Epidermal T Cells. Journal of Investigative Dermatology 126, 1052–1058.

Noguchi, M., Yi, H., Rosenblatt, H.M., Filipovich, A.H., Adelstein, S., Modi, W., McBride, W., Leonard, W.J., 1993. Interleukin-2 receptor γ chain mutation results in X-linked severe combined immunodeficiency in humans. Cell 73, 147–157.

Nonaka, S., Naito, T., Chen, H., Yamamoto, M., Moro, K., Kiyono, H., Hamada, H., Ishikawa, H., 2005. Intestinal γδ T cells develop in mice lacking thymus, all lymph nodes, Peyer's patches, and isolated lymphoid follicles. J. Immunol. 174, 1906–1912.

Ogg, S.L., Weldon, A.K., Dobbie, L., Smith, A.J.H., Mather, I.H., 2004. Expression of butyrophilin (Btn1a1) in lactating mammary gland is essential for the regulated secretion of milk–lipid droplets. Proc Natl Acad Sci USA, 101, 10084–10089.

Oh-hora, M., Komatsu, N., Pishyareh, M., Feske, S., Hori, S., Taniguchi, M., Rao, A., Takayanagi, H., 2013. Agonist-Selected T Cell Development Requires Strong T Cell Receptor Signaling and Store-Operated Calcium Entry. Immunity 38, 881–895.

Olivares-Villagómez, D., Mendez-Fernandez, Y.V., Parekh, V.V., Lalani, S., Vincent, T.L., Cheroutre, H., Van Kaer, L., 2008. Thymus leukemia antigen controls intraepithelial lymphocyte function and inflammatory bowel disease. Proc Natl Acad Sci USA 105, 17931–17936.

Oppenheim, D.E., Roberts, S.J., Clarke, S.L., Filler, R., Lewis, J.M., Tigelaar, R.E., Girardi, M., Hayday, A.C., 2005. Sustained localized expression of ligand for the activating NKG2D receptor impairs natural cytotoxicity in vivo and reduces tumor immunosurveillance. Nature immunology 6, 928–937.

Osborne, B.A., Smith, S.W., Liu, Z.G., McLaughlin, K.A., Grimm, L., Schwartz, L.M., 1994. Identification of genes induced during apoptosis in T lymphocytes. Immunological Reviews 142, 301–320.

Pang, D.J., Neves, J.F., Sumaria, N., Pennington, D.J., 2012. Understanding the complexity of γδ T-cell subsets in mouse and human. Immunology 136, 283–290.

Pardoll, D.M., 2012. The blockade of immune checkpoints in cancer immunotherapy. Nature Reviews Cancer 12, 252–264.

Park, S.H., Guy-Grand, D., Lemonnier, F.A., Wang, C.R., Bendelac, A., Jabri, B., 1999. Selection and expansion of CD8α/α+ T cell receptor α/β+ intestinal intraepithelial lymphocytes in the absence of both classical major histocompatibility complex class I and nonclassical CD1 molecules. Journal of Experimental Medicine. 190, 885–890.

Pathan, S., Gowdy, R.E., Cooney, R., Beckly, J.B., Hancock, L., Guo, C., Barrett, J.C., Morris, A., Jewell, D.P., 2009. Confirmation of the novel association at the BTNL2 locus with ulcerative colitis. Tissue Antigens 74, 322–329.

Payer, E., Elbe, A., Stingl, G., 1991. Circulating CD3+/T cell receptor Vγ3+ fetal murine thymocytes home to the skin and give rise to proliferating dendritic epidermal T cells. The Journal of Immunology 146, 2563–2543.

Pennington, D.J., Silva-Santos, B., Shires, J., Theodoridis, E., Pollitt, C., Wise, E.L., Tigelaar, R.E., Owen, M.J., Hayday, A.C., 2003. The inter-relatedness and interdependence of mouse T cell receptor γδ+ and αβ+ cells. Nature immunology 4, 991–998.

Pereira, P., Lafaille, J.J., Gerber, D., Tonegawa, S., 1997. The T cell receptor repertoire of intestinal intraepithelial γδ T lymphocytes is influenced by genes linked to the major histocompatibility complex and to the T cell receptor loci. Proc. Natl. Acad. Sci. U.S.A. 94, 5761–5766.

Pertel, T., Hausmann, S., Morger, D., Züger, S., Guerra, J., Lascano, J., Reinhard, C., Santoni, F.A., Uchil, P.D., Chatel, L., Bisiaux, A., Albert, M.L., Strambio-De-Castillia, C., Mothes, W., Pizzato, M., Grütter, M.G., Luban, J., 2011. TRIM5 is an innate immune sensor for the retrovirus capsid lattice. Nature 472, 361–365.

Pobezinsky, L.A., Angelov, G.S., Tai, X., Jeurling, S., Van Laethem, F., Feigenbaum, L., Park, J.-H., Singer, A., 2012. Clonal deletion and the fate of autoreactive thymocytes that survive negative selection. Nature immunology 13, 569–578.

Prinz, I., Sansoni, A., Kissenpfennig, A., Ardouin, L., Malissen, M., Malissen, B., 2006. Visualization of the earliest steps of γδ T cell development in the adult thymus. Nature immunology 7, 995–1003.

Ramond, C., Berthault, C., Burlen-Defranoux, O., de Sousa, A.P., Guy-Grand, D., Vieira, P., Pereira, P., Cumano, A., 2013. Two waves of distinct hematopoietic progenitor cells colonize the fetal thymus. Nature immunology 15, 27–35.

Rast, J.P., Anderson, M.K., Strong, S.J., Luer, C., Litman, R.T., 1997. α, β, γ, and δ T cell antigen receptor genes arose early in vertebrate phylogeny. Immunity 6, 1–11.

Reinherz, E.L., Meuer, S., Fitzgerald, K.A., Hussey, R.E., Herbert, L., Schlossman, S.F., 1982. Antigen recognition by human T lymphocytes is linked to surface expression of the T3 molecular complex. Cell 40, 735–743.

Reis, B.S., Rogoz, A., Costa-Pinto, F.A., Taniuchi, I., Mucida, D., 2013. Mutual expression of the transcription factors Runx3 and ThPOK regulates intestinal CD4+ T cell immunity. Nature immunology 14, 271–280.

Reis, B.S., van Konijnenburg, D.P.H., Grivennikov, S.I., Mucida, D., 2014. Transcription Factor T-bet Regulates Intraepithelial Lymphocyte Functional Maturation. Immunity 41, 244–256.

Rhodes, D.A., Chen, H.C., Price, A.J., Keeble, A.H., Davey, M.S., James, L.C., Eberl, M., Trowsdale, J., 2015. Activation of Human γδ T Cells by Cytosolic Interactions of BTN3A1 with Soluble Phosphoantigens and the Cytoskeletal Adaptor Periplakin. The Journal of Immunology 194, 2390–2398.

Rhodes, D.A., de Bono, B., Trowsdale, J., 2005. Relationship between SPRY and B30.2 protein domains. Evolution of a component of immune defence? Immunology 116, 411–417.

Rhodes, D.A., Reith, W., Trowsdale, J., 2016. Regulation of Immunity by Butyrophilins. Annual Review of Immunology 34, 6.1–6.22.

Rhodes, D.A., Trowsdale, J., 2007. TRIM21 is a trimeric protein that binds IgG Fc via the B30.2 domain. Molecular Immunology 44, 2406–2414.

Riaño, F., Karunakaran, M.M., Starick, L., Li, J., Scholz, C.J., Kunzmann, V., Olive, D., Amslinger, S., Herrmann, T., 2014. Vγ9Vδ2 TCR-activation by phosphorylated antigens requires butyrophilin 3A1 (BTN3A1) and additional genes on human chromosome 6. European Journal of Immunology 44, 2571–2576.

Ribeiro, S.T., Ribot, J.C., Silva-Santos, B., 2015. Five Layers of Receptor Signaling in γδ T-Cell Differentiation and Activation. Frontiers in Immunology 6, 1–9.

Ribot, J.C., Debarros, A., Pang, D.J., Neves, J.F., Peperzak, V., Roberts, S.J., Girardi, M., Borst, J., Hayday, A.C., Pennington, D.J., Silva-Santos, B., 2009. CD27 is a thymic determinant of the balance between interferon-γ- and interleukin 17–producing γδ T cell subsets. Nature immunology 10, 427–436.

Robenek, H., Hofnagel, O., Buers, I., Lorkowski, S., Schnoor, M., Robenek, M.J., Heid, H., Troyer, D., Severs, N.J., 2006. Butyrophilin controls milk fat globule secretion. Proc. Natl. Acad. Sci. U.S.A. 103, 10385–10390.

Robert, C., Long, G.V., Brady, B., Dutriaux, C., Maio, M., Mortier, L., Hassel, J.C., Rutkowski, P., McNeil, C., Kalinka-Warzocha, E., Savage, K.J., Hernberg, M.M., Lebbé, C., Charles, J., Mihalcioiu, C., Chiarion-Sileni, V., Mauch, C., Cognetti, F., Arance, A., Schmidt, H., Schadendorf, D., Gogas, H., Lundgren-Eriksson, L., Horak, C., Sharkey, B., Waxman, I.M., Atkinson, V., Ascierto, P.A., 2015. Nivolumab in Previously Untreated Melanoma without BRAFMutation. New England Journal of Medicine 372, 320–330.

Roberts, S.J., Smith, A.L., West, A.B., Wen, L., Findly, R.C., Owen, M.J., Hayday, A.C., 1996. T-cell αβ+ and γδ+ deficient mice display abnormal but distinct phenotypes toward a natural, widespread infection of the intestinal epithelium. Proc. Natl. Acad. Sci. U.S.A. 93, 11774–11779.

Rocha, B., Vassalli, P., Guy-Grand, D., 1991. The Vβ repertoire of mouse gut homodimeric α CD8+ intraepithelial T cell receptor α/β + lymphocytes reveals a major extrathymic pathway of T cell differentiation. Journal of Experimental Medicine. 173, 483–486.

Roth, S., Franken, P., van Veelen, W., Blonden, L., Raghoebir, L., Beverloo, B., van Drunen, E., Kuipers, E.J., Rottier, R., Fodde, R., Smits, R., 2009. Generation of a tightly regulated doxycycline-inducible model for studying mouse intestinal biology. genesis 47, 7–13.

Rothenberg, E.V., Moore, J.E., Yui, M.A., 2008. Launching the T-cell-lineage developmental programme. Nature Reviews Immunology 8, 9–21.

Saito, H., Kanamori, Y., Takemori, T., Nariuchi, H., Kubota, E., Takahashi-Iwanaga, H., Iwanaga, T., Ishikawa, H., 1998. Generation of intestinal T cells from progenitors residing in gut cryptopatches. Science 280, 275–278.

Saito, H., Kranz, D.M., Takagaki, Y., Hayday, A.C., Eisen, H.N., Tonegawa, S., 1984. A third rearranged and expressed gene in a clone of cytotoxic T lymphocytes. Nature 312, 36–40.

Salim, M., Knowles, T.J., Hart, R., Mohammed, F., Woodward, M.J., Willcox, C.R., Overduin, M., Hayday, A.C., Willcox, B.E., 2016. Characterization of a Putative Receptor Binding Surface on Skint-1, a Critical Determinant of Dendritic Epidermal T Cell Selection. Journal of Biological Chemistry 291, 9310–9321.

Sallusto, F., Lenig, D., Forster, R., Lipp, M., Lanzavecchia, A., 1999. Two subsets of memory T lymphocytes with distinct homing potentials and effector functions. Nature 401, 708–712.

Salomonsen, J., Chattaway, J.A., Chan, A.C.Y., Parker, A., Huguet, S., Marston, D.A., Rogers, S.L., Wu, Z., Smith, A.L., Staines, K., Butter, C., Riegert, P., Vainio, O., Nielsen, L., Kaspers, B., Griffin, D.K., Yang, F., Zoorob, R., Guillemot, F., Auffray, C., Beck, S., Skjødt, K., Kaufman, J., 2014. Sequence of a Complete Chicken BG Haplotype Shows Dynamic Expansion and Contraction of Two Gene Lineages with Particular Expression Patterns. PLoS Genetics 10, e1004417.

Sandstrom, A., Peigné, C.-M., Léger, A., Crooks, J.E., Konczak, F., Gesnel, M.-C., Breathnach, R., Bonneville, M., Scotet, E., Adams, E.J., 2014. The Intracellular B30.2 Domain of Butyrophilin 3A1 Binds Phosphoantigens to Mediate Activation of Human Vγ9Vδ2 T Cells. Immunity 40, 490–500.

Sarter, K., Leimgruber, E., Gobet, F., Agrawal, V., Dunand-Sauthier, I., Barras, E., Mastelic-Gavillet, B., Kamath, A., Fontannaz, P., Guéry, L., Duraes, F.D.V., Lippens, C., Ravn, U., Santiago-Raber, M.-L., Magistrelli, G., Fischer, N., Siegrist, C.-A., Hugues, S., Reith, W., 2016. Btn2a2, a T cell immunomodulatory molecule coregulated with MHC class II genes. Journal of Experimental Medicine 213, 177–187.

Schadendorf, D., Hodi, F.S., Robert, C., Weber, J.S., Margolin, K., Hamid, O., Patt, D., Chen, T.T., Berman, D.M., Wolchok, J.D., 2015. Pooled Analysis of Long-Term Survival Data From Phase II and Phase III Trials of Ipilimumab in Unresectable or Metastatic Melanoma. Journal of Clinical Oncology 1–7.

Schenkel, J.M., Fraser, K.A., Casey, K.A., Beura, L.K., Pauken, K.E., Vezys, V., Masopust, D., 2016. IL-15-Independent Maintenance of Tissue-Resident and Boosted Effector Memory CD8 T Cells. The Journal of Immunology 196, 3920–3926.

Schenkel, J.M., Masopust, D., 2014. Tissue-Resident Memory T Cells. Immunity 41, 886–897.

Schlissel, M.S., Durum, S.D., Muegge, K., 2000. The interleukin 7 receptor is required for T cell receptor gamma locus accessibility to the V(D)J recombinase. Journal of Experimental Medicine. 191, 1045–1050.

Schluns, K.S., Lefrançois, L., 2003. Cytokine control of memory T-cell development and survival. Nature Reviews Immunology 3, 269–279.

Schluns, K.S., Nowak, E.C., Cabrera-Hernandez, A., Puddington, L., Lefrançois, L., Aguila, H.L., 2004. Distinct cell types control lymphoid subset development by means of IL-15 and IL-15 receptor alpha expression. Proc. Natl. Acad. Sci. U.S.A. 101, 5616–5621.

Sebestyen, Z., Scheper, W., Vyborova, A., Gu, S., Rychnavska, Z., Schiffler, M., Cleven, A., Chéneau, C., van Noorden, M., Peigné, C.-M., Olive, D., Lebbink, R.J., Oostvogels, R., Mutis, T., Schuurhuis, G.J., Adams, E.J., Scotet, E., Kuball, J., 2016. RhoB Mediates Phosphoantigen Recognition by Vγ9Vδ2 T Cell Receptor. Cell 15, 1973–1985.

Shafi, S., Vantourout, P., Wallace, G., Antoun, A., Vaughan, R., Stanford, M., Hayday, A., 2011. An NKG2D-Mediated Human Lymphoid Stress Surveillance Response with High Interindividual Variation. Science Translational Medicine 3, 1–9.

Sharp, L.L., Jameson, J.M., Cauvi, G., Havran, W.L., 2004. Dendritic epidermal T cells regulate skin homeostasis through local production of insulin-like growth factor 1. Nature immunology 6, 73–79.

Shen, Y., Zhou, D., Qiu, L., Lai, X., Simon, M., Shen, L., Kou, Z., Wang, Q., Jiang, L., Estep, J., Hunt, R., Clagett, M., Sehgal, P.K., Li, Y., Zeng, X., Morita, C.T., Brenner, M.B., Letvin, N.L., Chen, Z.W., 2002. Adaptive immune response of Vγ2Vδ2+ T cells during mycobacterial infections. Science 295, 2255–2258.

Sheridan, B.S., Lefrançois, L., 2011. Regional and mucosal memory T cells. Nature immunology 131, 485–491.

Sheridan, B.S., Pham, Q.-M., Lee, Y.-T., Cauley, L.S., Puddington, L., Lefrançois, L., 2014. Oral Infection Drives a Distinct Population of Intestinal Resident Memory CD8. Immunity 40, 747–757.

Shibata, K., Yamada, H., Nakamura, M., Hatano, S., Katsuragi, Y., Kominami, R., Yoshikai, Y., 2014. IFN-γ-Producing and IL-17-Producing γδ T Cells Differentiate at Distinct Developmental Stages in Murine Fetal Thymus. The Journal of Immunology 192, 2210–2218.

Shin, S., El-Diwany, R., Schaffert, S., Adams, E.J., Garcia, C., Pereira, P., Chien, Y.-H., 2005. Antigen recognition determinants of γδ T cell receptors. Science 308, 252–255.

Shinkura, R., Kitada, K., Matsuda, F., Tashiro, K., Ikuta, K., Suzuki, M., Kogishi, K., Serikawa, T., Honjo, T., 1999. Alymphoplasia is caused by a point mutation in the mouse gene encoding Nf-κb-inducing kinase. Nature Genetics 22, 74–77.

Silva-Santos, B., Pennington, D.J., Hayday, A.C., 2005. Lymphotoxin-mediated regulation of gammadelta cell differentiation by αβ T cell progenitors. Science 307, 925–928.

Smith, I.A., Knezevic, B.R., Ammann, J.U., Rhodes, D.A., Aw, D., Palmer, D.B., Mather, I.H., Trowsdale, J., 2010. BTN1A1, the Mammary Gland Butyrophilin, and BTN2A2 Are Both Inhibitors of T Cell Activation. The Journal of Immunology 184, 3514–3525.

Smith-Garvin, J.E., Koretzky, G.A., Jordan, M.S., 2009. T Cell Activation. Annual Review of Immunology. 27, 591–619.

Stingl, G., Koning, F., Yamada, H., Yokoyama, W.M., Tschachler, E., Bluestone, J.A., Steiner, G., Samelson, L.E., Lew, A.M., Coligan, J.E., 1987. Thy-1+ dendritic epidermal cells express T3 antigen and the T-cell receptor γ chain. Proc. Natl. Acad. Sci. U.S.A. 84, 4586–4590.

Stonier, S.W., Schluns, K.S., 2010. Trans-presentation: A novel mechanism regulating IL-15 delivery and responses. Immunology Letters 127, 85–92.

Strid, J., Roberts, S.J., Filler, R.B., Lewis, J.M., Kwong, B.Y., Schpero, W., Kaplan, D.H., Hayday, A.C., Girardi, M., 2008. Acute upregulation of an NKG2D ligand promotes rapid reorganization of a local immune compartment with pleiotropic effects on carcinogenesis. Nature immunology 9, 146–154.

Strid, J., Sobolev, O., Zafirova, B., Polic, B., Hayday, A., 2011. The Intraepithelial T Cell Response to NKG2D-Ligands Links Lymphoid Stress Surveillance to Atopy. Science 334, 1293–1297.

Stritesky, G.L., Jameson, S.C., Hogquist, K.A., 2012. Selection of Self-Reactive T Cells in the Thymus. Annual Review of Immunology 30, 95–114.

Sumaria, N., Roediger, B., Ng, L.G., Qin, J., Pinto, R., Cavanagh, L.L., Shklovskaya, E., Fazekas de St Groth, B., Triccas, J.A., Weninger, W., 2011. Cutaneous immunosurveillance by self-renewing dermal γδ T cells. Journal of Experimental Medicine 208, 505–518.

Sutton, C.E., Lalor, S.J., Sweeney, C.M., Brereton, C.F., Lavelle, E.C., Mills, K.H.G., 2009. Interleukin-1 and IL-23 Induce Innate IL-17 Production from γδ T Cells, Amplifying Th17 Responses and Autoimmunity. Immunity 31, 331–341.

Suzuki, H., Duncan, G.S., Takimoto, H., Mak, T.W., 1997. Abnormal development of intestinal intraepithelial lymphocytes and peripheral natural killer cells in mice lacking the IL-2 receptor β chain. Journal of Experimental Medicine. 185, 499–505.

Suzuki, H., Jeong, K., Doi, K., 2002. Age-related changes in the regional variations in the number and subsets of intraepithelial lymphocytes in mouse small intestine. Developmental and Comparative Immunology 26, 589–595.

Suzuki, H., Jeong, K.I., Okutani, T., Doi, K., 2000. Regional variations in the distribution of small intestinal intraepithelial lymphocytes in three inbred strains of mice. Journal of Veterinary Medical Science 62, 881–887.

Suzuki, K., Oida, T., Hamada, H., Hitotsumatsu, O., Wantanabe, M., Hibi, T., Yamamoto, H., Kubota, E., Kaminogawa, S., Ishikawa, H., 2000. Gut cryptopatches: direct evidence of extrathymic anatomical sites for intestinal T lymphopoiesis. Immunity 13, 691–702.

Swamy, M., Abeler-Dörner, L., Chettle, J., Mahlakoiv, T., Goubau, D., Chakravarty, P., Ramsay, G., Sousa, C.R.E., Staeheli, P., Blacklaws, B.A., Heeney, J.L., Hayday, A.C., 2015. Intestinal intraepithelial lymphocyte activation promotes innate antiviral resistance. Nature Communications 6, 1–12.

Swamy, M., Jamora, C., Havran, W., Hayday, A., 2010. Epithelial decision makers: in search of the “epimmunome”. Nature immunology 11, 656–665.

Tamura, A., Soga, H., Yaguchi, K., Yamagishi, M., Toyota, T., Sato, J., Oka, Y., Itoh, T., 2003. Distribution of two types of lymphocytes (intraepithelial and lamina-propria-associated) in the murine small intestine. Cell and Tissue Research 313, 47–53.

Tesselaar, K., Xiao, Y., Arens, R., van Schijndel, G.M.W., Schuurhuis, D.H., Mebius, R.E., Borst, J., van Lier, R.A.W., 2003. Expression of the Murine CD27 Ligand CD70 In Vitro and In Vivo. The Journal of Immunology 170, 33–40.

Thurnher, M., Gruenbacher, G., 2015. T lymphocyte regulation by mevalonate metabolism. Science Signaling 8, re4.

Triebel, F., Jitsukawa, S., Baixeras, E., 1990. LAG-3, a novel lymphocyte activation gene closely related to CD4. Journal of Experimental Medicine. 171, 1393–1405.

Turchinovich, G., Hayday, A.C., 2011. Skint-1 Identifies a Common Molecular Mechanism for the Development of Interferon-γ-Secreting versus Interleukin-17-Secreting γδ T Cells. Immunity 35, 59–68.

Turchinovich, G., Pennington, D.J., 2011. T cell receptor signalling in γδ cell development: strength isn't everything. Trends in Immunology 32, 567–573.

Uhlen, M., Fagerberg, L., Hallstrom, B.M., Lindskog, C., Oksvold, P., Mardinoglu, A., Sivertsson, A., Kampf, C., Sjostedt, E., Asplund, A., Olsson, I., Edlund, K., Lundberg, E., Navani, S., Szigyarto, C.A.K., Odeberg, J., Djureinovic, D., Takanen, J.O., Hober, S., Alm, T., Edqvist, P.H., Berling, H., Tegel, H., Mulder, J., Rockberg, J., Nilsson, P., Schwenk, J.M., Hamsten, M., Feilitzen, von, K., Forsberg, M., Persson, L., Johansson, F., Zwahlen, M., Heijne, von, G., Nielsen, J., Ponten, F., 2015. Tissue-based map of the human proteome. Science 347, 1260419–1260419.

Valentonyte, R., Hampe, J., Huse, K., Rosenstiel, P., Albrecht, M., Stenzel, A., Nagy, M., Gaede, K.I., Franke, A., Haesler, R., Koch, A., Lengauer, T., Seegert, D., Reiling, N., Ehlers, S., Schwinger, E., Platzer, M., Krawczak, M., Müller-Quernheim, J., Schürmann, M., Schreiber, S., 2005. Sarcoidosis is associated with a truncating splice site mutation in BTNL2. Nature Genetics 37, 357–364.

van Beek, E., Pieterman, E., Cohen, L., Löwik, C., Papapoulos, S., 1999. Farnesyl pyrophosphate synthase is the molecular target of nitrogen-containing bisphosphonates. Biochem. Biophys. Res. Commun. 264, 108–111.

Van Rhijn, I., Rutten, V.P.M.G., Charleston, B., Smits, M., van Eden, W., Koets, A.P., 2007. Massive, sustained γδ T cell migration from the bovine skin in vivo. Journal of Leukocyte Biology 81, 968–973.

Vantourout, P., Hayday, A., 2013. Six-of-the-best: unique contributions of γδ T cells to immunology. Nature Reviews Immunology 13, 88–100.

Vantourout, P., Willcox, C., Turner, A., Swanson, C.M., Haque, Y., Sobolev, O., Grigoriadis, A., Tutt, A., Hayday, A., 2014. Immunological visibility: posttranscriptional regulation of human NKG2D ligands by the EGF receptor pathway. Science Translational Medicine 6, 231ra49.

Vavassori, S., Kumar, A., Wan, G.S., Ramanjaneyulu, G.S., Cavallari, M., Daker, El, S., Beddoe, T., Theodossis, A., Williams, N.K., Gostick, E., Price, D.A., Soudamini, D.U., Voon, K.K., Olivo, M., Rossjohn, J., Mori, L., De Libero, G., 2013. Butyrophilin 3A1 binds phosphorylated antigens and stimulates human γδ T cells. Nature immunology 14, 908–916.

Vidal, K., Grosjean, I., evillard, J.P., Gespach, C., Kaiserlian, D., 1993. Immortalization of mouse intestinal epithelial cells by the SV40-large T gene. Phenotypic and immune characterization of the MODE-K cell line. Journal of Immunological Methods 166, 63–73.

Waickman, A.T., Park, J.-Y., Park, J.-H., 2015. The common γ-chain cytokine receptor: tricks-and-treats for T cells. Cellular and Molecular Life Sciences. 73, 253–269.

Walker, C.R., Hautefort, I., Dalton, J.E., Overweg, K., Egan, C.E., Bongaerts, R.J., Newton, D.J., Cruickshank, S.M., Andrew, E.M., Carding, S.R., 2013. Intestinal Intraepithelial Lymphocyte-Enterocyte Crosstalk Regulates Production of Bactericidal Angiogenin 4 by Paneth Cells upon Microbial Challenge. PLoS ONE 8, e84553.

Weber, J.S., Minor, D., DAngelo, S.P., Hodi, F.S., Gutzmer, R., Neyns, B., Hoeller, C., Khushalani, N.I., Miller, W.H., Jr, Lao, C.D., Linette, G.P., Thomas, L., Lorigan, P., Grossmann, K.F., Hassel, J.C., Maio, M., Sznol, M., Ascierto, P.A., Mohr, P., Chmielowski, B., Bryce, A., Svane, I.M., MD, D.M., Grob, J.-J., Krackhardt, A.M., Horak, C., Lambert, A., Yang, A.S., Larkin, J., 2015. Nivolumab versus chemotherapy in patients with advanced melanoma who progressed after anti-CTLA-4 treatment (CheckMate 037): a randomised, controlled, open-label, phase 3 trial. Lancet Oncology 16, 375–384.

Wencker, M., Turchinovich, G., Di Marco Barros, R., Deban, L., Jandke, A., Cope, A., Hayday, A.C., 2013. Innate-like T cells straddle innate and adaptive immunity by altering antigen-receptor responsiveness. Nature Publishing Group.

Winoto, A., Littman, D.R., 2002. Nuclear hormone receptors in T lymphocytes. Cell 109, S57–S66.

Witherden, D.A., Verdino, P., Rieder, S.E., Garijo, O., Mills, R.E., Teyton, L., Fischer, W.H., Wilson, I.A., Havran, W.L., 2010. The Junctional Adhesion Molecule JAML Is a Costimulatory Receptor for Epithelial T Cell Activation. Science 329, 1205–1210.

Witherden, D.A., Watanabe, M., Garijo, O., Rieder, S.E., Sarkisyan, G., Cronin, S.J.F., Verdino, P., Wilson, I.A., Kumanogoh, A., Kikutani, H., Teyton, L., Fischer, W.H., Havran, W.L., 2012. The CD100 Receptor Interacts with Its Plexin B2 Ligand to Regulate Epidermal γδ T Cell Function. Immunity 37, 314–325.

Wolchok, J.D., Kluger, H., Callahan, M.K., Postow, M.A., Rizvi, N.A., Lesokhin, A.M., Segal, N.H., Ariyan, C.E., Gordon, R.-A., Reed, K., Burke, M.M., Caldwell, A., Kronenberg, S.A., Agunwamba, B.U., Zhang, X., Lowy, I., Inzunza, H.D., Feely, W., Horak, C.E., Hong, Q., Korman, A.J., Wigginton, J.M., Gupta, A., Sznol, M., 2013. Nivolumab plus Ipilimumab in Advanced Melanoma. New England Journal of Medicine 369, 122–133.

Woo, J.S., Imm, J.H., Min, C.K., Kim, K.J., Cha, S.S., 2006. Structural and functional insights into the B30.2/SPRY domain. The EMBO Journal 25, 1353–1363.

Xing, L., Dai, Z., Jabbari, A., Cerise, J.E., Higgins, C.A., Gong, W., de Jong, A., Harel, S., DeStefano, G.M., Rothman, L., Singh, P., Petukhova, L., Mackay-Wiggan, J., Christiano, A.M., Clynes, R., 2014. Alopecia areata is driven by cytotoxic T lymphocytes and is reversed by JAK inhibition. Nat Med 20, 1043–1049.

Xu, F., Liu, J., Liu, D., Liu, B., Wang, M., Hu, Z., Du, X., Tang, L., He, F., 2014. LSECtin Expressed on Melanoma Cells Promotes Tumor Progression by Inhibiting Antitumor T-cell Responses. Cancer Research 74, 3418–3428.

Yamagata, T., Mathis, D., Benoist, C., 2004. Self-reactivity in thymic double-positive cells commits cells to a CD8αα lineage with characteristics of innate immune cells. Nature immunology 5, 597–605.

Yamazaki, T., Goya, I., Graf, D., Craig, S., Martin-Orozco, N., Dong, C., 2010. A Butyrophilin Family Member Critically Inhibits T Cell Activation. The Journal of Immunology 185, 5907–5914.

Ye, S.K., Agata, Y., Lee, H.C., Kurooka, H., Kitamura, T., Shimizu, A., Honjo, T., Ikuta, K., 2001. The IL-7 receptor controls the accessibility of the TCRγ locus by Stat5 and histone acetylation. Immunity 15, 813–823.

Yu, A., Malek, T.R., 2000. The Proteasome Regulates Receptor-mediated Endocytosis of Interleukin-2. Journal of Biological Chemistry 276, 381–385.

Zarin, P., Wong, G.W., Mohtashami, M., Wiest, D.L., Zuniga-Pflucker, J.C., 2014. Enforcement of γδ-lineage commitment by the pre-T-cell receptor in precursors with weak γδ-TCR signals. Proc Natl Acad Sci USA 111, 5658–5663.

Zelenay, S., Sousa, C.R.E., 2013. Adaptive immunity after cell death. Trends in Immunology 34, 329–335.

Zhang, B., Wu, J., Jiao, Y., Bock, C., Dai, M., Chen, B., Chao, N., Zhang, W., Zhuang, Y., 2015. Differential Requirements of TCR Signaling in Homeostatic Maintenance and Function of Dendritic Epidermal T Cells. The Journal of Immunology 195, 4282–4291.

Zhang, Y., Cado, D., Asarnow, D.M., Komori, T., Alt, F.W., Raulet, D.H., Allison, J.P., 1995. The role of short homology repeats and TdT in generation of the invariant γδ antigen receptor repertoire in the fetal thymus. Immunity 3, 439–447.

Zhou, T., Cheng, J., Yang, P., Wang, Z., Liu, C., Su, X., Bluethmann, H., Mountz, J.D., 1996. Inhibition of Nur77/Nurr1 leads to inefficient clonal deletion of self-reactive T cells. Journal of Experimental Medicine. 183, 1879–1892.

Zinkernagel, R.M., Bachmann, M.F., Kundig, T.M., Oehen, S., Pirchet, H., Hengartner, H., 1996. On immunological memory. Annual review of Immunology 14, 333–367.

Zufferey, R., Nagy, D., Mandel, R.J., Naldini, L., Trono, D., 1997. Multiply attenuated lentiviral vector achieves efficient gene delivery in vivo. Nature Biotechnology. 15, 871–875.